SI-traceable quantification of clinically relevant proteins

PhD Chemistry

Department of Chemistry

Attila Ferenc Torma

March 2018

Abstract

Current requirements of the EU in-vitro diagnostic directive (IVDD) has established the requirement for routine devices to provide results that are traceable to higher order reference standards, where available. Routine blood tests are an essential component of prognostic and diagnostic medicine; however, these often use arbitrary international units (IU) to facilitate comparability, which lack metrological traceability. Whilst a number of certified reference materials (CRMs) are available for small molecules, little has been done in developing SI-traceable biological reference materials. In this thesis, the first task is to develop an SI-traceable quantified B-type natriuretic peptide (BNP) standard by adapting the current isotope dilution mass spectrometry (IDMS) methods. The standard is used to develop a reference method for the SI-traceable quantification of BNP in plasma. The difficulties associated with the purity assessment of synthetic peptides, stabilisation of BNP in plasma, measurement of large intact peptides by mass spectrometry (MS) and multiplexing the method for monitoring for the presence of degradation products are addressed.

Many circulating peptides such as BNP, are routinely measured and External Quality Assessment Schemes (EQAS) are already established. BNP is an essential biomarker for heart failure. The reference method was used to participate in EQAS to assess the capability of the method to supply reference values to EQAS samples. The ultimate goal of the reference method to develop a commutable certified reference material (CRM) to assist the standardization of BNP measurements and to ascertain the direct benefits of metrological traceability in clinical diagnostics and evidence based medicine.

Abstract

This project also aims to include the higher order reference method in the Joint Committee for Traceability in Laboratory medicine (JCTLM) database.

Acknowledgments

I would like to dedicate this thesis to my mother Nemeth Gabriella and to my wife-to-be Gazdag Szilvia. I am grateful to my mother for her relentless optimism and support throughout my endeavours in life.

To be able to describe my feeling towards Gazdag Szilvia I am going to have to resort to the medium of poetry.

Like
Written by: Torma Attila Ferenc
Presented by: Torma Attila Ferenc

Harmless little like. Innocuous and innocent,
I remember Szilvia. Shall we change or chat?
Would you visit me? There was no harm if we met.
Pretty girl on the outside, nothing else I bet.

We share the taste for coffee and have the same toothbrush,
Interesting, I thought. Let's not get excited too much.
There is no future for us, we live in different countries,
Does not matter that we look beautiful in selfies.

Now I hold a doctorate also known as PhD,
Always thinking about her, all day long I reverie,
There is nothing in the World that makes me more happy,
Than to be with Szilvia and to change some nappy.

Declaration

I confirm that this is my own work and the use of all material from other sources has been properly and fully acknowledged.

Attila Ferenc Torma

Table of Contents

Table of Contents

Table of Contents

Table of Figures

Table of Figures

List of Tables

List of Tables

List of Equations

List of Equations

Abbreviations

ABC	-	Ammonium bicarbonate
ACN	-	Acetonitrile
AEBSF	-	(4-(2-aminoethyl)benzenesulfonyl fluoride
AGC	-	Automatic gain control
APCI	-	Atmospheric pressure chemical ionisation
APPI	-	Atmospheric pressure photo ionisation
AQUA	-	Absolute quantification
ASMS	-	American society for mass spectrometry
BIPM	-	Bureau of weights and measures (Bureau international des poids et mesures)
BNP	-	B-type natriuretic peptide
BSA	-	Bovine serum albumin
CAD	-	Charged aerosol detector
CB	-	Calibration blend
CCQM	-	Committee for weights and measures (Comité consultatif pour la quantité de matére)
CEM	-	Chain ejection model
CHCA	-	α-cyano-4-hydroxycinnamic acid

Abbreviations

CHF	-	Congestive heart failure
CI	-	Chemical ionisation
CID	-	Collision induced dissociation
CIPM	-	Committee for weights and measures (Comité international des poids et mesures)
CK	-	Creatine kinase
CMC	-	Calibration and measurement capability
CPS	-	Counts per second
CRM	-	Charged residue model
CRM	-	Certified reference material
DAD	-	Diode array detector
dc, U	-	Direct current potential
DHB	-	2,5-dihydroxybenzoic acid
DMSO	-	Dimethyl sulfoxide
DNA	-	Deoxynucleic acid
DPP IV	-	Dipeptidyl peptidase
DSC	-	Differential scanning calorimetry
ECD	-	Electron capture dissociation
ECD	-	Electron capture detector

EDTA	-	Ethylenediaminetetraacetic acid
EI	-	Electron ionisation
EM-IDMS	-	Exact matching isotope dilution mass spectrometry
ESI	-	Electrospray ionisation
ETD	-	Electron transfer dissociation
FA	-	Formic acid
FAB	-	Fast atomic bombardment
FDA	-	Food and drug administration
FID	-	Flame ionisation detector
FT-ICR	-	Fourier-transform ion cyclotron resonance
GC	-	Gas chromatography
GPC	-	Gel permeation chromatography
IA	-	Immunoaffinity enrichment
IDE	-	Insulin degrading enzyme
IDMS	-	Isotope dilution mass spectrometry
IEM	-	Ion evaporation model
IFCC	-	International federation of clinical chemistry and laboratory medicine
ILAC	-	International laboratory accreditation cooperation

Abbreviations

ILM	-	Ionic liquid matrices
IS	-	International unit
IVD	-	In-vitro-diagnostics
JCTLM	-	Joint committee of traceability in laboratory medicine
LC	-	Liquid chromatography
LGC	-	Laboratory of the government chemist
LSM	-	Liquid support matrices
LTQ	-	Linear trap quadrupole
m	-	Mass (kg)
m/z	-	Mass-to-charge ratio
MALDI	-	Matrix-assisted laser desorption/ionisation
MBF	-	Median baseline filter
MMTS	-	S-methyl methanethiosulfonate
m-NBA	-	3-nitrobenzyl alcohol
MS	-	Mass spectrometry
MS/MS	-	Tandem mass spectrometry
MSI	-	Multisegment injection
MSIA	-	Mass spectrometry immunoassay
MSTFA	-	N-methyl-N-(trimethylsilyl)-trifluoroacetamide

MTBSTFA	-	N-*tert*-butyldimethylsilyl-N-methyltrifluoroacetamide
NEP	-	Neutral endopeptidase
NEQAS	-	National external quality assessment scheme
NIST	-	National institute of standards and technology
NMI	-	National measurement institute
NMIJ	-	National metrology institute of Japan
NMR	-	Nuclear magnetic resonance
NMWL	-	Nominal molecular weight limit
NT-proBNP	-	N-terminal proBNP
NYHA	-	New York heart association
PAWG	-	Protein analysis working group
PD	-	Plasma desorption
PICAA	-	Peptidic impurity corrected amino acid analysis
POC	-	Point of care
PPT	-	Protein precipitation
PSD	-	Post source decay
PTM	-	Post translational modification
Q	-	Quadrupole mass analyser
QqQ	-	Triple quadrupole

Abbreviations

Q-TOF	-	Quadrupole time-of-flight
RF, $Vcos(\omega t)$	-	Radiofrequency voltages
RP-HPLC	-	Reversed phase liquid chromatography
SA	-	Sinapinic acid
SB	-	Sample blend
SDS	-	Sodium dodecyl sulphate
SIM	-	Selected ion monitoring
SI-units	-	International system of units (Système international d'unités)
SLD	-	Soft laser desorption
SPE	-	Solid phase extraction
SPPS	-	Solid phase peptide synthesis
SRM	-	Selected reaction monitoring
SRM	-	Standard reference material
t	-	Time (s)
TBDMSCl	-	*tert*-Butyldimethylchlorosilane
TCEP-HCl	-	Tris(2-carboxyethyl)phosphine hydrochloride
TFA	-	Trifluoroacetic acid
Th	-	Thomson (*m/z*)
TMCS	-	Trimethylchlorosilane

TOF	-	Time-of-flight
TRIS-HCl	-	Tris(hydroxymethyl)aminomethane hydrochloride
TSQ	-	Triple quadrupole
UF	-	Ultrafiltration
UV	-	Ultraviolet
ω	-	Frequency (1/s,Hz)
WHO	-	The world health organisation
z	-	Charge number

Related publications

Some of the research and data used in this study have been published in a peer-reviewed journal. The abstract of the publication is presented below. The full manuscript is in Appendix C. All data was acquired by me, apart from the preliminary investigation of the dilution (Sabine Biesenbruch, Chapter 3.2.8) and the quantification of the BNP standard by the signature peptides (Kate Groves, Chapter 3.2.2). Data analysis was initiated by me and further discussed with the other authors. The digital version of the paper was written by me and edited by the other authors.

Clinical Chemistry and Laboratory Medicine 2017; 55(9): 1397–1406

"A candidate liquid chromatography mass spectrometry reference method for the quantification of the cardiac marker 1-32 B-type natriuretic peptide"

Attila F. Torma, Kate Groves, Sabine Biesenbruch, Chris Mussell, Alan Reid, Steve Ellison,

Rainer Cramer and Milena Quaglia

Abstract

Background: B-type natriuretic peptide (BNP) is a 32 amino acid cardiac hormone routinely measured by immunoassays to diagnose heart failure. While it is reported that immunoassay results can vary up to 45 %, no attempt of standardization and/or harmonization through the development of certified reference materials (CRMs) or reference measurement procedures (RMPs) has yet been carried out.

Methods: B-type natriuretic peptide primary calibrator was quantified traceably to the International System of Units (SI) by both amino acid analysis and through its signature peptides after tryptic digestion. A method for the stabilization of BNP in plasma followed by protein precipitation, solid phase extraction (SPE) and liquid chromatography (LC) mass spectrometry (MS) was then developed and validated for the quantification of BNP at clinically relevant concentrations (15-150 fmol/g).

Results: The candidate reference method was applied to the quantification of BNP in a number of samples from the UK NEQAS Cardiac Markers Scheme to demonstrate its applicability to generate reference values and to preliminarily evaluate the commutability of a potential CRM. The results from the reference method were consistently lower than the immunoassay results and discrepancy between the immunoassays was observed confirming previous data.

Conclusions: The application of the liquid chromatography-mass spectrometry (LC-MS) method to the UK NEQAS samples and the correlation of the results with the immunoassay results shows the potential of the method to support external quality assessment schemes, to improve understanding of the bias of the assays and to establish RMPs for BNP measurements. Furthermore, the method has the potential to be multiplexed for monitoring circulating truncated forms of BNP.

Chapter 1 Introduction

A large number of biomarkers, such as albumin, peptide hormones, C-reactive protein, troponin, myoglobin and alpha-1-antitrypsin,have been identified over the past years and are routinely used in clinical diagnostics to guide medical treatment. [1] While biomarker discovery is generally performed by liquid chromatography (LC) coupled to mass spectrometry (MS) [2], routine measurement of proteins is currently carried out by immunoassays. [3] Immunoassay measurements are based on specific reactions between an antibody and the analyte of interest: the antigen. The specific part of the molecule the antibody recognizes is called the epitope. Immunoassay platforms are easy to use, provide quick results and are highly sensitive. Detection of the proteins of interest, however, may be hindered by structural changes introduced by pre-analytical effects. Cross-reactivity of different isoforms and breakdown products of proteins or peptides are also not uncommon. The lack of certified reference materials renders the reliable calibration of the assays problematic. [4], [5] This ultimately causes immunoassay results to be highly variable. [6]–[8]

In order to support comparability, The World Health Organization (WHO) introduced International Standards (IS) for the harmonization of clinical measurements. [9] International Standards are value-assigned by collaborative studies and defined by International Units (IU). International Units are arbitrarily assigned describing biological activity per a given amount of the standard. IU is traceable to a defined portion of the product and not to a chemical entity. This makes comparability between different preparations difficult. The International Standards are produced periodically and value assigned by comparison of biological activity observed in the previous preparation. [10]

While IU will be comparable to the previous preparation, it may exhibit different molecular or matrix characteristics compared to the preceding reference material and the differences may affect immunoassay measurements. Discrepancies between biological activities of different preparations were highlighted by certification studies and the metrological community called for a critical evaluation of existing protocols. [11] Thus, the concept of traceability based on metrological principles for clinically relevant proteins and peptides emerged.

Following the EU legislation of medical devices for in vitro diagnostics (IVD) in 1998 [12], the Joint Committee of Traceability in Laboratory Medicine (JCTLM) was formed in 2002 to govern the global standardization of measurements in clinical laboratories. [13], [14] JCTLM was founded by the International Committee for Weights and Measures (Comité International des Poids et Mesures, CIPM), the International Federation of Clinical Chemistry and Laboratory Medicine (IFCC) and the International Laboratory Accreditation Cooperation (ILAC). [15] The organisation combines metrological and medical expertise and mediates between commercial suppliers and governmental bodies. It provides guidelines for standardization that will benefit patient care by helping in the earlier detection of diseases, promoting better understanding of pathological states and assisting in the monitoring of response to therapy.

According to JCTLM the ultimate realisation of a given quantity that can be used for standardization is a reference material where the quantity of the measurand is assigned by a reference measurement. [16]

Chapter 1.1 Metrological traceability

Modern metrology is based on the establishment of the International System of Units (Système International d'Unités) called “SI units” in 1960. The main driving force of this worldwide standardization initiative is to eliminate differences of measurement results of the same sample depending on the utilized measurement method, the geographical location or the time of the measurement. [17]

Comparability is achieved through the establishment of reference measurement systems that enable traceability to certified reference materials directly related to one of the seven SI units (kilogram, meter, second, mole, Ampere, Kelvin, candela) through an unbroken chain of comparisons all with stated uncertainties (i.e. accounting for all sources of measurement variability). [18]

An important prerequisite for the development of SI-traceable reference measurement systems is a value assignment of the primary standard using a primary reference method. For the development of such an analytical method the explicit definition of the measurand is required. Due to the complexity of proteins and biological matrices the definition of the measurand is often still unclear. The International Organization for Standardization (ISO) published a document controlling the measurement of biological quantities in 2003. According to ISO17511, calibrators and control materials used for IVD devices must achieve traceability to the *highest order* reference material available. In 2011the International Consortium for Harmonization of Clinical Laboratory Results was established to complement the work of IFCC for analytes where SI-traceable quantification is problematic, efforts were unsuccessful or the definition of the analyte (due to heterogeneity of circulating forms) and production of reference materials are not

yet feasible. If a measurement result is traceable to international standards or a reference measurement procedure exists, the measurement system is harmonized. If the measurement result is traceable to the SI the measurement system is standardized (see Figure 1:1). [9] Traceability to the SI is maintained by using primary standards to assign concentration values to matrix matched secondary and product calibrators. To avoid measurement bias the commutability between the primary standard and the matrix matched secondary and product calibrator must be demonstrated. The reference material is commutable if it mimics the behaviour of real patient samples. Commutability must be evaluated as part of the validation of a reference material before it can be utilized as a common calibrator for routine measurement procedures. [19]

To improve the metrological quality of the measurement systems primary methods must be developed for the measurement of proteins and peptides, factors affecting protein structure have to be evaluated and controlled and the biological implications of such changes fully understood. In order to achieve this progress in medical and analytical disciplines, advances in instrumental technology and cooperation between clinical and metrological experts on a global level is required. [9], [10], [20]

The ISO standard 17511:2003 (In vitro diagnostic medical devices - Measurement of quantities in biological samples - Metrological traceability of values assigned to calibrators and control materials) is currently under revision to refine traceability requirements of the results for patient samples. [19] The JCTLM database lists all currently available higher order reference materials, reference methods and accredited laboratories that are capable of value assignment of product calibrators. [21]

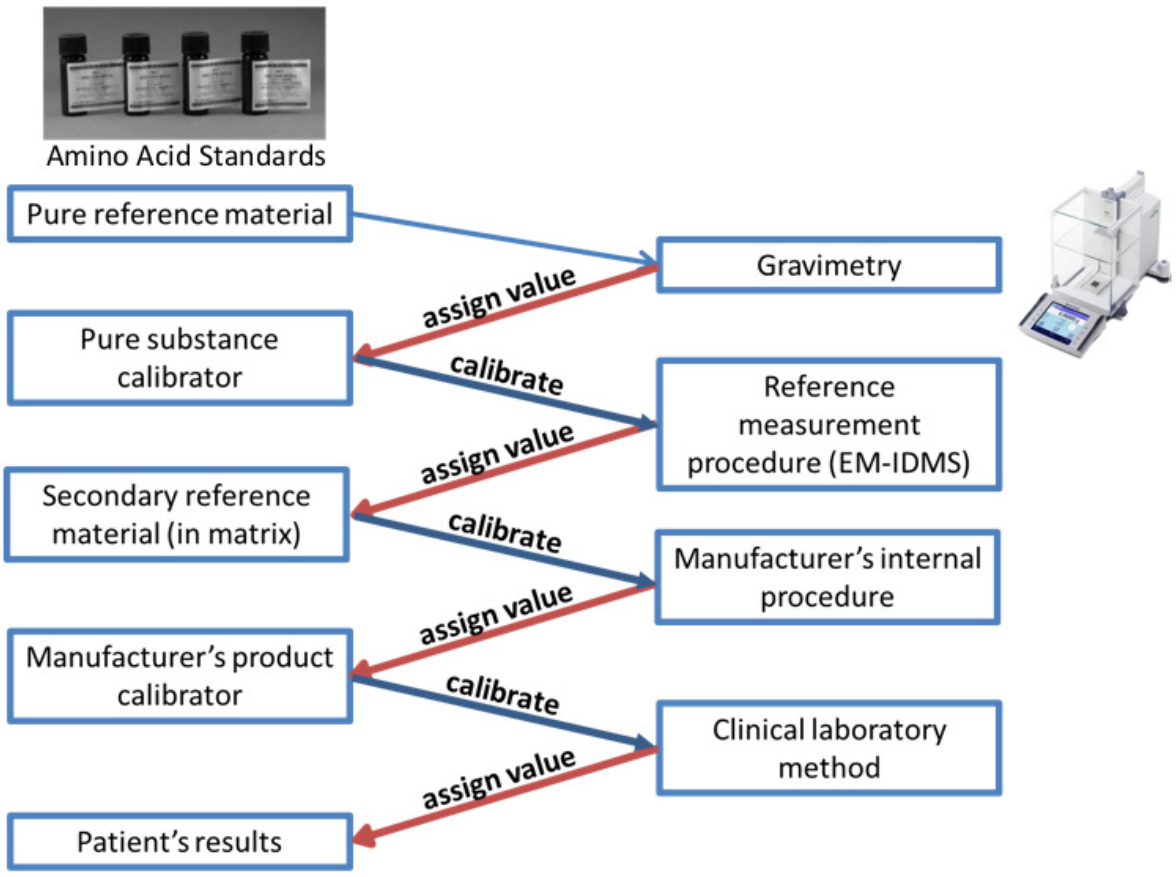

Figure 1:1. Requirement for practical realisation of SI-traceability in clinical testing applications. EM-IDMS: Exact Matching Isotope Dilution Mass Spectrometry (primary method).

In this thesis, the SI-traceable quantification of the pure substance calibrator will be discussed. The challenges associated with quantification of large intact peptides in plasma by MS will also be addressed. Finally, the direct comparison of immunoassay and MS results by participation in a National External Quality Assessment Scheme (NEQAS) will be presented.

For the development of an MS-based reference method, the most important prerequisite is the ability to measure the analyte by MS at amounts that are practically useful.

Chapter 1.2 Mass spectrometry-based peptide and protein measurements

Primary methods based on mass spectrometry, that can define the measured quantity and assign measurand concentrations unequivocally to calibrants used for immunoassays, are essential for successful standardization of clinical measurements.

The development of mass spectrometry was founded by the study of positive rays (canal rays) by J.J. Thomson. Thomson was able to determine the mass to charge ratio (*m/z*, Th) of different atoms and molecules present from a mixture in the discharge tube at relatively low concentrations. In his method he evaluated the parabolas, recorded by the emitted rays channelled through electric and magnetic fields, on a photographic plate. [22] His colleague and mentee Francis Aston received the Nobel Prize in Chemistry for the discovery of isotopes using a mass spectrograph in 1922. The first mass spectrometer was developed by Arthur Jeffrey Dempster in 1918. [23]

Mass spectrometers are capable of the measurement of the mass to charge ratio (*m/z*) of gas-phase ionised molecules. The ionised species, generated in an ion source, are manipulated by electric and/or magnetic fields enabling the separation of them according to their mass to charge ratio in the mass analyser. The relative abundance of the ions is recorded by a suitable detector to create a mass spectrum. Mass analysers and detectors are operated in high vacuum to increase the mean free path of the reactive ions and prevent them from losing their charge through collision.

Development in the technology of ion sources and mass analysers enabled physicists to improve the resolution and the sensitivity of mass measurements. The discovery of isotopes and the ability of mass spectrometers to separate them by their mass to charge ratio was used to enrich ^{235}Uby Alfred Nier. [24]

In chemistry, mass spectrometers were initially used for the quantitative analysis of hydrocarbons in the oil industry. [25] The establishment of fragmentation patterns and mechanisms by Fred McLafferty, Klaus Biemann and Carl Djerassi enabled chemists to link the mass spectrum to unknown structure and revolutionised analytical chemistry. [26] The technique was routinely used for thermally stable and volatile organic molecules ionised by electron ionisation (EI). [27] Thermo-labile biomolecules were first ionised by chemical ionisation (CI) [28], plasma desorption (PD) [29] or fast atom bombardment (FAB). [30] The transformation of large molecules (>2000 Da) into multiply charged gas phase ions without fragmentation however remained elusive.

New ionisation techniques discovered in the late 1980s (Electrospray Ionisation (ESI), matrix-assisted laser desorption/ionisation (MALDI) [31], [32] made macromolecules amenable to MS analysis. The introduction of nanolitre flow regimes in LC (1999) enabled MS platforms to achieve quantification of proteins and peptides in clinically relevant concentration ranges. [33], [34] The sequence information of peptides can be harvested by tandem mass spectrometry (MS/MS), making this method an invaluable tool in biological research. [35]

Introduction of higher amounts of naturally less abundant isotopes into proteins or peptides creates internal standards that are distinguishable by MS with identical behaviour as the target analyte. The use of isotopically labelled internal standards makes both relative and absolute quantification by MS and MS/MS possible.

Chapter 1.3 Ionisation techniques

Chapter 1.3.1 Electrospray ionisation (ESI)

The problem of producing gas phase ions of non-volatile molecules without degradation was ultimately solved by the phenomenon of droplet charging by electrospray. [36]

Fundamental theories on the properties of charged droplets were established by Lord Rayleigh in 1882. [37] Dole studied the behaviour of macromolecules in electrospray in 1968 in an attempt to generate ions from solution. [38] He used a nozzle skimmer system to produce a negatively charged ion beam of dilute polystyrene electrosprayed into an evacuation chamber. The nozzle skimmer system operates at atmospheric pressure. The oxygen content of the surrounding air adsorbs electrons and inhibits the formation of an electric discharge making this form of ionisation 10,000 times more effective than sources operating under reduced pressure. The speed of the molecules in the supersonic jet is proportional to their molecular weight. Macromolecules with uniform velocity are concentrated in the produced ion beam. Dole's experiments gave evidence for the existence of multiply charged macromolecules with the charge state being proportional to the surface area of the molecule.

Yamashita and Fenn investigated the introduction of liquid chromatography (LC) effluents to mass spectrometers using electrospray and reported the results at the American Society for Mass Spectrometry (ASMS) conference in 1984. [39]

In electrospray, a volatile liquid containing ions and the analyte of interest is flowing through a capillary at high voltage potential. Due to the small diameter of the capillary, the strength of the electric field at the tip of the capillary is extremely high and the

surface of the emerging liquid becomes charged. When the electric field is high enough to overcome the surface tension, the charged liquid forms a Taylor cone. [40]

Above the *onset voltage* small droplets are emitted from the tip of the cone. The charged droplets are driven by the electric field towards the inlet of the mass spectrometer (Figure 1:3). The droplets are commonly nebulized by an inert drying gas (usually N_2). The drying gas is heated to high temperatures to compensate for evaporative cooling. Evaporation of the solvent decreases the diameter of the droplets and increases their surface charge density. The efficient transfer of ions into gas phase requires small, highly charged droplets. Evolution of small droplets can occur by two mechanisms. Spherical droplets blast into microscopic charged droplets when the forces of surface tension equal the forces generated by Coulomb repulsion (Rayleigh limit). Larger droplets can be deformed and form a new Taylor cone ejecting highly charged droplets before the Rayleigh limit is reached. The process is repeated until the solvent completely evaporates and a stable flow of charged gas phase molecular ions enters the mass spectrometer.

The exact mechanism for the formation of gas phase ions from the charged droplet is not fully understood. Three models exist in the scientific literature. (Figure 1:2) The ion evaporation model (IEM) states that ion clusters (solvated ions) can be expelled from the charged droplet as long as the Coulombic repulsion between the escaping ion and electric field of the surface of the deformed parent droplet is greater than the attraction between the ion and the polarized solvent medium. [31], [41]

According to the charged residue model (CRM) the size of the droplet decreases through Coulombic fission or Taylor cone mechanism and solvent evaporation until it contains a

single macromolecule. As solvent evaporation occurs the macromolecule ion remains in the gas phase. This explains the unlimited mass scale of electrospray ionisation.

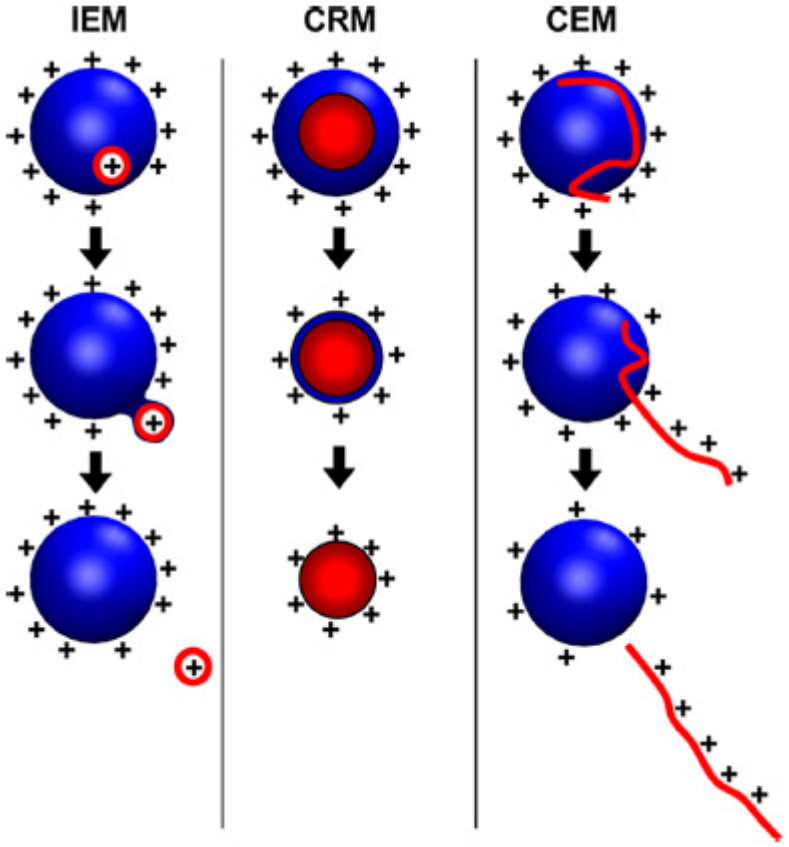

Figure 1:2. Schematic illustration of the three models describing the mechanisms of ion transfer from a charged droplet into the gas phase during ESI. IEM: ion evaporation model, CRM: charged residue model CEM: chain ejection model. Adopted from [42].

The consensus is that small molecule ions are formed following the ion evaporation model and the formation of macromolecule ions are explained by the charged residue model. It is also hypothesised that peptides and proteins can protrude into the gas phase and the repulsion between the charge carried on the end of the molecule and between the surface of the droplet promotes the escape of a single protein ion. (Chain ejection model (CEM)) [42], [43] Hydrophobic analytes accumulate on the surface of the droplet so their ionisation efficiency is higher. They can even suppress signal of hydrophilic components.

Nitrogen gas flowing perpendicular with the orifice and voltage applied to the repeller prevents small molecules and droplets entering the evacuated mass spectrometer.

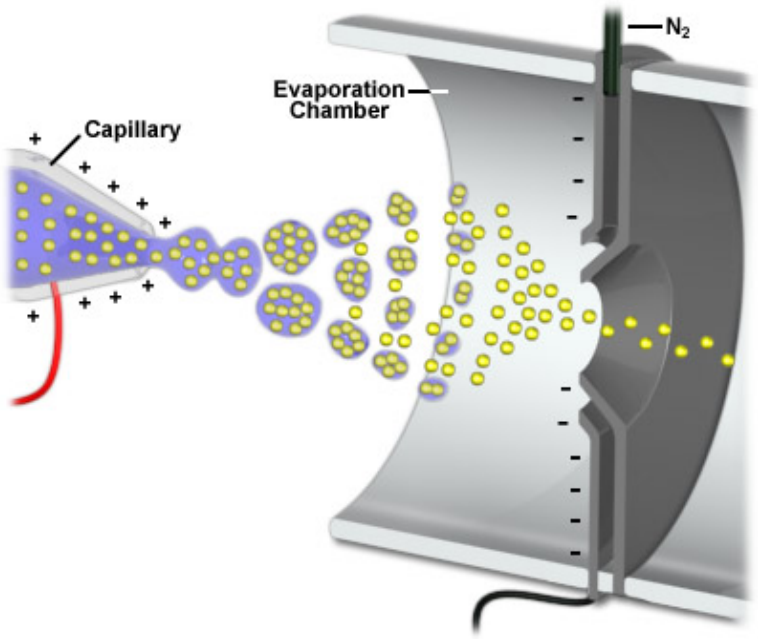

Figure 1:3. Illustration of the electrospray ionisation process. Picture from: http://www.magnet.fsu.edu.

Ionisation of a range of different types of analyte by electrospray with high efficiency is possible. The ions are in ground state, the ion beam produced is stable and, due to the multiply charged nature of ions, within the *m/z* range of conventional mass analysers.

Chapter 1.3.2 Superchargers

The charge state distribution and the intensity of the most intense charge state of peptides and proteins generated by ESI can be influenced by superchargers. [44]–[49] Superchargers are compounds that can be added to the mobile phase or directly into the ESI source to change the composition of the electrosprayed droplets. [47], [49] The exact mechanism for supercharging is unclear and a number of research groups have studied the phenomenon in search for a comprehensive theory that fits the experimental data.

Introduction

The charge state observed for large solute species depends on the density of available charge at the time of desorption of the ion into the gas phase and the ability of the macromolecule to accommodate them. [51] This in turn will depend on the conformation of the protein and the solvent composition of the charged droplet. The composition of the heated droplets changes before the gas phase ions are formed. The droplet temperature increases as the lower boiling point constituent evaporates which can promote the denaturation of proteins encapsulated in the electrosprayed droplet. [51], [52] The increase in surface area due to protein unfolding increases the maximum charge state as it exposes basic sites in the protein making them accessible to protonation. The effective temperature of the ESI droplet can be controlled by using a high boiling point additive, increasing the capillary temperature or by increasing the potential of the ESI source. Sterling *et al*. proposed that a higher potential promotes heating of the charged droplets through higher energy collisions with the heated gas molecules in the source interface. [53] The availability of charge in contrast depends on the proton transfer reactivity of the used superchargers. Supercharging ability has been shown to correlate with the dipole moment and gas phase basicity of the applied supercharging agent. [44] The effect of dimethyl sulfoxide (DMSO) was observed to depend on the amount added to the electrosprayed solution of lysozyme and myoglobin. [46] In low concentrations (5 %), DMSO promotes folding of the proteins resulting in a decrease in carried charge. If the amount of DMSO increased to 20 %, however, the charge of the protein increased as the proteins unfolded thanks to the higher boiling point solvent being enriched in the developing droplets. Hahne *et al*. reported enhanced ion intensities witnessed with the use of 5 % DMSO added to the mobile phases. [47] The presence of even a small amount of DMSO causes the droplets to be about 5 % smaller and the Rayleigh limit around 10-20 %

larger than without the additive leading to faster evaporation and a threefold improvement in ionisation efficiency. The maximum charge acquired by any protein is also influenced by the proximity of the charge bearing residues. [55] Electrostatic repulsion between the positive charges residing on neighbouring basic residues limit the highest charge state observed for proteins in electrospray. [47] Direct interaction with the analyte was given as an explanation for the increase in the highest charge states with the use of m-nitrobenzyl alcohol (m-NBA) or sulfolane. [45], [47] Adduct formation with superchargers can reduce the electrostatic repulsion by charge delocalisation through dipole reordering and reduce the barrier of proximal charging.

Molecular dynamics simulations conducted on native proteins with the superchargers m-NBA and sulfolane were compared to experimental results and a completely different mechanism for supercharging was proposed by Metwally *et al*. [49] When superchargers are used, solvent segregation occurs in the charged droplet. The protein is contained in an aqueous core that is surrounded by a shell formed by the supercharger. Unfavourable solvation of the charged particles in the supercharger limits charge ejection and increases ion concentration in the aqueous centre of the droplet. As water evaporates, the charge is transferred to the macromolecule ion. *Electrostatically driven* unfolding takes place over a longer timescale when the ionisation is already complete and a highly charged protein is released into the gas phase as the supercharger evaporates.

Chapter 1.3.3 Matrix-assisted laser desorption/ionisation (MALDI)

Matrix-assisted laser desorption/ionisation was first studied and reported by Franz Hillenkamp and Michael Karas while investigating the influence of the wavelength of ultraviolet laser irradiation on the desorption of organic molecular ions. They found that

10 times lower energy is required for the ionisation of alanine when mixed with tryptophan and irradiated with laser energy at the threshold irradiance specific to tryptophan(λ = 266 nm). [55] They recognized that the laser energy transferred to the condensed phase can be controlled by using a laser energy-absorbing matrix (chromophore) resulting in soft ionisation of thermally labile non-volatile molecules. [32]

In the first experiment when MALDI was successfully applied to biomolecules, reported by Karas and Hillenkamp in 1987 [38], the matrix was an aqueous solution of nicotinic acid and they used a pulsed Nd:YAG Laser (λ = 266 nm; 3 ns). Their correspondence contained a laser desorption spectrum of the 67 kDa bovine albumin. [57]

Based on similar results, Koichi Tanaka shared the Nobel Prize with Fenn in 2002 for the development of Soft Laser Desorption (SLD). [58] Tanaka used a nitrogen laser (λ = 337 nm) and ultra-fine cobalt powder as the laser energy-absorbing chromophore in glycerol and recorded a spectrum of carboxypeptidase-A (34 kDa).

In MALDI the analyte is mixed with an excess of laser energy-absorbing matrix molecules and deposited on a target plate. The matrix/analyte mixture is irradiated with a laser pulse tuned to excite the matrix material. The laser pulse induces rapid heating and desorption (ablation) of the matrix/analyte mixture from the surface producing a plume of ionised matrix and analyte molecules (Figure 1:4).

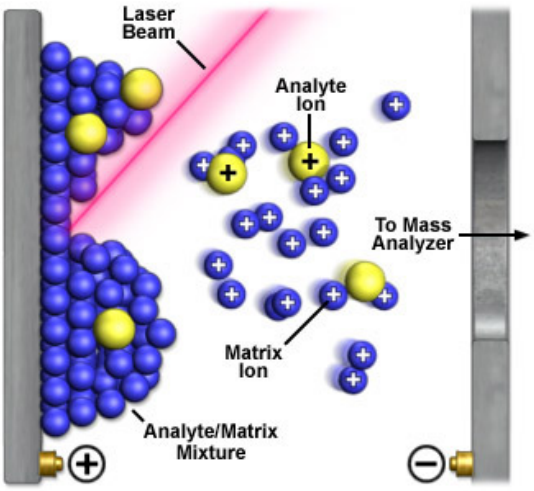

Figure 1:4. Matrix-Assisted Laser Desorption/Ionisation. Figure adopted from http://www.magnet.fsu.edu.

The transfer mechanism of the excess energy from the matrix ions to the analyte is still debated. It has been accepted, that the primary ionisation of the matrix is taking place in the condensed phase and secondary ion transfer is occurring in the expanding plume. [59], [60] The most common matrices currently applied with MALDI for proteins and peptides are 2,5-dihydroxybenzoic acid (DHB), α-cyano-4-hydroxycinnamic acid (CHCA) and sinapinic acid (SA). Ideal matrices display a strong absorbance at the laser irradiation wavelength, sufficient vacuum stability and chemical inertness. Since the ion signal generated by this technique is pulsed, it is best coupled with time-of-flight mass analysers (TOF). Ions observed by conventional MALDI are predominantly singly charged. Structural information of the analyte can be acquired by controlled fragmentation, e.g. using post-source decay (PSD). [61] This typically requires the separation of the fragments from the parent molecules using an ion reflector. [62]

Recent developments also concentrate on the use of liquid support matrices (LSM) and ionic liquid matrices (ILM). The self-healing attributes of the liquid matrix facilitates the generation of persistent ion yields from the same desorption (ablation) spot. Longevity of

the ion signal has been demonstrated in using matrices with viscous liquids such as glycerol. [62]

Chapter 1.4 Mass analysers

The ions formed in the ion source enter the evacuated mass analysers where they are separated by their mass to charge ratio (*m/z*). Depending on the principle of ion separation, mass analysers are divided into two different classes. Scanning devices employ dynamic electric and magnetic fields to manipulate ions and only transmit ions of a certain mass-over-charge (*m/z*) value at any given time (i.e. quadrupole). Non-scanning mass analysers record an entire mass spectrum from a single pulse of ions (i.e. TOF, orbitrap).

Table 1:1. Comparison of different type of mass spectrometers used in this study.

Instrument	Mass range (*m/z*)	Resolution	Dynamic range OME	Sensitivity RMS Agilent only	Scan/acquisition rate
AB Sciex 4000 QTRAP	5-2,800	> 3,000 at *m/z* 609	6	N/A	2,400 Da/s
Agilent 6490 QqQ	5-1,400	> 1,500 at *m/z* 609	6	> 60,000:1[a]	12,500 Da/s
Agilent 6530 Q-TOF	Q: 5-4,000 TOF: 100-20,000	> 10,000 at *m/z* 118 > 20,000 at *m/z* 1,522	5	> 500:1[a]	50 spectra/s
Waters Xevo G2 Q-TOF	Q: 20-4,000 TOF: 20-100,000	> 22,500 at *m/z* 956	4	N/A	40 spectra/s

OME: orders of magnitude estimate, SNR: signal to noise ratio, RMS: root mean square (of baseline, noise estimate), Q: quadrupole, TOF: time-of-flight, a) MS/MS, 1 pg injection of reserpine on the transition *m/z* 609 to 195.

Chapter 1.4.1 Quadrupole

The development of dynamic mass analysers is based on the strong ion-focusing principle of quadrupole electric fields. Quadrupole mass analysers (Q) separate ions using their stable and unstable ion trajectories through an electric quadrupole field. Wolfgang Paul was awarded the Nobel Prize in Physics for the discovery of the first quadrupole mass filter. [64] Quadrupoles consist of four hyperbolic rods set in parallel to each other. Opposing pairs of rods are connected and an oscillating electric field is generated by a combination of direct current potential (dc, U) superimposed on radiofrequency voltages (RF, $V\cos(\omega t)$, were ω is frequency and t is time). Two rods have a voltage of $+U + V\cos(\omega t)$ and the other two $-U - V\cos(\omega t)$. The focused ion beam enters the mass analyser and travels along the axis of the poles. Their *m/z* ratio determines their travel trajectory (Figure 1:5). Depending on the applied voltage the ions either reach the detector or get neutralized by colliding with the quadrupole rods; allowing the user to record an entire range of *m/z* values or to filter a particular ion from a mixture of ions.

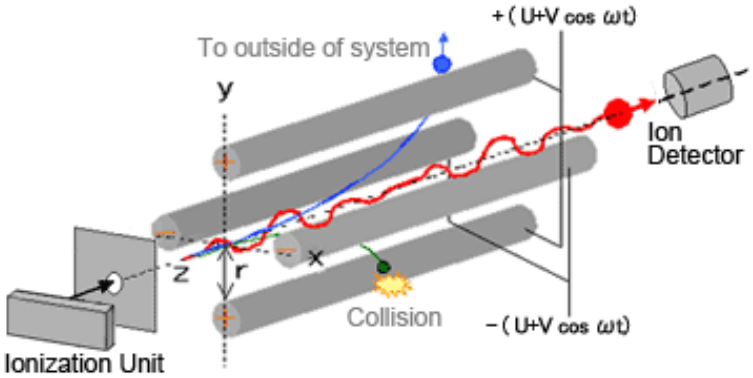

Figure 1:5. Schematic illustration of a quadrupole mass analyser. Adopted from www.shimadzu.com [64].

The differential equations describing the trajectories of the ions are highly complex but can be simplified mathematically and modelled to display the stable solutions where ions do not collide with the rods in the analyser with the help of Matthieu's differential equation.

In Figure 1:6 the shaded area represents the stable solutions of the equation. The *mass scan line* is a number line that contains the masses of all the particles entering the analyser. The slope of the mass line is $\frac{2U}{V}$. By changing the slope of the mass line (i.e. increasing *U* and *V* while keeping the ratio constant), only a small portion will lie within the stable areas of the diagram. The sharp tip of the a-q diagram can be used to create a narrow pass mass filter.

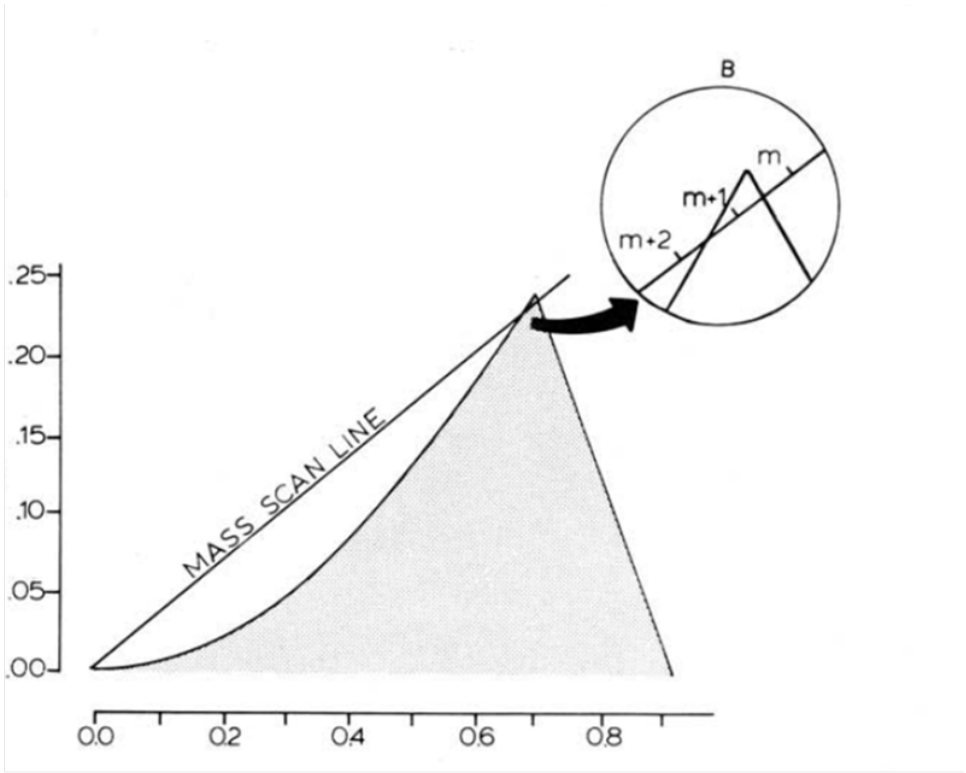

$$a = \frac{4zU}{mr^2\omega^2}$$

$$q = \frac{2zV}{mr^2\omega^2}$$

Figure 1:6. The a-q stability diagram. Shaded area represents the values for which the solutions of the Matthieu's differential equation are stable. B) Resolution of a narrow pass mass filter. Figure adopted from [66].

As *a* and *q* are inversely proportional to mass, the lighter particles are on the right, and higher masses are on the left side of the mass line. The complete mass spectrum with unit mass resolution can be recorded by simultaneously sweeping the direct and radiofrequency voltages applied to the rods. Similarly, reducing the slope will allow a larger portion of the mass scan line to pass through the stable area of the a-q stability diagram reducing the resolution of the mass filter. If the quadrupole is operated in RF only (i.e. *U*=0, slope is 0) it transmits and focuses all ions that are stable in the a-q stability diagram. [65] The main advantages of quadrupoles are: simple mechanical design, small size and electronic control.

The ability of quadrupoles to allow only ions in a small *m/z* window to traverse is used in MS/MS. In triple quadrupole instruments (QqQ) any mass can be filtered by the first quadrupole. The second quadrupole is used in RF only mode. It focuses the scattered ions and if filled with an inert gas (nitrogen, helium or argon) introduces fragmentation by low-energy (3-50 eV) collision-induced dissociation (CID). [44] If the selected precursor is subjected to CID the entire spectrum of its fragments can be recorded by scanning the third quadrupole. If the third quadrupole is set to monitor a particular fragment only, the experiment is called selected reaction monitoring (SRM). The high efficiency of the individual components, the focusing effect of the quadrupoles and the elimination of chemical noise enable these instruments to detect and quantify compounds in complex matrices with superior selectivity and sensitivity. [35]

Chapter 1.4.2 Orbitrap

For quadrupoles, scanning the entire *m/z* range is necessary to record a complete mass spectrum. Non-scanning analysers such as the orbitrap and time-of-flight analysers record the entire mass spectrum of ion packets by measuring their oscillation frequency and flight time, respectively.

The operation of the orbitrap is based on the principle of electrostatic trapping first described in 1923 by Kindon. [27] The orbitrap consists of a central spindle-like electrode (max diameter 12 mm) surrounded by a barrel-like outer electrode (inner diameter 30 mm). The ions are trapped by a rapid increase of the electric field by setting the central electrode to -3.5 kV (for positive ions), while the outer electrode is at ground potential. The ions enter the analyser 7.5 mm from the centre pane of the orbitrap at high kinetic energy and start oscillating around the central spindle (Figure 1:7).

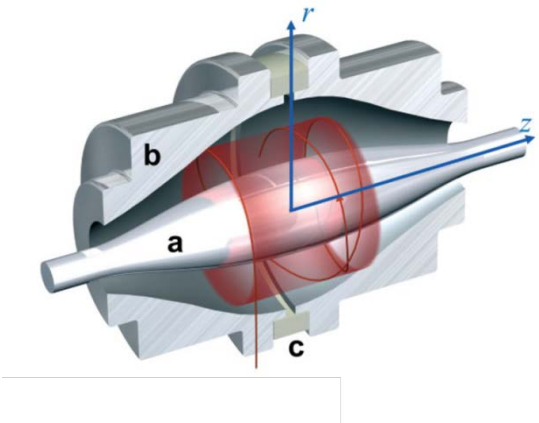

Figure 1:7. Schematic illustration of an orbitrap mass analyser. Adopted from [68].

Due to the unique design of the trap no additional excitation is required. The transient of the small AC current generated by the ion oscillations is recorded and Fourier-transformed to provide the mass spectrum according to Equation 1:1.

$$\omega_z = \sqrt{\frac{k}{m/z}}$$

Equation 1:1. Angular frequency (ω_z) dependence on mass-to-charge (m/z) ratio in an orbitrap analyser. k: axial restoring force.

Resolving power of the orbitrap is proportional to the time of oscillations. [68] If the transient is recorded longer the accuracy of the ion oscillation frequency measurement improves and results in higher resolution mass spectra. [68]

Makarov patented the device in 1996 and published his results in 2000. [69] ThermoFisher developed the first commercial orbitrap instrument in 2005. The commercial LTQ-Orbitrap uses a linear trap to transmit the ions and an rf-only curved quadrupole (C-trap) to store and to rapidly inject them into the orbitrap analyser. [71] The C-trap is filled with N_2 bath gas for collisional damping. The temperature of the analyser and its power supplies must be kept constant to maintain calibration stability and reduce thermal noise. High vacuum must be maintained for the measurement of large molecules such as proteins. A pre-scan using the linear trap (AGC automatic gain control) determines the optimal fill time to avoid space charging. With the above set up are solution exceeding 100,000 can be reached with the long term mass accuracy being better than 5 ppm. [71]

Chapter 1.4.3 Time-of-flight (TOF) analyser

While quadrupoles are designed to monitor a constant beam of ions, TOF analysers are best used with pulsed ion packages. The concept of relating the flight time of accelerated ions to their mass to charge ratio (*m/z*) was first reported in 1946 by W. E. Stephens. [71]

The first commercial instrument was built according to the design published by Wiley and McLaren in 1955. [73] With the TOF analyser a full mass spectrum can be obtained in

microseconds. It theoretically has an unlimited mass range and high sensitivity but early instrument designs suffered from poor mass resolution due to the dispersed energetic state of the ions leaving the ion source. In TOF mass analysers, ion packages generated in the ion source are accelerated into the flight tube of the TOF analyser by an electric field. The potential energy (E_p) of the ions is converted into kinetic energy (E_k). Ions with the same *m/z* ratio acquire the same amount of kinetic energy by the potential (*V)* applied in the accelerating region of the analyser. (Equation 1:2)

The time required to reach the detector for ions with the same *m/z* depends on their position after ionisation (space distribution) and their kinetic energy acquired in the ionisation region of the mass spectrometer (energy distribution). The difference in kinetic energies is addressed by delayed extraction and the use of a reflector. In delayed extraction [72], the ions are allowed to expand into the field free region when a high-energy pulse is applied to accelerate them towards the detector. Ions with higher initial velocity will be affected less by the applied electric field than slower ones reducing kinetic energy differences. Increasing the flight path by building longer flight tubes or decreasing the acceleration voltage also improves resolution but is impractical. [73] Reflectrons, discovered in 1973 by Mamyrin [61], increase the flight time and compensate for kinetic energy differences simultaneously. Reflectrons consist of an electrostatic ion reflector and use a retarding electric field to reverse the direction of ion travel. Faster ions penetrate deeper into the ion mirror than slower ones resulting in uniform flight times for ions with the same *m/z* value but different kinetic energies. [61] TOF mass analysers equipped with a reflectron and delayed extraction produce high-resolution mass spectra.

The amount of time for each ion to reach the detector will depend on their mass (*m*), the charge they are carrying (*q = ze,* where *z* = charge number and *e* = elementary charge)

and the distance (*d*) of the field free region between the source and the detector according to Equation 1:3 and Equation 1:4.

$$E_k = \frac{mv^2}{2} = qV = zeV = E_p$$

Equation 1:2. E_k : kinetic energy, *v*: velocity, *V*: electric potential, *Ep*: potential energy

$$t = \frac{d}{v}$$

Equation 1:3. *t*: flight time, *d*: length of flight tube

$$t^2 = \frac{m}{z}\left(\frac{d^2}{2Ve}\right)$$

Equation 1:4. Flight time (*t*) dependence on mass-to-charge (*m/z)*

As *d* and *V* are constant, the flight time *t* is directly proportional to the mass-to-charge ratio (*m/z*) (Equation 1:5).

$$t \sim \sqrt{\frac{m}{z}}$$

Equation 1:5. Flight time dependence on *m/z*

Small multiply charged molecules will get to the detector first, while larger molecules in lower charges states will take longer to reach the detector. The TOF analyser is ideally suited to pulsed ion sources and frequently coupled to the MALDI ionisation technique.

Quadrupoles followed by a collision cell can be coupled with a TOF analyser (Q-TOF) and used in tandem MS experiments providing the advantages of selectivity and high resolution. An illustration of a Q-TOF mass analyser is displayed in Figure 1:8.

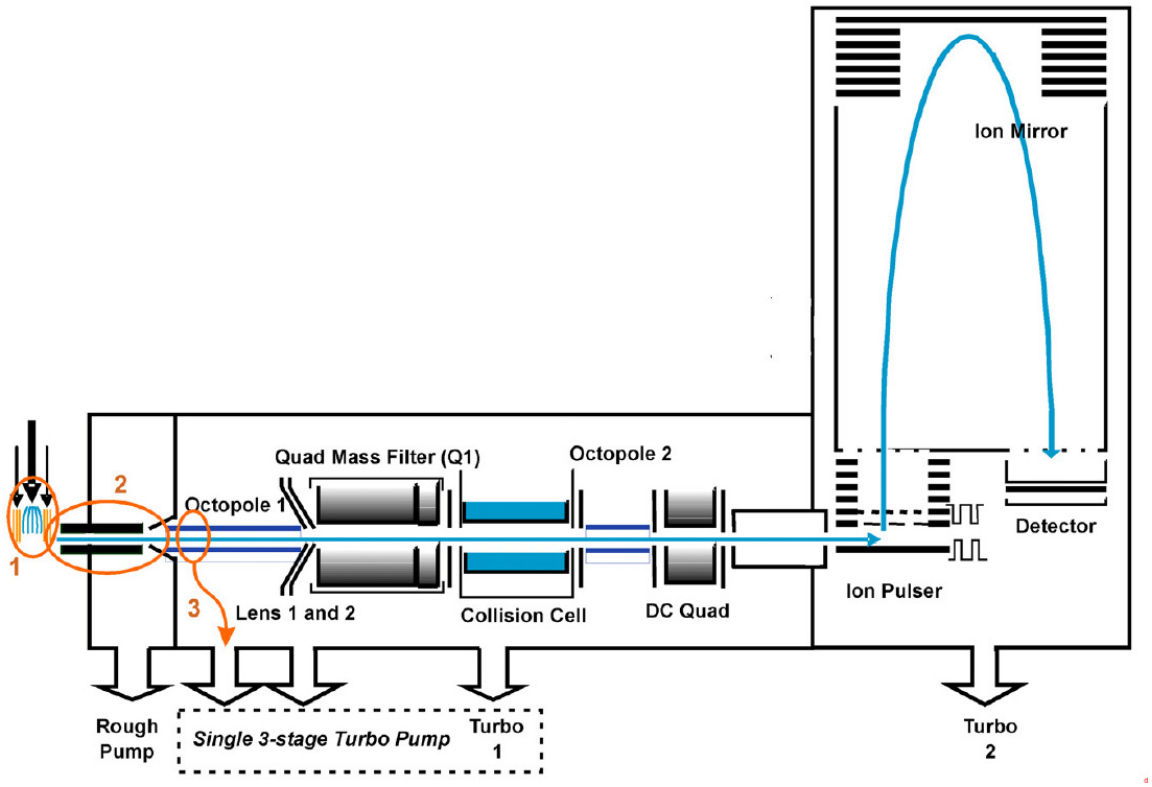

Figure 1:8. Schematic illustration of Agilent 6530 Q-TOF LC/MS. Adopted from www.Agilent.com.

When the Q-TOF instrument is operated to record MS spectra, the quadrupole is in RF mode and the collision cell is not pressurised. In tandem MS, the selected precursor is transmitted by the quadrupole and accelerated into a gas-filled hexapole collision cell where excitation and dissociation occurs. The focused beam of (fragment) ions is then pulsed into the TOF analyser by applying high voltage on the back plate of the pulser. The pulse rate depends on the *m/z* range of interest. [73]

Chapter 1.5 Peptide fragmentation

Peptide molecules fragment along the backbone when exposed to low energy CID during MS/MS analysis in QqQ or Q-TOF instruments. The translational energy of precursor ions selected in the first mass analyser is converted into internal energy by collisions with gas molecules (usually argon, nitrogen or helium) in the collision cell. The activated ions undergo spontaneous decomposition. The maximum energy converted into internal energy depends on the amount of kinetic energy of the ion, the mass of the ion and the mass of the gas molecule. Large ions require more energy to fragment and the higher the mass of the gas molecule in the collision cell the lower the energy that is required to fragment a certain peptide ($CE_{Ar\ (40)}$<$CE_{N_2(28)}$<$CE_{He\ (4)}$). The peptide CID fragmentation pattern is sequence and charge dependent. According to the mobile proton theory fragmentation is charge directed. Fragmentation depends on the number of ionizing protons and the number of arginine residues in the sequence. Basic residues (arginine (R), lysine (K), histidine (H)) attract the first positive charge in order of their gas phase basicity. Singly charged peptides containing arginine require high energy to mobilise the sequestered charge. [74] Sequence information for peptides with multiple basic residues is difficult to obtain. Acidic amino acid residues or protonated histidine can provide the additional proton required for fragmentation. Singly charged peptides with arginine selectively cleave at aspartic acid (D) or/and glutamic acid (E). [75] The annotation of the peptide fragments is governed by the position of the cleavage along the backbone and depends on the charge bearing side of the chain. If the charge is on the N-terminal the fragments are called *a, b* and *c*. If the charge is retained on the C-terminal of the chain the fragments are called *x, y* and *z*. [76], [77] Basic amino acids at the N-terminus give rise to *a* fragments. *b* Fragments are dominant for peptides without basic residues or acylated at

the N-terminus. Tryptic peptides contain arginine or lysine at the C-terminal hence predominantly produce *y* ions. [78]–[80] Peptide sequences containing basic side chains or amides (i.e. arginine (R), lysine (K), asparagine (N), glutamine (Q)) produce characteristic fragments missing 17 Da (NH_3). Side chains containing hydroxyl, or carboxyl moieties (i.e. serine (S), threonine (T), aspartic acid (D), glutamic acid (E)) loose water (-18 Da).

Additional sequence information can be gained by fragmentation of the amino acid side chains during high energy CID or utilizing post-source decay (PSD) in MALDI-TOF instruments. [81] Soft fragmentation techniques are available for the MS analysis of post-translational modifications such as phosphorylation and glycosylation by electron capture dissociation (ECD) [82] and electron transfer dissociation (ETD). [83]

The primary sequence of B-type Natriuretic Peptide (BNP) and the most intense fragment of its tryptic peptides observed in a triple quadrupole instrument are displayed in Figure 1:9.

B-type Natriuretic Peptide BNP-32

SPKMVQGSGCFGRKMDRISSSSGLGCKVLRRH

MVQGSGCFGR

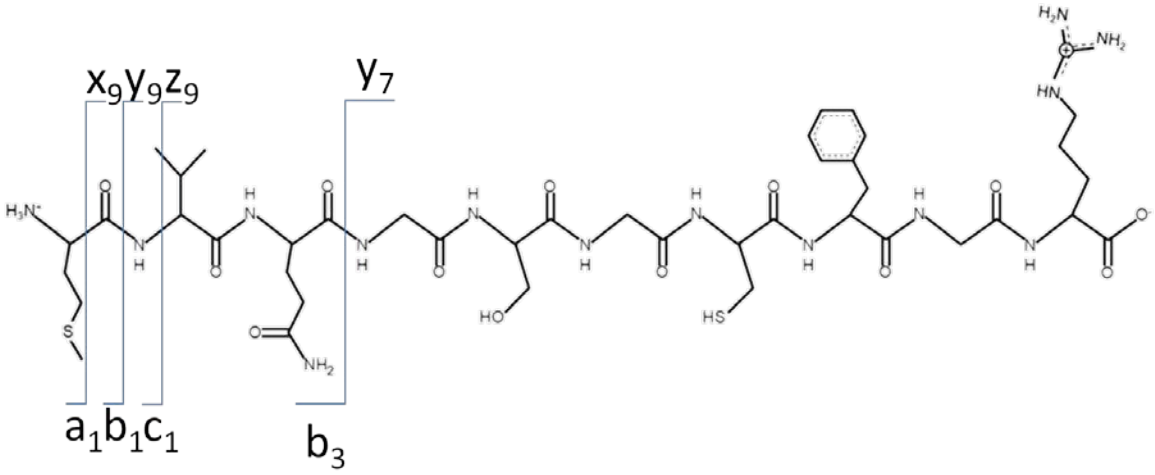

ISSSSGLGCK

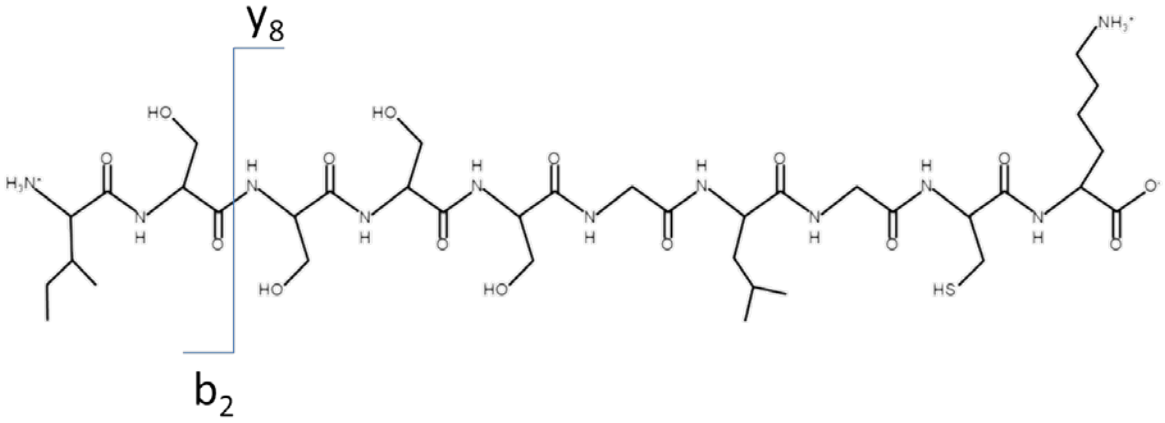

Figure 1:9. Amino acid sequence of BNP, tryptic peptides of BNP and fragments used for quantification. BNP contains a disulphide bridge between the underlined cysteine (C) residues. The number in the subscripts represent the position of the amino acid in the peptide bond where the fragmentation occurs.

Chapter 1.6 Isotope dilution mass spectrometry (IDMS)

Mass spectrometry combined with isotope dilution (IDMS) measurement is a definitive primary method that provides low uncertainty and accurate results for the assignment of SI-traceable concentrations of primary calibrators. [83], [84] The method is based on the MS measurement of the ratio of isotope fractions by mass spectrometry in a gravimetrically prepared blend of analyte spiked with isotopically labelled material. Provided that the concentration of either the labelled or the natural component is known the concentration of the other constituent of the blend can be calculated. [85]

The feasibility of this approach requires the existence of a stable isotopically labelled form of the analyte, its availability in a highly purified form and the ability to measure them accurately using mass spectrometry. [86] In order to acquire such an isotopic substance the measurand must be well defined. Due to production and purification difficulties, and the limited sensitivity of mass spectrometers at high *m/z*, direct IDMS on macromolecules is not yet possible.

Currently the primary standards with the highest metrological quality available with SI-traceable values assigned are amino acids. The National Institute of Standards and Technology (NIST) in the USA supplies a mixture of amino acids prepared gravimetrically and quantified by IDMS. [88] Their Japanese counterpart, The National Metrology Institute of Japan (NMIJ) provides pure amino acid standards quantified by titrimetry and more recently by quantitative NMR. [88]–[90]

The concentration of peptide standards can be assigned with the use of these primary amino acid standards and isotopically labelled amino acids. If IDMS is used as the

quantification method, the peptide concentration can be directly linked to the kg or the amount of substance, the mole. [92], [93]

Absolute Quantification (AQUA) of proteins with the use of labelled peptides has been introduced by Steve Gygi and colleagues at Harvard Medical School in 2001. [93] It uses an internal standard that contains isotopically labelled amino acids incorporated into the sequence of peptides that is typically generated by enzymatic digestion of the parent protein. Quantification is performed by adding a known amount of the isotopically labelled peptide before enzymatic digestion and monitoring the ion signal ratio between the unlabelled and the isotopically labelled peptide.

LGC and other National Measurement Institutes (NMIs) have further developed the method introduced by Gygi *et al.* by applying the principles of exact matching isotope dilution mass spectrometry on peptides. [94]–[97]

Exact matching IDMS involves an iterative procedure culminating in the gravimetric preparation of a calibration blend (CB) having the same ion abundance, ratio and molar amount content of unlabelled and labelled peptides as the sample blend (SB). [83], [84] For protein quantification, the calibration blend contains quantified synthetic signature peptides (i.e. MVQGSGCFGR, ISSSSGLGCK for BNP) and stable isotopically labelled peptides, whereas the sample blend contains the stable isotopically labelled peptides at known amounts and the peptide or protein to be quantified (i.e. BNP). Both calibration blend and sample blend are digested and analysed by LC-MS/MS using selected reaction monitoring (SRM) experiments.

Results are then obtained by applying the double exact matching IDMS equation (Equation 1:6).

$$w_x = w_z \frac{m_y}{m_x} \frac{m_z}{m_{yc}} \frac{R_B^{'}}{R_{BC}^{'}}$$

Equation 1:6. EM-IDMS equation

w_x	amount content of the amino acid, peptide or protein to be quantified (µg/g)
w_z	amount content of the pure standard material in the standard solution (µg/g)
m_z, m_{yc}	mass of the unlabelled standard and the labelled standard used to prepare the calibration blend (g)
m_y, m_x	mass of labelled standard and the sample in the sample blend (g)
R'_B, R'_{BC}	measured ratios of the unlabelled and labelled peptide signals in the sample and in the calibration blend

The measurement system requires the proteins to be enzymatically digested into peptides and the peptide standards to be traceably quantified by amino acid analysis against primary standards by IDMS. Figure 1:10 shows a schematic outline of the method.

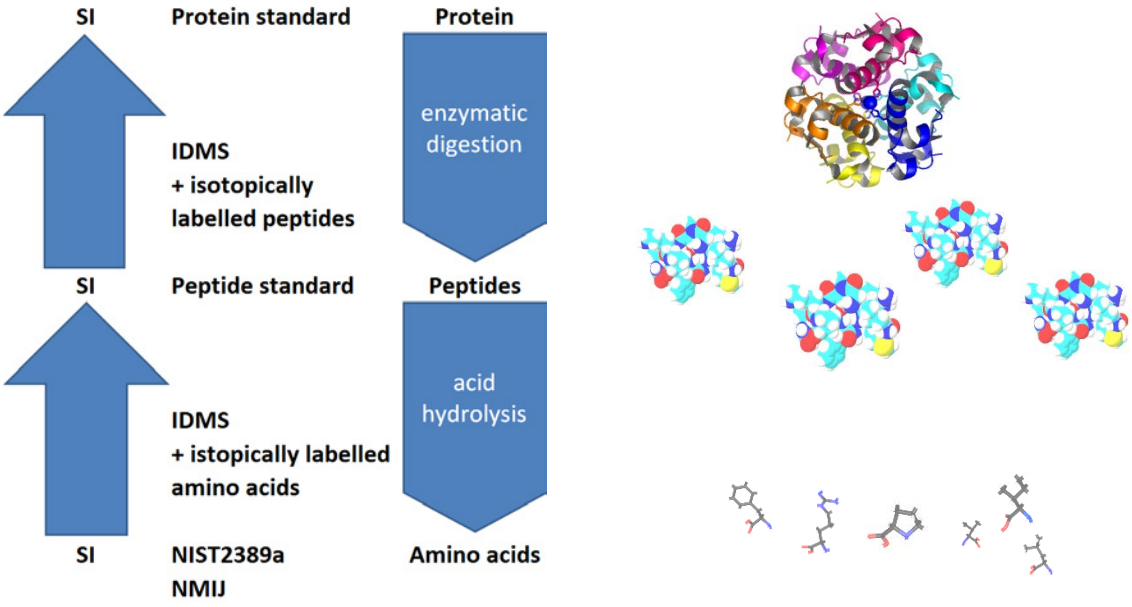

Figure 1:10. Workflow of SI-traceable protein quantification. IDMS: Isotope dilution mass spectrometry, NIST2389a: certified primary standards (mixed amino acid solution) supplied by NIST (National Institute of Standards and Technology, USA), NMIJ individual amino acid standards supplied by NMIJ (National Measurement Institute of Japan).

The chosen enzyme must liberate unique signature peptides from the parent protein in an equimolar manner. The peptides must not go under any post-translational modifications, must be amenable to synthesis in both the unlabelled and the labelled form and must contain at least three amino acids (arbitrary condition) that can be quantified by amino acid analysis (i.e. do not degrade during acid hydrolysis). [94], [98]

With the above approach, the SI-traceable value assignment of primary protein reference materials at the highest metrological quality is possible.

Chapter 1.7 Cardiovascular biomarkers

Cardiovascular events remain the biggest cause of mortality around the world. In the UK they kill over 180,000 people a year according to the Coronary Heart Disease Statistics published by the British Heart Foundation. [99] Heart failure costs the UK healthcare system £8.7 billion and £19 billion to the UK economy as a whole. Early detection of heart disease by monitoring cardiac markers is vital for appropriate treatment and prevention of death. Cardiac markers should be sensitive, specific, proportional to the degree of myocardial injury, stable enough to be detectable in patients after the event and must be validated by clinical studies. [8] From the initial discovery of biomarkers there is a long journey until they become validated and approved so they can be utilized in everyday clinical testing. While the currently proposed cardiac biomarkers include less specific enzymes and proteins such as creatine kinase (CK, CK-MB), myoglobin and C-reactive protein, official approval by the Food and Drug Administration (FDA) has only been attained for two: cardiac troponin (troponin T and I) and BNP, listed in Table 1:2.

Table 1:2. FDA-Approved Cardiac Markers

Marker	Disease	Sensitivity[a]	Specificity[b]
Troponin I	Myocardial Infarction	93 %	81 %
B-type Natriuretic Peptide	Congestive Heart Failure	98 %	92 %

a. Biomarker correctly identifies patients suffering from the condition (true positive rate).

b. Biomarker correctly identifies individuals not suffering from a medical condition (true negative rate). [101]

In 2004 NIST released a Human Cardiac Troponin Complex (SRM2921) standard in order to assist in the global standardization of immunoassay measurements. [101] The assignment of SI-traceable concentration to the reference material was hindered by the lack of clear definition of the measurand. Troponin contains three subunits (troponin C, troponin I, and troponin T) with unknown chemical structure. In an attempt to fully characterise the candidate reference material the subunits were separated by reversed phase liquid chromatography (RP-HPLC) and fraction collected for quantification by amino acid analysis. The nature of any post-translational modifications was investigated by combining proteolytic digestion and MALDI-TOF-MS.

Quantification of the standard was performed by a combination of comparing the ultraviolet (UV) signal of purified troponin I that was quantified by amino acid analysis and performing amino analysis on each fraction of the troponin complex after acid hydrolysis.SI-traceability was established by using certified amino acid standards for the calibration of the amino acid method. NIST has used three amino acid residues (alanine, valine and leucine) to assign amount of substance to the reference material.

During the development of the reference material it became evident that very little is known about the exact structure of troponin in patients with myocardial infarction, purification of large proteins extracted from human tissues is problematic and capabilities for the full characterization of the exact chemical structure of such a complex molecule are lacking. The project highlighted the fact that the definition of the measurand that can be explicitly targeted by MS methods is of paramount importance for the successful standardisation of measurements in laboratory medicine. [10]

Introduction

C-peptide is a 31 amino acid peptide where the implementation of a reference measurement system was successful. [103] The measurand is sufficiently well defined and its concentration can be assigned using SI units. [92] Primary reference materials and reference measurement procedures exist and equivalence of the results between different laboratories has been demonstrated. [102] A list of laboratories capable of a provision of reference measurements is available on the JCTLM database. [21] External quality assessment schemes are established and provide a platform for the monitoring of the standardisation efforts. [102]

Chapter 1.8 B-type natriuretic peptide (BNP)

BNP is a cardiac hormone secreted by the myocytes of the left ventricle in response to volume overload in an event of congestive heart failure. [103] The prohormone (proBNP) contains 108 amino acids and is naturally cleaved into the 32 amino acid long, biologically active BNP and the biologically inactive N-terminal (NT-proBNP, 76 amino acids) peptides by the putative enzymes corin and furin. [104] Corin degrades proBNP in the heart muscle, while furin is responsible for the processing of the secreted proBNP in circulation. [106], [107] The amino acid sequence of proBNP is shown in Figure 1:11.

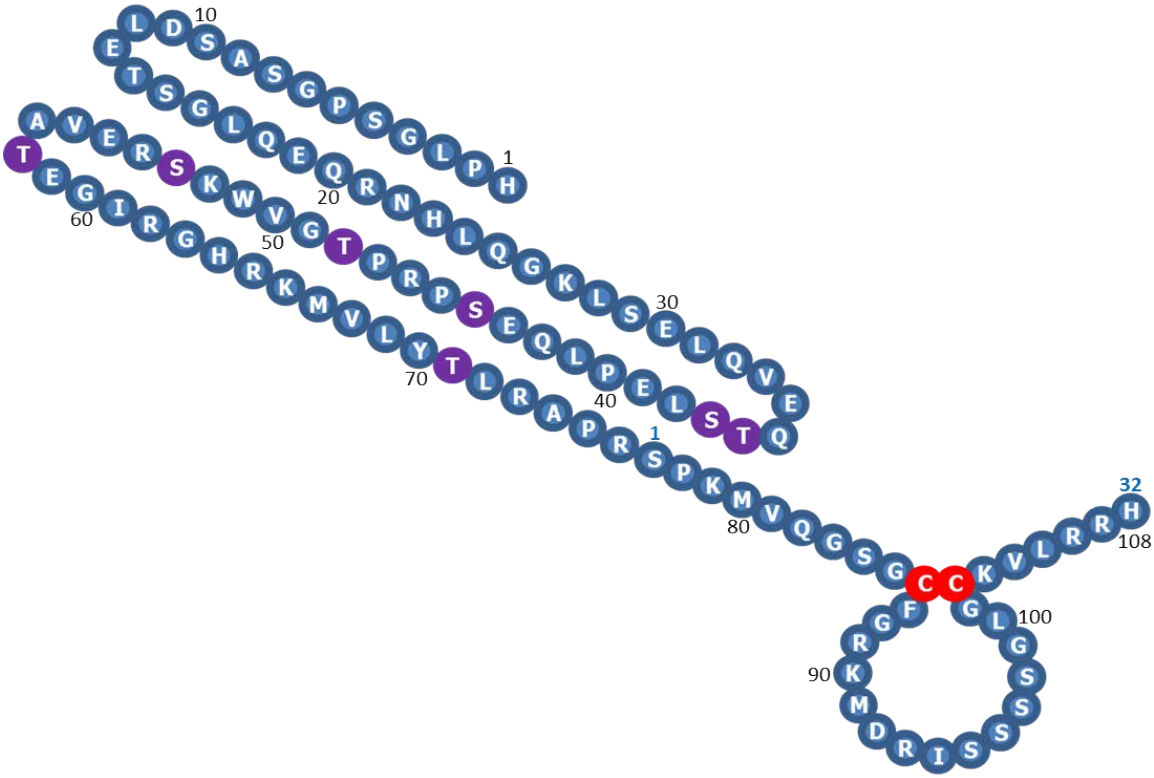

Figure 1:11. Amino acid sequence of proBNP. After proteolytic cleavage, NT-proBNP (1-76) and BNP (77-108 also BNP1-32) forms in circulation. Serine (S_{37}, S_{44}, S_{53}) and threonine (T_{36},T_{48}, T_{58}, T_{71}) residues highlighted in purple are O-glycosylated.

BNP contains a ring structure with 17 amino acid residues, shared by all natriuretic peptides, which plays an important role in the recognition of the peptides in cell signalling. [107] BNP reduces blood pressure and increases sodium excretion as part of the cardiac

endocrine function. The circulating concentration of BNP ranges from 15 pg/mL in healthy individuals to around 1,400 pg/mL in patients who suffered a severe heart attack. NT-proBNP and BNP levels reflect the severity of the heart attack and were found to correlate well with the classification of cases by the New York Heart Association (NYHA; see Table 1:3). [108]

Table 1:3. BNP concentration found by clinical assays in heart failure patient samples. [79]

NYHA Class	Patient Symptoms	BNP (pg/mL)	BNP (fmol/mL)
Class I (Mild)	No limitation of physical activity. Ordinary physical activity does not cause undue fatigue, palpitation or dyspnea (shortness of breath)	83-152	24-44
Class II (Mild)	Slight limitation of physical activity. Comfortable at rest but ordinary physical activity results in fatigue, palpitation or dyspnea	235-322	68-93
Class III (Moderate)	Marked limitation of physical activity. Comfortable at rest but less than ordinary activity causes fatigue, palpitation or dyspnea	459-590	133-170
Class IV (Severe)	Unable to carry out any physical activity without discomfort. Symptoms of cardiac insufficiency at rest. If any physical activity is undertaken discomfort is increased	960-1190	277-344

In 2007 the National Academy of Clinical Biochemistry published a document aimed at the utilization of test results of BNP/NT-proBNP. [110] BNP and its N-terminal co-metabolite NT-proBNP are valid biomarkers that can be used for the confirmation of heart failure in ambiguous patient cases. [110] Their measurement is also warranted when risk stratification is required. NT-proBNP and BNP concentrations are routinely measured by immunoassays for the diagnosis and prognosis of congestive heart failure (CHF). BNP and NT-proBNP levels below 100 pg/mL and 400 pg/mL respectively rule heart failure out while above 500 pg/mL and 1800 pg/mL confirm heart failure with 98 % sensitivity. The study has found that results from commercial assays (Biosite and Abbott)

and research assays (Shiongi) can differ by 15-20 %, making the establishment of decision limits or BNP/NT-proBNP guided therapy not reliable. [111]

In 2013 Franzini *et al.* published the results of heart failure patient and control samples distributed as part of the CardioOrmoCheck external quality assessment scheme. The BNP results showed a marked bias between the four assays (Siemens, Biosite, Abbot and TOSO) used in point of care (POC) testing in Italy, highlighting the need for standardisation of BNP measurements. [112]

Chapter 1.8.1 Glycosylation

proBNP is O-glycosylated at four threonine and three serine residues on the N-terminal of its sequence (Figure 1:11). In 2006 Schellenberger *et al*. investigated the post-translational modifications of proBNP. [113] Recombinant proBNP was purified by monoclonal antibodies developed to be specific to the C-terminal end of proBNP sequence (-CKVLRRH). The treatment of the recombinant proBNP expressed in Chinese hamster ovary (CHO) cells with a cocktail of deglycosylating enzymes resulted in two separate bands in Western blot analysis. The glycosylation sites were identified by digestion of the deglycosylated protein with trypsin and endoproteinase GluC followed by Edman degradation of the proteolytic peptides. Patient samples confirmed that the circulating form of proBNP is an O-linked glycoprotein and the extent of the glycosylation is not uniform. The high density of glycosylation of the T3 tryptic peptide (LS**E**LQV**E**QTSL**E**PLQ**E**SPRPTGVWK) prevented cleavage at glutamic acid residues (E) by GluC. Edman degradation of proBNP found a truncated sequence missing the first two N-terminal amino acid residues (-HP) (cf. Figure 1:11).In 2008 Hammerer-Lecher *et al*. used affinity chromatography coupling sheep monoclonal antibodies (mAB) recognizing the first 21 amino acid residues on NT-proBNP to silica beads to investigate the circulating

forms of BNP. The captured NT-proBNP was put through a tryptic reactor and the resulting peptides were analysed by LC-ESI MS/MS. The identified tryptic peptides originated from both NT-proBNP and BNP, confirming that the processing of proBNP is not complete and there is intact proBNP present in the blood of patients with heart failure. Deglycosylation of the collected peptide fractions by O-glycosidase and N-acetylneuraminidase corroborated the findings of Schellenberger *et al*. both proBNP and NT-proBNP are glycosylated monomers in vivo. [115]

Chapter 1.8.2 Incomplete processing of proBNP

Glycosylation also affects the processing of proBNP by furin. According to Semanov *et al*. the glycosylation at threonine 71 residue prevents the production of the bioactive BNP molecule.[105]

The first qualitative evidence of the overestimation of biologically active BNP in circulation was produced by Hawkridge *et al.* in 2005. The research group used nano-LC-FT-ICRMS to identify and quantify circulating forms of intact BNP in patients with high concentrations of BNP (c_{BNP}> 290 fmol/mL, i.e. 1000 pg/mL) determined by point of care tests (POCT). [116] To accomplish the required sensitivity an enrichment method was developed using antibodies specific to BNP. Quantification was based on the addition of synthetic BNP containing $U^{13}C$, $U^{15}N$ labelled glycines. The claimed detection limit of 15 fmol (52 pg) on column was achieved. However, there was no endogenous BNP detected even in patient samples that showed very high concentrations by clinical assays. The conclusion based on the MS results was that the immunoassay readings cannot be attributed to the biologically active intact BNP alone, strongly suggesting the existence of cross-reacting species in circulation introducing error to clinical assay results.

In 2007 Lian *et al*. used monoclonal antibodies reported to be selective for the C-terminal of BNP for immunoprecipitation of BNP in NYHA IV class patient samples. Western blot analysis of the purified glycosylated and deglycosylated patients' plasma samples showed substantial amount of proBNP. [116] Additionally, recombinant proBNP was found to be 6-8 times less potent than BNP in affecting the behaviour of cells involved in alleviating heart attack symptoms. They also demonstrated that two commercially available BNP immunoassays (Triage and Advia Centaur) were unable to distinguish between the prohormone (proBNP) and its mature proteolytic peptide (BNP). The NT-proBNP assay (Elecsys) did not recognize BNP but significantly underestimated proBNP concentration most likely due to the glycosylation of the recombinant proBNP blocking the recognition of the epitope.

An in depth study of cross-reactivity between clinical assays was conducted in 2008 by the IFCC Committee for the Standardisation of Markers of Cardiac Damage. [117] The comparison of five commercial assays for BNP and three for the analysis of NT-proBNP was performed by quantifying two BNP, two NT-proBNP and two proBNP calibration reagents. All assays were calibrated according to the manufacturer's instructions. The peptide standards from five different suppliers showed substantial variation in reactivity depending on the methods of peptide production (synthetic or recombinant), the degree of glycosylation and assay architectures. The study concluded that both BNP and NT-proBNP specific assays cross react with non-glycosylated proBNP. The IFCC urged the clinical field to gain better understanding of what is being measured by immunoassays and since 2014 the analytical characteristics of the major commercial immunoassays are available online. [118] In 2016, a cross-reactivity study was conducted with all BNP-related peptides on five different BNP, nine NT-proBNP and three proBNP platforms. The

conclusion of the immunoassay specificity experiment was that BNP and NT-proBNP or proBNP results are not transferable even between assays with the same antibody configuration due to substantial cross reactivity and lack of standardisation. [120]

Apart from the incomplete processing and the possibility of the glycosylation sites blocking epitope recognition, cross-reactivity may also be caused by degradation products of the biomarkers in human blood.

Chapter 1.8.3 Degradation of NT-proBNP and BNP

Measurement results of BNP by immunoassays are inherently heterogeneous. [111] Lack of exact definition of the measurand due to post-translational modifications (see Chapter 1.8.1) already makes the development of selective antisera for immunoassays unfeasible. [114], [116] Additional challenges are the incomplete processing of the prohormone (see Chapter 1.8.2) and the rapid degradation of both BNP and NT-proBNP in blood and plasma. [103], [120]

In 2006 Brandt and co-workers showed that BNP gets truncated into its des Ser-Pro form *in vivo* by the ubiquitous enzyme dipeptidyl peptidase IV (DPP IV). [120] BNP is also degraded in circulation by neprilysin (neutral endopeptidase, NEP), insulin degrading enzyme (IDE) and meprin. All of these enzymes are located in the heart. [121]

Rapid degradation of BNP in plasma and whole blood was studied in 2008 by Niederkofler *et al*. [123] A Mass Spectrometry ImmunoAssay (MSIA) method was developed to capture BNP by two different types of monoclonal antibodies recognizing both the C-terminal end (-CKVLRRH) and an epitope between amino acid residues 5-13 of intact BNP (-VQGSGCFGR-). The captured peptides were analysed by MALDI. Analysis of intact BNP spiked into plasma showed the complete hydrolysis of the full length peptide (BNP 1-32)

within an hour. Neither the addition of ethylenediamine-tetraacetic acid (EDTA, anticoagulant) nor cooling to 4 °C inhibited the DPP IV enzyme activity significantly. The most effective protease inhibitor combination was found to be (4-(2-aminoethyl) benzenesulfonyl fluoride (AEBSF) mixed with leupeptine or with benzamidine. The breakdown products are truncated forms of the BNP missing a combination of amino acid residues at both C- and N-terminus. External calibration with synthetic peptides allowed quantification of the most abundant species of the disintegrated BNP. To avoid bias due to differences in ionisation efficiencies the signals were normalized against biotinylated BNP internal standard. Comparison of the sum of the quantified breakdown product concentrations with results from clinical assays showed a significant overestimation of BNP concentrations by the latter. Unprocessed proBNP and further breakdown products, not captured by the antibody combination used, may be responsible for the difference between the results. A comparison of clinical assays with the above mentioned MSIA measurements was conducted in 2011 to unveil the circulating fragments of BNP in patient with chronic heart failure. [123] To prevent degradation of BNP a protease inhibitor “cocktail” of 10 mmol/L benzamidine and 5 mmol/L AEBSF was added to the centrifuged samples, split and kept at -70 °C until batch analysis by both MS and clinical antibody assays. A total of seventy patients were enrolled and statistically significant correlations between clinical characteristics and the concentrations between circulating levels of BNP (MS and clinical antibody assays) were evaluated. The study found that BNP 1-32 degrades regardless of the inhibitor added. Biologically inactive forms of BNP (3-32, 4-32 and 5-32) and proBNP were also detected suggesting that insufficient processing of the prohormone and degradation of BNP 1-32 are responsible for both the cross-

reactivity in immunoassays and the lack of clinical compensation in patients with congestive heart failure.

More recently the direct analysis of the peptidoforms was performed by capillary electrophoresis (CE) with ESI-MS detection. [125] Zhang *et al.* spiked synthetic BNP into heparin and EDTA plasma at high concentration (250 µg/g, 72 nmol/g) and analysed the degradation of BNP by multisegment injection (MSI). The same sample was injected every 34 minutes over fourteen hours. After the addition of BNP to plasma it was rapidly degraded by the DPPIV to form BNP 3-32. BNP 3-30 and 3-29 was detected after 40 and 100 minutes respectively with the simultaneous decrease of BNP 3-32 concentration. The level of 3-30 reached a plateau after about 120 minutes and remained high until the end of the time course experiment. (c.f. Figure 5:3) These data confirm that rapid degradation of BNP is taking place in plasma and suggests that degradation products are also substrates of various enzymes and their clearance take considerably longer. BNP related peptidoforms remain in circulation for at least over 14 hours after the complete disappearance of the biologically active cardiac hormone.

Chapter 1.9 Entresto™

In 2015, a new heart failure drug called Entresto™ gained approval by the FDA agency. The new medicine developed by Novartis contains two active ingredients. The first inhibits the angiotensin II receptor (valsartan) and the second blocks neprilysin activity (sacubitril). It was suggested that the measurement of BNP is no longer appropriate for the diagnosis of heart failure for patients administered with the drug. For patients taking Entresto™ BNP concentrations may be deceptively high, as both BNP and proBNP remain intact in circulation. [126]

The majority of the detected BNP by immunoassays, especially in chronic heart failure, is proBNP. To prove the assumption that measured BNP concentrations will be unaffected by blocking the enzyme, proBNP and BNP was incubated with neprilysin and their concentration was monitored. The measurements were made with two types of immunoassays with different epitope specificity.

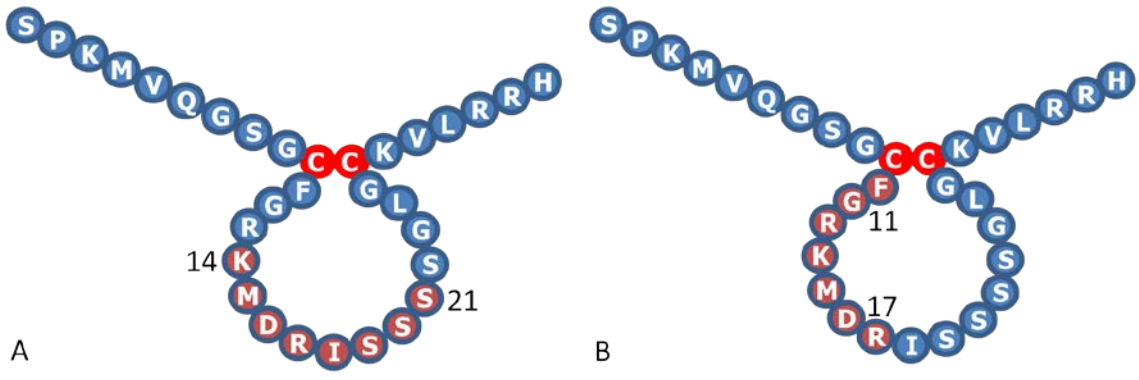

Figure 1:12. Platform, code and epitope specificity of capture antibodies used in the study. Epitopes are highlighted in red. a) Shionogi, BC-203, epitope 14-21 b) Hytest, mAb 24C5, epitope 11-27.

The epitope of the first antibody (A) recognises one of the cleavage sites of neprilysin (R_{17}-I_{18}) and the authors used the results to demonstrate the non-specificity of the immunoassays depending on the antibody they use for capturing BNP for analysis. MALDI-MS experiments were conducted to determine the location of the cleavage sites of the enzyme. Neprilysin lysed BNP at hydrophobic residues consecutively. BNP was cleaved between residues M_5-V_6 after 30 min. R_{17}-I_{18} after two hours, K_{14}-M_{15}, G_{23}-L_{24}, V_{28}-L_{29} after four hours.BNP concentrations were different depending on epitope specificity. Results of the first antibody (A) showed a rapid degradation of BNP as the cleaved BNP was no longer captured by the antibody.

The proBNP signal was constant in the same time period measured with the same BNP assays. Neither the glycosylated nor the non-glycosylated forms of proBNP were ideal substrates for neprilysin (i.e. there was no degradation of proBNP). The authors conclude that the effect of the new drug may not change immunoassay readings significantly, as proBNP is not degraded by neprilysin and remains the major part recognized by the immunoassays due to the cross-reactivity between BNP and proBNP. They also suggest that using different antibodies with varying epitope recognition can accommodate better understanding of the effects of Entresto™. [126]

All clinical studies related to the measurement of cardiac hormones are conducted by immunoassays. [106] Due to the lack of comparability between the results, complete understanding of their faith in circulation or the efficacy of cardiac medications does not exist. Even the MS-based methods use immunoaffinity enrichment to achieve the required quantification levels. A reference standard and a reference method that is capable of the measurement of BNP in clinically relevant concentration is required to support the clinical community in the establishment of common decision limits, to assist

standardisation of BNP testing and to enable the thorough understanding of the pathophysiology of heart failure.

Chapter 1.10 Aims of the work/project

BNP is routinely measured worldwide for the diagnosis of heart failure. Immunoassay measurements are highly variable and there is no reference method for the accurate quantification of calibrators. The structure of the thesis follows the steps necessary to fulfil the requirements for the development of a reference measurement system. Characterisation and quantification of the primary reference standard is described in Chapter 3 and the development of a reference measurement procedure in Chapter 4. The capability of the reference method for the provision of reference values to matrix matched calibrator is investigated by participation in the UK National External Quality Assessment Scheme (UK-NEQAS, Chapter 5). The equivalence of results between different laboratories is demonstrated by comparison samples analysed by LGC and NIST and BNP is a subject of an international comparison study between NMIs to assess their calibration capabilities in 2020. The final aim of the project is a development of a reference measurement procedure that is included on the JCTLM database as a higher order method for the accurate quantification of the cardiac hormone.

Chapter 2 Materials and Methods

Chapter 2.1 Materials

Chapter 2.1.1 Amino acid analysis of synthetic peptides

Synthetic BNP was purchased from Sigma-Aldrich (Gillingham, UK) and from Phoenix Pharmaceuticals, INC. (Burlingame, CA, USA). Synthetic isotopically labelled BNP was custom-synthesised by CPC Scientific (Sunnydale, CA, USA) as SPKMV($^{13}C_5$,^{15}N)Q-G($^{13}C_2$,^{15}N)S-G($^{13}C_2$,^{15}N)-CF-G($^{13}C_2$,^{15}N)-RKMDR-I($^{13}C_6$,^{15}N)-SSSSGLGC-K($^{13}C_6$,$^{15}N_2$)-VLRRH with a stated purity of 95 %. BNP stock solution was prepared in 0.1 % formic acid (FA)/10 % acetonitrile and stored at -80 °C ± 5 °C. Signature 'tryptic' peptides of BNP were custom-synthesised by AnaSpec (Fremont, CA, USA): MVQGSGCFGR, MVQGSGC-F($^{13}C_9$,^{15}N)-GR, ISSSSGLGCK and ISSSS-G($^{13}C_2$,^{15}N)-L($^{13}C_6$,^{15}N)-GCK, with stated purities of 95 %. Signature peptide solutions were prepared in water and stored at -20 °C ± 5 °C. All dilutions were carried out in Eppendorf Protein LoBind tubes from Thermo Fisher Scientific UK (Paisley, UK). Unlabelled amino acids were obtained from Fluka (Buchs, Switzerland): L-glycine, L-leucine, L-alanine, L-valine, L-lysine, L-isoleucine, L-proline, L-arginine, L-phenylalanine (purities > 99 %). Labelled amino acids were obtained from Cambridge Isotopes Laboratory (Andover, MA, USA): L-glycine($^{13}C_2{}^{15}N$, 98 %), L-leucine ($^{13}C_6{}^{15}N$, 98 %), L-alanine ($^{13}C_3{}^{15}N$, 98 %), L-valine ($^{13}C_5{}^{15}N$, 98 %), L-lysine/2HCl ($^{13}C_6$, $^{15}N_2$, 98 %), L-isoleucine (13C_6, 98 %), L-proline ($^{13}C_5{}^{15}N$, 98 %), L-arginine/HCl ($^{13}C_6$, 98 %), L-phenylalanine ($^{13}C_9{}^{15}N$, 99 %).The reference material used for the traceable mass fraction determination of unlabelled amino acids was SRM 2389a (National Institute of Standards and Technology [NIST], Gettysburg, PA, USA), which is a mixture of seventeen free amino acids in 100 mM hydrochloric acid solution (Gly (2.52 ± 0.07 mmol/L), Leu (2.44 ± 0.11 mmol/L), Ala (2.50 ± 0.07 mmol/L), Val (2.51 ± 0.10 mmol/L), Lys (2.41 ± 0.17 mmol/L), Ile

(2.44 ± 0.11 mmol/L), Pro (2.46 ± 0.11 mmol/L), Arg (2.51 ± 0.07 mmol/L), Phe (2.55 ± 0.09 mmol/L), Asp (2.50 ± 0.08 mmol/L), Cys (1.23 ± 0.06 mmol/L), Glu (2.50 ± 0.08 mmol/L), His (2.52 ± 0.07 mmol/L), Met (2.51 ± 0.07 mmol/L), Thr (2.49 ± 0.07 mmol/L), Tyr (2.54 ± 0.08 mmol/L), and Ser (2.44 ± 0.11 mmol/L)). Unlabelled amino acid standard solutions were prepared in 100 mM hydrochloric acid and calibrated against the NIST standard reference material using exact-matching isotope dilution mass spectrometry (EM-IDMS). The determined amino acid purities were: glycine 99.8 + 0.2/-2.1 %, leucine 96.5 ± 2.5 %, valine 98.9 + 1.1/-2.1 %, lysine 96.7 + 3.3/-3.9 %, isoleucine 99.0 + 1/-3.1 %, proline 99.0 ± 1.0 %, arginine 95.2 + 4.8/-5.3 % and phenylalanine 99.0 ± 1 %. The BNP primary standard was quantified using certified amino acids from the National Metrology Institute of Japan (NMIJ; Tsukuba, Japan). Glycine (CRM 6022-a, 99.9 ± 0.2 %), L-leucine (CRM 6012-a, 99.9 ± 0.2 %), L-alanine (CRM 6011-a, 99.9 ± 0.2 %), L-valine (CRM 6015-a, 99.8 ± 0.2 %), L-lysine monohydrochloride (CRM 6018-a, 99.8 ± 0.2 %), L-isoleucine (CRM 6012-a, 99.7 ± 0.2 %), L-proline (CRM 6016-a, 99.9 ± 0.2 %), L-arginine (CRM 6017-a, 99.8 ± 0.2 %), L-phenylalanine (CRM 6014-a, 99.9 ± 0.2 %). Concentrated hydrochloric acid was obtained from ROMIL (Ultra Purity Acid, ROMIL, UK) and N-methyl-N-(trimethylsilyl)-trifluoroacetamide (MSTFA) containing 1 % trimethylchlorosilane (TMCS) catalyst was bought from Restek Corporation (Belleforte, PA, USA). N-*tert*-Butyldimethylsilyl-N-methyltrifluoroacetamide (MTBSTFA) with 1 % *tert*-Butyldimethylchlorosilane (TBDMSCl) was purchased from Sigma-Aldrich (Gilliam, UK).

Chapter 2.1.2 MALDI-TOF MS

Trifluoroacetic acid (TFA) was from Thermo Scientific (Rockford, IL, USA). 2,5-dihydroxybenzoic acid (DHB) was purchased from Bruker Daltonics (Coventry, UK).

Chapter 2.1.3 ESI-Q-TOF MS, ESI-QqQ MS

Ultra-pure water (18.2 MΩ cm) was generated by the ELGA Process Water Flex 2 instrument (ELGA Process Water, UK). Formic acid (FA) 99.5 + %, Optima™ LC/MS Grade was acquired from Fisher Scientific (Loughborough, UK). HPLC Optigrade organic solvents were obtained from LGC Standards (Teddington, UK). Dimethyl sulfoxide (DMSO), sulfolane and 3-nitrobenzyl alcohol (m-NBA)were sourced from Sigma-Aldrich (Gillingham, UK).

Chapter 2.1.4 Tryptic digestion

Tris(hydroxymethyl)aminomethane hydrochloride (TRIS-HCl), ammonium bicarbonate (ABC), urea, sodium dodecyl sulfate, S-methyl methanethiosulfonate (MMTS) and calcium chloride dihydrate were purchased from Sigma-Aldrich (Gillingham, UK). Tris(2-carboxyethyl)phosphine hydrochloride (TCEP-HCl) was obtained from Thermo Fisher Scientific (Schwerte, Germany). Modified sequencing-grade trypsin and Zwittergent detergents were supplied by Roche Applied Science (Penzberg, Germany).

Chapter 2.1.5 Plasma and plasma clean-up

Human K2 EDTA mixed-gender plasma was purchased from Sera Laboratories International Ltd. (Haywards Heath, West Sussex, UK). The following solid phase extraction (SPE) cartridges were evaluated: Bond Elute PLEXA (60 mg/3 mL, 100 Å, 45 µm; Agilent Technologies Inc., Santa Clara, CA, USA), STRATA XL (200 mg/3 mL, 300 Å, 100 µm; Phenomenex, Macclesfield, UK), ZIC-HILIC SPE (200 mg/3 mL, 60 Å, 50 µm; Millipore UK

Ltd., Watford, UK) and EVOLUTE CX-50 (100 mg/3 mL, N/K, 50 µm; Biotage GB Ltd., Hengoed, UK). Ultracentrifugation was explored with Amicon Ultra 0.5 mL Centrifugal Filters Ultracel10 membrane (NMWL: 10 kDa; Millipore UK Ltd.).

Chapter 2.2 Methods

Chapter 2.2.1 Amino acid analysis

The traceable quantification of the peptides by amino acid analysis was achieved by acid hydrolysis followed by IDMS on the released amino acids. Vapour phase hydrolysis was performed at 190 °C with the use of MILESTONE ETHOZ EZ Microwave Digestion System (Milestone S.r.l., Sorisole (BG), Italy). The peptide concentration was calculated assuming complete release of the amino acids from the parent peptide (glycine, leucine, alanine, valine, lysine, isoleucine, proline, arginine and phenylalanine). The peptide solutions were prepared in a nominal concentration of 50 nmol/g (BNP) and 100 nmol/g (ISSSSGLGCK, MVQGSGCFGR) corrected for the peptide content supplied on the certificate of analysis. The quantification of peptide stock solutions was performed on six independent aliquots for both signature BNP peptides, and the intact BNP peptide. The hydrolysis was repeated three times. Amino acid standard solutions containing the expected molar concentrations of the amino acids from the parent peptide molecule were prepared and used as calibrants. The calibration blends were prepared by mixing the calibrants with the labelled amino acids in equimolar amounts. The peptide solutions were spiked with the same labelled amino acid solutions. All blends were prepared gravimetrically. The calibration and sample blends were frozen at -80 °C for 30 min and then freeze-dried in a vacuum centrifuge (Alpha 1-2LD, RVO 2-25, Christ, Osterode am Harz, Germany) at 0.1 mbar (-42 °C) for 2.5 h. The samples were hydrolysed at 190 °C for 30 min in the MILESTONE ETHOZ EZ Microwave Digestion System equipped with a protein hydrolysis kit,

containing 30 mL 6 M hydrochloric acid. The hydrolysed samples were lyophilized and reconstituted in 80 µL MSTFA or MTBSTFA. The samples were then analysed using a single quadrupole Finnigan TRACE DSQ GC-MS system (Thermo Fisher Scientific, Waltham, MA, USA) equipped with a CTC Combi-PAL Autosampler system (CTC Analytics AG, Zwingen, Switzerland). The amino acids were separated on a 30 m long Zebron ZB-5HT INFERNO GC column (0.25 µm i.d.) attached to 2 m long Zebron HT deactivated guard column (0.5 µm i.d.) both from Phenomenex (Macclesfield, UK). The inlet temperature was 280 °C and the split flow was set at 85 mL/min with splitless time for 0.75 min. 1 µL of the samples were injected. The temperature program was: hold at 90 °C for 2 min, then increase to 330 °C at a rate of 25 °C/min and hold the final temperature for 5 min. The ions monitored for each unlabelled/labelled amino acid pair in selected ion monitoring mode (SIM, in order of elution) are tabulated in Table 2:1.

Table 2:1. SIM ions used for the quantification of amino acids.

Amino acid	Quantifier mass (*m/z*, U/L) MSTFA	Quantifier mass (*m/z*, U/L) MTBSTFA
Alanine	116/119	158/161
Glycine	102/104	218/220
Valine	144/149	186/191
Leucine	158/164	200/206
Isoleucine	158/163	200/205
Proline	216/221	184/189
Phenylalanine	192/201	302/305
Lysine	84/90	300/307
Arginine	256/261	199/203

U: unlabelled; L: labelled.

Chapter 2.2.2 Purity assessment of synthetic peptides

Chapter 2.2.2.1 MALDI-TOF MS

The synthetic signature peptides ISSSSGLGCK, MVQGSGCFGR, ISSSSG*L*GCK and MVQGSGCF*GR (*:^{13}C and ^{15}N enriched amino acids) were cysteine-alkylated and mixed in equimolar amounts to obtain a concentration of 10.8 nmol/g for each peptide. 200 mg of 2,5-dihydroxybenzoic acid (DHB) was dissolved in 2 mL of water to make a saturated solution. On an AnchorChip plate (Bruker Daltonics) 0.5 µL of analyte solution was mixed with 0.5 µL of DHB matrix solution, air-dried and used for MS analysis. MALDI-TOF MS measurements were performed using an Ultraflex II mass spectrometer (Bruker Daltonics). The laser pulse repetition rate was set to 50 Hz and spectra were recorded by averaging 500 shots. For MS calibration, Peptide Calibration Standard II mixture (Bruker Daltonics, Cat. #222570) was prepared the same way as the samples.

Chapter 2.2.2.2 LC-ESI-Q-TOF MS

10 nmol (100 µL, 100 nmol/g) of the synthetic peptides were reduced using 200 nmol of TCEP (4 µL, 50 mM TCEP, 37 °C, 60 min) in 500 µL LowBind Eppendorf tubes. The cysteine residues were then alkylated with 400 nmol MMTS (4 µL, 100 mM MMTS, dark, 37 °C, 30 min). For MS analysis, an Agilent Q-TOF 6530 instrument was coupled to an Agilent 1200 capillary and nano pump system (Agilent Technologies, Inc., Santa Clara, CA, USA), providing a split flow of 4 µL/min for loading onto the trap and 0.6 µL/min for separation. An Agilent chip-cube assembly was used to interface the HPLC-chip with the MS. Chromatographic separation was achieved using an Agilent HPLC-chip (5 µm particle size, 300 Å mean pore diameter, Zorbax 300SB-C18 Protein ID Chip) that comprised of a 40 nL enrichment and a 75 µm x 43 mm analytical column. The trap was loaded using 0.1 % FA (solution A) while separation was performed with a linear gradient from 1-50 % of 0.1 %

FA in acetonitrile (solution B) in solution A within 9.5 min. The gas temperature of the source was 235 °C and the gas flow was set to 6 L/min. The capillary voltage was set to 1950 V and the fragmentor voltage was 210 V. The fragmentation of the signature peptides was performed by targeting the doubly charged ions, using a CID voltage of 20 V.

Chapter 2.2.3 Tryptic digestion and quantification of BNP

The calibration blend for the tryptic digestion contained the previously quantified synthetic peptide standards and their labelled analogues (MVQGSGCFGR, ISSSSGLGCK, ISSSSG*L*GCK and MVQGSGCF*GR). The sample blend was prepared with intact BNP peptide solution mixed with the labelled synthetic peptides. Digestion was optimised to achieve complete tryptic proteolysis by repeated addition of trypsin to the buffered solution and monitoring the ratio of unlabelled and labelled synthetic peptide signals until a plateau was reached. 5 µL of 10.8 nmol/g of the sample and calibration blends were diluted to 250 µL with 500 mM TRIS buffer, 10 mM Ca^{2+} solution (pH 8.10). This mixture was digested with 3.5 µg of trypsin (37 °C, 1 hour). 3.5 µg of trypsin (3.5 µL, 1 µg/µL trypsin) was added after an hour and the mixture was digested further at 37 °C for an hour. The digest was reduced with 200 nmol TCEP (4 µL, 50 mM TCEP, 37 °C, 60 min) and alkylated with 400 nmol MMTS (4 µL, 100 mM MMTS, dark, 37 °C, 30 min). Two sample blends and two calibration blends were treated with the same digestion protocol, in triplicate. A Q-TRAP 4000 quadrupole linear ion trap instrument (ABSciex, Framingham, MA, USA) coupled to an Agilent 1100 series HPLC system (Agilent Technologies, Inc.) was used for the quantification of the signature peptides. Separation was achieved on an XBridge BEH C18 Waters column (3.5 µm particle size, 2.1 mm i.d., 150 mm length, 130 Å mean pore diameter) from Waters Corporation (Milford, MA, USA) at a flow rate of 100 µL/min. Mobile phase solutions were: (A) 0.1 % FA and (B) 0.1 % FA in acetonitrile.

Peptides eluted with a linear gradient from 5 % to 40 % solution B within 30 min. The column effluent was introduced into the ESI source through a divert valve directing the solvent into waste after the peptides eluted. A Turbo V ESI ion source was used. Source temperature was 600 °C, ion spray voltage was 3000 V. Curtain gas pressure was 30 psi. Nebuliser and heater gas pressures were set to 70 psi each. The mass spectrometer was operated in positive ion mode. The doubly charged molecular ions were fragmented by CID. SRM and source conditions were optimized for the most abundant fragment ions. A collision cell voltage of 25 V was used for both peptides. Table 2:2 shows the monoisotopic and observed masses of the parent and the monitored fragment ions. The analytical column temperature was 60 °C.

Table 2:2. Masses monitored for the signature peptides.

Unlabelled	M (g/mol)	Monoisotopic Theoretical Mass *m/z* (z=2)	Observed Mass QTRAP
MVQGSGC(Methylthiol)FGR	1086.4409	544.2277	544.3
Monitored fragment y_7+	729.2807		729.4
ISSSSGLGC(Methylthiol)K	983.4416	492.7281	492.4
Monitored fragment y_8+	784.3328		784.4
Labelled	**M (g/mol)**	**Monoisotopic Theoretical Mass *m/z* (z=2)**	**Observed Mass QTRAP**
MVQGSGC(Methylthiol)**F***GR	1096.4684	549.2413	549.3
Monitored fragment y_7+	739.3079		739.4
ISSSS**G*L***GC(Methylthiol)K	993.4625	497.7385	**497.3**
Monitored fragment y_8+	794.3537		**793.5**

* :labelled amino acids ^{13}C, ^{15}N.

Chapter 2.2.4 ESI-Q-TOF MS purity assessment of BNP primary stock

The Agilent Q-TOF 6530 instrument was coupled to the Agilent 1290 HPLC system (Agilent Technologies, Inc.). The instrument was calibrated using the Agilent LC/MS low concentration tuning mix. (Cat. # G1969-85020) The chromatographic separation was performed using an Aeris PEPTIDE XB-C18 column (2.6 µm particle size; 2.1 mm i.d.; 250 mm length, pore size of 90 Å) from Phenomenex. A linear gradient from 1 % to 20 % solution B was applied over 20 min. Solution A was 0.5 % FA and solution B was 0.5 % FA in acetonitrile. The flow rate was set to 400 µL/min and the temperature to 60 °C. Samples were kept at 5 °C in the auto sampler. Dimethyl sulfoxide (DMSO) was infused post column with a separate pump (PU-1585 Intelligent HPLC Pump; JASCO Analytical Instruments, Dunmow, Essex, UK) at a flow rate of 1 µL/min. The Agilent JetStream ESI source was used with the following settings: Gas temperature was 300 °C and drying gas flow was set at 13 L/min. Nebuliser gas pressure was 50 psig. Sheath gas temperature was 350 °C and the flow was 12 L/min. Capillary voltage was set to 1500 V. Nozzle voltage was 1000 V. Fragmentor and skimmer voltage was 175 V and 65 V, respectively.

Chapter 2.2.5 UPLC-UV-ESI MS experiments

The purity of the BNP stock solution was determined by recording the chromatogram of the stock solution with UV and MS detectors connected in series. An Acquity UPLC Twin UV (TUV) Detector (Waters Corporation) was connected to the column and after the UV cell the eluent was directed to the ESI source of a Xevo G2-XS QToF MS instrument (Waters Corporation). The separation was performed using an Acquity UPLC H-Class system (Waters Corporation) on an Aeris PEPTIDE XB-C18 column (2.6 µm particle size; 2.1 mm i.d.; 250 mm length, pore size of 90 Å) from Phenomenex. Solvent A was 0.5 % FA and solvent B was 0.5 % FA in acetonitrile. A linear gradient from 1 % to 25 % solution B

was applied over 48 min. The flow rate was set to 250 µL/min and the column temperature to 70 °C. Samples were kept at 5 °C in the auto sampler. The Twin UV detector was set up to display absorption at 260 nm after correction with Median Baseline Filter (MBF). Sampling rate was 20 point/sec and the filter constant was set to Normal (0.1 sec). Sensitivity setting was 4 AUFS with positive polarity and a voltage offset of 0 mV. The ESI source temperature was 100 °C, desolvation temperature 450 °C, cone gas flow was 50 L/h and desolvation gas flow was set to 600 L/h. The MS instrument was operated in positive ion sensitivity mode. A capillary voltage of 3 kV and a cone voltage of 40 V were applied. The data acquisition range was *m/z* 50-1,800. [Glu1]-Fibrinopeptide lockmass solution (100 µg/µL, *m/z* 785.8427) was infused at a flow rate of 10 µL/min. The*m/z* scale was automatically corrected every 60 seconds.

Chapter 2.2.6 BNP LC-ESI MS Method development

Chapter 2.2.6.1 Superchargers

Both the Agilent Q-TOF 6530 instrument and the Agilent QqQ 6490 instrument were used and coupled to the Agilent 1290 HPLC system. The chromatographic separation was performed using an Aeris PEPTIDE XB-C18 column (2.6 µm particle size; 2.1 mm i.d.; 250 mm length; pore size of 90 Å) from Phenomenex. A linear gradient from 1 % to 20 % solution B was applied over 20 min. Solvent A was 0.5 % FA and solvent B was 0.5 % FA in acetonitrile. The flow rate was set to 400 µL/min and the temperature to 60 °C. Samples were kept at 5 °C in the auto sampler. Sulfolane, m-NBA and DMSO were infused post column with a separate pump (PU-1585 Intelligent HPLC Pump; JASCO Analytical Instruments) at a flow rate of 1 µL/min (0.25 %; v/v). The settings of the Agilent JetStream ESI source is displayed in Table 2:3. On the Q-TOF instrument the fragmentor and skimmer voltage was 175 V and 65 V, respectively.

Table 2:3. MS source conditions on the Agilent Q-TOF 6530 and Agilent QqQ 6490 instruments employed for the comparison of superchargers.

Gas Temperature (°C)	300
Gas Flow (l/min)	18
Nebulizer Gas Pressure (psi)	35
Sheath Gas Temperature (°C)	300
Sheath Gas Flow (L/min)	12
Capillary Voltage (V)	3500
Nozzle Voltage (V)	1500

Chapter 2.2.6.2 Optimisation of MS/MS conditions

Source optimisation was performed by monitoring the intensity of BNP signal with different source conditions. The LC described in Chapter 2.2.6.1 was delivering 10 % acetonitrile, 90 % water, 0.1 % FA (v/v/v) at 400 µL/min. BNP standard (1 nmol/g) was connected to the mobile phase through a t-piece and infused using a syringe pump at 10 µL/min. A second LC pump was delivering DMSO at 1 µL/min through another t-piece before the ESI source. The MS instrument was operated in positive ion mode. Full scan spectra were recorded from *m/z* 400-800. The capillary voltage was set to 3000 - 4000 V in 500 V increments, the nozzle voltage was varied from 0 - 1500 V in 500 V increments. Gas temperature was varied between 300 and 350 °C. Gas flow was set to 18 and 11 L/min. The nebuliser gas pressure was changed from 30 psi to 50 psi in 5 psi increments. For the SRM optimisation the product ion spectrum of the 6+ charge state of BNP (*m/z* 578.3) was monitored. Cell acceleration voltage was varied from 1 - 5 V by 1 V increments. The collision cell voltage was increased from 16 V to 22 V in 1 V increments. The electron multiplier voltage (EMV) was increased to +450 V.

Table 2:4. MS ion source and SRM transition optimisation results.

Source Conditions	Default	Optimised
Gas Temperature (°C)	300	300
Gas Flow (L/min)	18	18

Source Conditions	Default	Optimised
Nebuliser Gas Pressure (psi)	35	**50**
Sheath Gas Heater Temperature (°C)	300	**350**
Sheath Gas Flow (L/min)	12	12
Capillary Voltage (V)	3500	**1500**
Nozzle Voltage (V)	1500	**1000**

Transition Settings	Default	Optimised
EMV (V)	0	**+ 450**
Precursor (*m/z*)	Monoisotopic	**Average**
Product (*m/z*)	Monoisotopic	**Average**
Resolution	Unit/Unit	**Unit/Wide**
Dwell Time (ms)	200	**100**
Fragmentor Voltage (V)	380	380
Collision Cell Voltage (V)	16	**18**
Cell Accelerator Voltage (V)	5	**1**

The values in bold were attributed to the enhancement of signal intensity and optimised accordingly.

Chapter 2.2.6.3 Protein precipitation (PPT)

For the reference method a volume of 1.5 mL of water:acetonitrile (20:80; v/v) containing 0.5 % FA was added to the plasma samples, vortexed vigorously and centrifuged at 5,000 rpm at 4 °C for 60 min (Eppendorf Centrifuge 5804R; Thermo Fisher Scientific UK). The supernatant was transferred to pre-weighed 2 mL Eppendorf tubes and freeze-dried overnight in a CHRIST ALPHA 1-2 LD plus freeze dryer with a CHRIST RVC 2-25 centrifuge (SciQuip Ltd, Newtown, UK).

Chapter 2.2.6.4 Stabilisation experiments

Ten aliquots containing 60 fmol (200 pg) of BNP were freeze-dried. 0.5 g plasma was added gravimetrically to each aliquot. A volume of 1.5 mL of precipitation solvent was added at the beginning of the experiment to the first aliquot and at 10 min intervals to the remaining aliquots. Samples were centrifuged; the supernatant subjected to SPE and reconstituted in 100 µL of water containing 0.5 % FA (v/v) and an equimolar amount of

isotopically labelled BNP. The samples were then analysed by LC-ESI MS/MS SRM using the Agilent QqQ system.

Chapter 2.2.6.5 Solid phase extraction (SPE)

For the determination of elution characteristics of BNP, the STRATA XL cartridges were conditioned with 5 mL of methanol containing 0.5 % FA (v/v) followed by 5 mL of water containing 0.5 % FA (v/v). A solution containing 200 fmol of BNP was loaded (200 µL, 1 pmol/g BNP solution). The loaded cartridges were washed twice with 2 mL of water containing 0.5 % FA (v/v) and eluted with the sequential addition of 2 mL of water containing increasing percentages of acetonitrile (steps of 10 % from 10 to 100 % (v/v)). The washing and elution volumes were individually collected in 2 mL Protein LoBind vials. The solutions were freeze-dried and reconstituted in 100 µL of water with 0.5 % FA (v/v) containing an amount of isotopically labelled BNP equal to the amount of loaded BNP (200 fmol). The extracts were analysed by the LC-ESI MS/MS SRM reference method described in Chapter 2.2.7 and on the Agilent Q-TOF instrument in full scan mode. BNP recoveries were calculated by comparing the MS peak areas of the extracted ion chromatogram signal of the BNP recovered from the SPE and the extracted ion chromatogram signal of the isotopically labelled internal standard. For the reference method the STRATA XL SPE cartridges were conditioned with 5 mL of methanol containing 0.5 % FA (v/v) followed by 5 mL of water containing 0.5 % FA (v/v). The freeze-dried extracts from the protein precipitation experiments (PPT) were reconstituted in 2 mL of water containing 0.5 % FA (v/v), loaded onto the SPE cartridges, washed twice with 2 mL of water containing 0.5 % FA (v/v) and twice with 2 mL of water:acetonitrile (95:5; v/v) containing 0.5 % FA (v/v). All solvents contained 45 µg/g of methionine. Bound peptides were eluted into 5 mL Eppendorf vials with 4 mL of water:acetonitrile (65:35; v/v)

containing 0.5 % FA (v/v) and methionine at a concentration of 45 µg/g. The collection vials were pre-rinsed with an aqueous solution containing 0.5 % FA and 500 µg/g BSA to avoid any loss of BNP on the vessel surfaces. The extracts were lyophilized, reconstituted in 100 µL of water containing 0.5 % FA (v/v) and analyzed by LC-ESI MS/MS as described in Chapter 2.2.7.

Chapter 2.2.7 LC-ESI MS reference method

For the quantification of BNP by SRM, experiments were set up by fragmenting the 6+ charge state of the intact precursor ion (BNP: *m/z* 578.3, BNP*: *m/z* 583.3) and monitoring the 4+ y26 product ion (BNP: *m/z* 699.2, BNP*: *m/z* 705.2). Oxidation of methionine residues were monitored in separate windows. If one of the methionines was oxidized the precursor ion was at *m/z* 581.0 with the product ions of *m/z* 699.2 and *m/z* 703.5. If both of the methionines were oxidized the precursor ion was at *m/z* 583.7 and the product ion at *m/z* 703.5. The resolution was set to UNIT/WIDE (Q1: *m/z* 0.7/Q3: *m/z* 1.2). The mass spectrometer was operated in positive ion mode. The dwell time was set to 100ms and the fragmentor voltage was set to 380.0 V. Collision energies (CE) and cell acceleration voltages (CAV) were optimized (BNP: CE18, CAV 1; BNP*: CE18, CAV 1). The electron multiplier voltage (EMV) was set to +450 V. Volumes of 10 µL of the appropriate samples were injected. The chromatographic separation was performed by using an Aeris PEPTIDE XB-C18 column (2.6 µm particle size; 2.1 mm i.d.; 250 mm length, pore size of 90 Å) from Phenomenex. A linear gradient from 1 % to 20 % solution B was applied over 20 min. Solvent A was 0.5 % FA (v/v) and solvent B was 0.5 % FA in acetonitrile (v/v). The flow rate was set to 400 µL/min and the temperature to 60 °C. Samples were kept at 5 °C in the auto sampler. Dimethyl sulfoxide (DMSO) was infused post column with a separate

pump (PU-1585 Intelligent HPLC Pump; JASCO Analytical Instruments) at a flow rate of 1 µL/min.

Chapter 2.2.8 Final optimisation of sample clean-up

The recovery of the clean-up procedure was determined at every concentration level by comparing the ratio determined in the post-spiked samples to pre-spiked samples. Seven aliquots of the diluted BNP primary stock standard were prepared at the calibration range of the reference method (15 fmol/g-150 fmol/g, i.e. 52 pg/g-520 pg/g), spiked with 30 fmol isotopically labelled BNP and freeze-dried (pre-spike). Another set of BNP standard without the isotopically labelled internal standard was also prepared (post-spike). Labelled internal standard was added to the post-spikes after SPE. Plasma was added and the samples were subjected to PPT and SPE as described previously. Blank plasma samples were analysed with both sets of samples. The samples were analysed with the LC-ESI MS/MS SRM method.

Chapter 2.2.9 Analysis of NEQAS samples

Freeze-dried plasma samples were delivered by post and stored at 5 °C until analysis. The samples were reconstituted in the supplied reconstitution solvent by following the instructions provided by NEQAS. Immediately after reconstitution, 1.5 mL of the PPT solvent (water:acetonitrile (20:80; v/v)) was added. Seven plasma samples spiked with the BNP primary standard in a range of concentrations between 15 fmol/g-150 fmol/g (52 pg/g-520 pg/g) were also prepared. Blank plasma and the seven spiked plasma samples were used to construct the calibration curve. The same amount of isotopically labelled BNP (30 fmol) was added to the calibrants and the UK NEQAS samples. All samples were

processed and analysed as previously described in Chapter 2.2.7 by performing the two-step sample clean-up procedure prior to LC-ESI MS/MS analysis.

Chapter 3 Development of a primary B-type Natriuretic Peptide standard

Chapter 3.1 Introduction

Measurements must produce comparable results independent of the measurement platform used. Standardisation in clinical diagnostics can be achieved by means of Certified Reference Materials (CRMs) that can define the scale of quantity and link the measurement units to international references (i.e. SI unit), and by the existence of a reference measurement procedure that enables the transfer of SI-traceable values to calibrants with high precision and accuracy. Metrological traceability is defined as "the property of a measurement result whereby the result can be related to a reference through a documented unbroken chain of calibrations, each contributing to the measurement uncertainty". [18] Traceability is stipulated by international quality standards and requires the establishment of a calibration hierarchy. [12], [128] In chemistry, the realisation of the measurand as a high-purity primary reference material represents the highest metrological order in the calibration hierarchy. While well characterised primary reference standards with known purity are available for small organic molecules, where the measurand is well defined, methods for the purity assignment of more complex peptide and protein standards are still lacking. The purity of an organic substance is expressed as the mass fraction of the main compound in a nominally pure material. (Equation 3:1.)

$$w_A = \frac{m_A}{m_A + \sum m_x}$$

Equation 3:1. Definition of purity of organic standards, where w_A is the mass fraction of the main component A in the material, m_A is the gravimetric amount of the main component and $\sum m_x$ is the sum of the minor impurities present.

The purity can be determined directly by measuring the amount of substance of the main component or indirectly by determining the amount of impurities and subtracting it from the total value. Direct purity measurements require primary reference standards so the amount of substance can be assigned by gravimetry, titrimetry or by establishing comparison to the same chemical entity by isotope dilution mass spectrometry (IDMS) [129], [130], quantitative nuclear magnetic resonance (NMR) [90], [91] or by chromatographic response. The total amount of impurities can be determined indirectly by thermal methods such as differential scanning calorimetry (DSC) [131] or adiabatic calorimetry by evaluating phase-change phenomena (i.e. melting point depression). If the purity is determined indirectly by quantifying the impurities individually, the method is called “mass balance” approach. In the “mass balance” approach the impurities are categorised into well-established classes. [132] Table 3:1. Purity determination is performed by the systematic assessment of water content, related structure impurities, residual organic solvents and non-volatiles in the solid material. [133], [134]

Table 3:1. Analytical techniques used for the assessment of the purity of organic substances.

Class of impurity	Analytical technique
Related structure	Chromatographic techniques with universal and selective detectors
	GC-FID, GC-ECD, GC-MS/MS, LC-DAD, LC-UV, LC-MS/MS, LC-CAD, GPC-MALDI
	Elemental Microanalysis
Water	Karl Fischer Titration
	Thermogravimetric Analysis (TGA, TGA-MS)
Residual solvents	Headspace GC/MS
	Thermogravimetric Analysis (TGA, TGA-MS)
	Quantitative NMR
Non-volatiles	
Organic	Ion Chromatography
Inorganic	Inductively Coupled Plasma MS (ICP-MS)

GC: gas chromatography, ECD: electron capture detector, DAD: diode array detector, UV: ultraviolet detector, CAD: charged aerosol detector, GPC: gel permeation chromatography NMR: nuclear magnetic resonance.

Additional information such as synthetic production routes, potential side reactions and degradation pathways are particularly useful in the identification of impurities present in the material. The identity of the impurities is confirmed using orthogonal chromatographic techniques utilising different separation chemistries with universal (DAD, UV, FID, MS, CAD) and structure-specific detectors (i.e. electron capture detector, ECD) and ionisation techniques (ESI, atmospheric pressure chemical ionisation (APCI), atmospheric pressure photo ionisation (APPI)). [135], [133], [132], [136] Once the identity of every impurity is confirmed, impurity standards are used for accurate quantification by external calibration.

While analytical approaches to define the purity of small organic molecules are well established, there is a clear gap between the demand from clinicians and available CRMs for biological measurands. The Joint Committee for Traceability in Laboratory Medicine (JCTLM) database, maintained by the International Bureau of Weights and Measures (BIPM), is constantly updated with the list of available certified reference materials,

reference measurement procedures and laboratories with calibration facilities. As of August 2017 there are only twenty five CRMs available for peptides and proteins with values that provide traceability to the SI. Twenty-four of these are in matrix and only one, the human C-peptide, is available as a solid. [21] The number of CRMs for small organic molecules is over two hundred and fifty.

The lack of availability of higher order CRMs is mainly due to the complexity of large biomolecules and their potential impurities. The traditional “mass balance” approach for synthetic peptides is not always applicable because of the high costs associated with the production and purification of large quantities of the solid standard material. [137] Synthetic peptides are produced by solid phase peptide synthesis (SPPS). The peptide chain is built from the C-terminus towards the N-terminus. Resins with the C-terminal amino acid attached are commercially available. SPPS involves selective protection and de-protection of the reactive moieties of the coupled amino acid and the residue already attached to the growing peptide chain. [138] The advantage of solid phase synthesis versus solution chemistry is that the product remains attached to the polymeric material and the reagents can be washed away between each step minimising unwanted side reactions. The disadvantage is that in the case of incomplete coupling the main product will be contaminated with closely related peptidic impurities. Deletion sequences missing one or more amino acid residues are not uncommon. Imperfect washing of the resin between the coupling steps can result in multiple residues being built into the peptide sequence. As the yield of coupling efficiency is decreasing significantly with the number of residues in the sequence, proteins that contain more than 75 residues are produced by means of recombinant DNA technologies. For proteins used in clinical diagnostics the characterisation of different isoforms, post-translational modifications (PTM) and higher

order protein structure is also necessary and further increases the complexity of purity determinations.

National Metrology Institutes (NMI) are required to participate in comparison trials coordinated by the BIPM to demonstrate their measurement capabilities. The studies are organised and operated within the framework of the Consultative Committee for Amount of Substance (Comité Consultatif pour la Quantité de Matére, CCQM)- Metrology in Chemistry. Participation in a CCQM study allows NMIs to assess their calibration methods for the determination of organic purities and to compare and discuss results with fellow NMIs. Participation in CCQM studies also provides an opportunity for NMIs to demonstrate their Calibration and Measurement Capability (CMC) claims for the provision of organic pure substance CRMs. [133], [139]

A strategy for the SI-traceable value assignment of peptides and proteins was drafted by the Protein Analysis Working Group (PAWG) of the CCQM in 2017 to outline the timeframe for future CCQM studies. [140] The strategy classifies peptides and proteins by size and complexity. The first study for mass concentration assignment of small synthetic peptides of *unknown purity* was conducted in 2010. (CCQM-P55.1) In 2014, human C-peptide was distributed to participating NMIs to assess the capabilities for the purity assignment of a solid synthetic peptide standard without cross linking. (CCQM-K155) [141] The results of the key comparison study are displayed in Figure 3:1. The study highlighted the technical and metrological difficulties associated with the purity assignment of large synthetic peptides and the need for further research in the area.

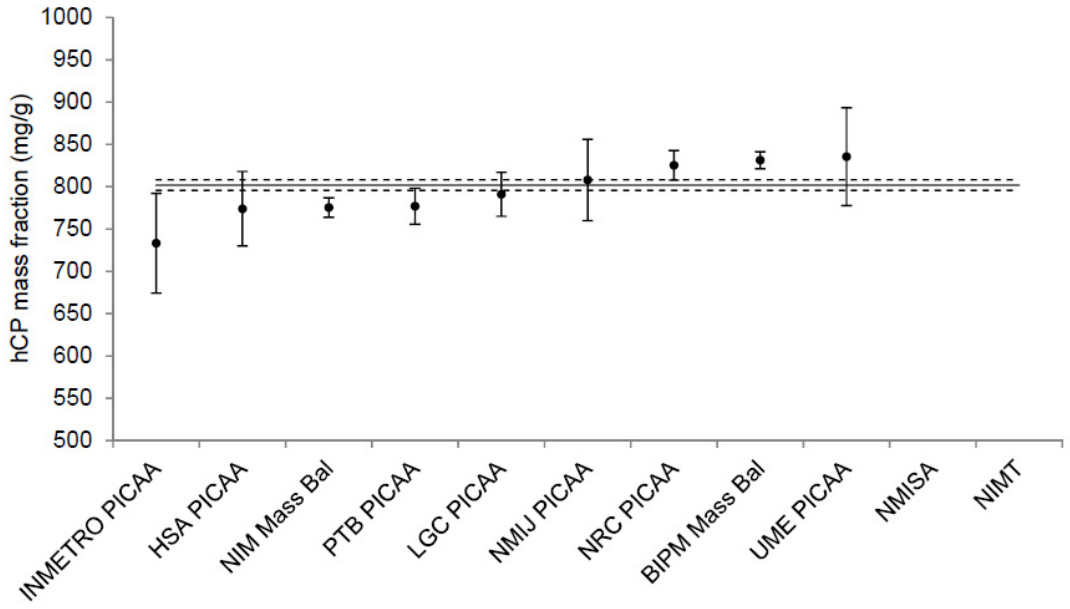

Figure 3:1. Mass fraction estimates by participants for human C-peptide (hCP) in CCQM-K115 with their reported expanded uncertainties (± U, *k*=2). Solid line: proposed reference value. Dashed lines: uncertainties. PICAA: Peptidic impurity corrected amino acid analysis.

Future studies are aimed at assessing technical capabilities for mass fraction assignment of peptides and proteins with disulfide bridges, post-translational modifications and from recombinant origin. While the metrological tools to determine the purity of complex biomolecules are still lacking, NMIs are developing “fit for purpose” approaches to fulfil the clinical demand.

Two methods are currently available for the SI-traceable quantification of proteins and peptides. The first is amino acid analysis and the second is quantification of proteins via their enzymatic peptides that had been quantified by amino acid analysis. For synthetic peptides the method of choice for SI-traceable quantification is amino acid analysis by EM-IDMS after acid hydrolysis. [128], [129], [141] Certified amino acid reference standards are readily available and provide traceability to the SI. Provided that the hydrolysis is complete, the concentration of the peptides can be derived by determining the concentration of the amino acids in their sequence. The drawback of this approach is

that full coverage of the sequence is not always possible as not all amino acids are stable during the harsh conditions employed during acid hydrolysis. Asparagine and glutamine are hydrolysed to aspartic acid and glutamic acid. Tyrosine and tryptophan decompose and serine and threonine are partially hydrolysed. Methionine is oxidised to methionine-sulfoxide or sulfone and cysteine is oxidised to cysteic acid. [143] As the main *related structure* impurities in synthetic peptides are deletion products or amino acid replacements during SPPS the results from the amino acid analysis represent the total peptidic content (peptide and peptidic impurities). Reliable quantification by amino acid analysis alone is only possible for high-purity proteins and peptides. [144] Even if the synthetic or recombinant standard is available in highly purified form difficulties still remain for macromolecules that display higher order structures. [145], [146]

An alternative to amino acid analysis is the SI-traceable quantification of macromolecules by performing EM-IDMS on the peptide level. Figure 1:10. The most widespread approach for the absolute quantification (AQUA) of large proteins entails the selection of signature peptides from the sequence, digestion to completeness by a suitable enzyme and quantification based on the postulation of equimolar release and sufficient stability during the measurement process. *In silico* digestion of the protein and a database search of the resulting peptides confirms that their sequence is unique and that these peptides can be used as signature peptides for quantification. [147], [97] Complete release and stability of the signature peptides is determined during the optimisation of the digestion step. Ideal signature peptides lack residues that are susceptible to post-translational modifications or degradation and contain at least three amino acids amenable to amino acid analysis. SI-traceability is maintained by assigning the concentration of the synthetic peptides by certified amino acid reference materials using EM-IDMS as previously

mentioned. When EM-IDMS is applied after enzymatic digestion for the absolute quantification of proteins, isotopically labelled peptides are used as internal standards and digested with the protein. A second blend containing the SI-traceable quantified synthetic standards and the isotopically labelled peptide standards is also digested and the EM-IDMS equation is applied on the peptide level. The most popular enzyme of choice for the quantitative digestion of macromolecules is trypsin. High-purity trypsin is available in sufficient quantity and produces reproducible results. Trypsin cleaves the peptide chain at the carboxylic side of arginine and lysine (unless they are followed by a proline). [148] As tryptic peptides originating from within the peptide sequence always contain a basic residue at the C-terminus they are predominantly observed as doubly charged species in positive ESI. The majority of the ions are often concentrated in one or two charge states only. This quality ensures maximum signal intensity when measured at low concentrations. The small size of the produced tryptic peptides makes them more likely to be amenable to SPPS in high purity and without a large number of deletion products. The impurities are relatively easy to separate from the main compound by LC and the determination of their sequence by MS/MS is possible.

Neither of the above mentioned quantification approaches is able to distinguish impurities from the main compound which can lead to overestimation of the assigned concentration. Breaking down peptides and proteins into their constituents (amino acids or peptides) also means that information about their secondary, tertiary or quaternary structure that determines biological activity in their natural environment is lost.

In this chapter the SI-traceable quantification of BNP is described. BNP was quantified using two different sets of amino acid CRMs and after tryptic digestion using its SI-traceable quantified signature peptides. New methods were tested for the reduction or

accurate estimation of the amount of peptidic impurities to avoid inaccuracies in the amino acid results. At the end of the chapter a fit for purpose method for the purity assessment of large synthetic peptides is proposed.

Chapter 3.2 Results and Discussion

Chapter 3.2.1 Amino acid analysis of BNP and signature peptide standards

In 2010, a method for the SI-traceable quantification of peptide standards via amino acid analysis was developed at LGC (Teddington, UK) and validated through the CCQM-P55.1 study organised by the BIPM. [149], [150] The study covered the traceable quantification of peptides of unknown purity in solution containing a maximum of 10 amino acid residues. Peptide hydrolysis traditionally takes place in vacuum at 110 °C for 24-56 hours. [151], [95], [129] The microwave-assisted vapour phase acid hydrolysis method developed by LGC reduced the required reaction time to three hours by increasing the temperature of the hydrolysis to 165 °C. As the rate of the reaction doubles with every 10 °C increase in the temperature, higher operating temperatures are desirable to reduce hydrolysis time. Due to pressure limitations of the CEM microwave instrument used for the CCQM-P55.1 study any further increase of the hydrolysis temperature was not possible. In 2012 the CEM instrument was replaced and a new method was developed using a MILESTONE ETHOZ EZ Microwave Digestion System. Because of the robust design of the hydrolysis kit, the new system allowed the use of temperatures up to 190 °C. At 190 °C the complete release of the amino acid residues was achieved in 30 min. The short hydrolysis time also prevented any degradation of the released amino acids before analysis.

BNP and the signature peptides of BNP (MVQGSGCFGR and ISSSSGLGSK)were quantified by amino acid analysis. BNP contains eight of the nine amino acid residues amenable to vapour phase acid hydrolysis providing excellent coverage of its sequence (60 %). The signature peptides contain six and five stable amino acid residues, respectively. The amino acid sequences of BNP and the signature peptides used in this study are displayed in Figure 3:2.

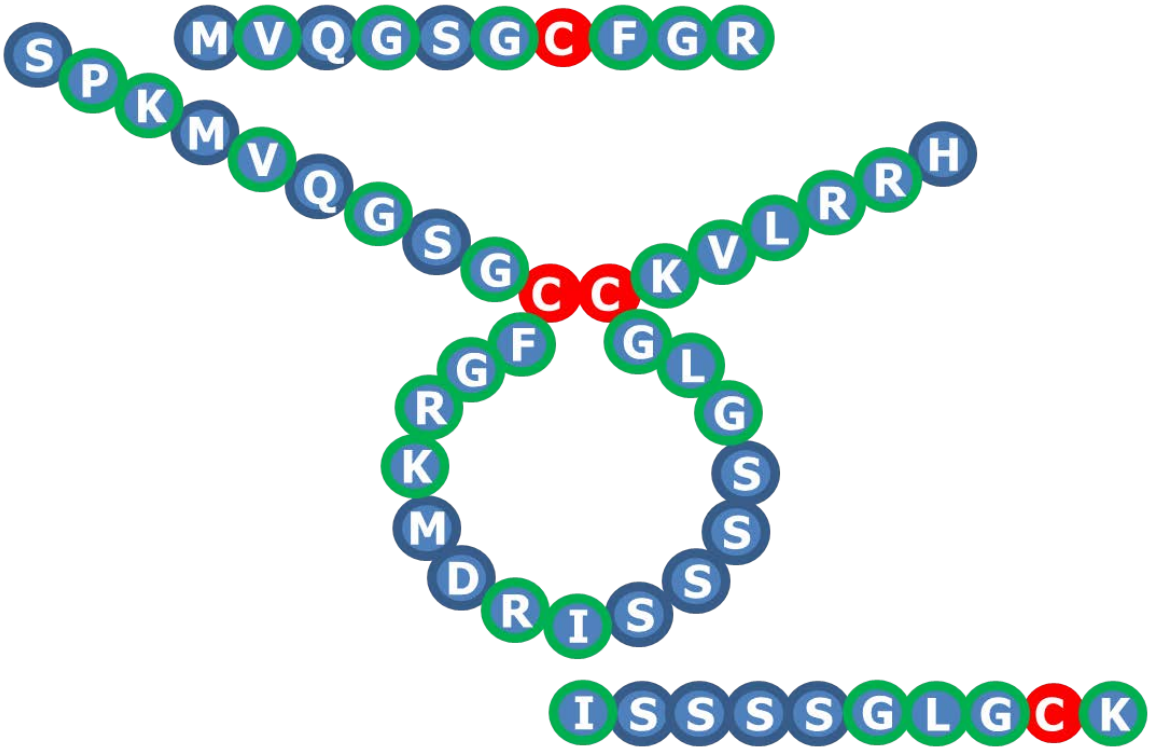

Figure 3:2. Amino acid sequences of BNP and two of its signature peptides after disulphide cleavage. Amino acids amenable to acid hydrolysis and used for SI-traceable value assignment are highlighted in green.

The SI-traceable quantification of BNP and its signature peptides was first performed against the NIST standard reference material SRM 2389a. [152] This NIST standard contains equimolar amount of seventeen amino acids in aqueous hydrochloric acid solution (100 mM). Amino acid quantification by exact matching isotope dilution mass spectrometry (EM-IDMS) requires the same amount of amino acids in the standard as is released from the peptide. Because the SRM 2389a contains amino acids in equimolar

amounts, exact matching of the correct molar ratios for the amino acids in BNP and the signature peptides was not directly possible. Therefore, individual amino acid standards were sourced from a commercial supplier and, to maintain SI-traceability, their concentration was determined *in-house* against the NIST amino acid SRM 2389a. For the EM-IDMS experiment two blends were prepared for each peptide gravimetrically. The calibration blend contained the *in-house* SI-traceable quantified amino acids mixed with isotopically labelled amino acids. The molar ratio of the amino acids was matched with the respective peptide sequence (e.g. ISSSSGLGCK: I, 2xG, L, K). The sample blend contained the peptide solution spiked with the same isotopically labelled amino acids as the calibration blend. Quantification of the peptide stock solutions was performed on three different days. Two aliquots of the BNP stock, MVQGSGCFGR and ISSSSGLGCK peptides were hydrolysed each day. The results for the signature peptides and BNP are displayed in Figure 3:3.

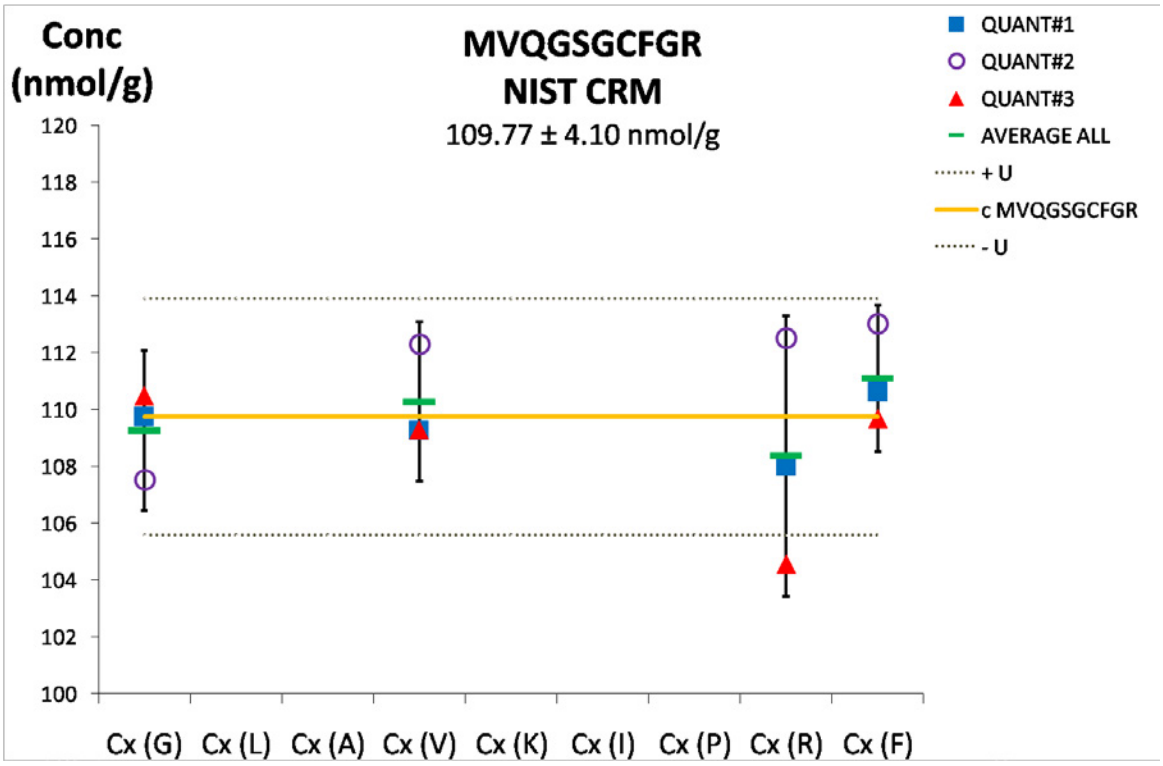

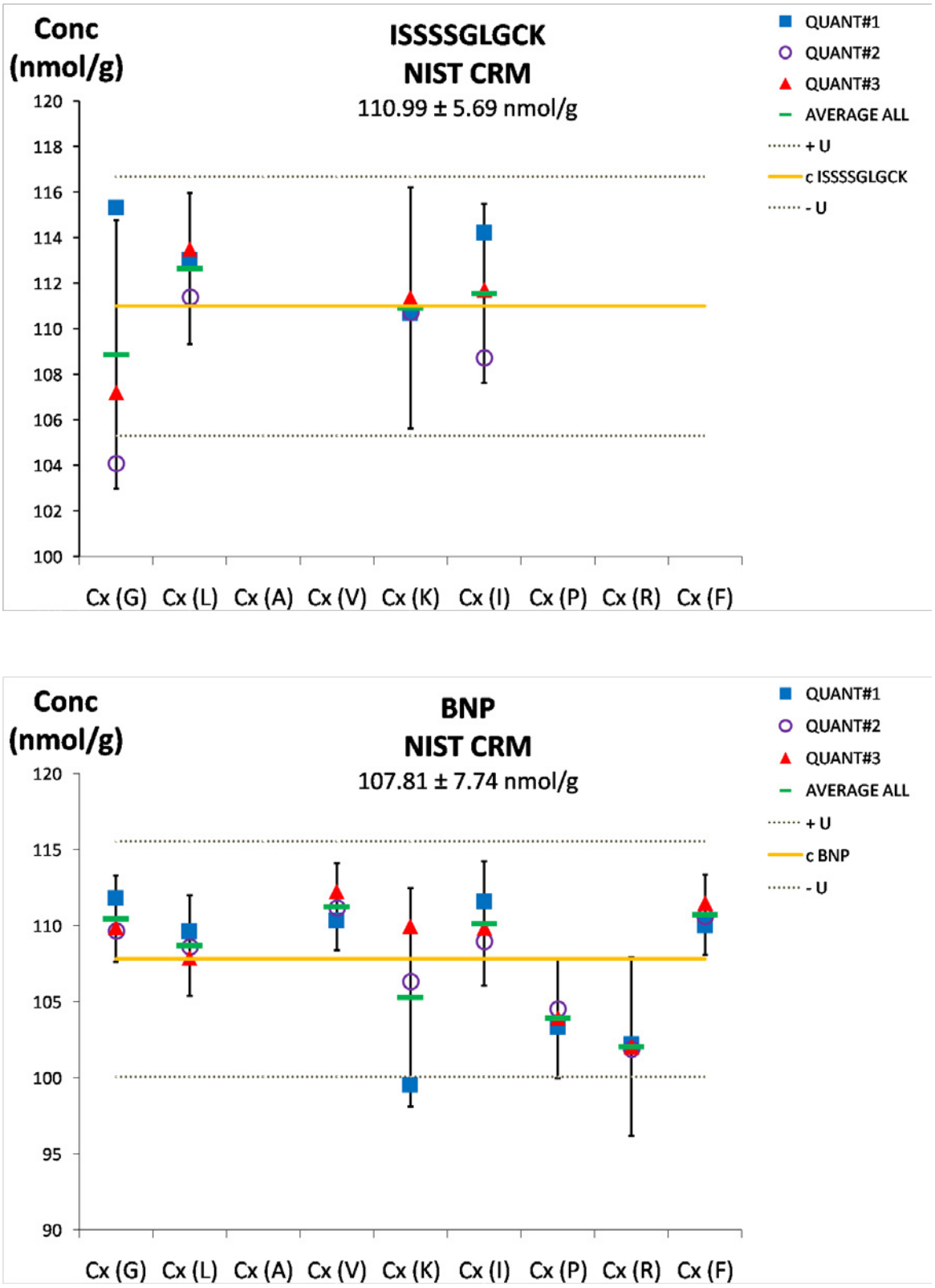

Figure 3:3. SI-traceable amino acid concentrations for the signature peptides (MVQGSGCFGR, ISSSSGLGCK) and BNP. Results are traceable to the NIST SRM 2389a. Each point represents the average of two results from each hydrolysis experiment. Error bars are the uncertainties of the individual amino acid results calculated by Equation 3:2.

Uncertainties associated with lysine and arginine concentrations are larger due to the instability of the derivatives. Trimethylsilyl derivative of arginine decomposes to ornithine and the derivative of the amine group on the side chain of lysine is unstable. [153] While the internal standard compensates for such degradation, peak broadening of the late eluting peaks and loss of sensitivity had a detrimental effect on the ratio precision of the measurement and led to higher uncertainties. The relative standard uncertainty of the amino acid concentrations in the NIST SRM was in the range of 1.39 - 7.43 %. [154] The uncertainties of the individual results are dominated by the uncertainty of the NIST amino acid SRM that was used to confirm the concentration of the commercially sourced amino acid stocks. Apart from the instability of arginine and lysine derivatives, the robustness of the GC-MS method was affected by the batch-to-batch variability of the derivatising agent. The inconsistent quality of the BSTFA reagent used in the original method necessitated the development of a GC-MS method for alternative amino acid derivatives. Transitions and separation conditions were determined using N-*tert*-butyldimethylsilyl-N-methyltrifluoroacetamide (MTBSTFA). MTBSTFA derivatives are ten thousand times more stable than their trimethylsilyl counterparts. The higher boiling point of the derivatives also improved resolution between the amino acid residues in the GC-MS experiments.

In 2015 the National Measurement Institute of Japan (NMIJ) released 17 individual pure amino acid primary standards with a relative standard uncertainty of 0.2 %. [136] Using the solid amino acid primary standards allowed the preparation of calibration solutions in the correct molar ratio and eliminated the need for SI-traceable concentration assignment of *in-house* calibrators. The BNP primary material was subsequently re-quantified using the NMIJ amino acid standards and MTBSTFA derivatization reagent. The determined concentration for the BNP using the newly available NMJI standards agreed

with the previous quantification data within the stated uncertainties. The concentration of the individual amino acid results determined by EM-IDMS using the NMIJ standards is displayed in Figure 3:4.

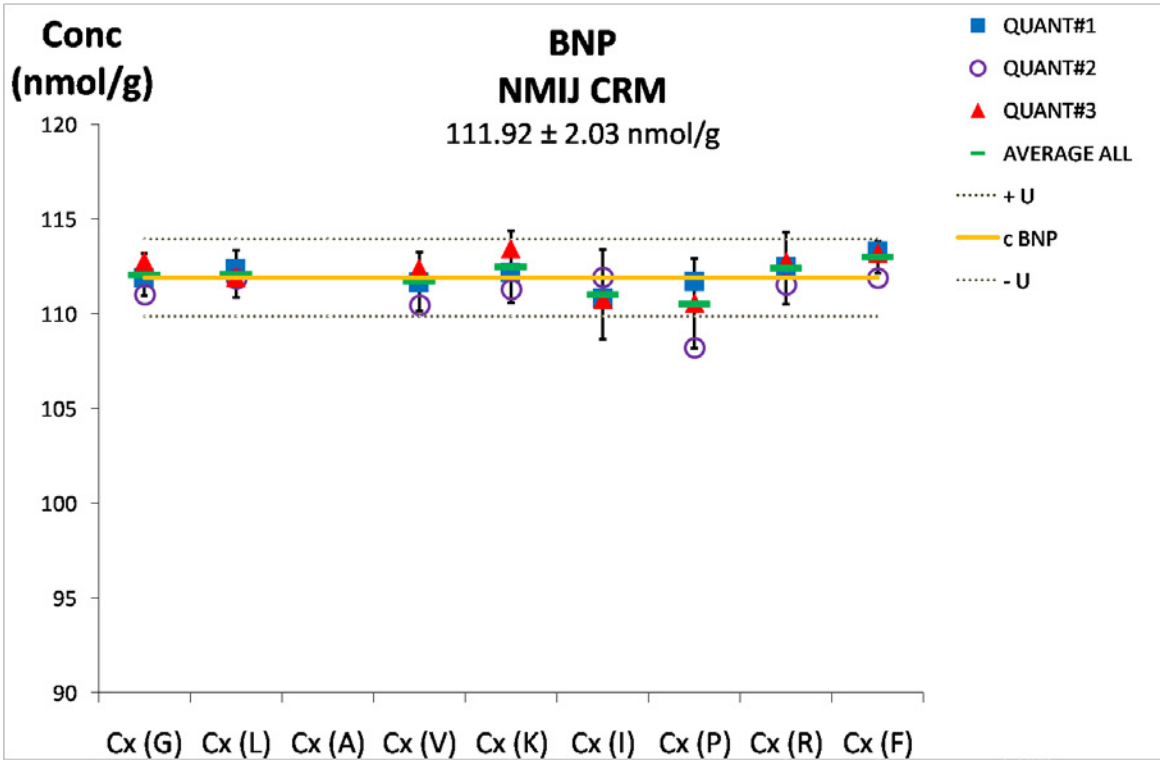

Figure 3:4. SI-traceable amino acid concentration values assigned by certified individual amino acid calibrators supplied by the NMIJ to the BNP primary standard. Each point represents the average of two results from each hydrolysis investigation. Error bars are the uncertainties of the individual amino acid results calculated by Equation 3:2.

Differences in the assigned uncertainty for the quantification results highlight the importance of the quality of the amino acid reference materials. Using individual high purity solid amino acid CRMs the expanded uncertainty (U, k=2, 95 % confidence level) of the SI-traceable concentration of BNP was reduced from ± 7.1 % to ± 1.8 %. (Chapter 3.2.3 Uncertainty calculations)

Chapter 3.2.2 Tryptic digestion of BNP

To increase the confidence in the determined SI-traceable concentration, the BNP primary stock was also quantified by IDMS applied on the peptide level following tryptic digestion. The signature peptides were sourced and quantified by amino acid analysis using *in-house* calibrators as described in Chapter 3.2.1. Peptides with isotopically labelled amino acids incorporated in their sequence were also purchased and used as internal standards. BNP produces two tryptic peptides which are long enough to be unique for the parent peptide (ISSSSGLGCK and MVQGSGFGR). These signature peptides are amenable to amino acid analysis but not ideal for quantification because they contain amino acids susceptible to post-translational modifications. The presence of cysteine and methionine require special precautions during the digestion and quantification experiments. The standard method for reduction of disulfide bridges involves heating to 60 °C with the reducing agent for an hour. Preliminary experiments with BNP indicated that these conditions lead to degradation of BNP. The reduction temperature was subsequently reduced to 37 °C. The alkylation agents were added in large excess to prevent the formation of dimers between the peptides with reduced cysteine residues. The release of the peptides was monitored by performing a digestion time course experiment. For the time course experiment four aliquots of the buffered pre-digestion BNP solution were spiked with the labelled synthetic peptides ISSSSG*L*GCK and MVQGSGCF*GR (*:^{13}C and ^{15}N enriched amino acids) and digested with trypsin. One aliquot was analysed after 2, 4, 18 and 20 hours. Fresh trypsin was added after 2, 4 and 18 hours. The samples were analysed on the Agilent Q-TOF instrument to determine digestion kinetics and to confirm equimolar release. The ratios were determined from integrating the extracted ion chromatograms of the doubly charged ions of the unlabelled

and labelled peptides. The equimolar release of the peptides was achieved after two hours of digestion and oxidation of the methionine residue in MVQGSGCFK was detected after four hours. Two-hour digestion was therefore adopted for the quantification experiments with the addition of trypsin at the beginning and after an hour. The two signature peptides quantified with the *in-house* calibrated amino acid standards were used for the quantification of BNP after tryptic digestion. The BNP concentration determined by the three methods is summarised in Figure 3:5.

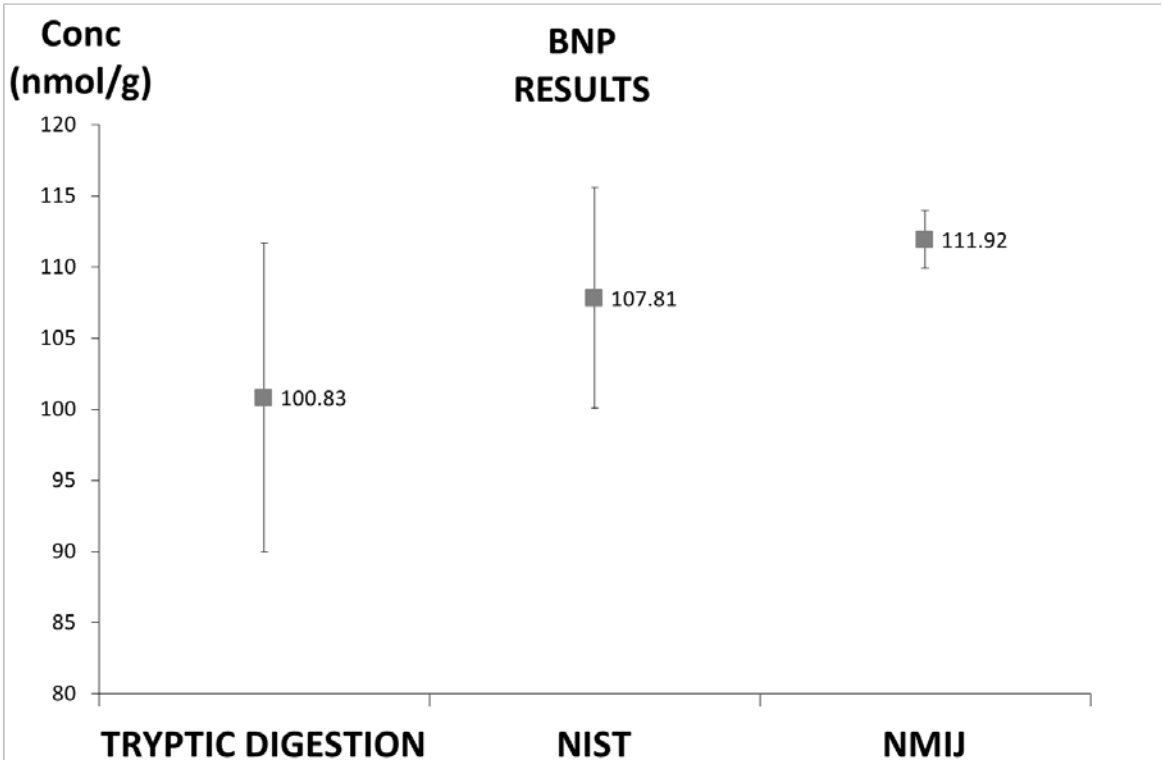

Figure 3:5. Quantification results for BNP, using the isotopically labelled synthetic peptides ISSSSG*L*GCK and MVQGSGCF*GR and tryptic digestion of the mixture and the results obtained by amino acid analysis using the NIST SRM 2389a and individual amino acid standards from the NMIJ. (see text for further information) The error bars represent the calculated combined expanded uncertainty (U) (*k*=2, at 95 % confidence level).

The BNP amino acid results agree with the result obtained from the signature BNP peptides within their uncertainties. The uncertainty of the amino acid measurement was greatly reduced when individual amino acid standards were used from NMIJ.

Development of BNP standard

Commercially available synthetic peptides used in this study are supplied in 95-98 % purities. The certificate of analysis provided by the manufacturer normally contains an LC-UV trace where the purity is calculated as the percentage area of the main peak compared to the sum of the total peak areas. When the peptides were received the peptide weights stated on the certificates were corrected with the purities and used to calculate the nominal concentrations for the stock solutions using the average molecular weights, i.e. 1 mg MVQGSGCFGR was made up in 10 mL water to give a concentration of 96.0 nmol/g. The nominal and SI-traceable concentrations are tabulated in Table 3:2.

Table 3:2. Nominal and SI-traceable concentrations of the synthetic peptide standards.

Sequence	Nominal Concentration (nmol/g)	AA Results (nmol/g)	U (*k*=2)
MVQGSGCFGR	96.0	110.1	3.1
ISSSSGLGCK	106.5	111.5	4.5
SPKMVQGSGCFGRKMDRISSSSGLGCKVLRRH NIST	57.7	107.8	7.7
SPKMVQGSGCFGRKMDRISSSSGLGCKVLRRH NMIJ	57.7	111.9	2.0
SPKMVQGSGCFGRKMDRISSSSGLGCKVLRRH EM-IDMS SIGNATURE PEPTIDES	57.7	100.8	10.8

NIST: results obtained with NIST SRM2389a; NMIJ: results obtained with the individual NMIJ amino acid standards; SIGNATURE PEPTIDES: results obtained with the signature peptides after enzymatic digestion, U: expanded uncertainty, *k*: coverage factor at 95 % confidence level.

For BNP, the determined concentration is almost twice of what was expected. Without amino analysis or a certified reference material to assign accurate concentration to calibrators a significant bias can be introduced into quantification results based on commercially available synthetic peptides.

Chapter 3.2.3 Uncertainty calculations

The standard and combined uncertainties were calculated in accordance with ISO Guide to the Expression of Uncertainty in Measurement [155] and EURACHEM guidelines [156].

The peptide concentration values determined by amino acid analysis ($w_{peptide}$) were calculated by averaging the individual amino acid results (w_{AAP}). The uncertainty (u) of the individual amino acid results, associated with the exact matching IDMS values were calculated according to Equation 3:2.

$$u_{w_{AAP}} = w_{AAP}\sqrt{\left(\frac{u_{w_{AA}}}{w_{AA}}\right)^2+\left(\frac{u_{m_y}}{m_y}\right)^2+\left(\frac{u_{m_x}}{m_x}\right)^2+\left(\frac{u_{m_z}}{m_z}\right)^2+\left(\frac{u_{m_{yc}}}{m_{yc}}\right)^2+\left(\frac{s_{\frac{R'_B}{R'_{BC}}}}{\sqrt{n}}\right)^2}$$

Equation 3:2. Uncertainty calculated for the exact matching isotope dilution equation, where the standard uncertainty (u) for each amino acid concentration is expressed as the concentration of the amino acid in the hydrolysed peptide (w_{AAP}) and multiplied by the square root of the sum of the variances of uncertainty contributions from the EM-IDMS equation. Equation 1:6.

w_{AA}	Amino acid standard concentration (NIST SRM or NMIJ CRM)	m_{yc}	mass of the labelled amino acid standard added to the calibration blend
w_{AAP}	Amino acid concentration determined in the hydrolysed peptide	R'_B	measured ratio (unlabelled peak area/labelled peak area) in the sample blend
m_x	mass of the peptide used	R'_{BC}	measured ratio (unlabelled peak area/labelled peak area) in the calibration blend
m_y	mass of the labelled amino acid standard added to the sample blend		
m_z	mass of the unlabelled amino acid standard added to the calibration blend		

Each sample blend was injected five times. The standard deviation of the mean of the measured ratio was used to calculate the uncertainty associated with instrument variability.

The uncertainty arising from sample preparation and hydrolysis was then combined using Equation 3:3 to give the combined uncertainty for the assigned peptide concentration (u_{peptide});

$$u_{peptide} = \sqrt{\left(\frac{\overline{u(w_{AAP})}}{w_{AAP}}\right)^2 + \left(\frac{s_{w_{peptide}}}{\sqrt{n}}\right)^2}$$

Equation 3:3. Calculation of the combined uncertainty of the determined peptide concentration w_{peptide}.

Peptide concentration uncertainty was calculated by taking the square root of the sum of the squares of the average standard uncertainty of the stable amino acid results and the standard deviation of the mean of the calculated peptide concentrations, where '*n*' represents the number of samples used for quantification (n=6). Finally, the uncertainty was expanded using a coverage factor value of two (*k*=2) to give the final uncertainty (*U*) with a 95 % confidence.

The uncertainty of the BNP stock after enzymatic digestion was calculated in the same way as after hydrolysis using the assigned concentration and uncertainty values of the signature peptide standards instead of amino acids.

Chapter 3.2.4 Qualitative assessment of signature peptide standards

The identity of the signature peptides and isotopically labelled internal standards was confirmed by exact mass using MALDI-TOF MS and LC-Q-TOF MS. MALDI-TOF MS experiments were performed on equimolar mixtures of the unlabelled and labelled form of the reduced and alkylated signature peptides. The resulting mass spectra are displayed in Figure 3:6 and Figure 3:7.

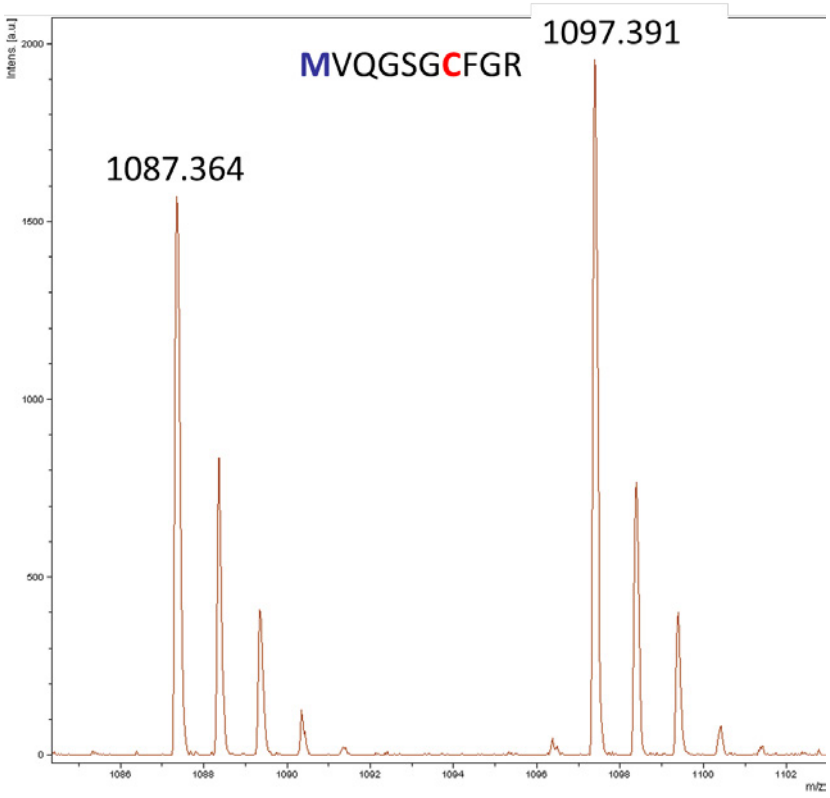

Figure 3:6. MALDI-TOF mass spectrum of alkylated (-S-CH_3) signature peptide MVQGSGCFGR (*m/z* 1087.448), and the internal standard MVQGSGCF*GR (*m/z* 1097.475). ( ): Monoisotopic *m/z* values *: amino acids containing ^{13}C and ^{15}N isotopes.

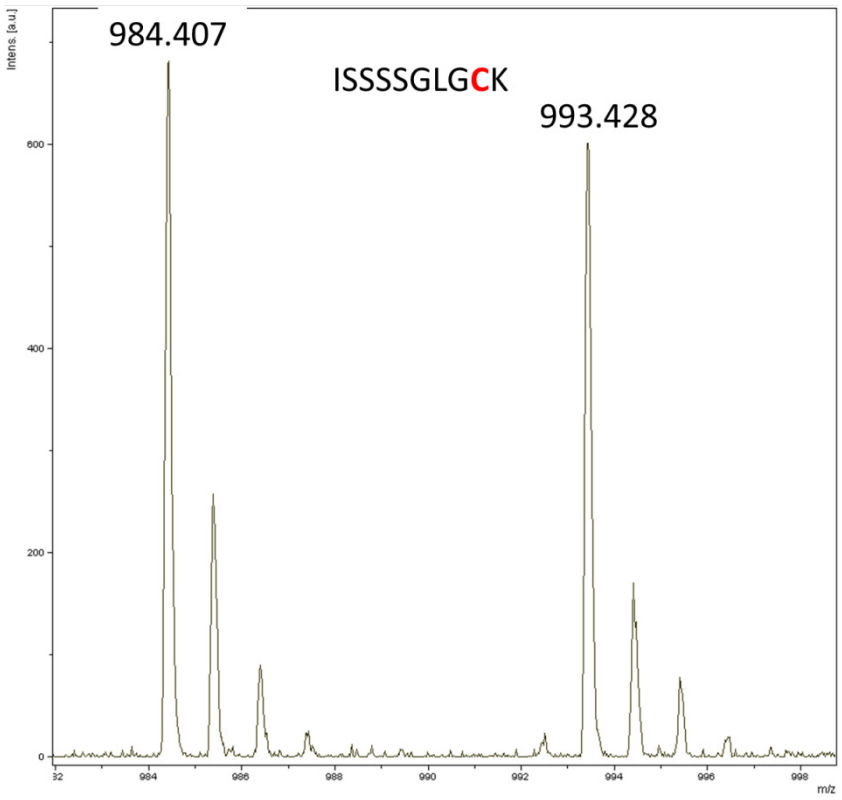

Figure 3:7. MALDI-TOF mass spectrum of alkylated (-S-CH_3) signature peptide ISSSSGLGCK (m/z 984.470) and the internal standard ISSSSG*L*CK (*m/z* 994.470). ( ): Monoisotopic *m/z* values: *: amino acids containing ^{13}C and ^{15}N isotopes.

The labelled internal standard for the ISSSSGLGCK peptide displayed an incorrect mass in the MALDI-TOF and ESI-Q-TOF spectra. Isotopically labelled glycine and leucine (G($^{13}C_2$, ^{15}N), L($^{13}C_6$, ^{15}N)) was requested to be incorporated into the sequence to result in a mass difference of + 10 Da relative to the unlabelled peptide.

The sequence of the signature peptides was confirmed by MS/MS using an Agilent Q-TOF 6530 instrument coupled with liquid chromatography. All y-ions were present in the MS/MS spectrum for the unlabelled peptides. MS/MS sequencing of the labelled peptide confirmed that the leucine residue was not enriched with the ^{15}N isotope. The ESI-Q-TOF MS/MS spectrum and the identification of the peptide fragments are displayed in Figure 3:8.

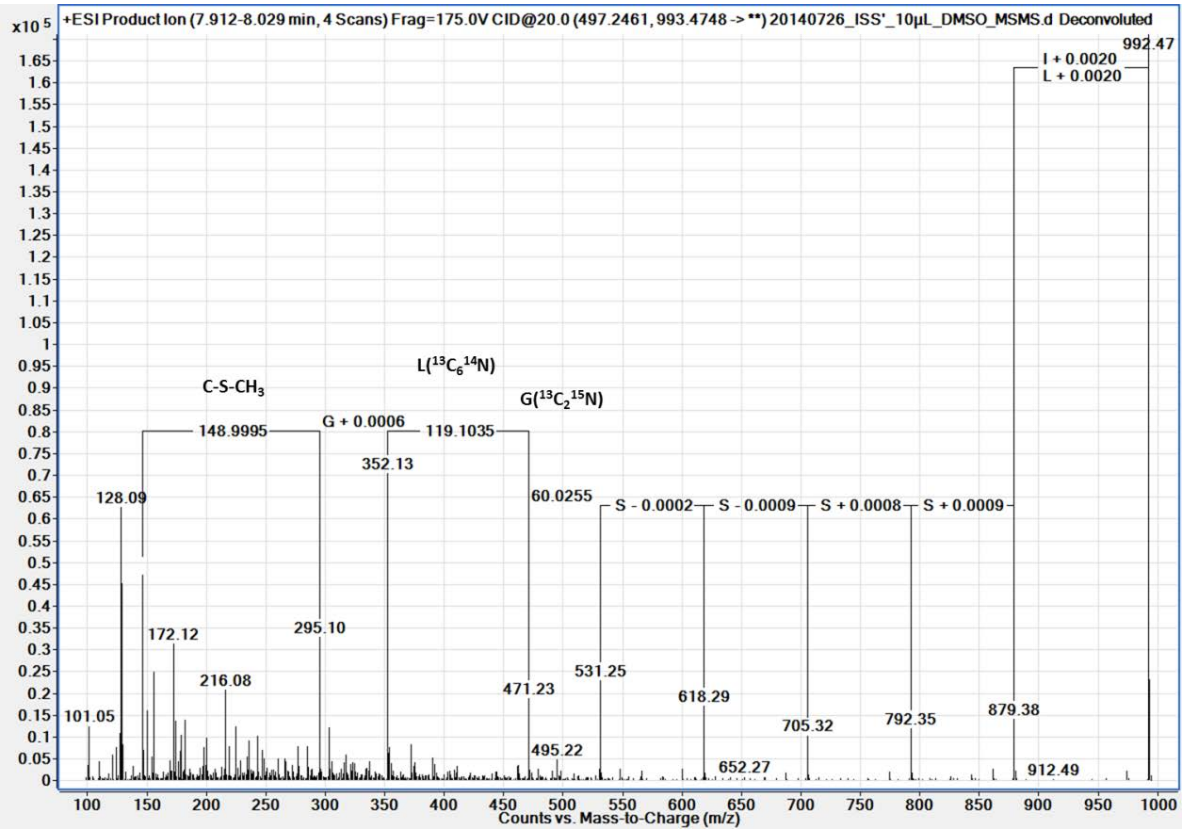

Figure 3:8. Deconvoluted ESI-Q-TOF MS/MS spectrum of the alkylated (-S-CH_3) peptide ISSSSG*L*GCK obtained on the Agilent 6530 Q-TOF instrument. CID voltage 20 eV.

The 1 Da difference was not readily identified for the doubly charged peptide ion on the quadrupole instrument used for the quantification of the BNP stock solution because of the lower resolution of quadrupole analysers.

Chapter 3.2.5 Purity assessment of BNP

The initial assessment of the primary BNP stock was performed by the evaluation of the high-resolution MS spectrum of high-concentration standards recorded using nano-flow LC-ESI-Q-TOF MS. The nano-flow LC chromatogram of the primary BNP stock is displayed in Figure 3:9.

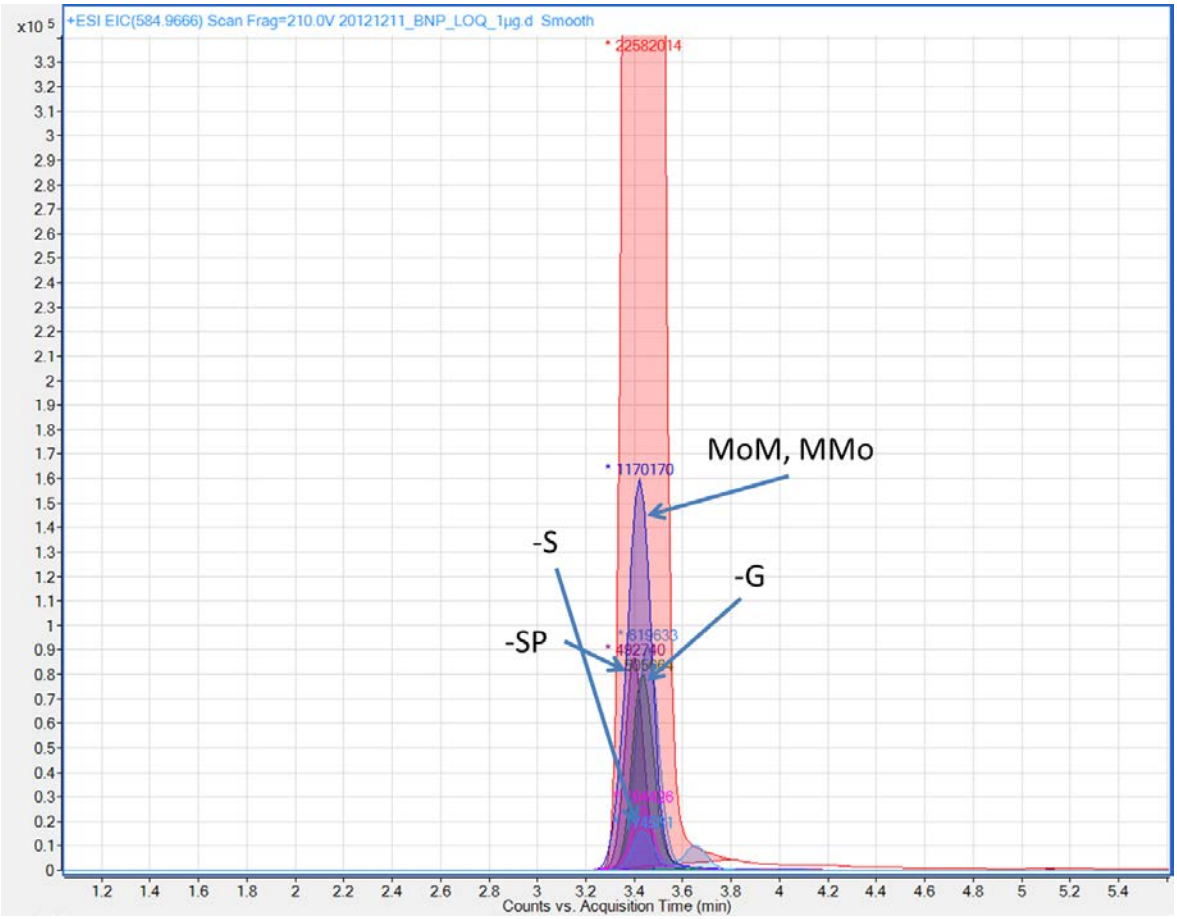

Figure 3:9. Nano-flow LC-ESI MS chromatograms of the primary BNP stock. Extracted ion chromatograms of the identified impurities (± 10 ppm of the monoisotopic *m/z* peaks)are displayed. MoM: methionine sulfoxide in position 4. MMo: methionine sulfoxide in position 15. -S: one serine residue, -G one glycine residue, -SP: a serine and a proline residue missing from the sequence.

The impurities were confirmed by exact mass and their relative amount estimated by comparing the area of the integrated extracted chromatograms to the main peak. The main impurities are deletion products of the sequence (-SP, -G, -S) and oxidation of methionine residues in the stock solution. Because the highest-intensity charge state observed for BNP was 6+, only impurities with a 6+ charge state produced detectable signals. The resolution of the Q-TOF instrument is 20,000. This is sufficient to distinguish differences of ≥12 Da in molecular weight for the 6+ charge state of the potential impurities or post-translational modifications. Oxidised methionine was detected but was not fully resolved in the mass spectrum due to saturation of the detector with the intact

BNP ions. MS instruments using ESI sources can produce different signal intensities for the main compound and the impurities depending on ionisation behaviour of the analytes. Without the use of isotopically labelled internal standards purity estimation by ESI-Q-TOF MS is not quantitative but gives an estimation of the amount and the identity of the impurities. Due to the close nature of the found impurities they could not be separated on the nano-flow LC system. The lack of baseline separation of the impurities leads to the overestimation of their relative amount. Products of in-source fragmentation of BNP can also be incorrectly identified as coeluting impurities.

At the method development stage the BNP stock was quantified by the *in-house* calibrated amino acid standards and the assigned uncertainty was ± 7.18 %.The purity assessment of the primary stock showed that the total amount of peptidic impurities was below 6 %. Therefore any differences caused by their presence are encompassed in the assigned uncertainty value. When the BNP stock standard was re-quantified against the NMIJ amino acid standards the uncertainty for the determined concentration was reduced to ± 1.8 %. An optimised LC separation for the oxidised methionine species was also available and investigated. (Chapter 4.3.1.1). The purity assessment of the BNP stock was repeated with the LC conditions developed for the reference method. A gradient from 1-20 % ACN (0.5 % FA) was used in 20 minutes. The resulting chromatogram is displayed in Figure 3:10.

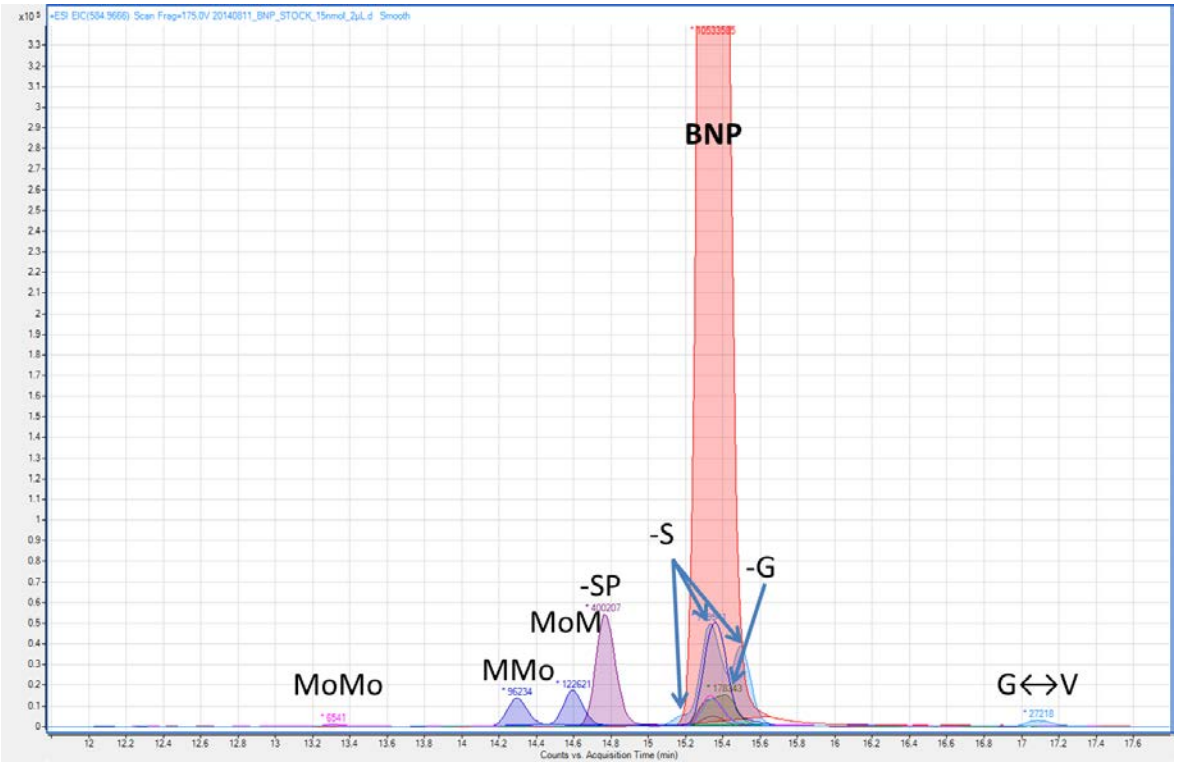

Figure 3:10. Normal flow LC-ESI ion chromatograms of the primary BNP stock with a gradient of 1-20 % ACN (0.5 % FA) in 20 minutes. Extracted ion chromatograms of the identified impurities (± 10 ppm of the monoisotopic *m/z* peaks) are displayed. MoM: methionine sulfoxide in position 4. MMo: methionine sulfoxide in position 15. MoMo: methionine sulfoxide in position 4 and 15. -S: one serine residue, -G one glycine residue, -SP: a serine and a proline residue missing from the sequence.

Baseline separation of the BNP molecules that contain methionine sulfoxide allowed the more accurate determination of their relative amount (< 1 %). The impurity missing the first two amino residues (-SP) was also separated chromatographically confirming that it is not a product of in-source fragmentation. The relative area of this impurity was ≅ 1.6 %. The determined amino acid concentration was lower for proline, indicating the presence of the impurity missing -SP. (cf. Figure 3:4). Impurities missing one serine and one glycine from the sequence were also detected and separated but not fully resolved under the conditions utilised. A small amount of an additional impurity corresponding to a mass difference of + 42 Da was found (< 0.1 %). The 42 Da mass difference agrees with an acetylated BNP impurity or a valine/glycine amino acid replacement in the sequence. In an attempt to further increase chromatographic resolution, the elution gradient was

reduced by increasing the ACN composition of the mobile phase from 1 % to 20 % in 40 minutes. (Figure 3:11)

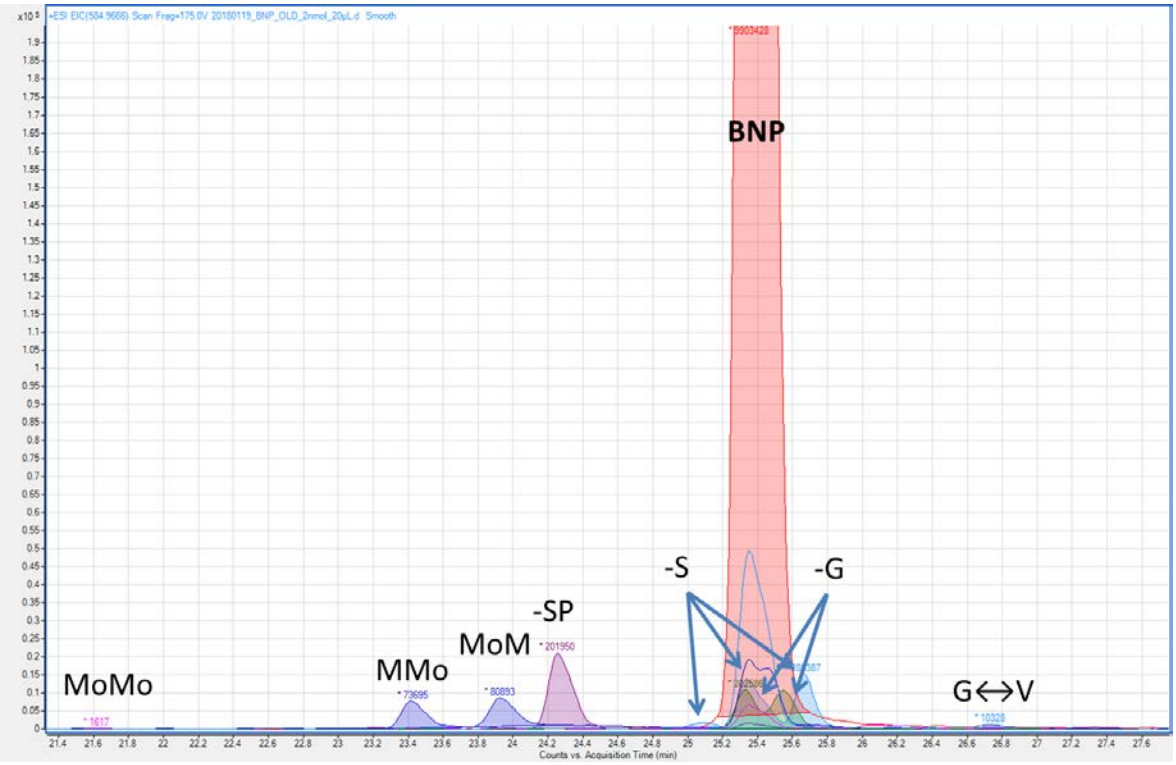

Figure 3:11. Normal flow LC-ESI ion chromatograms of the primary BNP stock with a gradient 1-20 % ACN (0.5 % FA) in 40 minutes. Extracted ion chromatograms of the identified impurities (± 10 ppm of the monoisotopic *m/z* peaks) are displayed. MoM: methionine sulfoxide in position 4. MMo: methionine sulfoxide in position 15. MoMo: methionine sulfoxide in position 4 and 15. -S: one serine residue, -G one glycine residue, -SP: a serine and a proline residue missing from the sequence.

The separation improved between the oxidised methionine species and for the impurities missing a single amino acid residue (G, S). The relative area of the impurities missing a glycine and a serine was ≅ 2.3 % and 1.5 % respectively. The extracted ion chromatograms suggest that there are three isobaric impurities present missing one serine and two impurities missing one glycine residue from the sequence. BNP contains six serine and five glycine residues. Methionine and serine are not amenable to amino acid quantification as they are not stable during acid hydrolysis but the signature peptides used for quantification (MVQGSGCFGK and ISSSSGLGCK) include one of the methionines and five of the serine residues increasing the coverage of the BNP sequence from 60 % to

87.5 %. The agreement between the results obtained with the signature peptides and with amino acid analysis increases the confidence in the assigned SI-traceable concentration value. For the development and validation of the LC-ESI MS/MS reference method the results obtained by the NMIJ amino acid standards were used. It is reasonable to assume that the concentration uncertainty incorporates the differences caused by the small amount of impurities present in the BNP stock.

Chapter 3.2.6 Purification

Current metrological approaches for the quantification of peptide-related impurities are based on the correction of the amino analysis results (PICAA) with the amount of peptidic impurities and quantification of the amount of the impurities by external calibration using the “mass balance” approach. The availability of authentic impurity standards is limited; therefore alternative ways of assigning purity to synthetic peptide solutions is desirable. One option is to reduce the number of impurities present by purification.

To investigate the feasibility of an adequate purification approach, a new batch of synthetic BNP was acquired from Phoenix Pharmaceuticals LTD (Phoenix stock) and analysed by LC-ESI-Q-TOF MS. An example ion chromatogram of the Phoenix stock with the identified impurities is displayed in Figure 3:12. The amount of impurity of the Phoenix material was higher than in the BNP stock making it an ideal candidate for the purification experiments.

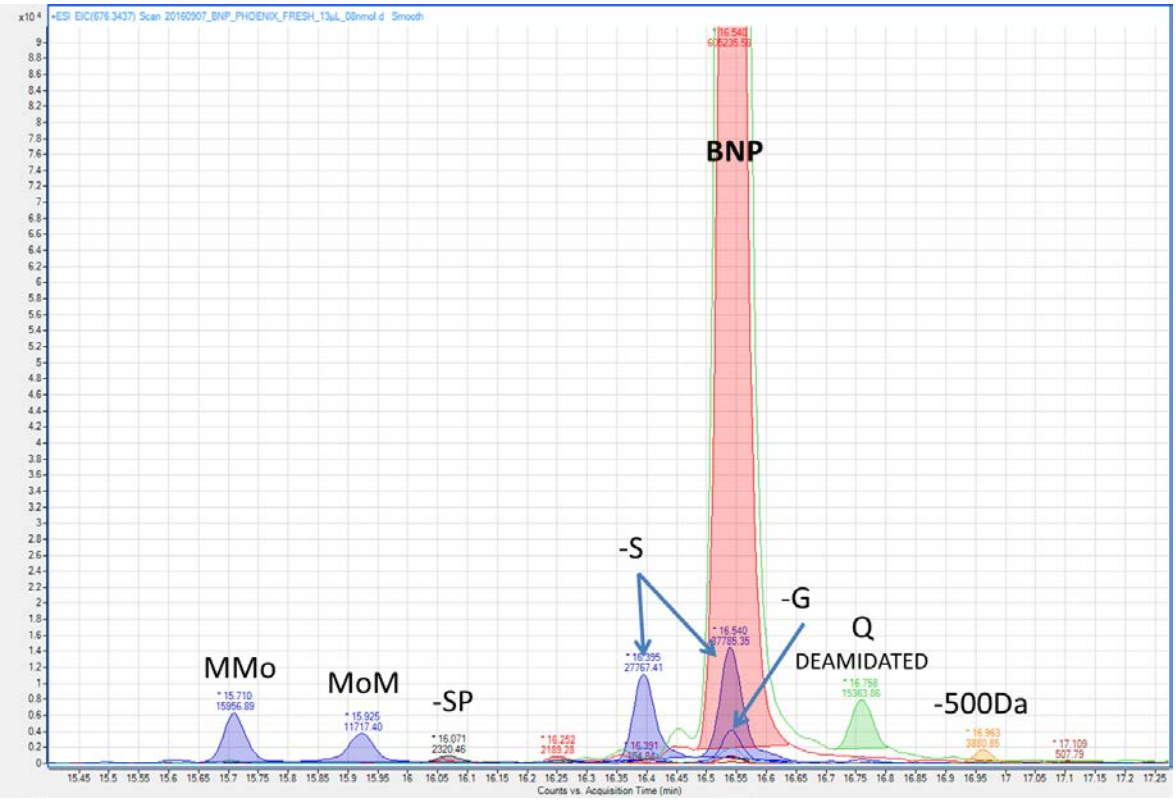

Figure 3:12. Normal flow LC-ESI ion chromatograms of BNP obtained from Phoenix Pharmaceuticals LTD, with a gradient 1-20 % ACN (0.5 % FA) in 20 minutes. Extracted ion chromatograms of the identified impurities (± 10 ppm of the monoisotopic *m/z* peaks) are displayed. MoM: methionine sulfoxide in position 4.MMo: methionine sulfoxide in position 15. MoMo: methionine sulfoxide in position 4 and 15.-S: one serine residue, -G one glycine residue, -SP: a serine and a proline residue missing from the sequence.

In order to maximise the separation between the impurities and BNP, two 25-cm long columns were connected in series and the LC was run with the isocratic composition of 10 % ACN. The full spectrum was monitored and the eluent was collected for 1 min when only BNP was detected in the full MS spectrum. (centre of the peak). 40 µL of the concentrated Phoenix stock was injected ten times. The collected fractions were freeze dried and combined. The chromatogram of the purified Phoenix material is displayed in Figure 3:13. Approximately 20 % of the BNP content was recovered during the LC purification.

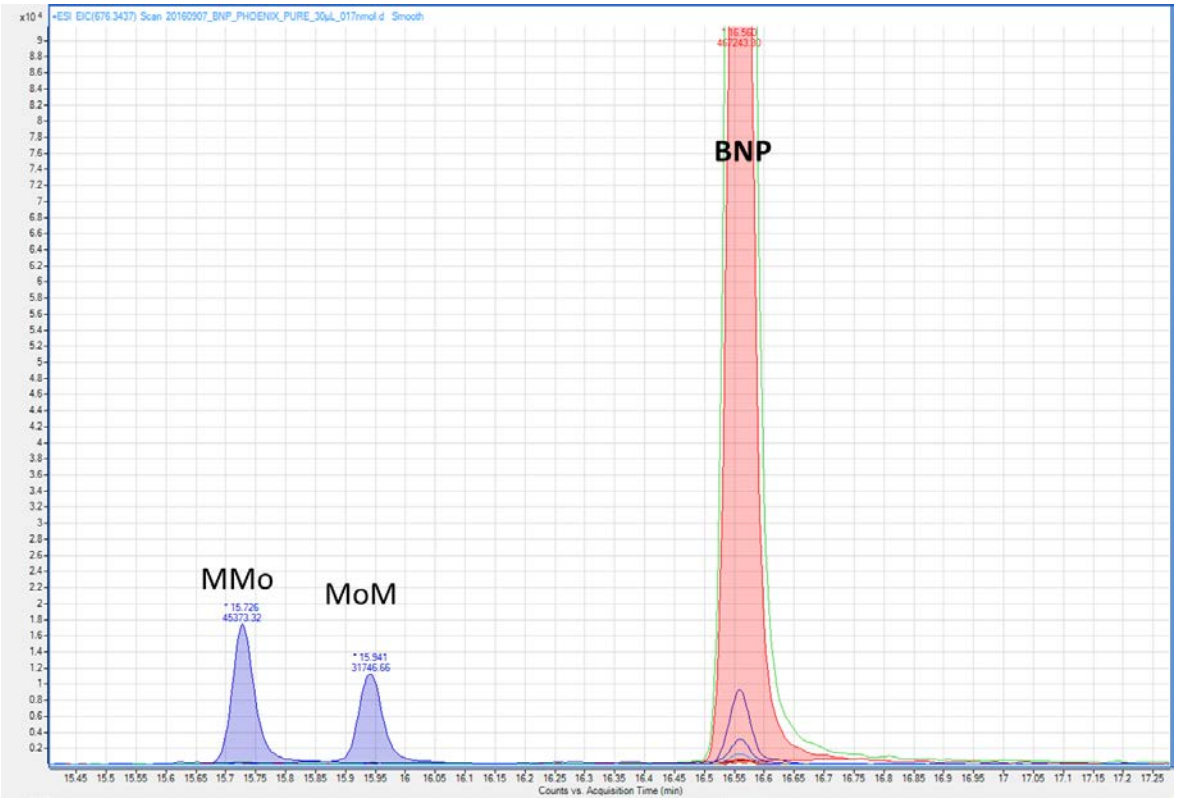

Figure 3:13. Normal flow LC-ESI ion chromatograms of the purified Phoenix BNP with a gradient 1-20 % ACN (0.5 % FA) in 20 minutes. Extracted ion chromatograms of the identified impurities (± 10 ppm of the monoisotopic *m/z* peaks) are displayed. MoM: methionine sulfoxide in position 4.MMo: methionine sulfoxide in position 15.

The purification experiments show that the approach can be used for the production of pure synthetic peptide CRMs, however, further optimisation of the process is required as the manipulation of the standard may introduce post-translational modifications to peptides with unstable amino acid residues in their sequence. In this case an increase in the relative amount of oxidised methionine residues was observed most likely introduced during the freeze drying step of the purified standard material.

Chapter 3.2.7 LC-UV-ESI MS purity estimation

Purity assessment of small organic molecules is normally performed using a number of different chromatographic techniques coupled with universal detectors. (e.g. GC-FID, LC-UV c.f. Table 3:1) The purity of the compound is assigned by integrating all peaks in the resulting chromatogram and calculating the relative area of the main compound to the sum of the integrated areas. The mass fraction is determined by multiplying the weight used for the gravimetric preparation of the standard solution with the relative area percentage of the main peak. Water content, residual solvents, non-volatile and inorganic impurities are determined separately and used to correct the weight of the solid material used to prepare the standard solution.

The assumption is made that all related structure impurities produce a signal in the detector and the response of the detector is the same for the impurities and the main compound, i.e. relative response factor (RRF) equals 1. If the identity of the impurity is known and an impurity standard is available the RRF is determined by comparing the slope of the linear calibration curve obtained with the impurity standard to the slope of the main compound. For synthetic peptides, the amount of solid material is seldom available in sufficient quantities to perform a full purity assessment. The amino acid analysis results can be used to define the concentration of the main component if the concentration and the identity of the impurities are known. As the determined amino acid concentration is a result of all stable amino acids released from the peptide solution, the relative amount of the peptidic impurities is sufficient to calculate their concentration if their sequence is known. It is possible to determine the relative response factors for the impurities without having the solid impurity standards if the linear calibration is performed by injecting increasing amounts of the stock solution. Because the impurities

are normally at very low concentrations compared to the main compound the sensitivity and dynamic range of the detector used for recording the chromatograms must be high. UV is a universal detector that fulfils these requirements but does not provide qualitative information on the nature of the impurities. As UV is non-destructive it is possible to record the UV chromatogram before MS detection to combine the benefits of high dynamic range and molecular selectivity. High-resolution mass spectra and MS/MS sequencing can be used for the identification of the different impurities and UV for the quantification of their relative amounts.

BNP is an excellent example where this approach would be extremely useful. A proof-of-concept study was conducted at LGC and the results are displayed in Table 3:3. Different volumes of the concentrated Phoenix stock were injected in triplicate. The chromatograms were recorded with UV and ESI-Q-TOF MS. The UV traces were integrated and the slopes were determined by linear regression using the injection volumes as independent variables. The slopes are divided by the relative % area to get the response factor (RF) and the response factors relative to BNP were calculated. The purity of BNP was then corrected with the determined RRF values. The purity of the Phoenix stock determined from the relative peak area of the UV chromatogram was found to be 90.98 %.

Table 3:3. Mass fraction assignment of the impurities calculated from the UV trace at each injection level (the slope was calculated from linear regression using injection volumes as x-variable)

Injection (µL)	Relative % Area (average of 3 injections)						
	MMo	MoM	-SP	-S	BNP	Q	-500Da
3	0.23	0.41	0.42	1.84	91.06	4.79	1.25
5	0.34	0.41	0.50	1.75	91.01	4.78	1.20
7	0.31	0.37	0.55	1.72	91.01	4.90	1.14
9	0.36	0.35	0.54	1.70	91.04	4.92	1.07
(m/m) %	0.31	0.39	0.50	1.76	91.03	4.85	1.17
Slope	0.99	0.91	1.53	4.46	242.90	13.23	2.78
Slope/(m/m) %	3.19	2.36	3.05	2.54	2.67	2.73	2.39
RRF	1.20	0.88	1.14	0.95	1.00	1.02	0.89
Corrected m/m %	0.26	0.44	0.44	1.84	90.98	4.74	1.30

MoM: methionine sulfoxide in position 4.MMo: methionine sulfoxide in position 15.MoMo: methionine sulfoxide in position 4 and 15. -S: one serine residue, -SP: a serine and a proline residue missing from the sequence, 500 Da: acetyl BNP 6-32.

Amino acid analysis was performed on the Phoenix stock as previously reported and the individual amino acid results were corrected with the amino acid content of the peptidic impurities. BNP concentration in the Phoenix stock determined from the average of the amino acid results before correction was 151 nmol/g (523 µg/g) after correction the value was 138 nmol/g (476 µg/g, 91.00 %). Although the full validation of this method was not possible further experiments will be conducted on a number of synthetic peptides to validate its applicability for the purity assessment of peptide solutions.

Chapter 3.2.8 Dilution of BNP stock

The determined SI-traceable concentration of the BNP standard is 111.9 ± 2.0 nmol/g. The clinically relevant concentration of BNP in plasma is in the fmol/g range. In order to maintain SI-traceability the quantitative dilution of the quantified stock must be evaluated and confirmed. BNP stock was initially diluted in water when the sensitivity of the instrument was investigated during the development of the reference method.

(Chapter 4) The dilution experiments provided inconsistent results. Repeated injection of the stock solution diluted in water alone resulted in decaying BNP signal detected. No BNP was found after a day when glass autosampler vials were used. BNP contains seven basic residues and has an overall 6+ charge in neutral aqueous medium. The most likely explanation for the drop in signal is that the positively charged peptide binds to the free silanol groups of the glass vials over time. Reduction and alkylation of the disulfide bridge did not improve the reproducibility of the dilution. Decreasing the pH of the dilution medium by the addition of 0.5 % FA and using polypropylene vials allowed the dilution of the stock solution to the 100 pmol/g (350 ng/g) level. Below 100 pmol/g, the addition of a carrier protein was also necessary. [157] Thus, the optimised dilution medium contains 0.05 % bovine serum albumin BSA and 0.5 % FA. All solutions used for the manipulation of BNP in future experiments of the study contained 0.5 % FA.

Chapter 3.3 Conclusions

A synthetic BNP solution was quantified for future use as a primary calibrator as part of the development of a reference method to quantify BNP in plasma. Metrological traceability of the results to the SI was established by relating the concentrations directly to amino acid reference materials by EM-IDMS. The concentration determined by amino acid analysis was confirmed by quantification of BNP using signature peptides after tryptic digestion. Using the two different approaches 87.5 % of the sequence was accurately quantified. Purity assessment of the BNP stock was performed and the peptidic impurities were identified. The relative amount of the found impurities was sufficiently small to be accounted for in the assigned uncertainty of the SI-traceable concentration. Two novel approaches were tested for the production of certified reference materials for BNP. In the first, BNP stock solution was purified. The results show that without sufficient control of

sample handling conditions unintended modifications can occur to peptides that contain unstable amino acid residues during purification. In the second approach the combination of a universal detector with MS was investigated for the identification and accurate assessment of the concentration of peptidic impurities. The relative (detector) response ratios for the impurities can be determined without the use of solid impurity standards, and the determination of the purity of a peptide solution by the evaluation of the UV chromatogram is possible. The SI-traceable concentration of the peptide solution can be determined by PICCA. There are certain limitations to the applicability of the method. The peptide and its impurities must absorb UV light and the impurities must be baseline-separated. The preliminary results are encouraging and further experiments are needed to validate the method for the determination of the purity of potential peptide calibrators.

The ability for National Measurement Institutes to accurately assign purity values to protein and peptide calibrators is a fundamental requirement. Due to the complexity of production and close nature of the potential impurities, establishing SI-traceability for the quantification results of synthetic peptides requires extensive research and is a subject of future metrological trials. The uncertainty determined for the BNP standard solution was deemed fit for purpose for the development of the reference method described in the next chapter.

Chapter 4 Development and validation of a reference method for BNP in plasma

Chapter 4.1 Introduction

Measurement of large biomolecules in plasma by MS is a formidable challenge complicated by a number of issues. Clinical levels of biomolecules are very low and often not within the practical detection limits of mass spectrometers. The structural complexity and high dynamic range of plasma proteins often compete for available charge and can cause (analyte-specific) suppression of ionisation in MS sources. The multiply charged nature of molecular ions generated by ESI is advantageous because it brings the analyte ions into the working range of conventional mass analysers but limit signal abundance at low concentrations as the ions are split between the different charge state populations.

Diagnosis of heart failure is based on two distinct BNP concentration levels. BNP concentration below 100 pg/g rules out heart failure with 98 % sensitivity (true positive rate) and BNP concentration above 500 pg/g confirms heart failure event with 92 % specificity (true negative rate). Table 1:2. Over the past decade a number of papers have been published on the development of methods for the quantification of BNP by MS. [123], [158]–[162] The gap between the sensitivity limitation of MS and the low levels of circulating BNP in plasma was bridged by using immunoaffinity enrichment of BNP by selective capture antibodies, large volume sample injections or performing quantification after enzymatic digestion (i.e. using signature tryptic peptides). [123], [158], [160], [162]

The MS methods used for the quantification of *intact* BNP in plasma are listed in Table 4:1. In 2005, Hawkridge *et al.* used nano-LC-ESI-FT-ICR MS for the quantification of intact BNP in patient samples. [158] The authors used bulk plasma spiked with commercially available BNP standard to develop an immunoaffinity enrichment method and a custom-

synthesised isotopically labelled internal standard for quantification. To reach the required levels of sensitivity, 1 mL of plasma was used for the capture of BNP. The eluent containing the released BNP was filtered, lyophilised and reconstituted in 50 µL of 0.0001 % Zwittergent 3-16. The entire volume of the reconstituted extract (50 µL) was injected on a nano-LC column. The robustness of the system was affected by the quick deterioration of the column because of the presence of high-abundance proteins (e.g. albumin) in the immunoprecipitated samples. Only the most intense 5+ charge state of BNP was observed at low concentrations and there was no BNP detected in the patient samples even though the immunoassay readings were above 420 fmol/mL. In a bid to overcome the disconnect between the practical detection limits of the MS system and the low levels of BNP in biological samples, the research group followed up the study in 2009, investigating the chromatographic performance for intact BNP and its tryptic peptides. [159]

Table 4:1. Summary of MS quantification methods for *intact* BNP in plasma.

Authors	Plasma (mL)	Strategy	Final volume (µL)	Loading volume (µL)	LOQ plasma (fmol/g)	Instrument
Hawkridge *et al.* 2005 [158]	1	IA	50 (20x)	50	150	Nano-LC-ESI-FT-ICR
Niederkofler *et al*. 2008 [123]	0.5	IA	3.5 (143x)	3.5	50	MALDI-TOF
Sobhi *et al*. 2011 [161]	0.75	PPT UF 30 kDa	-	2 x 750	250	Nano-LC-LTQ
Chappell *et al*. 2016 [162]	1	IA	50 (20x)	30	5	Nano-LC-TSQ

IA: immunoaffinity enrichment, PPT protein precipitation, UF: ultrafiltration, FT-ICR: Fourier-transform ion cyclotron resonance (Thermo), MALDI-TOF: MALDI time-of-flight (Bruker), LTQ: linear ion trap quadrupole (Thermo), TSQ: triple quadrupole (Waters) In brackets ( ): the concentration factor relative to the original sample volume.

In 2008,a mass spectrometry immunoassay (MSIA) method was developed by Niederkofler *et al.* using MALDI-TOF. [123] 500 µL plasma was processed and eluted in 3.5 µL of a solution containing the MALDI matrix straight onto MALDI plates. The group observed rapid degradation of BNP in EDTA plasma and quantified the degradation

products by external calibration with synthetic peptides. The mass error of less than 212 ppm (0.742 *m/z* at 3,500) was used for positive identification of BNP and BNP-related degradation products. BNP degradation was stopped by the addition of (4-(2-aminoethyl) benzenesulfonyl fluoride (AEBSF) mixed with leupeptine or with benzamidine to the plasma samples before immunoaffinity enrichment.

BNP was quantified in plasma by Sobhi *et al.* in 2011. [161]The approach involved a two-step plasma extraction procedure: protein precipitation followed by ultrafiltration. Two volumes of 750 µL of the depleted extracts were injected, trapped and back-flushed onto the nano-LC analytical column. The limit of quantification of the method was 250 fmol/g (866 pg/g). No protease inhibitors were used in the study.

More recently, Chappell *et al.* published a novel immunoaffinity LC-MS assay where 1 mL plasma was used to reach the limit of quantification of 5 fmol/g (17.3 pg/g) for BNP. [162] The method used 50 µL of 0.1 % FA/100 µL/mL bovine serum albumin (BSA)/0.001 % Zwittergent to elute the captured BNP and BNP-related species from the antibodies conjugated to magnetic beads. 30 µL of the extract was used to quantify intact BNP 1-32, and its degradation products (BNP 3-32, 4-32, 5-32 and 5-31). The remaining 20 µL was digested with trypsin and used to determine the total BNP-related content captured by the immunoassay by quantifying the ISSSSGLGCK peptide. The authors used P800 plasma containing a proprietary cocktail of inhibitors and observed that BNP concentration was relatively unchanged when it was measured by the IA-MS method after an hour.

MS methods with an ESI source used nano-LC to improve ionisation efficiency. The latter two methods used selective reaction monitoring (SRM) to increase the selectivity by fragmenting either the 4+ or the 5+ charge state of BNP.

BNP was also quantified by SRM using its tryptic peptides by Keshishian *et al.* in 2009. [160] The assay used immunoaffinity depletion of high abundance proteins prior to tryptic digestion and quantification of the tryptic peptides with the use of isotopically labelled internal standards. In this case, the sensitivity was increased by performing the quantification on the tryptic peptides instead of the intact BNP molecule. The doubly charged nature of tryptic peptides ensures higher ion abundances at low levels. The corresponding limit of quantification achieved for BNP was 222 fmol/g (768 pg/g).

This chapter describes the development of a reference method for the quantification of intact BNP in plasma. To quantify BNP in a clinically relevant range (52-520 pg/g, 15-150 fmol/g) an iterative optimisation of the LC-MS/MS and sample clean-up conditions were required to maximize the selectivity and the sensitivity of the method.

Chapter 4.2 Results and Discussion

The development of the reference method took place in several stages. First, a preliminary LC method was developed using high-concentration BNP standards and the sensitivity of the system was tested by analysing gravimetric dilutions of the BNP stock. MS source conditions were optimised for all observed charge states of BNP on a triple quadrupole (QqQ) system in single ion monitoring mode (SIM). An SRM method was then developed to increase specificity and optimised for the transition used for quantification. The development of the plasma extraction protocol started when the required limit of detection and limit of quantitation for solvent standards was achieved.

Development of reference method

Chapter 4.2.1 Preliminary LC method

For the preliminary test of the sensitivity of the system, LC separation was achieved on an Atlantis dC18 Waters column (5 µm particle size, 2.1 mm i.d., 150 mm length, 100 Å pore size). The flow rate was 400 µL/min. The gradient of 1-20 % ACN containing 0.1 % FA was run in 11 min. The QqQ method was set up to monitor the most intense charge states (5+, 6+, 7+) of BNP in SIM mode. The 6+ charge state was observed with the highest intensity. The intensity of the 5+ and 7+ charge states were 28 and 31 % of the 6+ ions. Gravimetric dilution of the quantified stock solution was prepared and analysed with the LC-SIM method. With the above settings the 10 pmol/g (350 ng/g) concentration produced a peak area of 5,000 (arbitrary units), when an injection volume of 40 µL was used.

Chapter 4.2.2 Superchargers

The sensitivity of the system was not adequate for the quantification of BNP in the clinically relevant range (15-150 fmol/g). It has been reported that the charge state distribution and signal abundance of peptides and proteins generated by ESI can be influenced by superchargers. [43]–[48]; therefore the use of supercharging additives were investigated. Sulfolane (γ 50.18 mN/m, 285 °C, 120.17 g/mol), m-nitrobenzyl alcohol (m-NBA, γ 52.7 mN/m, 175-180 °C, 153.15 g/mol) and dimethyl-sulfoxide (DMSO, γ 43.54 mN/m, 198 °C, 78.13 g/mol) have been studied extensively [46]–[48], [52], [53], [163], [164] in relation to their ability to influence the charge state distribution of macromolecules and were chosen for the experiments. In order to adjust the amount of supercharger present and to avoid disturbance of the chromatographic separation or contamination of the LC system a second pump was used after the analytical column for the controlled infusion of the selected charge enhancers. The introduction of superchargers after elution but before electrospraying has the same effect on

electrospray ionisation as adding them earlier to the mobile phase. [50] High-concentration BNP solutions were injected while the three superchargers were infused post-column on the Agilent 6530 Q-TOF (100 pmol/g, 0.35 µg/g) and Agilent 6490 QqQ (750 pmol/g, 2.6 µg/g) instruments with otherwise identical LC and ESI source conditions. The resulting full scan spectra are presented in Appendix A Superchargers. The numerical values for the charge state abundances are displayed in Figure 4:1. In the absence of superchargers the most intense charge state of BNP was found to be 6+ on both instruments. On the Q-TOF instrument the most intense charge state increased to 7+ in the presence of the three supercharging reagents. Apart from the shift in the most intense charge state, the intensity of the 6+ and 7+ charge states also increased while the intensity of the 5+ charge state decreased. Up to an eighteen fold improvement in ion intensity was observed in the presence of 0.25 % DMSO, in agreement with the more efficient ionisation reported by Hahne *et al*. [48]

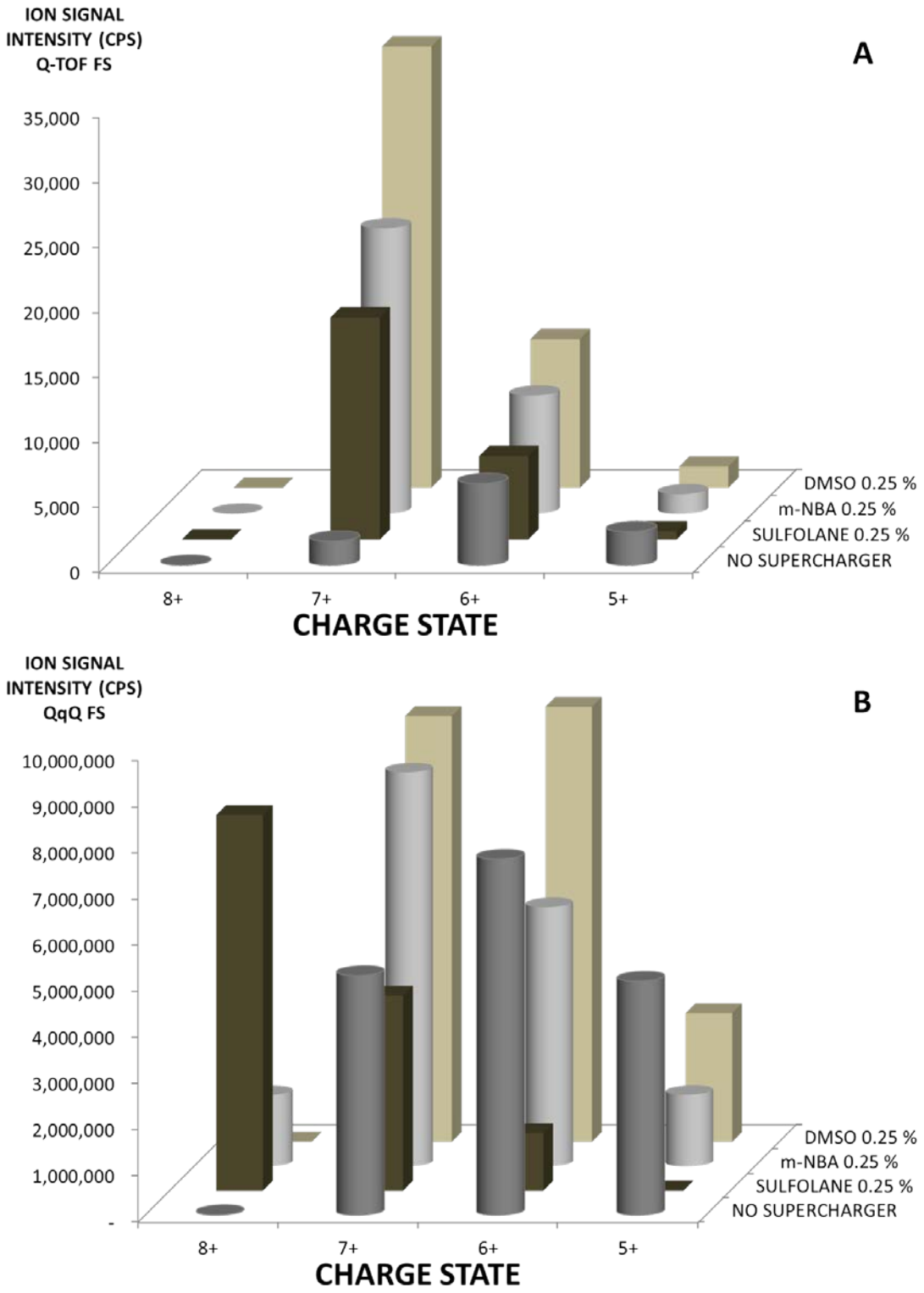

Figure 4:1. MS ion signal abundances of different charge states detected in full scan experiments for BNP when infusing a range of different superchargers. 445.7 *m/z* (8+), 495.8 *m/z* (7+), 578.2 *m/z* (6+) and 693.6 *m/z* (5+) A: Agilent Q-TOF 6530 results. B: Agilent QqQ 6490 results. CPS: counts per second.

On the QqQ instrument the most intense charge state shifted in the presence of sulfolane and m-NBA to 8+ and 7+ respectively and remained 6+ with DMSO. The highest ion signal

intensity on the QqQ system was detected for the 6+ charge state in the presence of DMSO. The increase in ion signal intensities was not as significant as on the Q-TOF instrument. This was unexpected because the LC and ESI source conditions were the same on both instruments. The increase in the most intense charge state with the use of the superchargers was initially attributed in the literature to thermal denaturation due to the increase in the temperature of the ESI droplet as it is enriched in the high-boiling point additives. [46], [165] As BNP has no tertiary structure the reason for the increase in the most intense charge state cannot be thermal denaturation caused by the supercharging reagents. The formation of a supercharger shell that restricts ion evaporation and increases ion density at the time of evaporation, as described by molecular dynamics simulations, is a more likely reason for the observed experimental results. [49] The full scan spectra in Appendix A Superchargers show little evidence of adducts of BNP formed with the different superchargers but another plausible explanation for the observed increase in the most intense charge states is the stabilising effect arising from the formation of adducts between the charged BNP ions and the highly polar supercharger molecules. [46] Without the supercharger, the neighbouring basic residues in the BNP sequence (R_{13}/K_{14} and R_{30}/R_{31}, Figure 3:2) cannot accommodate protons. Adduct formation may lead to the reduction of the electrostatic repulsion between closely located positively charged basic residues and allows the BNP molecule to be protonated to 7+ or 8+.Even though the same source conditions were used, the internal designs of the two mass spectrometers are different. The QqQ instrument has a high pressure ion funnel (8-12 Torr) after the source while on the Q-TOF instrument the ions enter a region of the mass spectrometer evacuated to lower pressures (1.5-2.5 Torr). Less effective evaporation and the loss of ions through collision in the high-pressure ion

funnel at the front of the QqQ instrument may be responsible for the difference in ion abundances detected on the two instruments. DMSO and m-NBA were selected for further experiments on the QqQ system. The experiments were repeated with the two superchargers infused at different concentrations while monitoring the different BNP charge states in SIM. Both m-NBA and DMSO improved signal intensities of the selected charge states. The greatest increase of the 6+ charge state (300 %) was observed when DMSO was infused at a concentration of 0.25 % (v/v) relative to the flow rate of the mobile phase (1 µL/min vs 400 µL/min).Increasing the concentration of DMSO above 0.25 % did not improve signal intensity further. With the infusion of 0.25 % DMSO, a twenty fold increase in intensity was achieved using the Atlantis dC18 Waters column (5 µm particle size, 2.1 mm i.d., 150 mm length, 100 Å pore size) and the LC-SIM method.

Chapter 4.2.3 Optimisation of LC and MS/MS conditions

In order to enhance chromatographic performance the method was then transferred to an Acquity BEH C18 UPLC column (1.7 µm particle size, 2.1 mm i.d., 50 mm length, 130 Å pore size). The use of a smaller particle size column improved resolution and peak intensities. Increasing the concentration of FA in the mobile phases from 0.1 % to 0.5 % reduced peak asymmetry and tailing and allowed the detection of BNP at the level of 100 fmol/g (346 pg/g) using the LC-SIM method. For the SRM method, 0.25 % DMSO was infused and ESI source conditions were optimised to maximise the intensity of the 6+ charge state of BNP. A table of the default and optimised source and transition settings can be found in the Materials and Methods section.(Chapter 2.2.6.2) Product ion scan experiments of the 6+ charge state were performed and the fragments used for quantification and confirmation selected. Finally, the collision cell voltage, collision cell

acceleration voltage, dwell time and electron multiplier voltage for the selected transitions were optimised.

The most intense observed fragment for BNP and BNP* after CID was the quadruply charged y26 fragment ion. Figure 4:2.

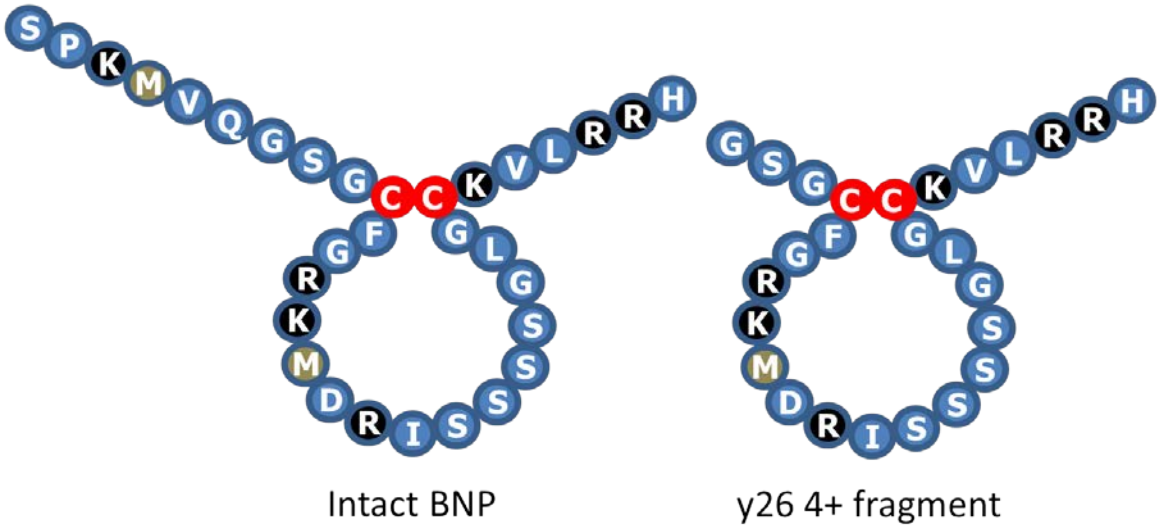

Figure 4:2. Sequence of BNP and the most abundant MS/MS fragment observed when fragmenting the most intense charge state (6+). Methionine residues are labelled in grey.

For the quadruply charged y26 fragment ion, the theoretical monoisotopic *m/z* values for BNP and BNP* are 698.8549 and 704.8655, respectively. Most elements that make up organic molecules occur as a mixture of isotopes in nature. (Table 4:2) For large peptides and proteins the multiply charged ions are displayed as an envelope of the isotopomers and isotopologues in low-resolution mass spectra. For BNP ($C_{143}H_{244}N_{50}O_{42}S_4$) the envelope of the 6+ charge state spans an *m/z* range of 1.5. Quadrupole settings can affect signal intensities in SRM experiments if the *m/z* selection windows and resolution settings are incorrect.

Table 4:2. List of heavy isotopes sorted by natural abundance.

Isotope	Mass [Da]	% Abundance (molar fraction)
^{34}S	33.967868	4.21
^{13}C	13.003355	1.10
^{33}S	32.971459	0.75
^{15}N	15.000109	0.37
^{18}O	17.999159	0.20
^{17}O	16.999131	0.038
^{2}H	2.014102	0.015

To confirm that the first quadrupole accurately transmits the majority of the BNP precursor in the presence of DMSO, the intensity of the SRM transition was recorded for an equimolar blend of high-concentration solutions (BNP + BNP* 1 pmol/g). The solutions were analysed using the optimised source and MS/MS conditions determined previously. The *m/z* selection of the first quadrupole was increased by *m/z* 0.1 intervals while the average mass of the quadruply charged y26 fragment ions was monitored (*m/z* 699.5 and 705.0). The resolution of the quadrupoles was set to unit (± *m/z* 0.35). The results of triplicate injections of a 1 pmol/g BNP + BNP* solution are displayed in Figure 4:3.

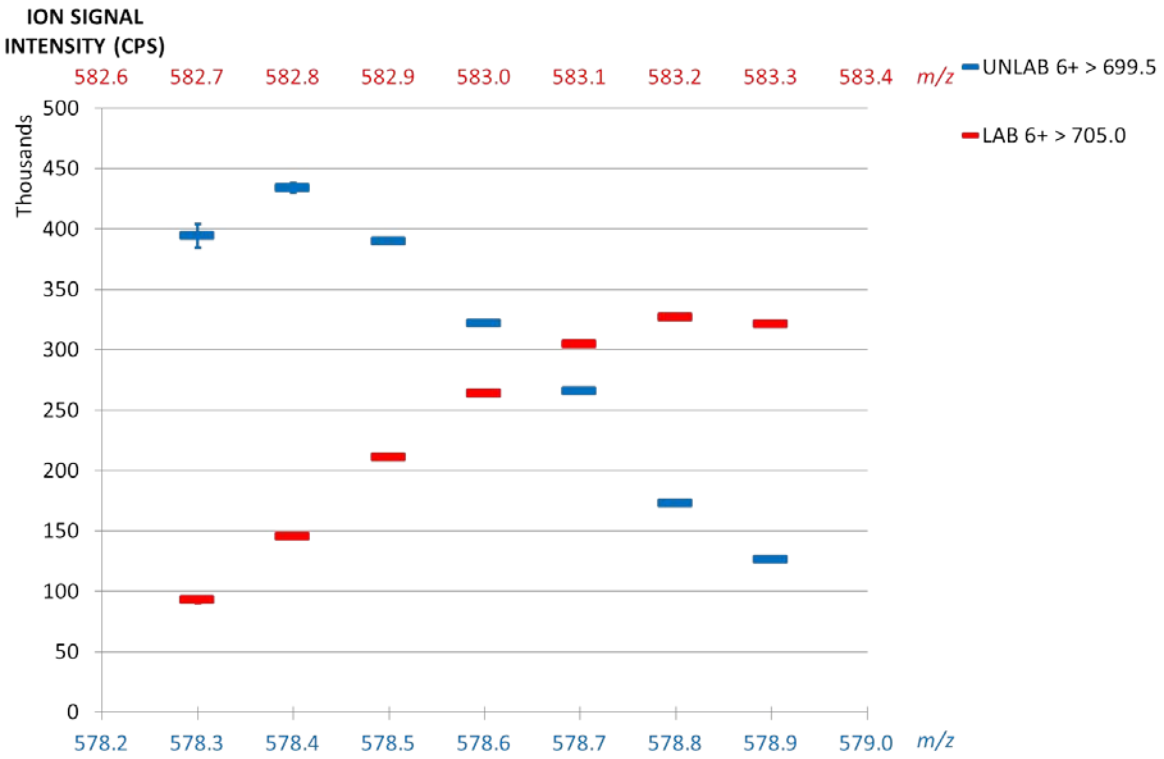

Figure 4:3. Effect of quadrupole settings on signal intensity of the SRM transitions (UNLAB 6+ 578.2 - 579.0 → y_{24}^{4+} 699.5, LAB 6+ 582.6 - 583.4 → y_{24}^{4+} 705.0) used for quantification. The resolution used was UNIT/UNIT (Q1/Q3). CPS: counts per second.

The results confirmed that selecting the average *m/z* values for the 6+ charge states provides the maximum transmission of the analyte in unit resolution.

Figure 4:4 shows the summary of the effects of optimisation on the intensity of BNP signal in SRM. Triplicate injections of an equimolar blend of BNP + BNP* (1 pmol/g) were performed with default source and SRM conditions, optimised source and SRM conditions and optimised source and SRM conditions while DMSO was infused. The figure shows that the most significant intensity increase is attributed to the addition of DMSO. Signal intensity could be increased further by reducing the resolution on the first quadrupole to allow more ions to enter the collision cell but this would decrease selectivity and results in higher variability in the intensity of the SRM transitions.

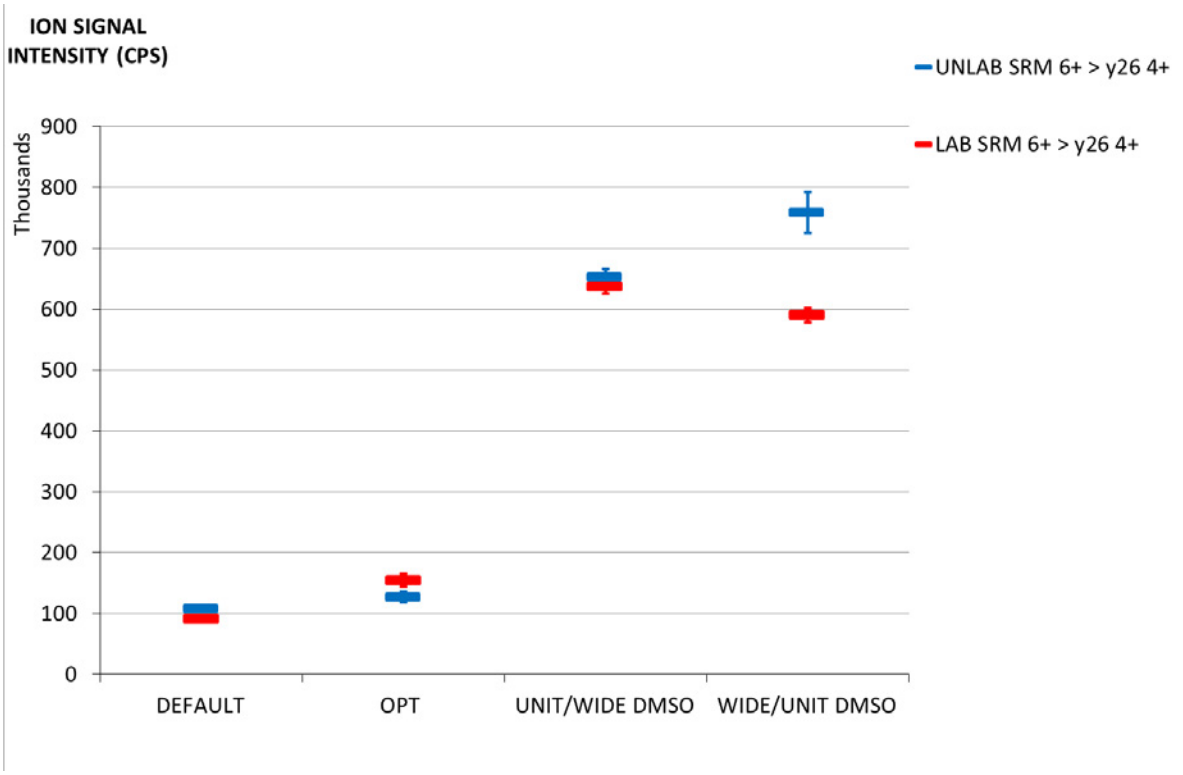

Figure 4:4. Results of MS/MS method optimisation and effect of resolution settings on SRM transition intensities. DEFAULT: default MS/MS conditions, OPT: optimised setting for selected SRM, DMSO: optimised settings with DMSO infused, 6+ *m/z* NAT/LAB 578.3/583.3, y26 4+ NAT/LAB 699.5/705.0,quadrupole resolution settings: UNIT: ± *m/z* 0.35 WIDE: ± *m/z* 0.60. CPS: counts per second.

For the quantification method the quadruple setting of Q1/Q3 UNIT/WIDE resulted in the best intensity, signal to noise and ratio precision values.

Chapter 4.2.4 Final LC-MS/MS method

To improve the retention of the hydrophilic BNP molecule the method was transferred to a 250 mm Aeris PEPTIDE UPLC core shell column (2.6 µm particle size, 2.1 mm i.d., 250 mm length, 90 Å pore size). Chromatographic conditions were optimised with the new column geometry. The effect of the mobile phase composition during the isocratic period at the start of the LC run on ion peak shape and signal intensity are displayed in Figure 4:5. The results show that extending the isocratic step with high aqueous mobile phase content in the LC method improves peak symmetry and the intensity of the BNP ion peak most likely due to a stacking effect at the head of the column.

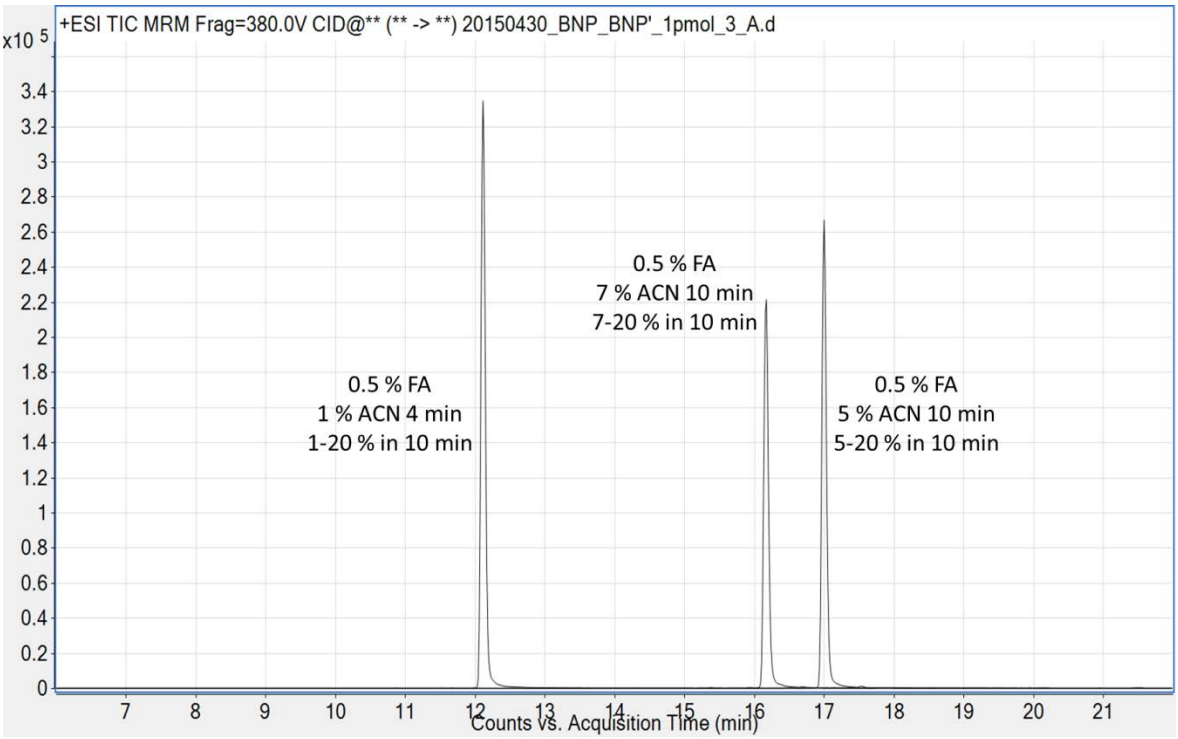

Figure 4:5. 1pmol/g BNP + BNP* analysed with the optimised MS/MS settings and different elution conditions.

The LC method was modified to include a 6 min 1 % ACN isocratic segment after injection. The gradient of 1-20 % ACN in 14 minutes with 0.5 % FA in the mobile phases was adopted with the wash of 50 % ACN before column conditioning. Increasing the column temperature improves peak shape and resolution by decreasing the viscosity of the solvent and increasing the diffusion rate of the molecules into and out of the pores of the stationary phase. [30] The column compartment temperature was set to 60 °C for the final LC method. The limit of detection of the optimised LC-MS/MS method using the Aeris PEPTIDE column for BNP was 6 fmol/g (22 pg/g) and the limit of quantitation was 21 fmol/g (72 pg/g) with only 10 µL injected (210 amol on column).

To demonstrate the effect of the optimised conditions on the observed BNP signal intensity, a standard corresponding to the lowest calibration point for the reference method (75 fmol/g, 260 pg/g) was injected using default SRM settings, optimised SRM

conditions and the optimised settings with DMSO infused. The chromatograms are displayed in Figure 4:6.

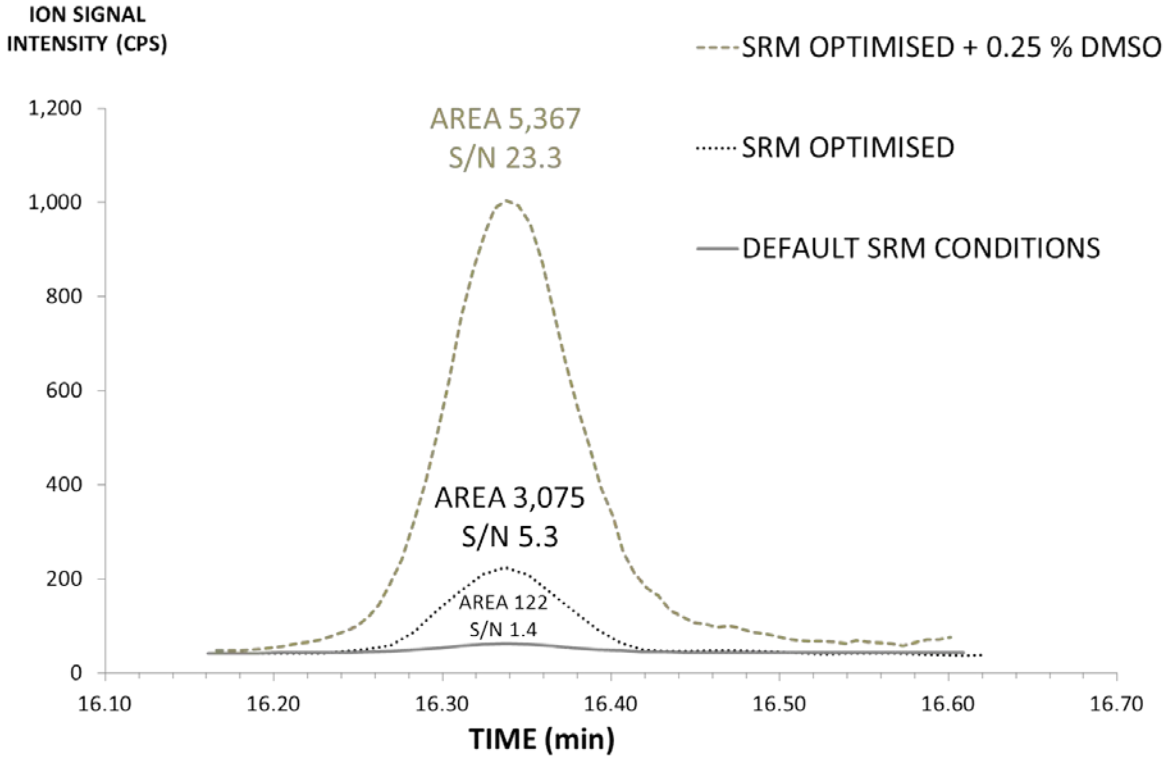

Figure 4:6. Chromatographic trace of the BNP transition used for quantification (*m/z* 578.3→699.2) using default SRM settings (solid), optimised source and SRM conditions (dotted) and 0.25 % DMSO infusion with the optimised source and SRM settings (dashed). The concentration of the injected BNP solution was 75 fmol/g (250 pg/g). CPS: counts per second.

The optimised source and SRM conditions increased the area of the BNP peak by a factor of twenty-five. With DMSO infused, a forty four-fold increase was achieved together with a seventeen-fold increase in the signal-to-noise ratio. While achieving the same signal intensities is not expected in plasma as with BNP standard solutions due to matrix suppression, the method was deemed to be appropriate for the development of a suitable concentration and clean-up strategy at the levels required for the analysis of clinical samples.

Chapter 4.3 Development of a clean-up method

The complexity of the blood plasma matrix is such that without a reasonable reduction of interferences from high-abundance proteins BNP cannot be analysed by LC-MS/MS. Plasma proteins are proteins that are secreted by the liver and the intestines and remain in circulation as they are larger than the kidney filter cut off (≈ 45 kDa). [166] High-abundance proteins in plasma include albumin (60 % w/w), globulins (25 % w/w) and fibrinogen (3 % w/w). Albumin concentration in plasma is around 50 mg/g. [165] This reference method is aimed at the quantification of BNP for concentrations six orders of magnitude lower than albumin, i. e. in the range of 52-520 pg/g.The majority of the methods published on the quantification of intact BNP used immunoaffinity enrichment. However, antibodies lack molecular specificity and are not compatible with the acidified solutions used for the quantitative dilution of the BNP stock standard; therefore they were not considered in the current study. Preliminary experiments with ultracentrifugation, solid phase extraction and protein precipitation indicated that a single step sample preparation would not be sufficient for the removal of abundant plasma proteins. A combination of two sample clean-up procedures will be necessary.

Sobhi *et al.* used ultrafiltration after protein precipitation and concentrated BNP on a trap column using high injection volumes. [160] To avoid the need for complex column-switching configurations, protein precipitation was chosen as the first step of the clean-up procedure and BNP was captured and separated from the remaining plasma proteins by solid phase extraction.

Apart from the complexity another major concern when working with plasma is the instability of BNP. BNP degrades rapidly in plasma (half-life ≈ 23 min) due to the activity of the enzymes displayed in Table 4:3. [122], [127], [167]

Table 4:3. Enzymes degrading BNP in blood circulation.

Enzyme	pH_{opt}	BNP cleavage sites	
		Major	Minor
Neprilysin, Neutral endopeptidase (NEP)	7.0	M_4-V_5	R_{17}-I_{18} K_{14}-M_{15} G_{23}-L_{24} V_{28}-L_{29}
Dipeptidyl peptidase IV (DPPIV)	7.4-8.7	P_2-K_3	-
Insulin degrading enzyme (IDE)	6.0-8.5	L_{29}-R_{30} R_{30}-R_{31} K_3-M_4	G_{12}-R_{13} R_{13}-K_{14} D_{16}-R_{17} C_{26}-K_{27}
Meprin	7.5-9.5	Q_6-G_7	G_7-S_8

pH_{opt} is the pH at which enzyme activity is maximum. Major and minor cleavage sites are indicated with the amino acid residue codes. The position of the amino acids is displayed in the subscript.

The enzymes degrading BNP operate at or slightly above physiological pH. It was hypothesised that performing protein precipitation in acidified solution blocks enzymatic degradation and precipitates high-abundance proteins in a single step. Plasma samples treated with protein precipitation alone cannot be injected on LC-MS/MS without deterioration to the LC column. Before performing protein precipitation experiments on spiked plasma samples a solid phase extraction step was developed for the selective capture of BNP.

Chapter 4.3.1 Solid phase extraction (SPE)

Preliminary experiments with different SPE chemistries showed that the STRATA XL cartridges offered the most suitable combination of bed-size, pore diameter and stationary phase for the enrichment of BNP in the second step of the clean-up procedure. To investigate retention behaviour of BNP on the STRATA XL cartridges serial elution experiments were conducted using various elution solvents. (Chapter 2.2.6.5) The most appropriate elution solvent composition was initially determined by loading and eluting aqueous BNP solutions and analysing the extract with the developed LC-SRM method. Recoveries were calculated by spiking the extracts with labelled BNP* post-elution. BNP

was detected in the 20, 30 and 40 % ACN elution steps. The sum of the recoveries in the individual elution steps, however, was below 50 %. Poor recovery of BNP was considered to be partially caused by the oxidation of the methionine residues during SPE that were not detected using the LC-SRM method. Whereas the use of the labelled internal standard compensates for any bias during quantification, oxidation of BNP will compromise the sensitivity of the method.

Chapter 4.3.1.1 Oxidation of methionine residues during SPE

BNP contains two methionine residues in position 4 and 15. Either of these can be oxidized to methionine sulfoxide or sulfone. MALDI MS experiments conducted at the University of Reading showed extensive oxidation of BNP when dissolved in water and exposed to air (i.e. spotted/dried on MALDI plates). The methionine residues were oxidised to methionine sulfoxide. Oxidation to methionine sulfone was not detected.

In order to verify that oxidation of the methionine residues is the reason for the low recoveries of BNP during SPE, the collected fractions were analysed using a Q-TOF instrument. Three additional baseline separated peaks were detected in the SPE fractions. The full scan mass spectrum indicated the presence of one doubly oxidised and two singly oxidised methionine species. The location of the oxidised methionine residue and the extent of the oxidation could not be identified from the full scan spectra.

The oxidised species can be distinguished on a triple quadrupole (QqQ) instrument in SRM mode by fragmenting the most intense charge state (6+) and monitoring the most abundant fragment ion (quadruply charged y26) because the y26 fragment ion only contains the second methionine residue (M_{15}) in the sequence. (Figure 4:2) The theoretical precursor and fragment *m/z* values for all plausible oxidation products were calculated and the transitions were included in the SRM method. The SPE extract were

subsequently re-analysed and the resulting chromatogram is displayed in Figure 4:7. The transitions for the intact and different oxidised BNP forms detected in the SPE fractions are tabulated in Table 4:4.

Table 4:4. Monitored *m/z* values for intact BNP and the oxidised-methionine sulfoxide forms of BNP.

Description	precursor *m/z* BNP	fragment *m/z* BNP	precursor *m/z* **BNP***	fragment *m/z* **BNP***
INTACTBNP	578.3	699.2	583.3	705.2
MMo	581.0	699.2	585.9	705.2
MoM	581.0	703.5	585.9	709.2
MoMo	583.7	703.5	588.9	709.2

MoM: M4 is oxidised. MMo: M15 is oxidised. MoMo: M4 and M15 are oxidised.

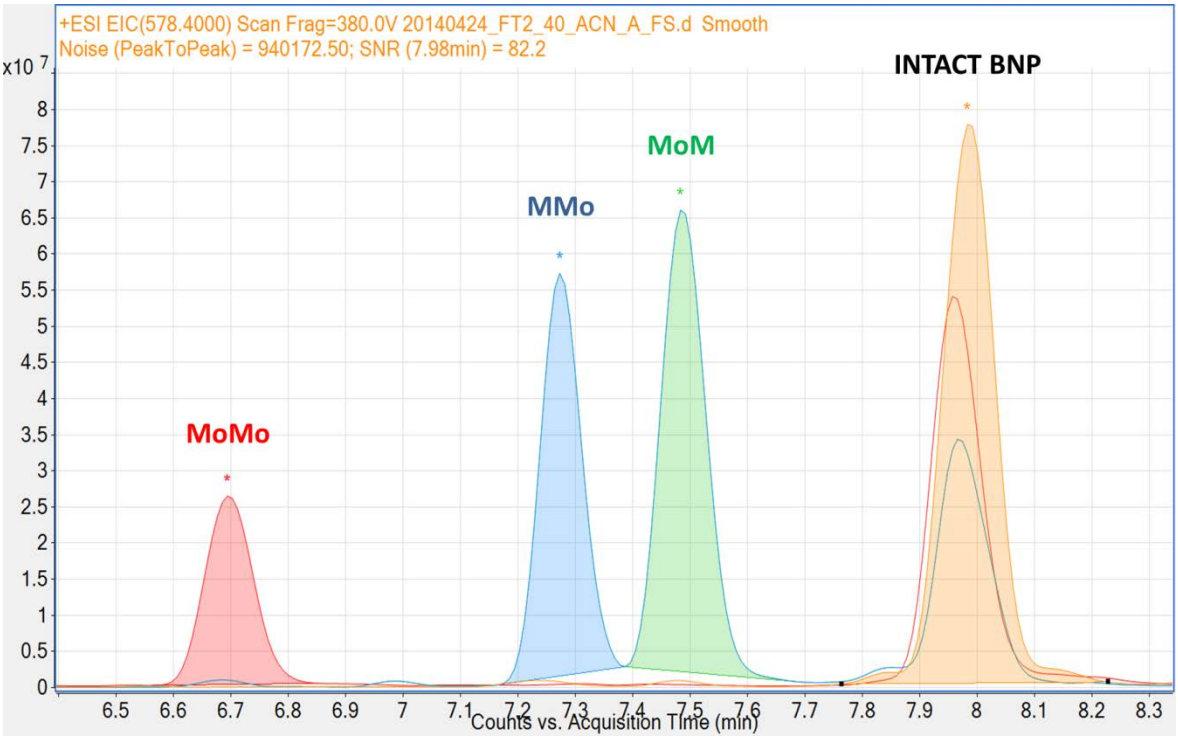

Figure 4:7. Chromatogram of the 40 % ACN SPE fraction analysed with selective SRM transitions to determine the elution order of BNP and the different BNP forms containing methionine sulfoxide. MoMo: both methionines 4 and 15 are oxidised. MMo: methionine 15 is oxidised. MoM: methionine 4 is oxidised.

The transitions for the oxidised BNP products were added to the final SRM method and their presence was monitored in all future experiments. Excess amount of methionine added to peptide/protein solutions can act as an antioxidant. [168] To investigate that methionine can act as a scavenger during the SPE process, 45 µg/g (0.3 µmol/g) of methionine was added to the washing and elution solvents. The solid phase extraction experiments previously described were repeated in the presence of methionine. The SPE extracts were analysed by SRM. There was no oxidised BNP detected in the solvent standards after SPE or in the reconstituted solution of the freeze-dried aliquots. The addition of 45 µg/g methionine into the elution solvents prevented oxidation of methionine residues and was therefore employed in the final clean-up procedure. The highest recovery of BNP was found by using 4 mL of 35 % ACN (water:ACN, 65:35, v/v) for the elution of BNP from the STRATA XL SPE cartridges.

Chapter 4.3.2 Protein precipitation (PPT) and stabilisation

To confirm that the addition of the acidified PPT solvent blocks the degradation of BNP thirteen aliquots of the BNP stock were prepared gravimetrically and freeze dried. Plasma was added to all thirteen aliquots at the start. The enzymatic degradation of BNP was stopped when acidified PPT solution was added and the sample was vigorously vortexed. For the first three samples the PPT solution was added directly after the plasma to establish the start point (T=0). The PPT solution was added at ten minute intervals to the remaining aliquots. Following both PPT and SPE, the final extracts were made up in a solution containing an equimolar amount of the isotopically labelled BNP* compared to the initially loaded amount of BNP. The samples were analysed by LC-MS/MS and the results are displayed in Figure 4:8.

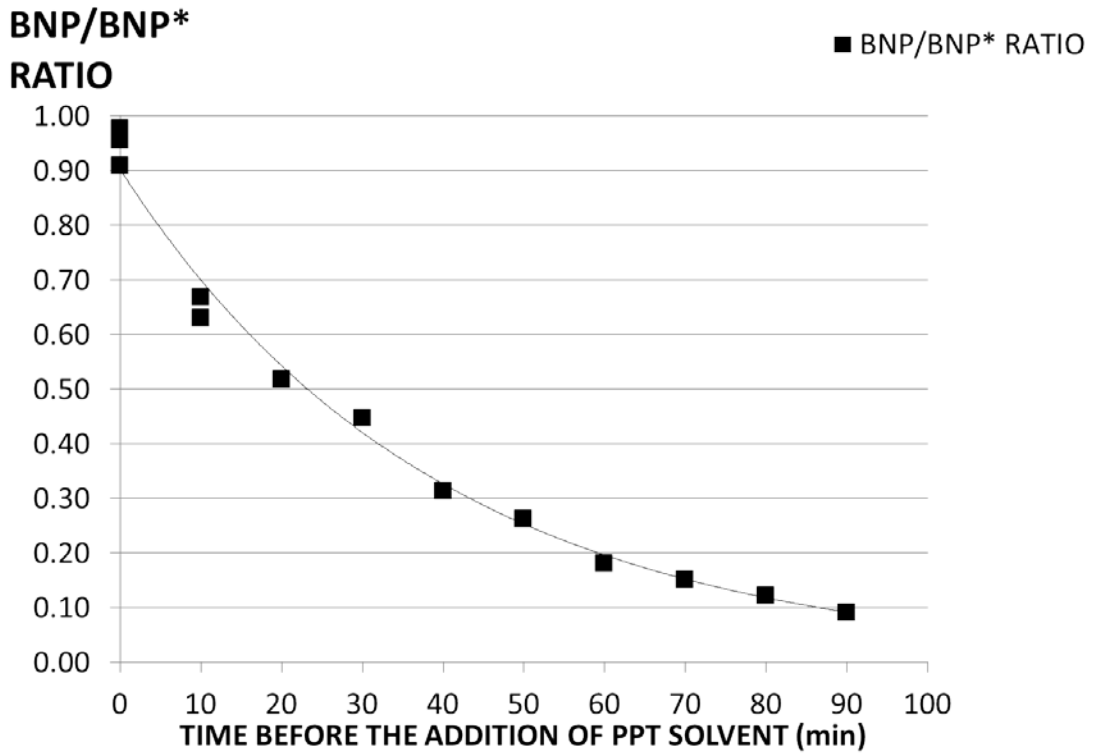

Figure 4:8. BNP spiked into 0.5 g plasma and PPT solvent added at 10 minute intervals. After freeze drying the samples were subjected to solid phase extraction (SPE) clean-up. The SPE extracts were spiked with labelled BNP (BNP*) using equal amounts of BNP* compared to the initial BNP loading. y-axis: Ratio of the integrated area of intact unlabelled BNP divided by the integrated area of labelled BNP (small black squares). The spiking concentration was 120 fmol/g (400 pg/g).

BNP degrades rapidly once it comes in contact with EDTA plasma. 65 % of the initial concentration was determined after only 10 minutes before the acidified protein precipitation solvent was added. The half-life determined by these experiments agrees very well with the literature data (23 min). Once the pH is decreased, BNP is stable in solution. Enzymatic degradation of BNP was successfully blocked by decreasing the pH and the samples are stable at room temperature while being processed and for more than 2 days while kept at 5 °C in the autosampler.

Chapter 4.3.3 Final optimisation of the sample clean-up

Next, the proposed clean-up strategy was investigated for the recovery of BNP across the desired calibration range of 15-150 fmol/g (52-520 pg/g). The recovery was determined by comparing the measured ratio of the integrated area of the unlabelled and isotopically labelled BNP* determined in the samples spiked with the isotopically labelled BNP* internal standard at the beginning (pre-spikes; pre-clean-up) and at the end of the clean-up process (post-spikes; post-clean-up). The recovery of BNP from plasma was 51 %. Matrix suppression was also investigated by comparing the intensities of the internal standard in the post-spiked samples with the signal intensity of the internal standard solution prepared at the same concentration. Matrix suppression was 65 %. As the final step of the method development process a systematic evaluation of the two-stage sample clean-up procedure was performed in an attempt to reduce matrix suppression and improve BNP recovery. Spiked plasma samples were prepared containing BNP corresponding to the proposed quantification limit for the reference method (15 fmol/g, 52 pg/g). The composition of the SPE eluent was varied in the first experiment with the precipitation solvent composition kept constant.

Precipitation was performed in 70 % ACN (water:ACN, 30:70 v/v)and the amount of ACN in the SPE elution solvent was increased in 5 % increments. Extracts were analysed in SRM and full scan (FS) mode on the QqQ instrument. Full scan experiments showed a significant decrease in ion abundance at the expected retention time of BNP (16.4 minutes) due to co-eluting matrix components. Figure 4:9.

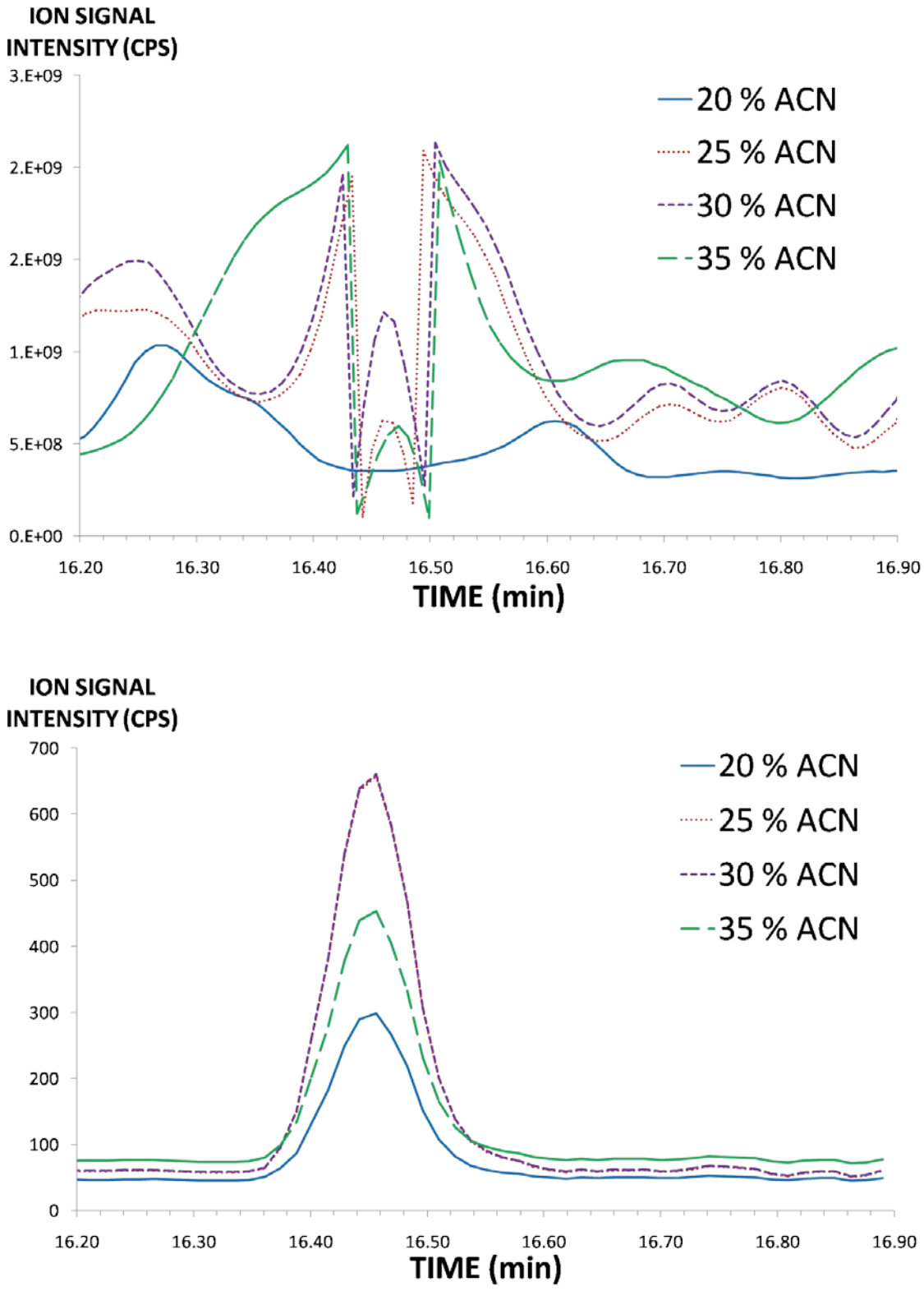

Figure 4:9. Full scan and SRM chromatograms of plasma extracts spiked with unlabelled BNP and precipitated using 70 % ACN (water:ACN, 30:70 v/v) solvent. ACN composition of the SPE elution solvent was increased in 5 % increments.CPS: counts per second.

The chromatographic behaviour implies that the polarities of the interferences are very similar to BNP. Increasing the organic content of the SPE elution solvent above 20 %

(water:ACN 80:20/75:25/70:30/65:35, v/v) resulted in large decrease in ion abundances observed in the FS experiments. It is likely that due to the similar elution characteristics of BNP and the interference and the poor resolution of the SPE cartridges, they could not be separated in the SPE step. The summary of the results is presented in Figure 4:10.

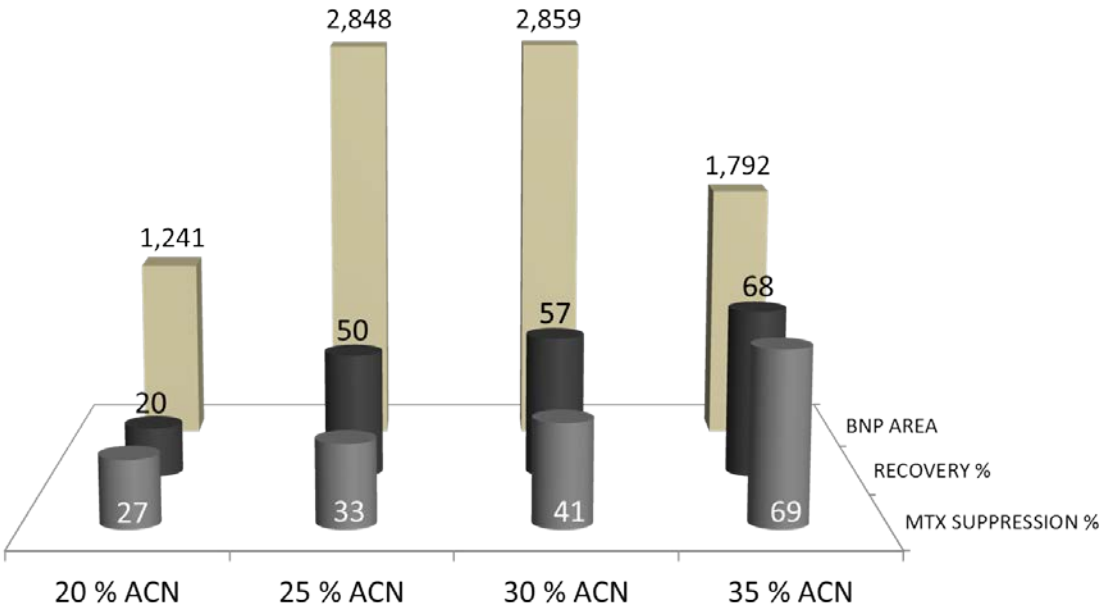

Figure 4:10. The relationship between matrix suppression, BNP recovery and signal intensity related to the amount of ACN in the SPE solution. PPT solvent composition was 70 % ACN (water:ACN, 30:70, v/v). Data shown is an average of three measurements.

In the second experiment the amount of ACN in the precipitation solvent was varied. The composition of the SPE elution solvent was kept constant (water:ACN, 65:35 v/v).The full scan and SRM chromatograms are displayed in Figure 4:11 and the summary of the results is displayed in Figure 4:12.

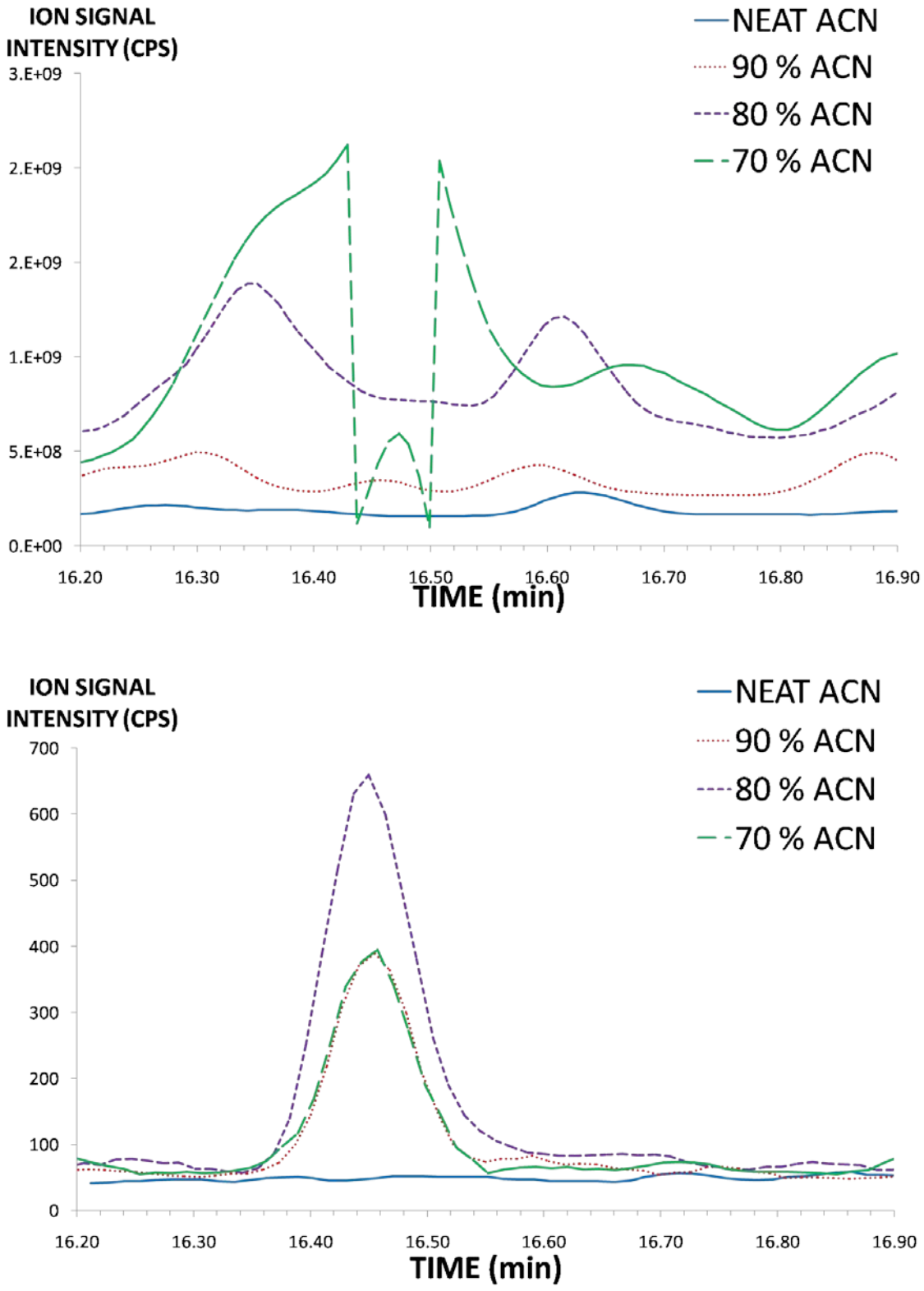

Figure 4:11. Full scan and SRM chromatograms of plasma extracts spiked with unlabelled BNP and PPT was performed using water:ACN (0:100/10:90/20:80/30:70, v/v) solvent. ACN composition of the SPE elution solvent was kept constant (water:ACN 65:35, v/v).CPS: counts per second.

No BNP was recovered when neat ACN was used for precipitation. The presence of the coeluting impurity causing ion signal suppression decreased significantly when 80 % or more ACN was used in the PPT solution.

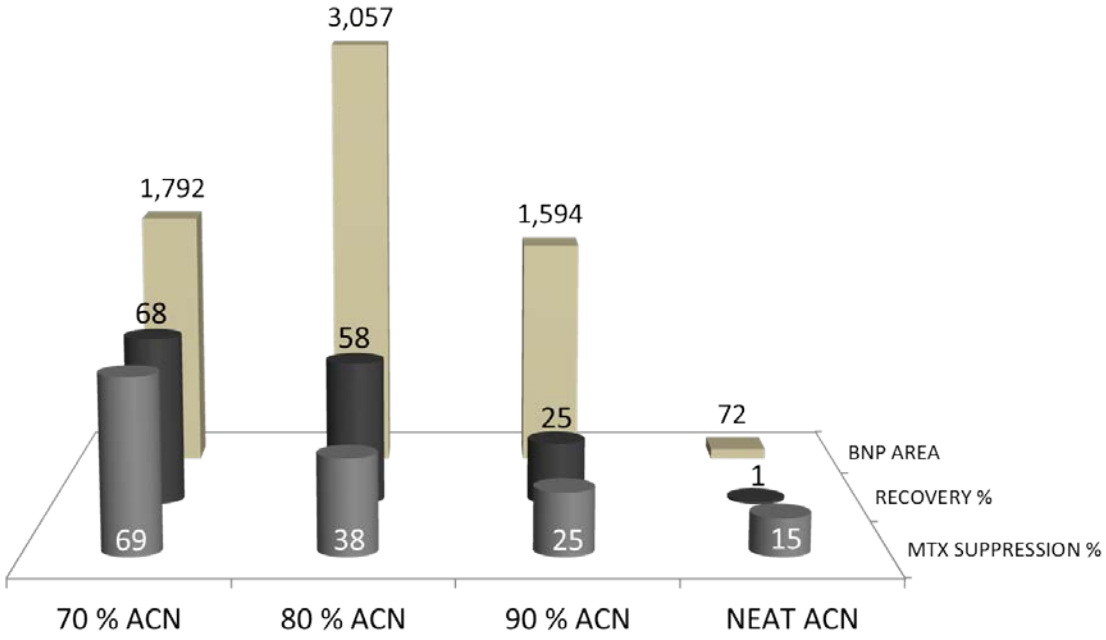

Figure 4:12. Matrix suppression, recovery and signal intensity dependence on the composition of the precipitation solvent. SPE solvent composition was water:ACN (65:35, v/v). Data shown is an average of three measurements.

The highest recovery of BNP (68 %) was achieved when precipitation was performed with 70 % ACN (water:ACN, 30:70, v/v) and SPE with 35 % ACN (water:ACN, 65:35, v/v). Matrix suppression with this combination was high so the signal intensities remained relatively low. The best conditions with the BNP recovery of 58 % and matrix suppression of 38 % were reached when PPT was performed with 80 % ACN (water:ACN, 20:80, v/v) and the elution solvent used for SPE was 35 % ACN (water:ACN, 65:35, v/v). The workflow of the final method is displayed in Figure 4:13.

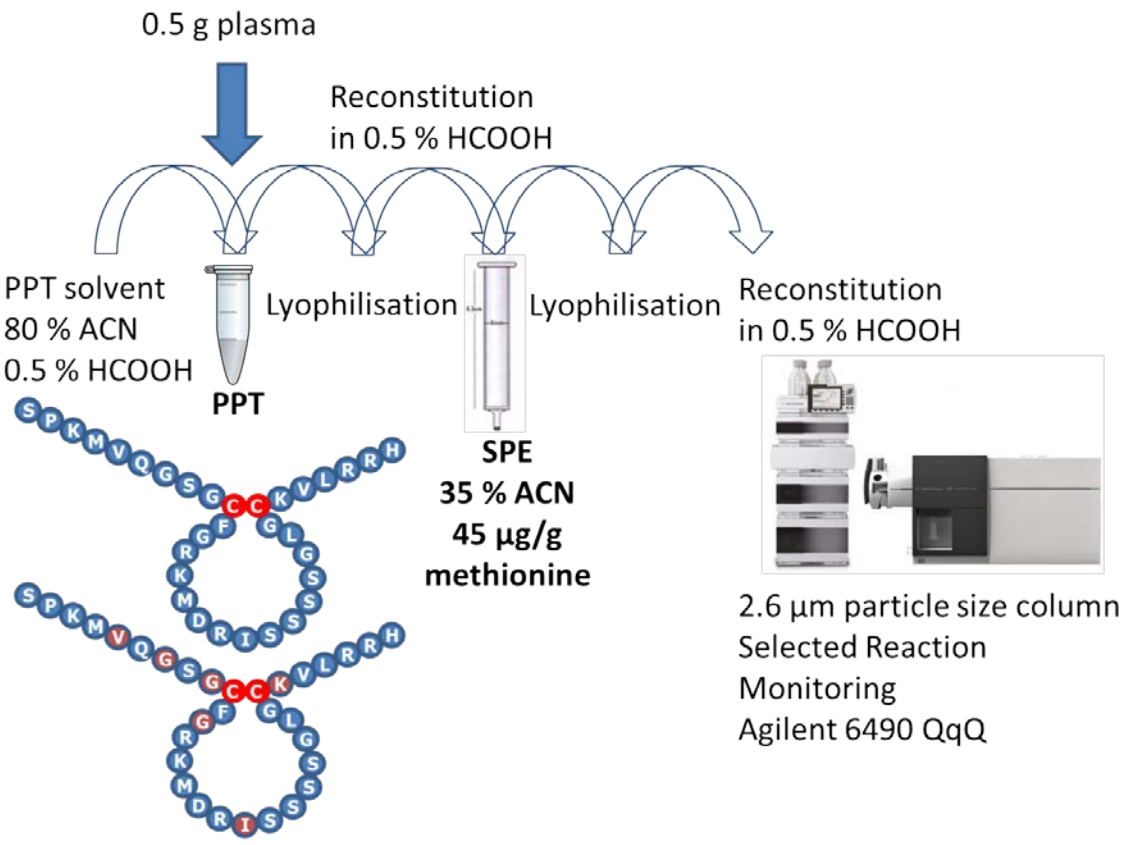

Figure 4:13. Diluted stock solutions of the BNP primary standard is gravimetrically dispensed into 2 mL Protein LoBind Eppendorf tubes. The solutions were spiked with equal amount of labelled BNP*. Isotopically labelled amino acids are highlighted in purple add a mass difference of +30 Da. After freeze drying 0.5 g plasma was added gravimetrically and the samples were subjected to protein precipitation (PPT) and solid phase extraction (SPE) clean-up. The final extracts are reconstituted in 100 µL and analysed by LC-MS/MS.

Chapter 4.4 Method validation

The limit of detection and quantification, repeatability, intermediate precision, linearity and accuracy of the method were assessed. Three sets of plasma samples were gravimetrically prepared containing isotopically labelled BNP (BNP*) at 60 fmol/g and seven calibration points with increasing amounts of unlabelled BNP at concentrations between 52-520 pg/g corresponding to 15-150 fmol/g. PPT and SPE were performed as previously described before analysis by LC-MS/MS. The observed ratio of the ion signal area of the unlabelled BNP divided by the ion signal area of the labelled BNP ($AREA_{UNLAB}/AREA_{LAB}$ (y)) was corrected for the gravimetric amount of isotopically labelled

BNP* ($n_{LABELLED}$) added and plotted against the gravimetric amount of unlabelled BNP in each sample ($m_{UNLABELLED}$ (pg) (x)).Equation 4:1.

$$\frac{AREA_{UNLAB}^{BNP}}{AREA_{LAB}^{BNP*}} * n_{LAB}^{BNP*} = b * m_{UNLAB}^{BNP} + c$$

Equation 4:1. Linear regression equation used for the determination of the amount of unlabelled BNP in plasma. b: slope, c: intercept.

The calibration points from the three experiments were combined to construct the calibration curve displayed in Figure 4:14.

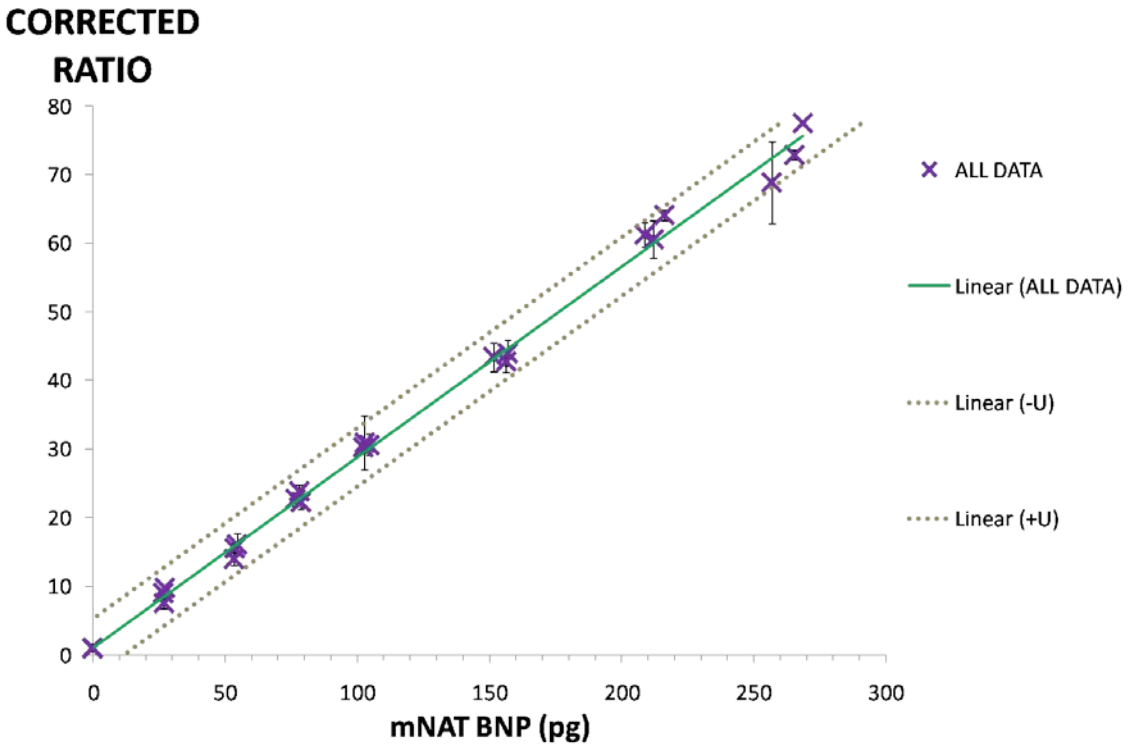

Figure 4:14. Calibration curve obtained by combining the data points of three independent sets of samples. Each point represents the average of three injections. ± U: expanded uncertainty.

The accuracy of the method was assessed by calculating the difference (bias) between the amounts of BNP determined from the constructed linear regression curve with the gravimetric values. This was performed by considering each plasma extract as an unknown sample and by quantifying its content of BNP using the calibration curve constructed without this unknown sample. Repeatability was calculated as the average

standard deviation of the replicate injections (n=3) determined from the individual calibration curves and the intermediate precision was calculated as the standard deviation of the results for each injection determined from the combined calibration curve and reported in Table 4:5.

The calculation of the error of the concentrations determined by linear calibration requires the estimation of the random error associated with both the intercept and the slope. [169], [170]The confidence limits in Table 4:5 (± U) were determined by calculating the concentration of each sample from the calibration curve and expanding the standard deviation (s_{xo}) of the determined concentrations (x_0) with the t-value at 95 % confidence level, with (n-2) degrees of freedom according to Equation 4:2.

$$x_0 \pm t_{(n-2)} s_{x_0}$$

Equation 4:2.Uncertainty associated with concentrations determined by linear regression.

Where *n* is the number of calibration points. Analysis of variance (ANOVA) of the calculated concentrations at each level from experiments performed on different days confirmed that the inter-day variability is not statistically significant. A limit of detection of 4.37 fmol/g (15.15 pg/g) was determined by calculating the standard deviation of the analytical response of the blank plasma samples (n=9).

Table 4:5. Concentration levels for the calibration curve and calculated statistics from the validation experiments.

pg/g plasma[1]	± U[2]	Bias pg/g	Repeatability	Intermediate precision
0.00	15.49	-	-	-
53.99	15.41	6.86	4.57	7.92
107.97	15.36	9.82	7.87	9.83
155.85	15.33	7.21	7.07	7.85
206.71	15.31	11.28	14.81	15.71
310.21	15.34	10.51	13.34	12.29
425.01	15.47	20.80	12.78	16.73
527.56	15.62	33.28	16.49	34.60

[1]Gravimetrically prepared concentration of BNP;[2]Expanded uncertainty.

The uncertainties assigned to the concentrations determined by linear calibration are dominated by variability arising from the construction of the calibration curve (47.5 %). Uncertainties can be reduced by improving the quality of the calibration standard and performing EM-IDMS.

Chapter 4.5 Conclusions

A reference method was developed for the SI-traceable quantification of BNP in plasma at the clinically relevant concentrations between 52 and 520 pg/g (15-150 fmol/g). The effects of incremental improvements in sensitivity by optimisation of the LC separation, ionisation efficiency, SRM conditions and sample preparation were demonstrated. Unlike previously reported MS-based methods, quantification of BNP in the pg/g range was achieved without the use of immunoaffinity enrichment. The classical sample clean-up techniques used in the reference method are not affected by the inconsistencies associated with the lack of specificity of enrichment antibodies. Stabilisation of the unstable cardiac hormone was achieved by reducing plasma pH and creating unfavourable conditions for enzymatic activity.

The sensitivity of the MS system was increased by the use of a supercharger reagent. Due to the improved ionisation efficiency observed with the use of 0.25 % DMSO, normal flow chromatography with low injection volumes can be used allowing repeated analysis of the same sample extracts. Results determined by the newly developed reference method are traceable to the SI and can be used for the accurate quantification of BNP in external quality assessment scheme and/or clinical samples. Determination of intact BNP concentration can be used to provide confirmation of the efficacy of cardiac drugs targeting BNP in clinical trials, it can be utilised in enzyme-substrate studies or to determine the effectiveness of plasma stabilisation protocols. The versatility of MS detection was utilised to distinguish between oxidised methionine species using SRM. The developed method is capable of the selective detection of oxidised BNP metabolites and can extend the scope of research into cardiovascular disease pathophysiology. The method was applied to the quantification of BNP in the UK NEQAS samples and the results of this are presented in the next chapter.

Chapter 5 National External Quality Assessment Scheme (NEQAS)

Chapter 5.1 Introduction

Clinical laboratories providing BNP tests must participate in an external quality assessment scheme (EQAS) to demonstrate their competence and comply with accreditation. [171] In order to verify that correlation between the immunoassays and the LC-MS/MS method results exists, the method described in the previous chapter was used to quantify samples distributed by the UK NEQAS cardiac marker scheme. The results of the reference method provide evidence that the major immunoreactive form in the samples is BNP and a tool for the assessment of the consistency and the stability of the samples. Furthermore, a method for monitoring enzymatic products of BNP was developed to support the understanding of cross-reactivity issues with the antibodies in three of the commercially available immunoassay analysers. The laboratories participating in the UK NEQAS use the same antibody configurations on different automated platforms. These BNP analysers are manufactured by Abbott Laboratories (Architect), Siemens (ADVIA Centaur CP, ADVIA Centaur XP, ADVIA Centaur XPT) and Beckmann Coulter (Access 2, DxI).

The samples distributed by NEQAS are EDTA plasma samples spiked with synthetic unlabelled BNP. EDTA is an additive used in blood collection tubes to block the activity of metalloproteases by chelating divalent metal ions (DPPIV, IDE, NEP listed above in Table 4:3). BNP was found to be unstable in EDTA plasma [123] therefore an enzyme inhibitor cocktail (Sigma-Aldrich) is added during the preparation of the samples. Using plasma spikes instead of pooled clinical samples is also beneficial for the comparison as the immunoassay results cannot be attributed to any cross-reactivity originating from unprocessed proBNP. The results are reported to the scheme organiser by all laboratories

and the data presented below are based on the average of all reported results for the different immunoassays and the LC-MS/MS measurement.

Chapter 5.2 Results and discussion

Eighty four samples from the UK NEQAS Cardiac Marker scheme were analysed by the method described in Chapter 4. Three samples were received every month and quantified by the developed reference method. The samples were provided as freeze-dried aliquots, which were reconstituted according to the instructions provided by NEQAS and transferred into Eppendorf vials containing the isotopically labelled internal standard BNP*. Quantification of the NEQAS samples was performed as described in Chapter 4.2.4. Briefly, seven plasma samples spiked with the unlabelled BNP primary calibrator in a range of concentrations between 52-520 pg/g (15-150 fmol/g) were prepared and used to construct the calibration curve. The same amount of isotopically labelled BNP* was added to the calibrants and the UK NEQAS samples.

The results from the calibrants were plotted as the gravimetric amount of primary calibrator *vs.* the MS ion signal area ratios of the unlabelled BNP divided by the area of the isotopically labelled BNP. From this ion signal ratio, the amount of BNP in the UK NEQAS samples was calculated. The uncertainties associated with the values reported for the unknown samples were calculated by applying Equation 5:1.

$$\frac{u(c_{BNP})}{c_{BNP}} = \sqrt{\left(\frac{u(c_{BNPstock})}{c_{BNPstock}}\right)^2 + \left(\frac{u(m_{BNP})}{m_{BNP}}\right)^2 + \left(\frac{s_{MS_{RATIO}}}{MS_{RATIO}}\right)^2 + \left(\frac{u(m_{plasma})}{m_{plasma}}\right)^2}$$

Equation 5:1. Calculation of uncertainty of BNP concentration for the NEQAS samples, where $u(c_{BNPstock})/(c_{BNPstock})$ is the relative standard uncertainty associated to the stock solution; $u(m_{BNP})/m_{BNP}$ is the relative standard uncertainty of the amount of BNP in the sample determined by the calibration function; $s_{MS\ RATIO}/\sqrt{n}$ is the standard deviation of the mean of the measured mass spectrometry ratio; $u(m_{plasma})/m_{plasma}$ is the relative standard uncertainty of the UK NEQAS sample weights.

To visualise the correlation between the LC-MS/MS and the immunoassay methods the results were plotted in pairs and displayed in Figure 5:1. Only the results that were within the calibration range of the LC-MS/MS method were included. The individual results for all NEQAS samples can be found in Appendix B UK NEQAS .

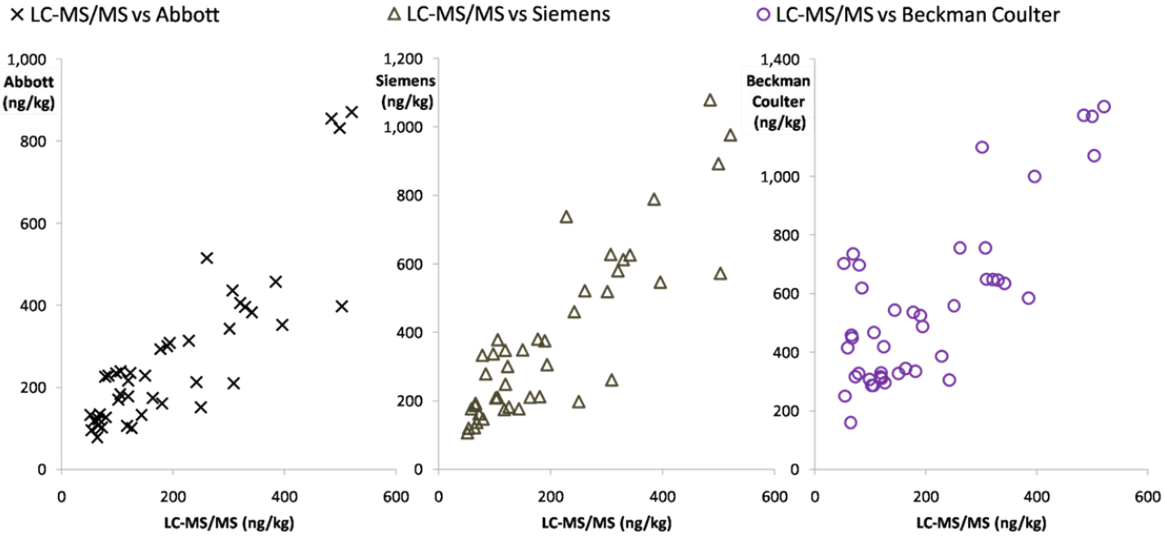

Figure 5:1. Correlation between the BNP results determined by the reference method and the Abbott, Siemens and Beckman Coulter immunoassay methods. x-axis: LC-MS/MS results, y-axis: average of the immunoassay results reported by the clinical laboratories for the same samples.

The results of the LC-MS/MS method were in most cases lower and correlate with the results of the immunoassays. The existence of a mathematical relationship between the results of immunoassays and the reference measurement procedure is the prerequisite for the success of any harmonisation or standardisation efforts in clinical chemistry.

Chapter 5.2.1 Multiplexing the LC-MS/MS method

Immunoassays are highly selective and specific to the epitope they are designed to recognise but due to the similar nature of the enzymatic degradation products of BNP cross-reactivity is not uncommon. [118], [120] An MS method for the determination of these products would be extremely valuable for the correct interpretation of the immunoassay results. Table 5:1 contains the list of the truncated BNP products and the enzymes responsible for their formation.

Table 5:1. Degradation products of BNP reported in literature.[122], [127], [167]

Sequence		M[a]	pI[b]	Charge[c]	Enzyme[d]
SPKMVQGSGCFGRKMDRISSSSGLGCKVLRRH	1-32	3464.1	12.1	6	-
KMVQGSGCFGRKMDRISSSSGLGCKVL	3-29	2830.4	11.5	4	DPPIV/ID
KMVQGSGCFGRKMDRISSSSGLGCKVLR	3-30	2986.6	11.9	5	DPPIV/ID
KMVQGSGCFGRKMDRISSSSGLGCKVLRRH	3-32	3279.9	12.1	6	DPPIV
MVQGSGCFGRKMDRISSSSGLGCK	4-27	2489.9	11.4	3	Corin/IDE
MVQGSGCFGRKMDRISSSSGLGCKVL	4-29	2702.2	11.4	3	Corin/IDE
MVQGSGCFGRKMDRISSSSGLGCKVLR	4-30	2858.4	11.9	4	Corin/IDE
MVQGSGCFGRKMDRISSSSGLGCKVLRR	4-31	3014.6	12.1	5	Corin/IDE
MVQGSGCFGRKMDRISSSSGLGCKVLRRH	4-32	3151.7	12.1	5	Corin
SPKMVQGSGCFGRKMDRISSSSGLGCKVL	1-29	3014.5	11.5	6	IDE
SPKMVQGSGCFGRKMDRISSSSGLGCKVLR	1-30	3170.7	11.9	7	IDE
VQGSGCFGRKMDRISSSSGLGCKVL	5-29	2571.0	11.4	5	NEP/IDE
VQGSGCFGRKMDRISSSSGLGCKVLRR	5-31	2883.4	12.1	7	NEP/IDE
VQGSGCFGRKMDRISSSSGLGCKVLRRH	5-32	3020.5	12.1	7	NEP
PKMVQGSGCFGRKMDRISSSSGLGCKVLRR	2-31	3239.8	12.2	6	-
SPKMVQGSGCFGRKMDRISSSSGLGCKV	1-28	2901.4	11.5	6	NEP
KMVQGSGCFGRKMDRISSSSGLGC	3-26	2489.9	11.4	5	DPPIV/ID
MVQGSGCFGRKMDRISSSSGLGC	4-26	2361.7	11.2	4	Corin/IDE
SPKMVQGSGCFGRKMDRISSSSGLGC	1-26	2674.1	11.4	5	IDE
VQGSGCFGRKMDRISSSSGLGC	5-26	2230.5	11.2	4	NEP/IDE
VQGSGCFGRKMDRISSSSGLGCK	5-27	2358.7	11.4	5	NEP

a: monoisotopic molecular weight (g/mol), b: calculated isoelectric point, c: positive charge at pH 7, [171] d: enzyme responsible, NEP: Neprilysin, DPPIV: Dipeptidyl peptidase IV, IDE: Insulin degrading enzyme.

The list is not comprehensive as additional enzymes likely to be involved in the degradation of BNP. [122], [167], [173] Meprin listed in Table 4:3.produces a truncated form of BNP 8-32 by cleaving between G_7 and S_8 in mice but not in humans therefore it was not included in the degradation study. [174] All listed degradation products share the ring structure of the intact BNP and truncated at the N-terminal and/or the C-terminal of the sequence. It is not unreasonable to assume that they are similarly recovered during the developed PPT and SPE conditions.

Because the synthetic peptides standards were not purchased, an experiment similar to the one used for the determination of the stabilisation effect of the acidified PPT (Chapter 4.3.2.) was used for the deliberate degradation of BNP. Five aliquots of a highly concentrated BNP solution were mixed with labelled BNP* in equimolar amounts (10 pmol, 2.9 µg) and freeze dried. The degradation products were generated in plasma by adding 0.5 g plasma to the aliquots resulting in a final concentration of 20 pmol/g (5.8 µg/g). PPT solvent was then added at the start (0 min) after 30, 60 and 90 min. These aliquots were used to study the degradation kinetics of BNP within the timeframes normally expected with sample processing. One aliquot was kept at room temperature and the degradation stopped after 54 hours to detect any BNP-related products formed after prolonged storage. (Figure 5:2.)

The identification of the degradation products was achieved by simultaneously monitoring specific transitions for the degradation products and the isotopically labelled internal standard based on the presumption that the internal standard degrades in an identical manner to the native analyte. Detection of the same transition for the unlabelled and labelled BNP was used as a confirmation of identity for the corresponding

product. Comparing the different time points the evolution of the different degradation products can be visualised and followed. Skyline was used for method development.

Skyline is an open source software tool that can be used to create SRM transition lists for peptides and proteins that can be exported into existing MS methods. [175] Skyline is compatible with Agilent platforms and was used for the generation of the SIM and SRM methods for monitoring the formation of products in the degradation experiments. The measurements were performed on the Agilent 6490 QqQ system. The number of plausible transitions that includes all possible fragments and charge states for BNP alone is over 200 (y- and b-ions only). The use of the isotopically labelled internal standard is invaluable in the identification of degradation products but doubles the number of transitions that are monitored. For the more than twenty degradation products listed in Table 5:1, the number of plausible transitions was more than 4,000. In reality not all charge states are observed and there are algorithms for the prediction of peptide charge states. Two formulas were used to try to reduce the number of transitions monitored for the screening methods. In the first, the net charge of peptides at a given pH was estimated by using the theoretical pKa/pKb values of the amino acid constituents. [176] The calculation is simple but neglects any interaction between the amino acid residues. The second method is based on the assumption that a minimum of three residues are required between acidic or basic residues to accommodate a charge. [55] Unfortunately, using either of the above methods resulted in an overestimation of the observed charge state for BNP. The relative position of the amino acids in the sequence, secondary structure and the use of superchargers affect the amount of protons accommodated on the peptide ion and make the prediction of the highest observed charge state cumbersome. Experiments were set up to monitor the charge states corresponding to ± 1

charge relative to the net charge calculated at pH 7 in single ion monitoring mode (SIM) (e.g. BNP 3-32, net charge at pH 7: 6+, monitored SIM: 5+/6+/7+). This method resulted in a total of 120 SIM transitions, which led to three MS methods.

For the degradation products that were identified in the SIM experiments, SRM transitions were set up to fragment the most intense charge state and monitor the y fragment ions only with the charge state equal to the precursor and - 1 and - 2 charge states relative to the precursor. The determined transitions for the detected peptides are listed in Table 5:2. The results of the degradation experiment are displayed in Figure 5:2.

Table 5:2. SRM *m/z* transitions for the monitored degradation products.

	Cleaved residues	UNLABELLED		LABELLED		Precursor charge state	Monitored fragment
		Precursor	Fragment	Precursor	Fragment		
1-32		578.3	699.2	583.3	705.3	6+	y26 4+
3-30	SP-/-RH	598.3	715.6	604.3	723.0	5+	y27 4+
3-32	SP-	547.7	699.2	552.6	705.3	6+	y26 4+
4-32	SPKM-	631.3	731.3	637.3	737.3	5+	y27 4+
8-31	SPKMVQG-	548.2	586.7			5+	y20 4+

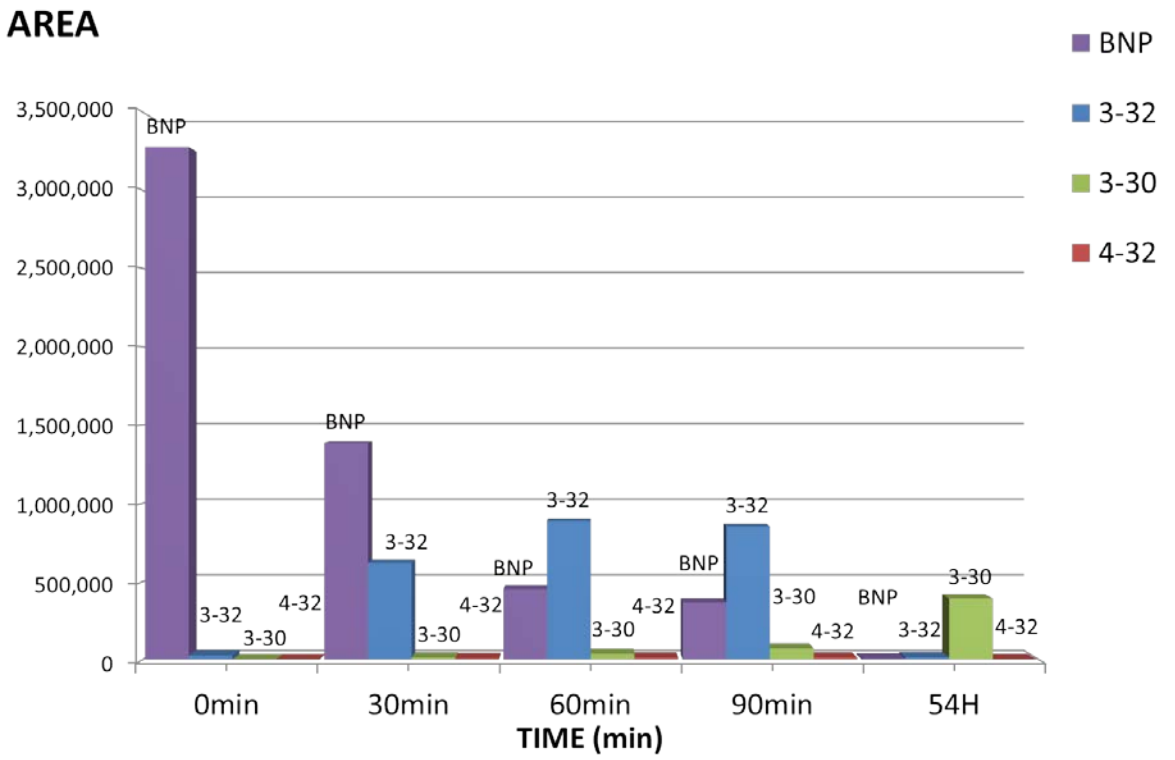

Figure 5:2. Results of the degradation experiments of BNP in plasma. Three degradation products were identified and monitored: BNP 3-32, BNP 3-30 and BNP 4-32. The integrated area of the SRM transitions corresponding to the unlabelled peptides is plotted vs time of degradation. Concentration of BNP in spiked plasma: 20 pmol/g (5.8 µg/g).

The degradation of BNP follows the same kinetics as determined in Chapter 4.3.2. As BNP degrades the ion signal for the peptide missing the first two amino acid residues (3-32) evolves due to the activity of the DPPIV enzyme. [121] The degradation product truncated at both the C-terminal and the N-terminal (3-30) was detected after 30 min and its ion signal increased as the degradation continued. BNP 4-32 was detected in the sample after 30 min and its ion signal intensity peaked after 90 min, only a small amount remained after 54 hours. These results agree with the findings of Zhang *et al.* when the peptidoforms of BNP were analysed by CE-MS. [125] The results of both experiments suggest that BNP 3-30 and 3-29 remain stable after an extended period of time. Assays targeting 3-30 may be more appropriate for the heart failure diagnosis. Relative amounts of 3-30 and 3-29 could be indicative of the time of the cardiac event.

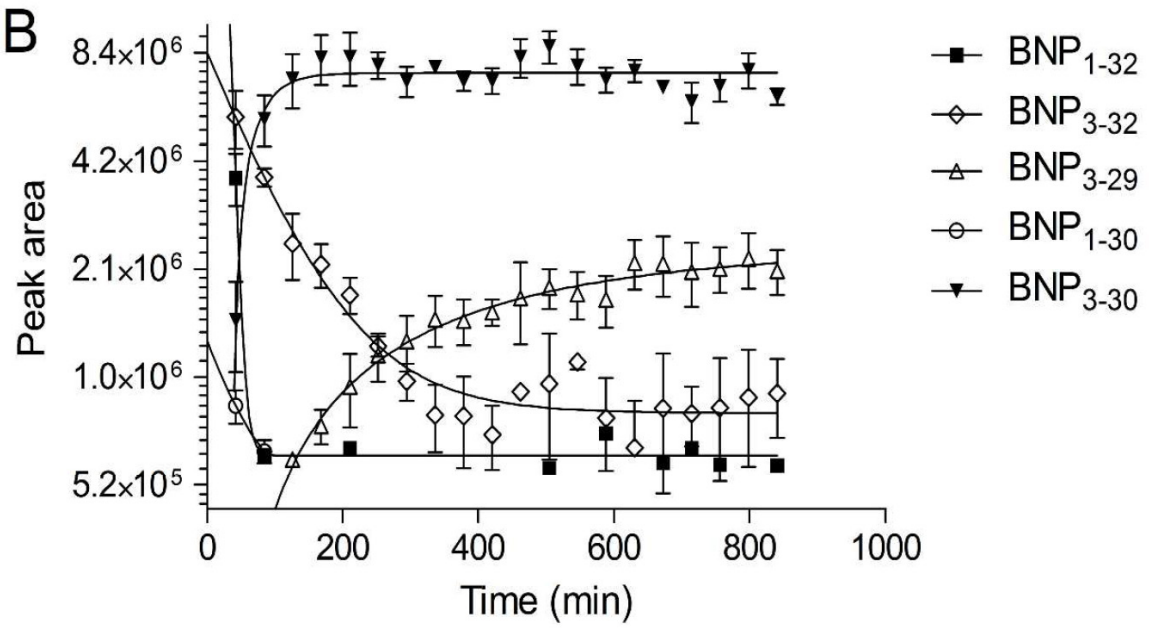

Figure 5:3. Time course profile of BNP peptidoforms detected by CE-MS by Zhang *et al*. Concentration of BNP in spiked plasma: 250 ng/µL (250 µg/g). [125]

Although without the use of isotopically labelled internal standard the results are not quantitative, they provide further evidence of the instability of BNP. In addition, the method can be used to monitor for the presence of any degradation products in the EQA samples.

In the course of the year samples from the same preparations were sent out on several occasions by NEQAS. The results corresponding to the same preparations (A, B, C, LGC1 and LGC2) and the degradation profiles determined for each sample are displayed in Figure 5:4.

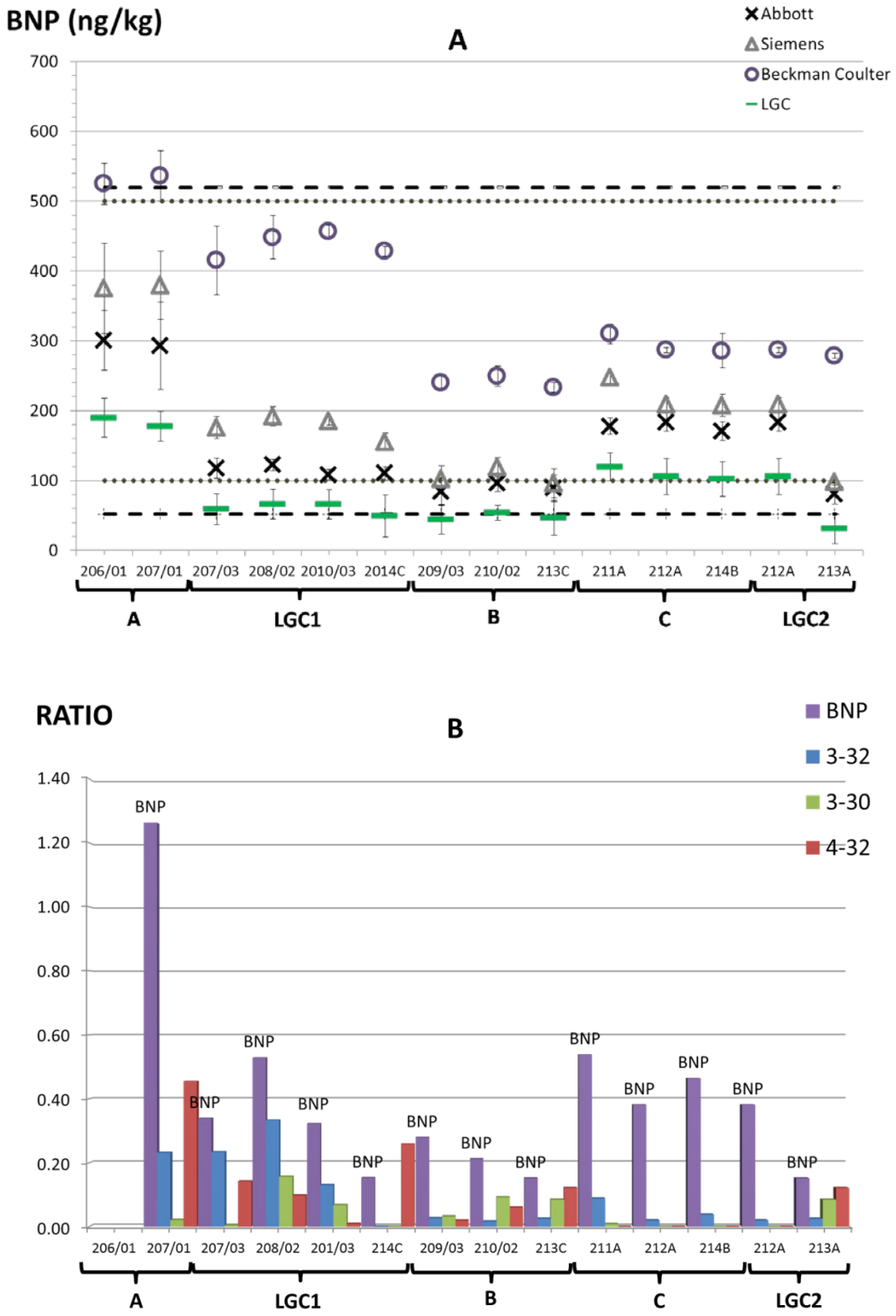

Figure 5:4. BNP quantitation results (A, top) and degradation profiles (B, bottom) of NEQAS samples. Dashed lines: range of the reference method (52-520 pg/g). Dotted lines: lower and higher decision limits (100/500 pg/g). RATIO: BNP, 3-32, 3-30 and 4-32 area over the labelled BNP* area. A, B, C, LGC1 and LGC2: samples are coming from the same preparation.

The LC-MS/MS results for replicate measurements agree within the determined uncertainty of the reference method. The results of the immunoassay measurements also show high reproducibility. The lower values of the newly developed LC-MS/MS reference method could indicate the non-specificity of the immunoassays. Additional reasons for the observed discrepancy could be a lack of characterisation of the BNP material used for the preparation of the EQAS samples, differences in the standards used for the calibration of immunoassays and degradation of BNP before analysis. The synthetic peptide employed by NEQAS could contain high amounts of closely related peptidic impurities that could cross-react with the immunoassays. [177], [178] To test this hypothesis, concentrated aliquots of the newly developed BNP primary standard were sent to NEQAS and used for the preparation of two sets of samples (LGC1 and LGC2). Using this BNP primary standard for spiking the plasma samples did not improve the agreement between the four assays. Because the primary BNP standard material was assessed for the presence of impurities and it was shown that it contained less than 4 % of peptidic impurities (Chapter 3), the difference between the immunoassay and the reference method was not caused by the quality of the BNP spiking material.

The agreement between the results for the replicate measurements of the same preparations is very good for all samples with the three immunoassays and the reference method. The only exception is sample 213A. (LGC2, Figure 5:4). In sample 231A a high amount of BNP products was detected by LC-MS/MS. The LC-MS/MS reference method and two of the immunoassays reported lower BNP concentrations, while the Beckman Coulter assay reported roughly the same value. This can be explained with the different epitope specificity of the antibodies used in the different immunoassays. Immunoassay manufacturers are required to publish epitope specificity of the antibodies used in their

kits. [119] The specificity of capture and detection antibodies for the three assays participating in the study is listed in Table 5:3.

Table 5:3. Epitope specificities of the antibodies used in immunoassays in the UK NEQAS.

Assay	Capture	Detection	Calibrant
Abbott	NH_2 terminus and part of the ring structure (Scios) Murine monoclonal AB (5-13)	COOH terminus Murine monoclonal AB (26-32)	Synthetic BNP
Siemens	COOH terminus (BC-203) (Shionogi) Murine monoclonal AB (27-32)	KY-hBNP-II (Shionogi) Murine monoclonal AB (14-21)	Synthetic BNP
Beckman Coulter	BNP (Biosite) Murine omniclonal AB epitope not characterized	NH_2 terminus and part of the ring structure (Scios) Murine monoclonal AB(5-13)	Recombinant BNP

Omniclonal: mixture of different antibody molecules.

The Abbott assay uses a combination of antibodies specific to the intact N-terminus of BNP and to amino acids 5-13 of the sequence. The detection antibody requires an intact C-terminus. This means that the Abbott assay will capture all the degradation products as long as the 5-13 amino acids are intact and detects everything that is not truncated at the C-terminal (i.e. 3-32, 4-32 and 5-32). The Siemens assay captures peptides with an intact C-terminus and detects everything that has an unbroken ring structure. (3-32, 4-32, 5-32, 8-32). The Beckman Coulter assay uses a mixture of different antibodies for capture and detects everything that has an intact N-terminal and the sequence corresponding to 5-13 amino acids of BNP. (1-29, 1-30, 1-28, 1-26). Recombinant BNP is used for the calibration of the Beckman Coulter assay while the other two immunoassays are calibrated by synthetic BNP.

In preparation C, sample 211A shows an increased amount of 3-32 peptide present in the extracts. The Siemens and Beckman Coulter assay reported higher BNP results than for sample 212A and 214B which came from the same preparation. In preparation B, the Abbott and the Siemens assay agree (100 ng/kg) but the Beckman Coulter assay reports

over 200 ng/kg BNP concentrations for the three samples. All three degradation products (3-32, 3-30, 4-32) were found in these samples. The high amount of 3-30 and 4-32 found in sample 213A also suggests that some of the differences between the immunoassay results can be explained by cross-reactivity with the products from the degrading BNP.

In order to investigate the possible cross-reactivity of the immunoassays, two samples distributed by NEQAS were spiked with BNP 8-32 peptide instead of BNP. BNP 8-32 is the degradation product of enzymatic activity of Meprin and the only BNP product peptide that is commercially available. The spiking experiment was devised to demonstrate the existence of cross-reactivity of immunoassays with different epitope specificities. The results reported by the four methods are displayed in Figure 5:5.

As expected, no BNP 1-32 was detected by LC-MS/MS. The Siemens assay detected BNP in the second sample. The capture antibody of the Siemens assay recognised the intact C-terminal of the 8-32 peptide and as the truncated peptide contains the 14-21 residues of the BNP sequence the detection antibody incorrectly gave positive readings for the NEQAS sample. The result successfully demonstrates how the use of nonspecific capture and detection antibodies can lead to erroneous results in clinical laboratories and the utility of a reference method for the correct value assignment of quality assessment samples.

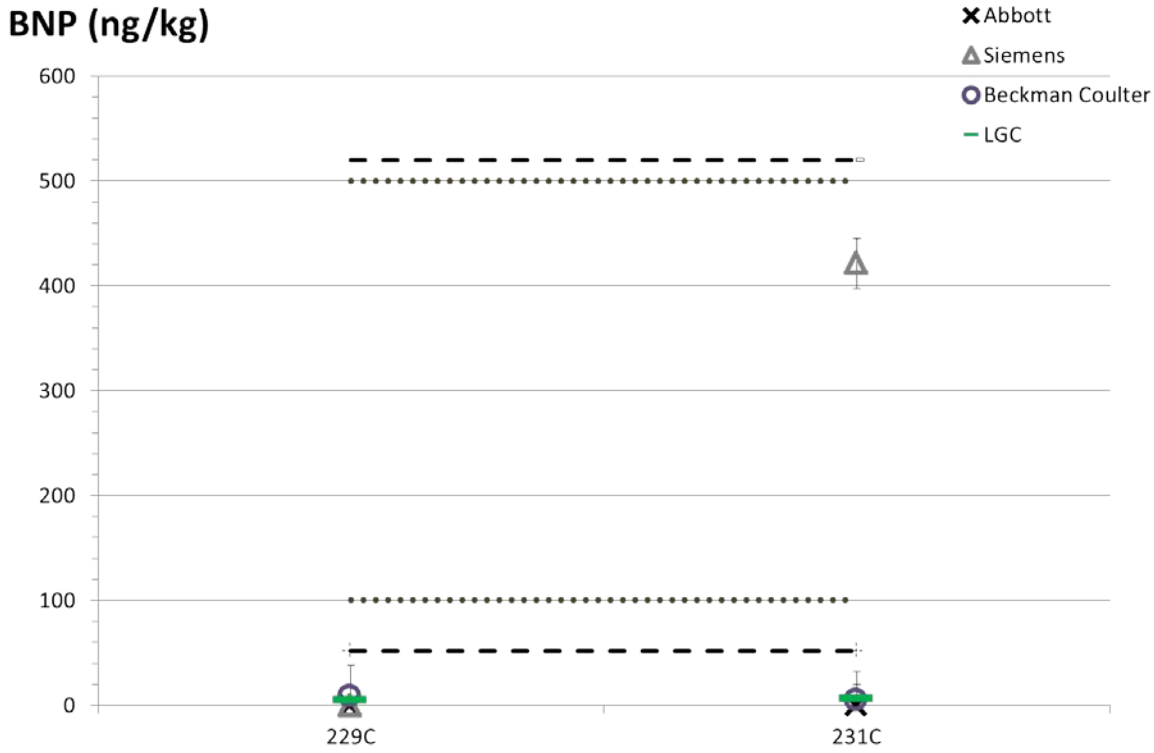

Figure 5:5. Results reported for the NEQAS preparations of samples 229C and 231C spiked with BNP 8-32 but no BNP. Dashed lines: range of the reference method (52-520 pg/g). Dotted lines: lower and higher decision limits (100/500 pg/g).

The capture antibody of the Abbott assay did not react and the detection antibody of the

Beckman Coulter assay did not recognise the 8-32 peptide.

Chapter 5.3 Conclusions

The reference method was successfully applied to the analysis of EQA samples for the determination of BNP concentration in plasma samples spiked with synthetic BNP. The LC-MS/MS results correlated with the results reported by the three immunoassays and therefore can be applied for the harmonisation or standardisation of clinical BNP measurements. The results of repeated analyses of EQA samples are very consistent for both the immunoassays and the reference method. The absolute BNP results in most cases are higher than the LC-MS/MS results. The differences between the (absolute) results reported by the immunoassays can be due to differences in the amount of BNP in the calibrants provided by the manufacturers, the lack of specificity of capture and/or detection antibodies and cross-reactivity between the immunoassays and BNP degradation products. As no certified BNP reference material in plasma is currently available, immunoassay manufacturers supply the calibrants to be used with the assays. The source and quality of these calibrants is not known.

With the use of isotopically labelled internal standard, MS detection enabled the reliable identification of degradation products without the need for synthetic peptide standards. The results from these experiments demonstrate that some of the differences between the immunoassay results are caused by the different specificity of the assays for BNP and BNP degradation products in plasma. The reference method can be extended to quantify multiple degradation products for BNP. Quantitative information on the presence and stability of degradation products can be used to develop assays not affected by cross-reactivity and could account for differences between results from existing immunoassays.

Chapter 6 Future work

The utility of LC-MS/MS for the development of a reference method for the quantification of an unstable intact peptide in plasma was demonstrated. The results of the reference method correlate with the immunoassay results for spiked plasma samples therefore it can potentially be used for the harmonisation and standardisation of external quality assessment schemes by assigning reference values to EQA samples.

The developed method provided insight into the possible causes for the variability between the different immunoassay results. The quality of the calibrants used by the immunoassay manufacturers, the lack of molecular specificity of antibodies and degradation of BNP in plasma have been identified as likely causes for the discrepancies in the reported absolute BNP values by different clinical laboratories.

Future work is aimed at the extension of the LC-MS/MS method for the quantification of BNP degradation products and the analysis of patient samples.

With the availability of a reliable platform for the detection and quantification of BNP and BNP degradation products alternative cardiac markers which have a longer half-life in circulation can be identified and targeted in clinical diagnostics. As the degradation kinetics is different for the products, their relative concentration could be indicative of the onset of the original cardiac injury. Information on the biological activity of BNP degradation products is not available in literature. An MS based method could be an extremely useful tool in medical research for the unambiguous confirmation of the efficacy of cardiac drugs or for therapeutic drug monitoring.

The results from patient samples can provide further understanding into the extent of cross reactivity with unprocessed proBNP and the availability of the biologically active

cardiac hormone (or biologically active degradation products of BNP) in heart failure patients. If correlation with the patient samples exists between the reference method and immunoassay results, the development of a commutable reference material is a possibility.

The work here carried out represents the background for a CCQM study for the quantification of BNP in plasma. The study will enable NMIs to demonstrate their competence and use their methods to provide reference values to samples distributed by their corresponding national EQA schemes.

A concerted effort in studying (biological) activity of degradation products, epitope mapping of antibodies used in commercial assays and reference laboratories capable of the value assignment of EQA samples could greatly benefit our understanding of cardiac health and efforts in the harmonisation and standardisation of clinical BNP measurements.

References

[1] M. Polanski and N. L. Anderson, 'A List of Candidate Cancer Biomarkers for Targeted Proteomics', *Biomark. Insights*, vol. 1, pp. 1–48, Feb. 2007.

[2] E. Boschetti, M. C. M. Chung, and P. G. Righetti, '"The quest for biomarkers": Are we on the right technical track?', *PROTEOMICS – Clin. Appl.*, vol. 6, no. 1–2, pp. 22–41, 2012.

[3] A. I. Barbosa and N. M. Reis, 'A critical insight into the development pipeline of microfluidic immunoassay devices for the sensitive quantitation of protein biomarkers at the point of care', *The Analyst*, vol. 142, no. 6, pp. 858–882, 2017.

[4] M. Bidlingmaier and P. U. Freda, 'Measurement of human growth hormone by immunoassays: Current status, unsolved problems and clinical consequences', *Growth Horm. IGF Res.*, vol. 20, no. 1, pp. 19–25, 2010.

[5] M. Bidlingmaier and C. J. Strasburger, 'Growth hormone assays: current methodologies and their limitations', *Pituitary*, vol. 10, no. 2, pp. 115–119, 2007.

[6] H. Schimmel, I. Zegers, and H. Emons, 'Standardization of protein biomarker measurements: Is it feasible?', *Scand. J. Clin. Lab. Invest.*, vol. 70, no. s242, pp. 27–33, 2010.

[7] S. Bruins *et al.*, 'High Intraindividual Variation of B-Type Natriuretic Peptide (BNP) and Amino-Terminal proBNP in Patients with Stable Chronic Heart Failure', *Clin. Chem.*, vol. 50, no. 11, pp. 2052–2058, Nov. 2004.

[8] K. Lewandrowski, A. Chen, and J. Januzzi, 'Cardiac markers for myocardial infarction. A brief review', *Am. J. Clin. Pathol.*, vol. 118 Suppl, pp. S93-99, Dec. 2002.

[9] L. M. Thienpont, K. Van Uytfanghe, and A. P. De Leenheer, 'Reference measurement systems in clinical chemistry', *Clin. Chim. Acta Int. J. Clin. Chem.*, vol. 323, no. 1–2, pp. 73–87, 2002.

[10] W. Greg Miller *et al.*, 'Roadmap for Harmonization of Clinical Laboratory Measurement Procedures', *Clin Chem*, vol. 57, no. 8, pp. 1108–1117, Aug. 2011.

[11] G. Merlini, S. Blirup-Jensen, A. M. Johnson, J. Sheldon, and I. Zegers, 'Standardizing plasma protein measurements worldwide: a challenging enterprise', *Clin. Chem. Lab. Med.*, vol. 48, no. 11, pp. 1567–1575, 2010.

[12] Directive 98/79/EC, 'Directive 98/79/EC of the European Parliament and of the Council of 27 October 1998 on In Vitro Diagnostic Medical Devices', vol. L331, pp. 1–37, 1998.

[13] D. Armbruster and R. R. Miller, 'The Joint Committee for Traceability in Laboratory Medicine (JCTLM): a global approach to promote the standardisation of clinical laboratory test results', *Clin. Biochem. Rev. Aust. Assoc. Clin. Biochem.*, vol. 28, no. 3, pp. 105–113, Aug. 2007.

[14] 'ISO 17511:2003 - In vitro diagnostic medical devices -- Measurement of quantities in biological samples -- Metrological traceability of values assigned to calibrators and control materials'. [Online]. Available: http://www.iso.org/iso/catalogue_detail.htm?csnumber=30716. [Accessed: 21-Nov-2012].

[15] G. R. D. Jones and C. Jackson, 'The Joint Committee for Traceability in Laboratory Medicine (JCTLM) – its history and operation', *Clin. Chim. Acta*, vol. 453, pp. 86–94, Jan. 2016.

[16] L. M. Thienpont and S. K. Van Houcke, ‘Traceability to a common standard for protein measurements by immunoassay for in-vitro diagnostic purposes’, *Clin. Chim. Acta*, vol. 411, no. 23–24, pp. 2058–2061, Dec. 2010.
[17] V. Barwick and E. Prichard, Eds., *Eurachem Guide: Terminology in Analytical Measurement - Introduction to VIM 3*, 1st ed. Eurachem, 2011.
[18] ISO/IEC Guide 99, *International vocabulary of metrology -- Basic and general concepts and associated terms (VIM)*, 3rd ed. Geneva, Switzerland: International Organisation for Standardisation, 2007.
[19] W. G. Miller, ‘Why Commutability Matters’, *Clin. Chem.*, vol. 52, no. 4, pp. 553–554, Feb. 2006.
[20] L. M. Thienpont and S. K. Van Houcke, ‘Traceability to a common standard for protein measurements by immunoassay for in-vitro diagnostic purposes’, *Clin. Chim. Acta*, vol. 411, no. 23–24, pp. 2058–2061, 2010.
[21] ‘Database of higher-order reference materials, measurement methods/procedures and services’. [Online]. Available: http://www.bipm.org/jctlm/. [Accessed: 04-Aug-2016].
[22] J. J. Thomson, *Rays of positive electricity and their application to chemical analyses*, vol. 1. Longmans, Green and Company, 1921.
[23] A. Dempster, ‘A new Method of Positive Ray Analysis’, *Phys. Rev.*, vol. 11, no. 4, pp. 316–325, 1918.
[24] A. O. Nier, ‘A Mass Spectrometer for Routine Isotope Abundance Measurements’, *Rev. Sci. Instrum.*, vol. 11, no. 7, pp. 212–216, Jul. 1940.
[25] R. A. Hites, ‘Development of Gas Chromatographic Mass Spectrometry’, *Anal. Chem.*, vol. 88, no. 14, pp. 6955–6961, Jul. 2016.
[26] J. Griffiths, ‘A Brief History of Mass Spectrometry’, *Anal. Chem.*, vol. 80, no. 15, pp. 5678–5683, Aug. 2008.
[27] A. O. Nier, ‘A Mass Spectrometer for Isotope and Gas Analysis’, *Rev. Sci. Instrum.*, vol. 18, no. 6, pp. 398–411, Jun. 1947.
[28] M. S. B. Munson and F. H. Field, ‘Chemical Ionization Mass Spectrometry. I. General Introduction’, *J. Am. Chem. Soc.*, vol. 88, no. 12, pp. 2621–2630, Jun. 1966.
[29] R. Macfarlane and D. Torgerson, ‘Californium-252 plasma desorption mass spectroscopy’, *Science*, vol. 191, no. 4230, pp. 920–925, Mar. 1976.
[30] M. Barber, R. S. Bordoli, R. D. Sedgwick, and A. N. Tyler, ‘Fast atom bombardment of solids (F.A.B.): a new ion source for mass spectrometry’, *J. Chem. Soc. Chem. Commun.*, no. 7, pp. 325–327, Jan. 1981.
[31] J. B. Fenn, M. Mann, C. K. Meng, S. F. Wong, and C. M. Whitehouse, ‘Electrospray Ionization for Mass-Spectrometry of Large Biomolecules’, *Science*, vol. 246, no. 4926, pp. 64–71, 1989.
[32] M. Karas, D. Bachmann, U. Bahr, and F. Hillenkamp, ‘Matrix-assisted ultraviolet laser desorption of non-volatile compounds’, *Int. J. Mass Spectrom. Ion Process.*, vol. 78, pp. 53–68, 1987.
[33] E. de Hoffmann and V. Stroobant, *Mass Spectrometry: Principles and Applications*, 2nd ed. Wiley, 2001.
[34] M. Wilm and M. Mann, ‘Analytical Properties of the Nanoelectrospray Ion Source’, *Anal. Chem.*, vol. 68, no. 1, pp. 1–8, 1996.
[35] R. A. Yost and C. G. Enke, ‘Triple Quadrupole Mass Spectrometry’, *Anal. Chem.*, vol. 51, no. 12, pp. 1251A-1264A, Oct. 1979.

[36] C. M. Whitehouse, R. N. Dreyer, M. Yamashita, and J. B. Fenn, 'Electrospray interface for liquid chromatographs and mass spectrometers', *Anal. Chem.*, vol. 57, no. 3, pp. 675–679, 1985.

[37] Lord Rayleigh, 'XX. On the equilibrium of liquid conducting masses charged with electricity', *Philos. Mag. Ser. 5*, vol. 14, no. 87, pp. 184–186, Sep. 1882.

[38] M. Dole, L. L. Mack, R. L. Hines, R. C. Mobley, L. D. Ferguson, and M. B. Alice, 'Molecular Beams of Macroions', *J. Chem. Phys.*, vol. 49, no. 5, pp. 2240–2249, Sep. 1968.

[39] M. Yamashita and J. B. Fenn, 'Electrospray ion source. Another variation on the free-jet theme', *J. Phys. Chem.*, vol. 88, no. 20, pp. 4451–4459, Sep. 1984.

[40] G. Taylor, 'Disintegration of Water Drops in an Electric Field', *Proc. R. Soc. Lond. Math. Phys. Eng. Sci.*, vol. 280, no. 1382, pp. 383–397, Jul. 1964.

[41] M. Wilm, 'Principles of Electrospray Ionization', *Mol. Cell. Proteomics*, vol. 10, no. 7, Jul. 2011.

[42] L. Konermann, E. Ahadi, A. D. Rodriguez, and S. Vahidi, 'Unraveling the Mechanism of Electrospray Ionization', *Anal. Chem.*, vol. 85, no. 1, pp. 2–9, Jan. 2013.

[43] L. Konermann, 'A simple model for the disintegration of highly charged solvent droplets during electrospray ionization', *J. Am. Soc. Mass Spectrom.*, vol. 20, no. 3, pp. 496–506, 2009.

[44] S. G. Valeja, J. D. Tipton, M. R. Emmett, and A. G. Marshall, 'New Reagents for Enhanced Liquid Chromatographic Separation and Charging of Intact Protein Ions for Electrospray Ionization Mass Spectrometry', *Anal. Chem.*, vol. 82, no. 17, pp. 7515–7519, Sep. 2010.

[45] S. H. Lomeli, I. X. Peng, S. Yin, R. R. Ogorzalek Loo, and J. A. Loo, 'New Reagents for Increasing ESI Multiple Charging of Proteins and Protein Complexes', *J. Am. Soc. Mass Spectrom.*, vol. 21, no. 1, pp. 127–131, Jan. 2010.

[46] H. J. Sterling, J. S. Prell, C. A. Cassou, and E. R. Williams, 'Protein Conformation and Supercharging with DMSO from Aqueous Solution', *J. Am. Soc. Mass Spectrom.*, vol. 22, no. 7, pp. 1178–1186, Jul. 2011.

[47] K. A. Douglass and A. R. Venter, 'Investigating the role of adducts in protein supercharging with sulfolane', *J. Am. Soc. Mass Spectrom.*, vol. 23, no. 3, pp. 489–497, Mar. 2012.

[48] H. Hahne *et al.*, 'DMSO enhances electrospray response, boosting sensitivity of proteomic experiments', *Nat. Methods*, vol. 10, no. 10, pp. 989–991, Oct. 2013.

[49] H. Metwally, R. G. McAllister, V. Popa, and L. Konermann, 'Mechanism of Protein Supercharging by Sulfolane and m-Nitrobenzyl Alcohol: Molecular Dynamics Simulations of the Electrospray Process', *Anal. Chem.*, vol. 88, no. 10, pp. 5345–5354, May 2016.

[50] S. M. Miladinović, L. Fornelli, Y. Lu, K. M. Piech, H. H. Girault, and Y. O. Tsybin, 'In-Spray Supercharging of Peptides and Proteins in Electrospray Ionization Mass Spectrometry', *Anal. Chem.*, vol. 84, no. 11, pp. 4647–4651, Jun. 2012.

[51] J. B. Fenn, 'Ion formation from charged droplets: Roles of geometry, energy, and time', *J. Am. Soc. Mass Spectrom.*, vol. 4, no. 7, pp. 524–535, Jul. 1993.

[52] S. H. Lomeli, S. Yin, R. R. Ogorzalek Loo, and J. A. Loo, 'Increasing Charge While Preserving Noncovalent Protein Complexes for ESI-MS', *J. Am. Soc. Mass Spectrom.*, vol. 20, no. 4, pp. 593–596, Apr. 2009.

[53] H. J. Sterling and E. R. Williams, 'Origin of Supercharging in Electrospray Ionization of Noncovalent Complexes from Aqueous Solution', *J. Am. Soc. Mass Spectrom.*, vol. 20, no. 10, pp. 1933–1943, Oct. 2009.

[54] H. J. Sterling, C. A. Cassou, A. C. Susa, and E. R. Williams, 'Electrothermal Supercharging of Proteins in Native Electrospray Ionization', *Anal. Chem.*, vol. 84, no. 8, pp. 3795–3801, Apr. 2012.

[55] K. A. Douglass and A. R. Venter, 'Predicting the Highest Intensity Ion in Multiple Charging Envelopes Observed for Denatured Proteins during Electrospray Ionization Mass Spectrometry by Inspection of the Amino Acid Sequence', *Anal. Chem.*, vol. 85, no. 17, pp. 8212–8218, Sep. 2013.

[56] M. Karas, D. Bachmann, and F. Hillenkamp, 'Influence of the wavelength in high-irradiance ultraviolet laser desorption mass spectrometry of organic molecules', *Anal. Chem.*, vol. 57, no. 14, pp. 2935–2939, Dec. 1985.

[57] M. Karas and F. Hillenkamp, 'Laser desorption ionization of proteins with molecular masses exceeding 10,000 daltons.', *Anal. Chem.*, vol. 60, no. 20, pp. 2299–301, Oct. 1988.

[58] K. Tanaka *et al.*, 'Protein and polymer analyses up to m\z 100 000 by laser ionization time-of-flight mass spectrometry', *Rapid Commun. Mass Spectrom.*, vol. 2, no. 8, pp. 151–153, 1988.

[59] R. Knochenmuss, 'Ion formation mechanisms in UV-MALDI', *Analyst*, vol. 131, no. 9, pp. 966–986, Aug. 2006.

[60] M. F. Mirabelli and R. Zenobi, 'Observing Proton Transfer Reactions Inside the MALDI Plume: Experimental and Theoretical Insight into MALDI Gas-Phase Reactions', *J. Am. Soc. Mass Spectrom.*, pp. 1–11, 2017.

[61] N. Bache, K. D. Rand, P. Roepstorff, and T. J. D. Jørgensen, 'Gas-phase fragmentation of peptides by MALDI in-source decay with limited amide hydrogen (1H/2H) scrambling', *Anal. Chem.*, vol. 80, no. 16, pp. 6431–6435, Aug. 2008.

[62] B. A. Mamyrin, V. I. Karataev, D. V. Shmikk, and V. A. Zagulin, 'The mass-reflectron, a new nonmagnetic time-of-flight mass spectrometer with high resolution', *Sov. J. Exp. Theor. Phys.*, vol. 37, p. 45, Jul. 1973.

[63] M. W. Towers, J. E. Mckendrick, and R. Cramer, 'Introduction of 4-Chloro-α-cyanocinnamic Acid Liquid Matrices for High Sensitivity UV-MALDI MS', *J. Proteome Res.*, vol. 9, no. 4, pp. 1931–1940, Apr. 2010.

[64] W. Paul and H. Steinwedel, 'Ein neues Massenspektrometer ohne Magnetfeld', *Z. Für Naturforschung A*, vol. 8, no. 7, pp. 448–450, 1953.

[65] 'Introduction to LC-MS : SHIMADZU (Shimadzu Corporation)'. [Online]. Available: http://www.shimadzu.com/an/hplc/support/lib/lctalk/61/61intro.html. [Accessed: 20-Oct-2017].

[66] P. E. Miller and M. B. Denton, 'The Quadrupole Mass Filter - Basic Operating Concepts', *J. Chem. Educ.*, vol. 63, no. 7, pp. 617–622, 1986.

[67] K. H. Kingdon, 'A Method for the Neutralization of Electron Space Charge by Positive Ionization at Very Low Gas Pressures', *Phys. Rev.*, vol. 21, no. 4, pp. 408–418, Apr. 1923.

[68] 'Orbitrap Mass Analyzer – Overview and Applications in Proteomics - Scigelova - 2006 - PROTEOMICS - Wiley Online Library'. [Online]. Available: http://onlinelibrary.wiley.com/doi/10.1002/pmic.200600528/full. [Accessed: 11-May-2017].

[69] R. A. Zubarev and A. Makarov, 'Orbitrap Mass Spectrometry', *Anal. Chem.*, vol. 85, no. 11, pp. 5288–5296, Jun. 2013.
[70] A. A. Makarov, 'Electrostatic axially harmonic orbital trapping: A high-performance technique of mass analysis', *Anal. Chem.*, vol. 72, no. 6, pp. 1156–1162, 2000.
[71] A. A. Makarov *et al.*, 'Performance evaluation of a hybrid linear ion trap/orbitrap mass spectrometer', *Anal. Chem.*, vol. 78, no. 7, pp. 2113–2120, 2006.
[72] W. E. Stephens, 'A pulsed mass spectrometer with time dispersion', in *Physical Review*, 1946, vol. 69, pp. 691–691.
[73] W. C. Wiley and I. H. McLaren, 'Time-of-Flight Mass Spectrometer with Improved Resolution', *Rev. Sci. Instrum.*, vol. 26, no. 12, p. 1150, 1955.
[74] H. R. Morris *et al.*, 'High Sensitivity Collisionally-activated Decomposition Tandem Mass Spectrometry on a Novel Quadrupole/Orthogonal-acceleration Time-of-flight Mass Spectrometer', *Rapid Commun. Mass Spectrom.*, vol. 10, no. 8, pp. 889–896, Jun. 1996.
[75] I. Haller, U. A. Mirza, and B. T. Chait, 'Collision induced decomposition of peptides. Choice of collision parameters', *J. Am. Soc. Mass Spectrom.*, vol. 7, no. 7, pp. 677–681, Jul. 1996.
[76] V. H. Wysocki, G. Tsaprailis, L. L. Smith, and L. A. Breci, 'Mobile and localized protons: a framework for understanding peptide dissociation', *J. Mass Spectrom.*, vol. 35, no. 12, pp. 1399–1406, Dec. 2000.
[77] P. Roepstorff and J. Fohlman, 'PROPOSAL FOR A COMMON NOMENCLATURE FOR SEQUENCE IONS IN MASS-SPECTRA OF PEPTIDES', *Biomed. Mass Spectrom.*, vol. 11, no. 11, p. 601, 1984.
[78] K. Biemann, 'Contributions of mass spectrometry to peptide and protein structure', *Biomed. Environ. Mass Spectrom.*, vol. 16, no. 1–12, pp. 99–111, Oct. 1988.
[79] P. Roepstorff and J. Fohlman, 'Proposal for a common nomenclature for sequence ions in mass spectra of peptides', *Biomed. Mass Spectrom.*, vol. 11, no. 11, p. 601, Nov. 1984.
[80] R. S. Johnson, S. A. Martin, and K. Biemann, 'Collision-induced fragmentation of (M + H)+ ions of peptides. Side chain specific sequence ions', *Int. J. Mass Spectrom. Ion Process.*, vol. 86, pp. 137–154, Dec. 1988.
[81] B. Spengler, 'Post-source decay analysis in matrix-assisted laser desorption/ionization mass spectrometry of biomolecules', *J. Mass Spectrom.*, vol. 32, no. 10, pp. 1019–1036, Nov. 1997.
[82] R. A. Zubarev, N. L. Kelleher, and F. W. McLafferty, 'Electron Capture Dissociation of Multiply Charged Protein Cations. A Nonergodic Process', *J. Am. Chem. Soc.*, vol. 120, no. 13, pp. 3265–3266, Apr. 1998.
[83] J. E. P. Syka, J. J. Coon, M. J. Schroeder, J. Shabanowitz, and D. F. Hunt, 'Peptide and protein sequence analysis by electron transfer dissociation mass spectrometry', *PNAS*, vol. 101, no. 26, pp. 9528–9533, 2004.
[84] K. G. Heumann, 'Isotope dilution mass spectrometry of inorganic and organic substances', *Fresenius Z. Anal. Chem.*, vol. 325, no. 8, pp. 661–666, 1986.
[85] P. D. Bièvre and H. S. Peiser, 'Basic equations and uncertainties in isotope-dilution mass spectrometry for traceability to SI of values obtained by this primary method', *Fresenius J. Anal. Chem.*, vol. 359, no. 7–8, pp. 523–525, Dec. 1997.
[86] A. Henrion, 'Reduction of systematic errors in quantitative analysis by isotope dilution mass spectrometry (IDMS): an iterative method', *Fresenius J. Anal. Chem.*, vol. 350, no. 12, pp. 657–658, 1994.

[87] D. M. Bunk, ‘Reference materials and reference measurement procedures: an overview from a national metrology institute’, *Clin. Biochem. Rev. Aust. Assoc. Clin. Biochem.*, vol. 28, no. 4, pp. 131–137, 2007.

[88] M. S. Lowenthal, J. Yen, D. M. Bunk, and K. W. Phinney, ‘Certification of NIST standard reference material 2389a, amino acids in 0.1 mol/L HCl--quantification by ID LC-MS/MS’, *Anal. Bioanal. Chem.*, vol. 397, no. 2, pp. 511–519, May 2010.

[89] NMIJ, ‘Reference Material Certificate NMIJ CRM 6013-a’. National Metrology Institute of Japan, 2009.

[90] T. Yamazaki and A. Takatsu, ‘Quantitative NMR spectroscopy for accurate purity determination of amino acids, and uncertainty evaluation for different signals’, *Accreditation Qual. Assur.*, vol. 19, no. 4, pp. 275–282, Aug. 2014.

[91] T. Yamazaki, S. Eyama, and A. Takatsu, ‘Concentration Measurement of Amino Acid in Aqueous Solution by Quantitative ^{1}H NMR Spectroscopy with Internal Standard Method’, *Anal. Sci.*, vol. 33, no. 3, pp. 369–373, 2017.

[92] T. Kinumi, M. Goto, S. Eyama, M. Kato, T. Kasama, and A. Takatsu, ‘Development of SI-traceable C-peptide certified reference material NMIJ CRM 6901-a using isotope-dilution mass spectrometry-based amino acid analyses’, *Anal. Bioanal. Chem.*, vol. 404, no. 1, pp. 13–21, May 2012.

[93] N. Stoppacher, R. D. Josephs, A. Daireaux, T. Choteau, S. Westwood, and R. I. Wielgosz, ‘Accurate quantification of impurities in pure peptide material – angiotensin I: Comparison of calibration requirements and method performance characteristics of liquid chromatography coupled to hybrid tandem mass spectrometry and linear ion trap high-resolution mass spectrometry’, *Rapid Commun. Mass Spectrom.*, vol. 29, no. 18, pp. 1651–1660, Sep. 2015.

[94] S. A. Gerber, J. Rush, O. Stemman, M. W. Kirschner, and S. P. Gygi, ‘Absolute quantification of proteins and phosphoproteins from cell lysates by tandem MS’, *Proc. Natl. Acad. Sci. U. S. A.*, vol. 100, no. 12, pp. 6940–6945, Jun. 2003.

[95] W. I. Burkitt, C. Pritchard, C. Arsene, A. Henrion, D. Bunk, and G. O’Connor, ‘Toward Système International d’Unité-traceable protein quantification: from amino acids to proteins’, *Anal. Biochem.*, vol. 376, no. 2, pp. 242–251, May 2008.

[96] C. G. Arsene *et al.*, ‘Protein quantification by isotope dilution mass spectrometry of proteolytic fragments: cleavage rate and accuracy’, *Anal. Chem.*, vol. 80, no. 11, pp. 4154–4160, 2008.

[97] C. G. Arsene, A. Henrion, N. Diekmann, J. Manolopoulou, and M. Bidlingmaier, ‘Quantification of growth hormone in serum by isotope dilution mass spectrometry’, *Anal. Biochem.*, vol. 401, no. 2, pp. 228–235, 2010.

[98] C. Pritchard, M. Quaglia, A. E. Ashcroft, and G. O’Connor, ‘Considering the advantages and pitfalls of the use of isotopically labeled protein standards for accurate protein quantification’, *Bioanalysis*, vol. 3, no. 24, pp. 2797–2802, 2011.

[99] C. Pritchard, F. A. Torma, C. Hopley, M. Quaglia, and G. O’Connor, ‘Investigating microwave hydrolysis for the traceable quantification of peptide standards using gas chromatography-mass spectrometry’, *Anal. Biochem.*, vol. 412, no. 1, pp. 40–46, May 2011.

[100] B. H. Foundation, ‘View Publication’, 25-Oct-2010. [Online]. Available: http://www.bhf.org.uk/publications/view-publication.aspx?ps=1002097. [Accessed: 20-Nov-2012].

[101] D. G. Altman and J. M. Bland, ‘Diagnostic tests. 1: Sensitivity and specificity’, *BMJ*, vol. 308, no. 6943, p. 1552, Jun. 1994.

[102] D. M. Bunk, J. J. Dalluge, and M. J. Welch, 'Heterogeneity in human cardiac troponin I standards', *Anal. Biochem.*, vol. 284, no. 2, pp. 191–200, 2000.
[103] R. R. Little *et al.*, 'Implementing a Reference Measurement System for C-peptide: Successes and Lessons Learned', *Clin. Chem.*, p. clinchem.2016.269274, Jan. 2016.
[104] H. Ruskoaho, 'Cardiac hormones as diagnostic tools in heart failure', *Endocr. Rev.*, vol. 24, no. 3, pp. 341–356, Jun. 2003.
[105] A. G. Semenov *et al.*, 'Processing of Pro–B-Type Natriuretic Peptide: Furin and Corin as Candidate Convertases', *Clin. Chem.*, vol. 56, no. 7, pp. 1166–1176, Jul. 2010.
[106] A. G. Semenov and K. R. Seferian, 'Biochemistry of the human B-type natriuretic peptide precursor and molecular aspects of its processing', *Clin. Chim. Acta*, vol. 412, no. 11–12, pp. 850–860, May 2011.
[107] J. Mair *et al.*, 'Will sacubitril-valsartan diminish the clinical utility of B-type natriuretic peptide testing in acute cardiac care?', *Eur. Heart J. Acute Cardiovasc. Care*, p. 2048872615626355, Jan. 2016.
[108] J. Mair, 'Biochemistry of B-type natriuretic peptide--where are we now?', *Clin. Chem. Lab. Med. CCLM FESCC*, vol. 46, no. 11, pp. 1507–1514, 2008.
[109] S. J. Wieczorek *et al.*, 'A rapid B-type natriuretic peptide assay accurately diagnoses left ventricular dysfunction and heart failure: A multicenter evaluation', *Am. Heart J.*, vol. 144, no. 5, pp. 834–839, Nov. 2002.
[110] W. H. W. Tang *et al.*, 'National Academy of Clinical Biochemistry Laboratory Medicine Practice Guidelines: Clinical Utilization of Cardiac Biomarker Testing in Heart Failure', *Clin. Biochem.*, vol. 41, no. 4–5, pp. 210–221, Mar. 2008.
[111] A. Palazzuoli, 'Natriuretic peptides (BNP and NT-proBNP): measurement and relevance in heart failure', *Vasc. Health Risk Manag.*, p. 411, May 2010.
[112] A. Clerico *et al.*, 'State of the art of BNP and NT-proBNP immunoassays: The CardioOrmoCheck study', *Clin. Chim. Acta*, vol. 414, pp. 112–119, Dec. 2012.
[113] M. Franzini *et al.*, 'Systematic differences between BNP immunoassays: Comparison of methods using standard protocols and quality control materials', *Clin. Chim. Acta*, vol. 424, pp. 287–291, Sep. 2013.
[114] U. Schellenberger, J. O'Rear, A. Guzzetta, R. A. Jue, A. A. Protter, and N. S. Pollitt, 'The precursor to B-type natriuretic peptide is an O-linked glycoprotein', *Arch. Biochem. Biophys.*, vol. 451, no. 2, pp. 160–166, Jul. 2006.
[115] A. Hammerer-Lercher *et al.*, 'Analysis of Circulating Forms of proBNP and NT-proBNP in Patients with Severe Heart Failure', *Clin. Chem.*, vol. 54, no. 5, pp. 858–865, May 2008.
[116] A. M. Hawkridge, D. M. Heublein, H. R. Bergen 3rd, A. Cataliotti, J. C. Burnett Jr, and D. C. Muddiman, 'Quantitative mass spectral evidence for the absence of circulating brain natriuretic peptide (BNP-32) in severe human heart failure', *Proc. Natl. Acad. Sci. U. S. A.*, vol. 102, no. 48, pp. 17442–17447, Nov. 2005.
[117] F. Liang *et al.*, 'Evidence for functional heterogeneity of circulating B-type natriuretic peptide', *J. Am. Coll. Cardiol.*, vol. 49, no. 10, pp. 1071–1078, Mar. 2007.
[118] K. N. Luckenbill *et al.*, 'Cross-Reactivity of BNP, NT-proBNP, and proBNP in Commercial BNP and NT-proBNP Assays: Preliminary Observations from the IFCC Committee for Standardization of Markers of Cardiac Damage', *Clin. Chem.*, vol. 54, no. 3, pp. 619–621, Mar. 2008.
[119] 'Natriuretic Peptide Assay Analytical Characteristics - IFCC'. [Online]. Available: http://www.ifcc.org/ifcc-scientific-division/documents-of-the-sd/natriureticpeptideassayanalyticalcharacteristics1/. [Accessed: 29-May-2017].

[120] A. K. Saenger *et al.*, 'Specificity of B-Type Natriuretic Peptide Assays: Cross-Reactivity with Different BNP, NT-proBNP, and proBNP Peptides', *Clin. Chem.*, p. clinchem.2016.263749, Jan. 2016.

[121] I. Brandt, 'Dipeptidyl-Peptidase IV Converts Intact B-Type Natriuretic Peptide into Its des-SerPro Form', *Clin. Chem.*, vol. 52, no. 1, pp. 82–87, Jan. 2006.

[122] T. G. Yandle and A. M. Richards, 'B-Type Natriuretic Peptide circulating forms: Analytical and bioactivity issues', *Clin. Chim. Acta*.

[123] E. E. Niederkofler *et al.*, 'Detection of endogenous B-type natriuretic peptide at very low concentrations in patients with heart failure', *Circ. Heart Fail.*, vol. 1, no. 4, pp. 258–264, Nov. 2008.

[124] W. L. Miller *et al.*, 'Comparison of mass spectrometry and clinical assay measurements of circulating fragments of B-type natriuretic peptide in patients with chronic heart failure', *Circ. Heart Fail.*, vol. 4, no. 3, pp. 355–360, May 2011.

[125] S. Zhang, K. Raedschelders, M. Santos, and J. E. Van Eyk, 'Profiling B-Type Natriuretic Peptide Cleavage Peptidoforms in Human Plasma by Capillary Electrophoresis with Electrospray Ionization Mass Spectrometry', *J. Proteome Res.*, Sep. 2017.

[126] V. C. Vasile and A. S. Jaffe, 'Natriuretic Peptides and Analytical Barriers', *Clin. Chem.*, p. clinchem.2016.254714, Jan. 2016.

[127] A. G. Semenov and A. G. Katrukha, 'Different Susceptibility of B-Type Natriuretic Peptide (BNP) and BNP Precursor (proBNP) to Cleavage by Neprilysin: The N-Terminal Part Does Matter', *Clin. Chem.*, vol. 62, no. 4, pp. 617–622, Apr. 2016.

[128] 'ISO/IEC 17025:2017(en), General requirements for the competence of testing and calibration laboratories'. [Online]. Available: https://www.iso.org/obp/ui/#iso:std:iso-iec:17025:ed-3:v1:en. [Accessed: 14-Jan-2018].

[129] T. Kinumi, R. Ichikawa, H. Arimoto, and A. Takatsu, 'Traceable Amino Acid Analyses of Proteins and Peptides by Isotope-Dilution Mass Spectrometry Using Precolumn Derivatization Reagent', *Anal. Sci.*, vol. 26, no. 9, pp. 1007–1010, 2010.

[130] J.-S. Jeong, H.-M. Lim, S.-K. Kim, H.-K. Ku, K.-H. Oh, and S.-R. Park, 'Quantification of human growth hormone by amino acid composition analysis using isotope dilution liquid-chromatography tandem mass spectrometry', *J. Chromatogr. A*, vol. 1218, no. 38, pp. 6596–6602, 2011.

[131] C. Plato, 'Differential scanning calorimetry as a general method for determining purity and heat of fusion of high-purity organic chemicals. Application to 64 compounds', *Anal. Chem.*, vol. 44, no. 8, pp. 1531–1534, Jul. 1972.

[132] S. Westwood, T. Choteau, A. Daireaux, R. D. Josephs, and R. I. Wielgosz, 'Mass Balance Method for the SI Value Assignment of the Purity of Organic Compounds', *Anal. Chem.*, Feb. 2013.

[133] R. D. Josephs, A. Daireaux, S. Westwood, and R. I. Wielgosz, 'Simultaneous determination of various cardiac glycosides by liquid chromatography–hybrid mass spectrometry for the purity assessment of the therapeutic monitored drug digoxin', *J. Chromatogr. A*, vol. 1217, no. 27, pp. 4535–4543, Jul. 2010.

[134] R. D. Josephs *et al.*, 'State-of-the-art and trends for the SI traceable value assignment of the purity of peptides using the model compound angiotensin I', *TrAC Trends Anal. Chem.*, vol. 101, pp. 108–119, Apr. 2018.

[135] T. Goff, E. Champarnaud, and F. Fardus, 'HPLC direct purity assay using ultra-purified materials as primary standards', *Anal. Bioanal. Chem.*, vol. 398, no. 7–8, pp. 3183–3192, 2010.

[136] M. Kato *et al.*, 'Development of High-purity Certified Reference Materials for 17 Proteinogenic Amino Acids by Traceable Titration Methods', *Anal. Sci.*, vol. 31, no. 8, pp. 805–814, 2015.

[137] R. D. Josephs *et al.*, 'Pilot study on peptide purity—synthetic human C-peptide', *Metrologia*, vol. 54, no. 1A, p. 08011, 2017.

[138] R. B. Merrifield, 'Solid Phase Peptide Synthesis. I. The Synthesis of a Tetrapeptide', *J. Am. Chem. Soc.*, vol. 85, no. 14, pp. 2149–2154, Jul. 1963.

[139] R. D. Josephs, A. Daireaux, T. Choteau, S. Westwood, and R. I. Wielgosz, 'Normal phase-liquid chromatography-tandem mass spectrometry with atmospheric pressure photoionization for the purity assessment of 17β-estradiol', *Anal. Bioanal. Chem.*, vol. 407, no. 11, pp. 3147–3157, Apr. 2015.

[140] R. D. Josephs *et al.*, 'Concept paper on SI value assignment of purity-Model for the classification of peptide/protein purity determinations', *J. Chem. Metrol.*, vol. 11, no. 1, p. 1, 2017.

[141] R. D. Josephs *et al.*, 'Key comparison study on peptide purity—synthetic human C-peptide', *Metrologia*, vol. 54, no. 1A, p. 08007, 2017.

[142] T. Kinumi, M. Goto, S. Eyama, M. Kato, T. Kasama, and A. Takatsu, 'Development of SI-traceable C-peptide certified reference material NMIJ CRM 6901-a using isotope-dilution mass spectrometry-based amino acid analyses', *Anal. Bioanal. Chem.*, vol. 404, no. 1, pp. 13–21, May 2012.

[143] I. Davidson, 'Hydrolysis of samples for amino acid analysis', *Methods Mol. Biol. Clifton NJ*, vol. 211, pp. 111–122, 2003.

[144] A. Muñoz, R. Kral, and H. Schimmel, 'Quantification of protein calibrants by amino acid analysis using isotope dilution mass spectrometry', *Anal. Biochem.*, vol. 408, no. 1, pp. 124–131, Jan. 2011.

[145] D. M. Bunk, J. J. Dalluge, and M. J. Welch, 'Heterogeneity in Human Cardiac Troponin I Standards', *Anal. Biochem.*, vol. 284, no. 2, pp. 191–200, Sep. 2000.

[146] D. M. Bunk and M. J. Welch, 'Characterization of a New Certified Reference Material for Human Cardiac Troponin I', *Clin. Chem.*, vol. 52, no. 2, pp. 212–219, Feb. 2006.

[147] C. Pritchard, M. Quaglia, W. I. Burkitt, C. Mussell, G. O'Connor, and H. Parkes, 'Fully traceable absolute protein quantification of somatropin: allowing independent comparison of somatropin standards', *Clin. Chem.*, vol. 55, no. 11, pp. 1984–1990, 2009.

[148] J. V. Olsen, S. Ong, and M. Mann, 'Trypsin cleaves exclusively C-terminal to arginine and lysine residues', *Mol. Cell. Proteomics*, vol. 3, no. 6, pp. 608–614, 2004.

[149] 'CCQM: Report of the 18th meeting (2012)'. [Online]. Available: http://www.bipm.org/utils/common/pdf/CCQM18.pdf. [Accessed: 18-Nov-2013].

[150] C. Pritchard, F. A. Torma, C. Hopley, M. Quaglia, and G. O'Connor, 'Investigating microwave hydrolysis for the traceable quantification of peptide standards using gas chromatography-mass spectrometry', *Anal. Biochem.*, vol. 412, no. 1, pp. 40–46, May 2011.

[151] J. Csapá *et al.*, 'Hydrolysis of proteins performed at high temperatures and for short times with reduced racemization, in order to determine the enantiomers of - and - amino acids', *Anal. Chim. Acta*, vol. 339, no. 1–2, pp. 99–107, Feb. 1997.

[152] M. S. Lowenthal, J. Yen, D. M. Bunk, and K. W. Phinney, 'Certification of NIST standard reference material 2389a, amino acids in 0.1 mol/L HCl—quantification by ID LC-MS/MS', *Anal. Bioanal. Chem.*, vol. 397, no. 2, pp. 511–519, May 2010.

[153] H. Kaspar, K. Dettmer, W. Gronwald, and P. J. Oefner, 'Advances in amino acid analysis', *Anal. Bioanal. Chem.*, vol. 393, no. 2, pp. 445–452, 2009.

[154] NIST, 'Certificate of Analysis; standard reference material 2389a'. National Institute of Standards & Technology, 2010.

[155] 'ISO/IEC Guide 98-3:2008 - Uncertainty of measurement -- Part 3: Guide to the expression of uncertainty in measurement (GUM:1995)'. [Online]. Available: http://www.iso.org/iso/home/store/catalogue_tc/catalogue_detail.htm?csnumber=50461. [Accessed: 06-Nov-2013].

[156] S. L. R. Ellison and A. Williams, 'Eurachem/CITAC guide: Quantifying Uncertainty in Analytical Measurement, Third edition, (2012) ISBN 978-0-948926-30-3. Available from www.eurachem.org.' [Online]. Available: http://www.eurachem.org/index.php/publications/guides/quam. [Accessed: 06-Nov-2013].

[157] K. Maes, I. Smolders, Y. Michotte, and A. Van Eeckhaut, 'Strategies to reduce aspecific adsorption of peptides and proteins in liquid chromatography–mass spectrometry based bioanalyses: An overview', *J. Chromatogr. A*, vol. 1358, pp. 1–13, Sep. 2014.

[158] A. M. Hawkridge, D. M. Heublein, H. R. Bergen, A. Cataliotti, J. C. Burnett, and D. C. Muddiman, 'Quantitative mass spectral evidence for the absence of circulating brain natriuretic peptide (BNP-32) in severe human heart failure', *Proc. Natl. Acad. Sci. U. S. A.*, vol. 102, no. 48, pp. 17442–17447, Nov. 2005.

[159] G. L. Andrews, C. M. Shuford, J. C. Burnett, A. M. Hawkridge, and D. C. Muddiman, 'Coupling of a Vented Column with Splitless NanoRPLC-ESI-MS for the Improved Separation and Detection of Brain Natriuretic Peptide-32 and its Proteolytic Peptides', *J. Chromatogr. B Analyt. Technol. Biomed. Life. Sci.*, vol. 877, no. 10, pp. 948–954, Apr. 2009.

[160] H. Keshishian *et al.*, 'Quantification of cardiovascular biomarkers in patient plasma by targeted mass spectrometry and stable isotope dilution', *Mol. Cell. Proteomics MCP*, vol. 8, no. 10, pp. 2339–2349, Oct. 2009.

[161] H. R. Sobhi, B. Vatansever, A. Wortmann, E. Grouzmann, and B. Rochat, 'Generic approach for the sensitive absolute quantification of large undigested peptides in plasma using a particular liquid chromatography–mass spectrometry setup', *J. Chromatogr. A*, vol. 1218, no. 47, pp. 8536–8543, Nov. 2011.

[162] D. L. Chappell, A. Y. Lee, H. S. Bernstein, M. E. Lassman, and O. F. Laterza, 'Development and validation of an IA-LC/MS method to quantitate active and total B-type natriuretic peptide in human plasma', *Bioanalysis*, vol. 8, no. 22, pp. 2341–2349, Oct. 2016.

[163] A. T. Iavarone and E. R. Williams, 'Supercharging in electrospray ionization: effects on signal and charge', *Int. J. Mass Spectrom.*, vol. 219, no. 1, pp. 63–72, Aug. 2002.

[164] H. J. Sterling *et al.*, 'Effects of Supercharging Reagents on Noncovalent Complex Structure in Electrospray Ionization from Aqueous Solutions', *J. Am. Soc. Mass Spectrom.*, vol. 21, no. 10, pp. 1762–1774, Oct. 2010.

[165] M. Šamalikova and R. Grandori, 'Testing the role of solvent surface tension in protein ionization by electrospray', *J. Mass Spectrom.*, vol. 40, no. 4, pp. 503–510, Apr. 2005.

[166] N. L. Anderson and N. G. Anderson, 'The human plasma proteome: history, character, and diagnostic prospects', *Mol. Cell. Proteomics MCP*, vol. 1, no. 11, pp. 845–867, Nov. 2002.
[167] V. C. Vasile and A. S. Jaffe, 'Natriuretic Peptides and Analytical Barriers', *Clin. Chem.*, Oct. 2016.
[168] X. M. Lam, J. Y. Yang, and J. L. Cleland, 'Antioxidants for prevention of methionine oxidation in recombinant monoclonal antibody HER2', *J. Pharm. Sci.*, vol. 86, no. 11, pp. 1250–1255, Nov. 1997.
[169] J. C. Miller and J. N. Miller, 'Basic statistical methods for analytical chemistry. Part I. Statistics of repeated measurements. A review', *Analyst*, vol. 113, no. 9, pp. 1351–1356, 1988.
[170] J. N. Miller, 'Basic statistical methods for Analytical Chemistry. Part 2. Calibration and regression methods. A review', *Analyst*, vol. 116, no. 1, pp. 3–14, Jan. 1991.
[171] 'ISO 15189:2012 - Medical laboratories -- Requirements for quality and competence'. [Online]. Available: https://www.iso.org/standard/56115.html. [Accessed: 14-Jul-2018].
[172] 'PepCalc.com - Peptide calculator'. [Online]. Available: http://www.pepcalc.com/. [Accessed: 06-Sep-2017].
[173] A. G. Semenov and A. G. Katrukha, 'Analytical Issues with Natriuretic Peptides – has this been Overly Simplified?', *EJIFCC*, vol. 27, no. 3, pp. 189–207, Jul. 2016.
[174] D. M. Dickey and L. R. Potter, 'Human B-type natriuretic peptide is not degraded by meprin A', *Biochem. Pharmacol.*, vol. 80, no. 7, pp. 1007–1011, Oct. 2010.
[175] B. MacLean *et al.*, 'Skyline: an open source document editor for creating and analyzing targeted proteomics experiments', *Bioinformatics*, vol. 26, no. 7, pp. 966–968, Apr. 2010.
[176] D. S. Moore, 'Amino acid and peptide net charges: A simple calculational procedure', *Biochem. Educ.*, vol. 13, no. 1, pp. 10–11, Jan. 1985.
[177] C. M. Sturgeon, 'Common decision limits — The need for harmonised immunoassays', *Clin. Chim. Acta*, vol. 432, pp. 122–126, May 2014.
[178] W. G. Miller, 'Time to Pay Attention to Reagent and Calibrator Lots for Proficiency Testing', *Clin. Chem.*, p. clinchem.2016.255802, Mar. 2016.

Appendices

Appendix A Superchargers

Agilent6530 Q-TOF 0.25 % sulfolane

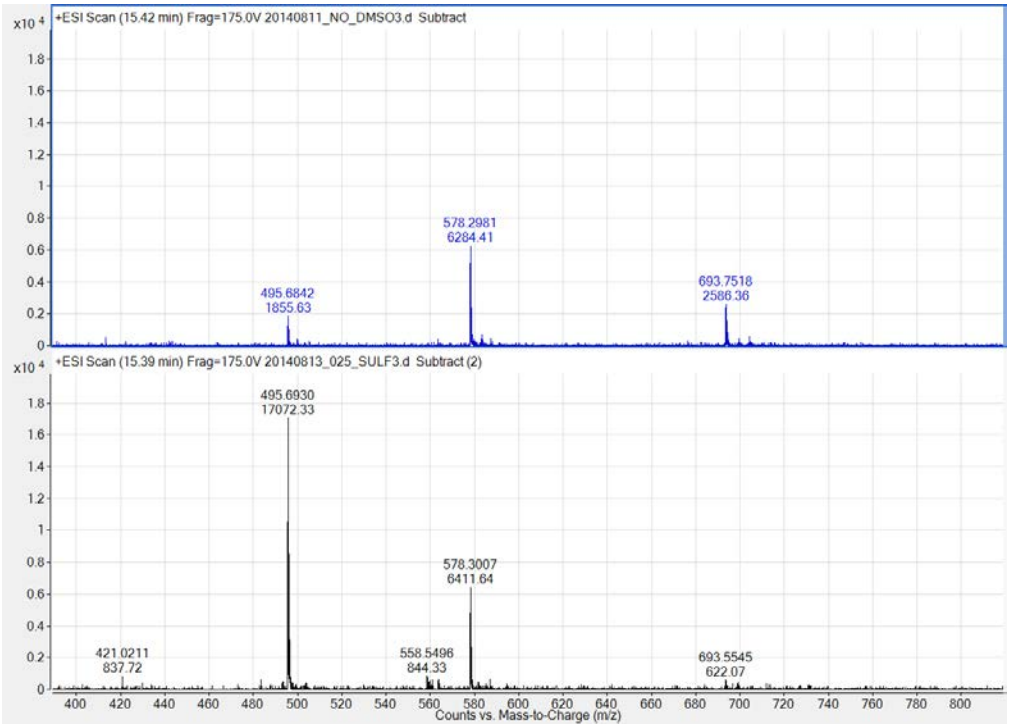

Appendix A 1MS ion signal abundances in full scan experiments for BNP (top) and when infusing sulfolane (bottom). 495.8 *m/z* (7+), 578.2 *m/z* (6+) and 693.6 *m/z* (5+).

Agilent 6530 Q-TOF 0.25 % m-NBA

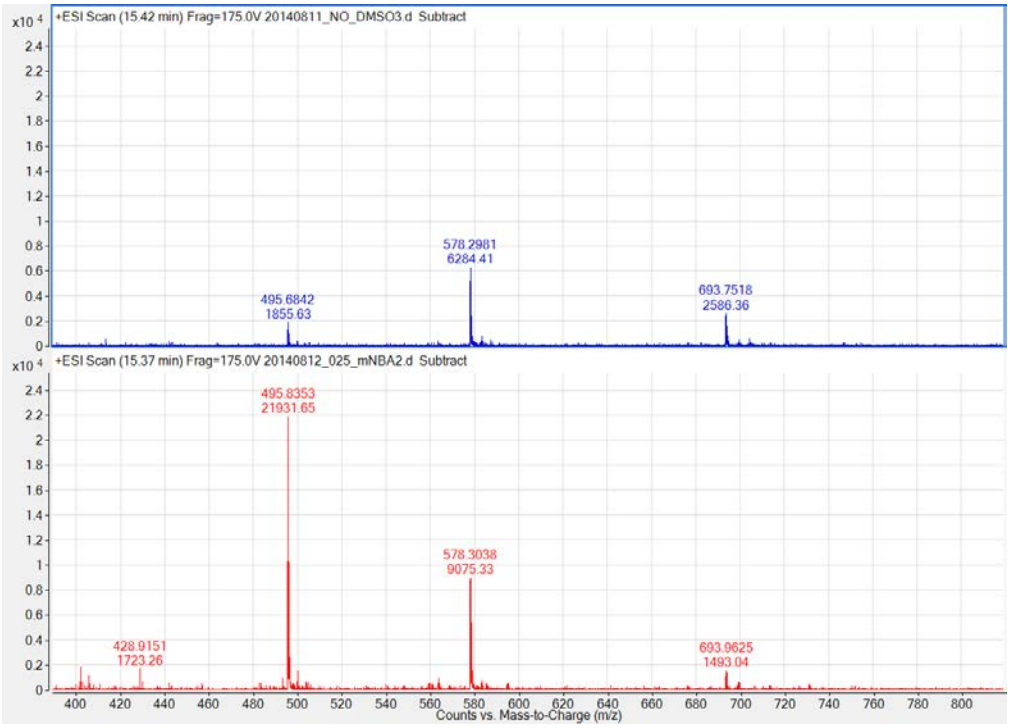

Appendix A 2MS ion signal abundances in full scan experiments for BNP (top) and when infusing m-NBA (bottom). 495.8 *m/z* (7+), 578.2 *m/z* (6+) and 693.6 *m/z* (5+).

Agilent 6530 Q-TOF 0.25 % DMSO

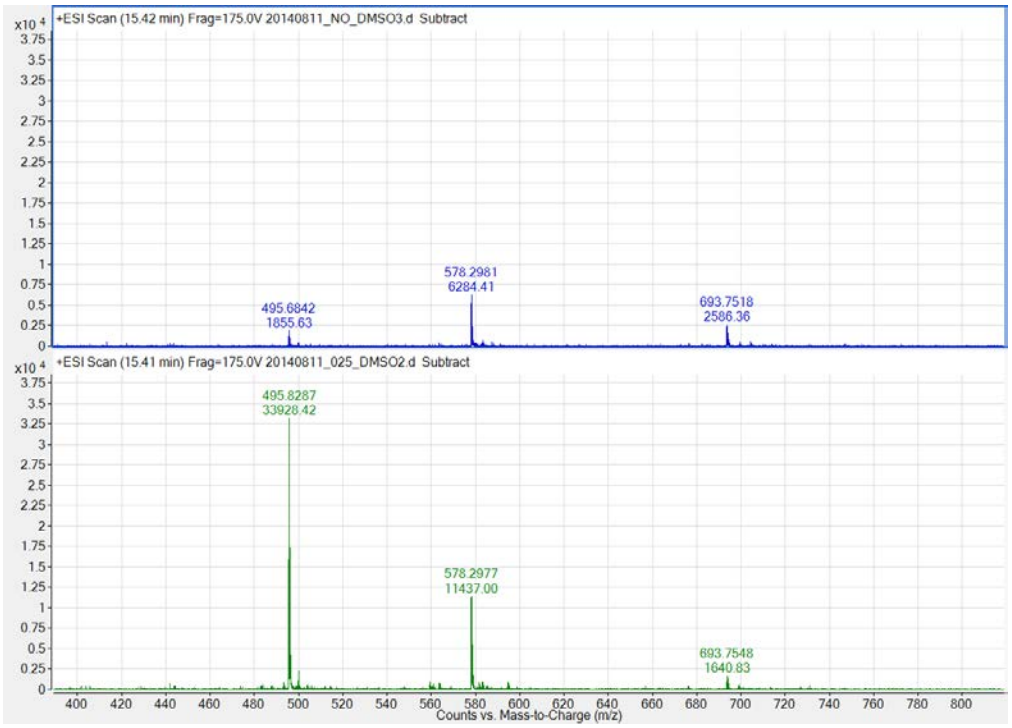

Appendix A 3MS ion signal abundances in full scan experiments for BNP (top) and when infusing DMSO (bottom). 495.8 *m/z* (7+), 578.2 *m/z* (6+) and 693.6 *m/z* (5+).

Agilent 6490 QqQ 0.25 % sulfolane

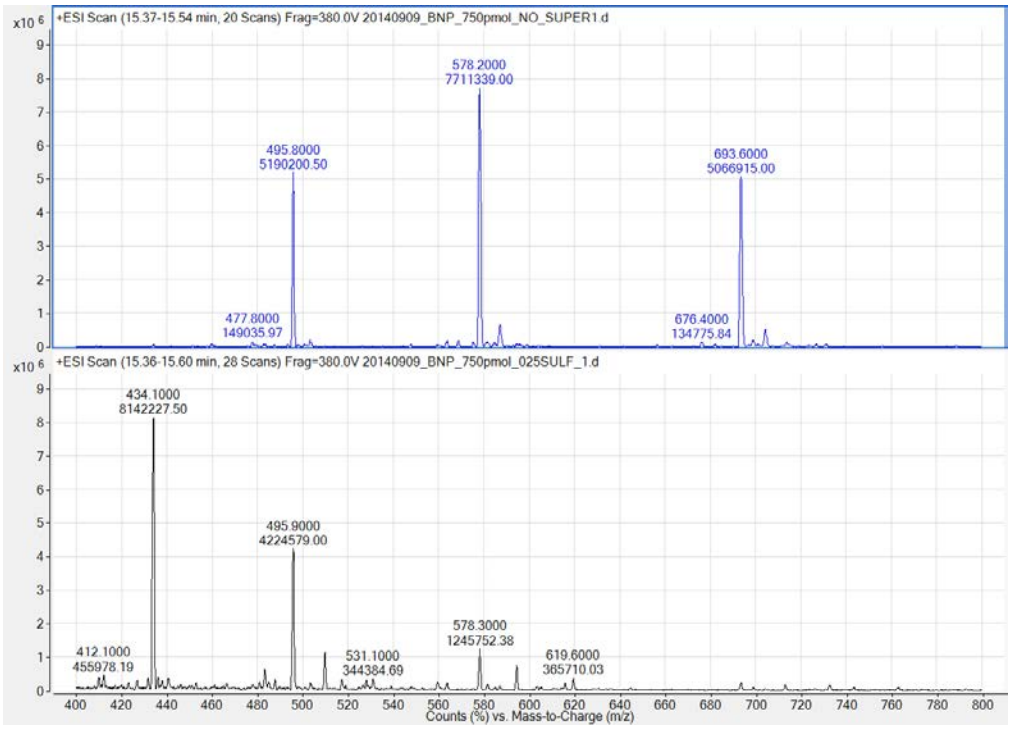

Appendix A 4MS ion signal abundances in full scan experiments for BNP (top) and when infusing sulfolane (bottom). 434.1 *m/z* (8+), 495.8 *m/z* (7+), 578.2 *m/z* (6+) and 693.6 *m/z* (5+).

Appendices

Agilent 6490 0.25 % m-NBA

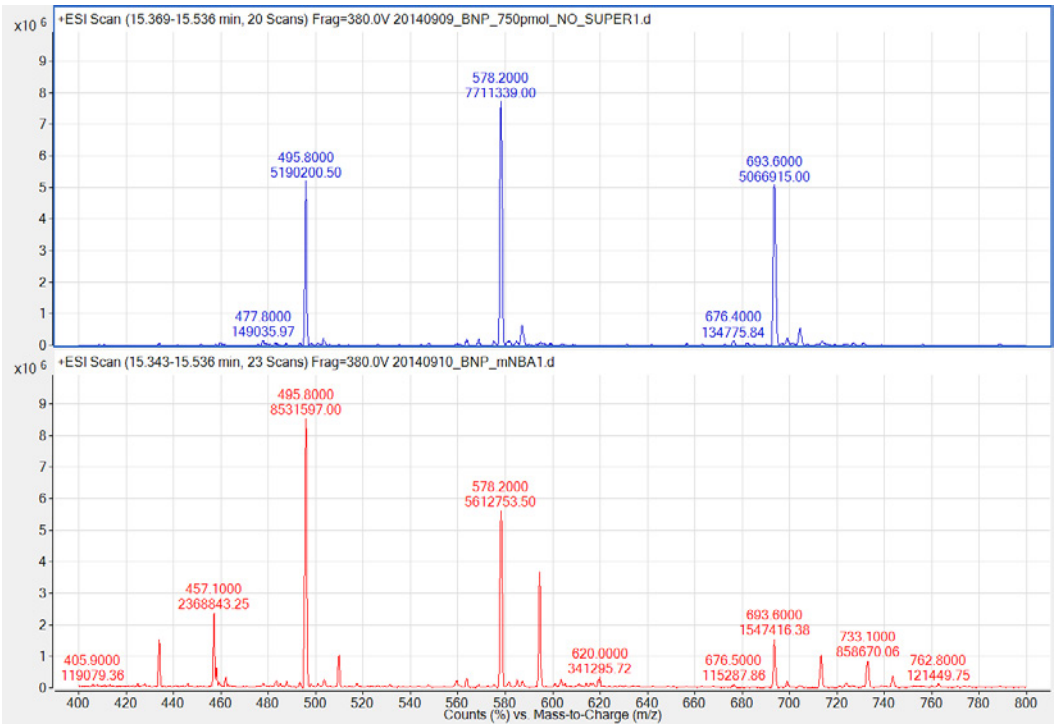

Appendix A 5MS ion signal abundances in full scan experiments for BNP (top) and when infusing m-NBA (bottom). 434.1 *m/z* (8+), 495.8 *m/z* (7+), 578.2 *m/z* (6+) and 693.6 *m/z* (5+).

Agilent 6490 0.25 % DMSO

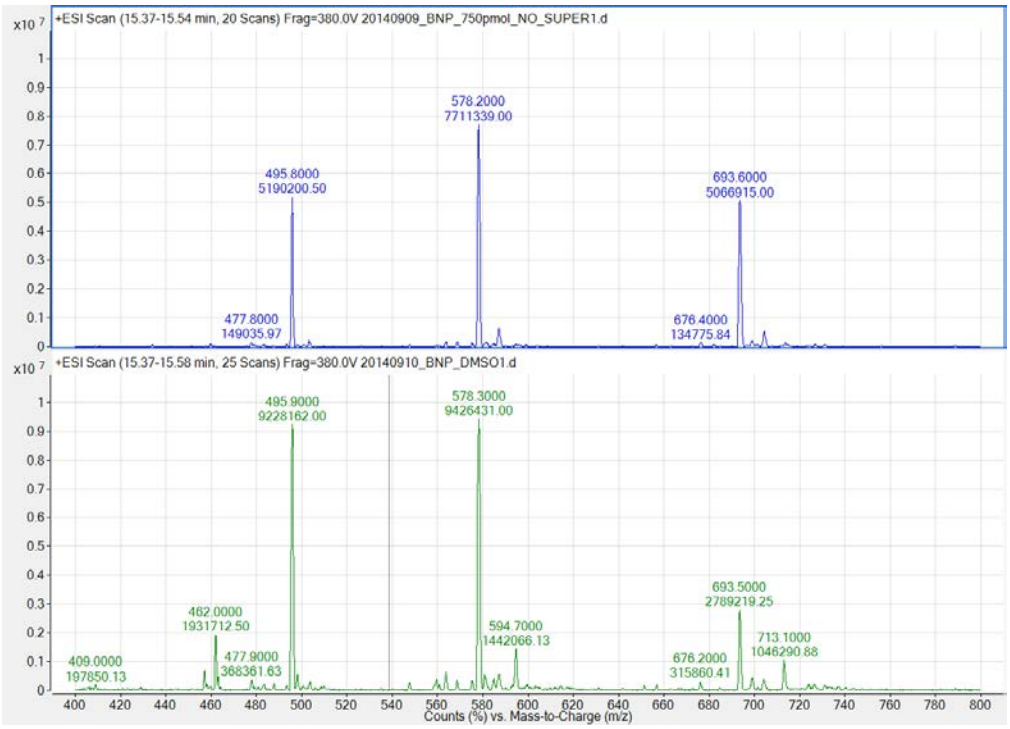

Appendix A 6MS ion signal abundances in full scan experiments for BNP (top) and when infusing DMSO (bottom). 495.8 *m/z* (7+), 578.2 *m/z* (6+) and 693.6 *m/z* (5+).

Appendix B UK NEQAS results

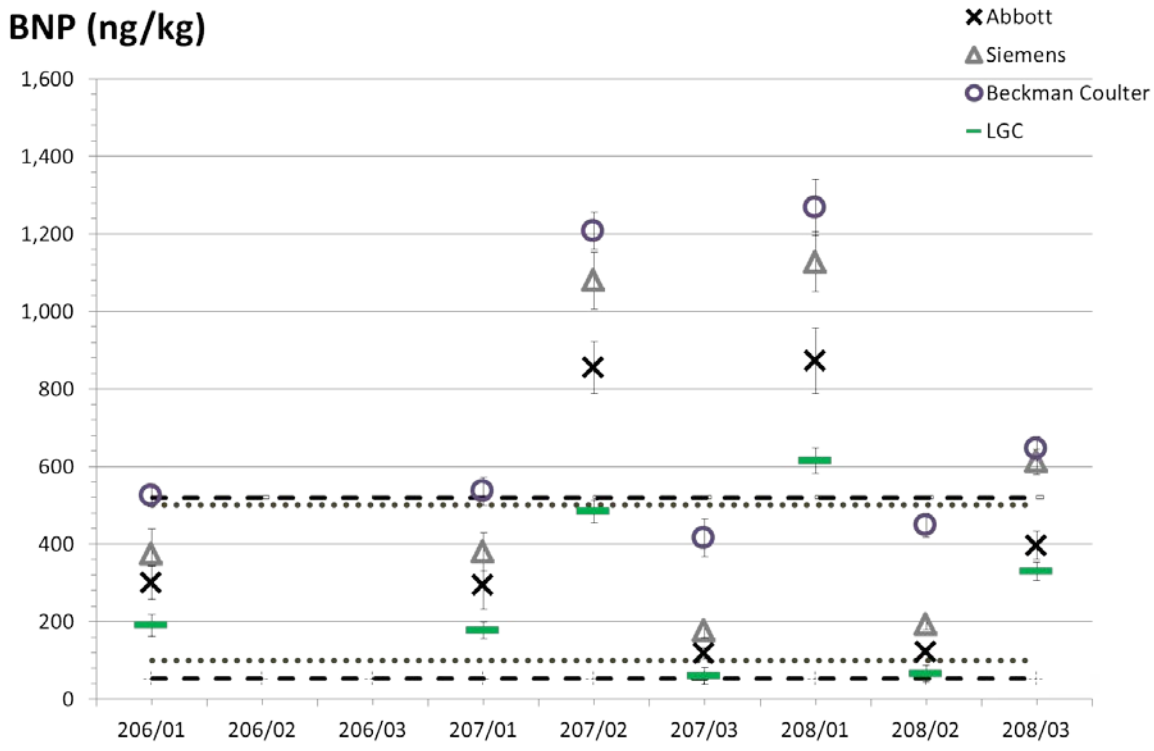

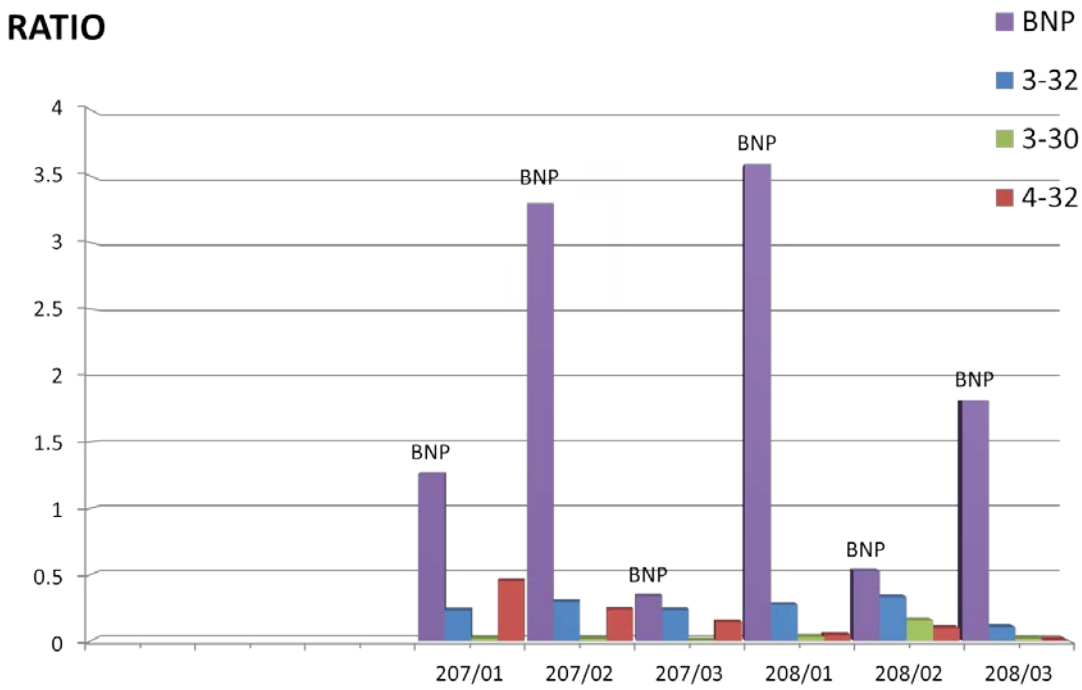

Appendix B 1 BNP quantitation results and degradation profiles of NEQAS samples. Dashed lines: range of the reference method (52-520 pg/g). Dotted lines: lower and higher decision limits (100/500 pg/g). RATIO: BNP, 3-32, 3-30 and 4-32 area over the labelled BNP* area. Results 207-208.

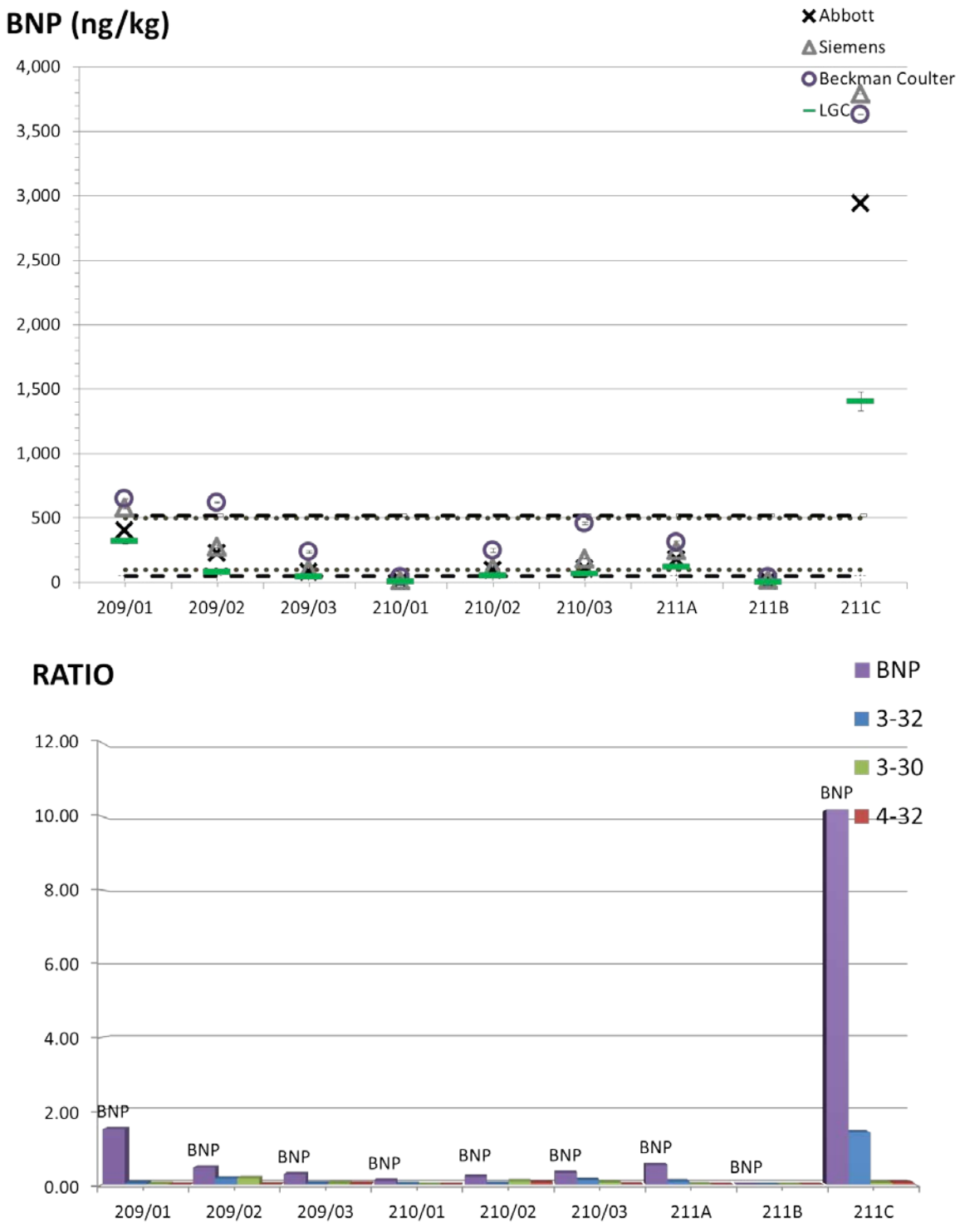

Appendix B 2 BNP quantitation results and degradation profiles of NEQAS samples. Dashed lines: range of the reference method (52-520 pg/g). Dotted lines: lower and higher decision limits (100/500 pg/g). RATIO: BNP, 3-32, 3-30 and 4-32 area over the labelled BNP* area. Results 209-211.

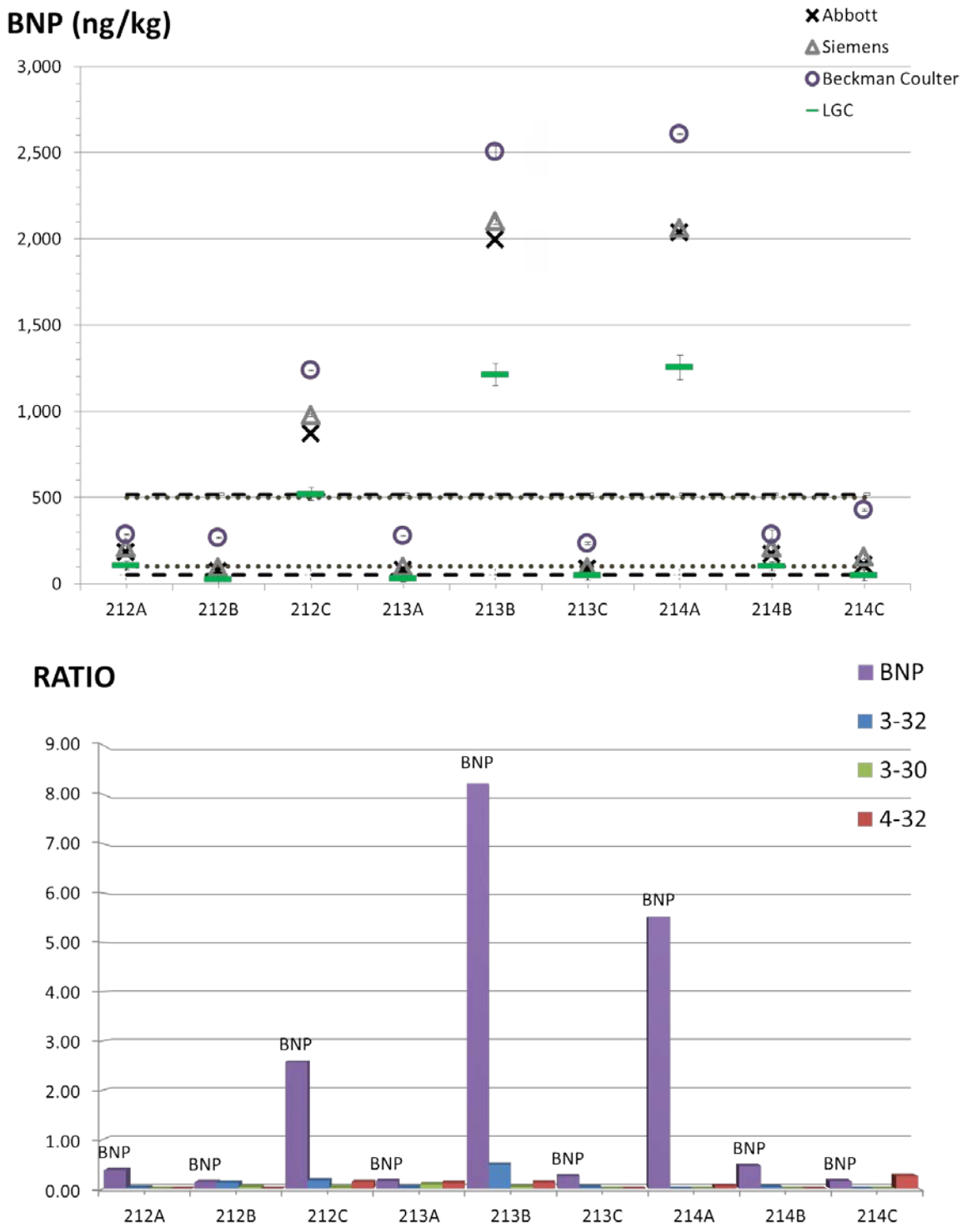

Appendix B 3 BNP quantitation results and degradation profiles of NEQAS samples. Dashed lines: range of the reference method (52-520 pg/g). Dotted lines: lower and higher decision limits (100/500 pg/g). RATIO: BNP, 3-32, 3-30 and 4-32 area over the labelled BNP* area. Results 212-214.

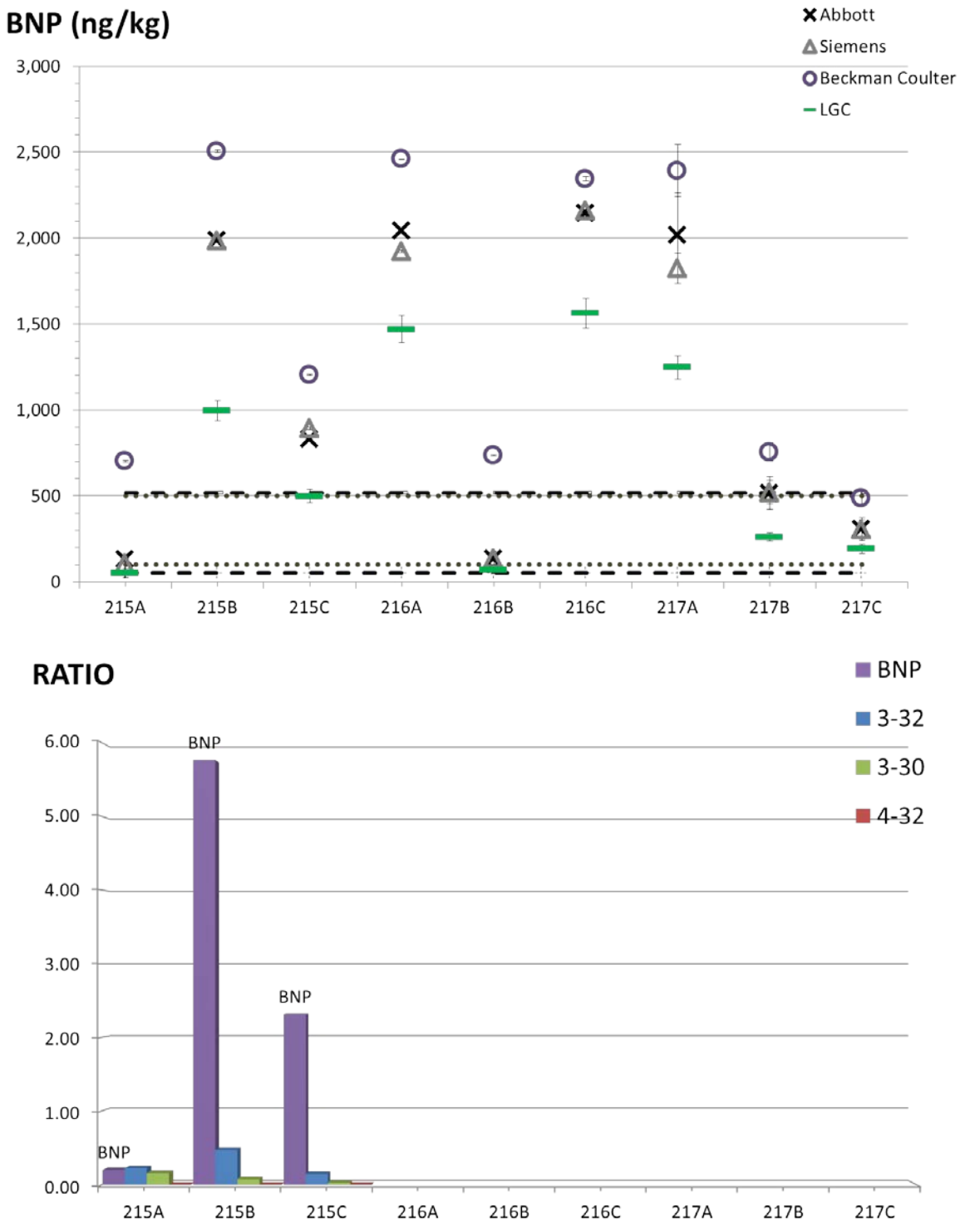

Appendix B 4 BNP quantitation results and degradation profiles of NEQAS samples. Dashed lines: range of the reference method (52-520 pg/g). Dotted lines: lower and higher decision limits (100/500 pg/g). RATIO: BNP, 3-32, 3-30 and 4-32 area over the labelled BNP* area. Results 215-217.

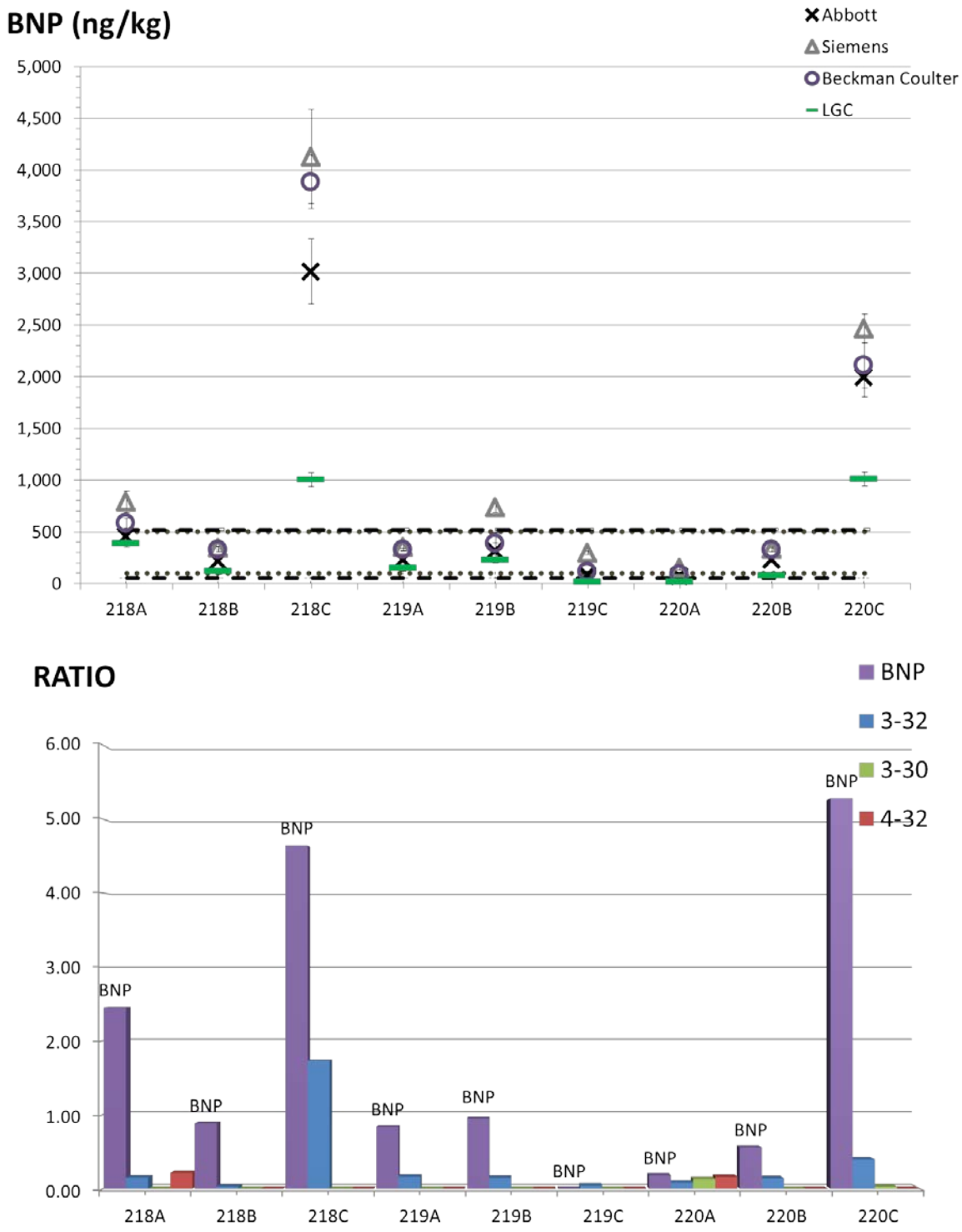

Appendix B 5 BNP quantitation results and degradation profiles of NEQAS samples. Dashed lines: range of the reference method (52-520 pg/g). Dotted lines: lower and higher decision limits (100/500 pg/g). RATIO: BNP, 3-32, 3-30 and 4-32 area over the labelled BNP* area. Results 218-220.

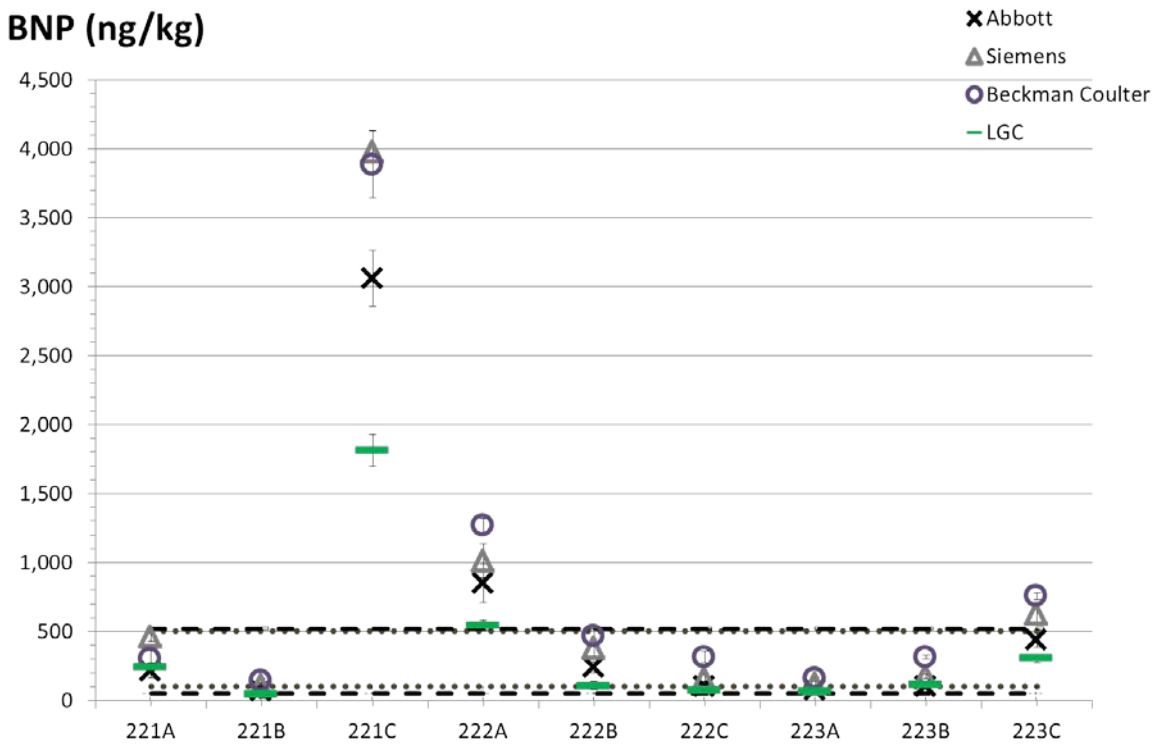

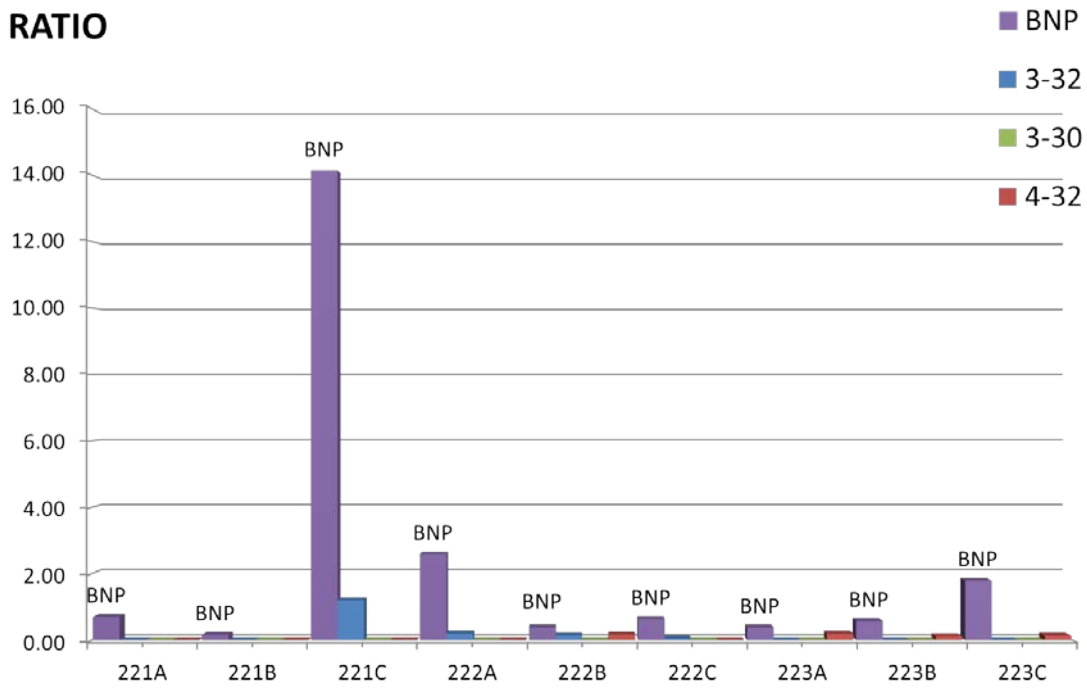

Appendix B 6 BNP quantitation results and degradation profiles of NEQAS samples. Dashed lines: range of the reference method (52-520 pg/g). Dotted lines: lower and higher decision limits (100/500 pg/g). RATIO: BNP, 3-32, 3-30 and 4-32 area over the labelled BNP* area. Results 221-223.

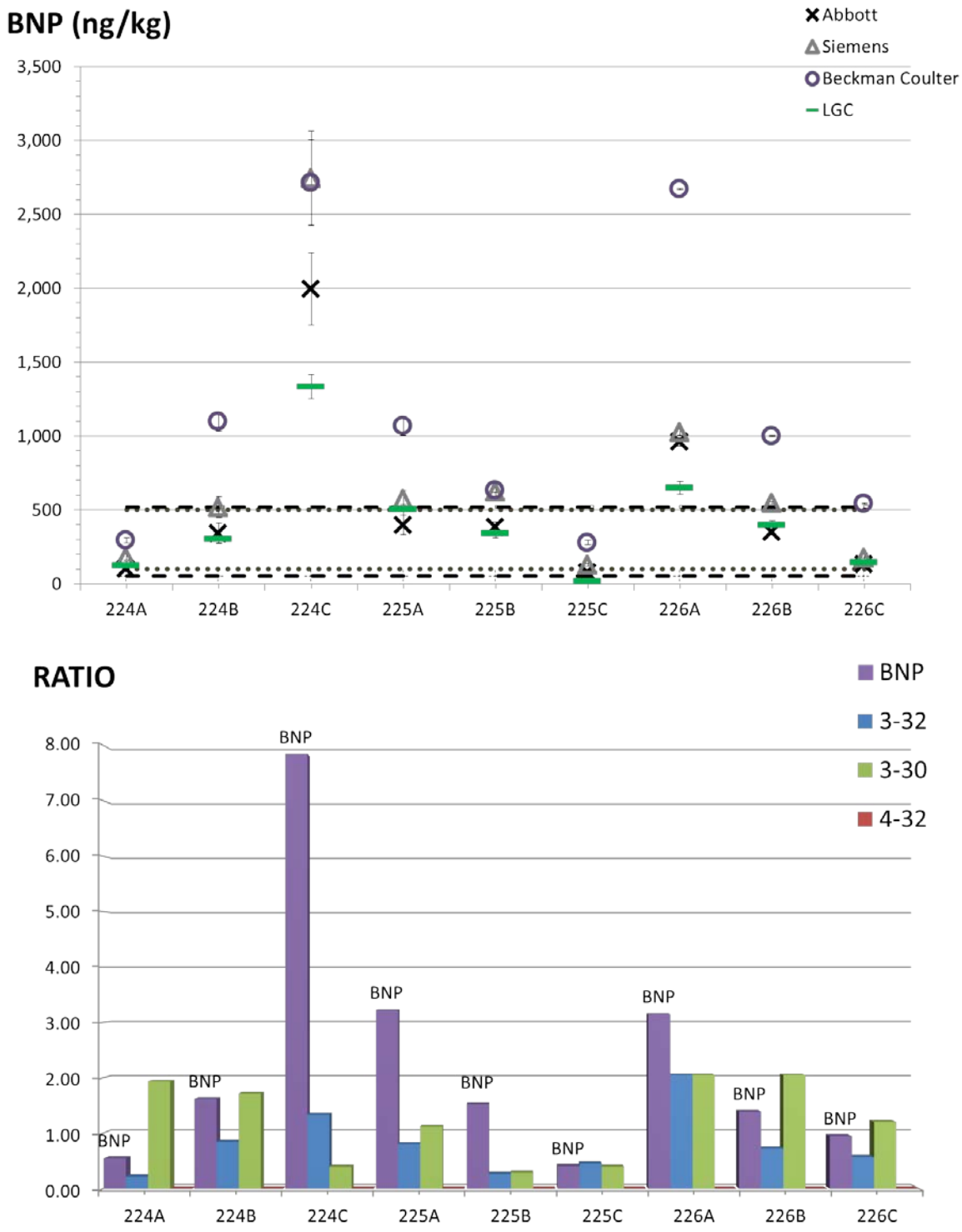

Appendix B 7 BNP quantitation results and degradation profiles of NEQAS samples. Dashed lines: range of the reference method (52-520 pg/g). Dotted lines: lower and higher decision limits (100/500 pg/g). RATIO: BNP, 3-32, 3-30 and 4-32 area over the labelled BNP* area. Results 224-226.

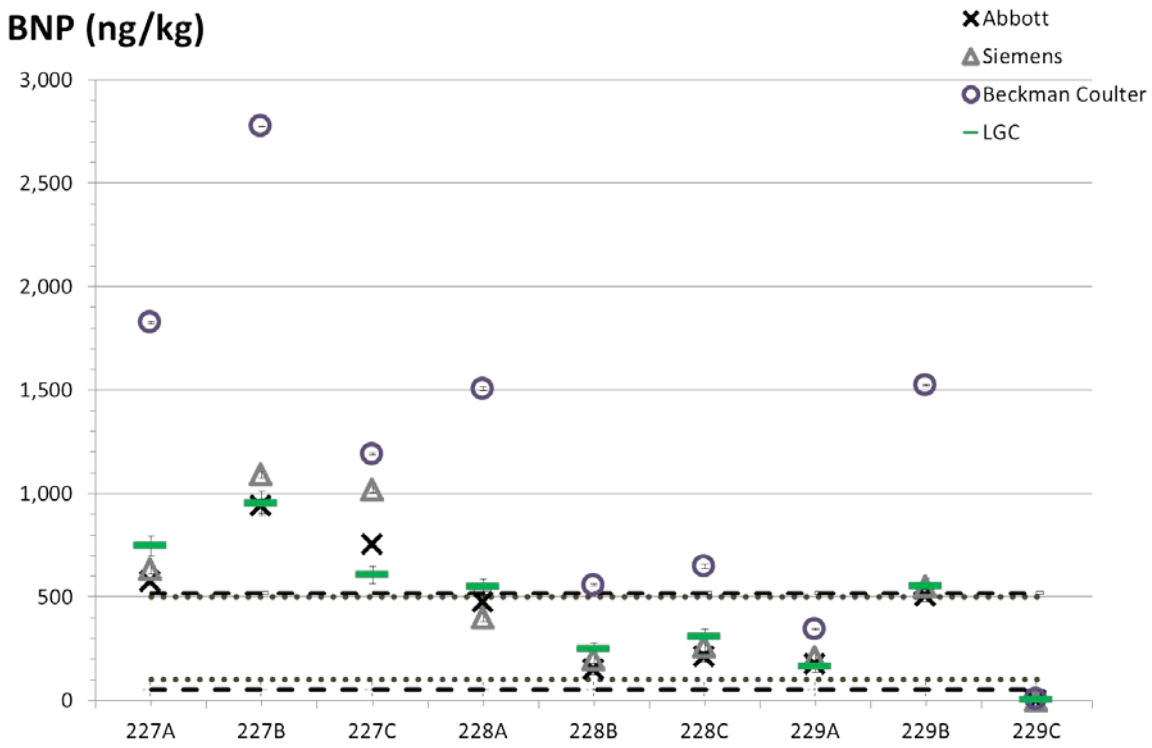

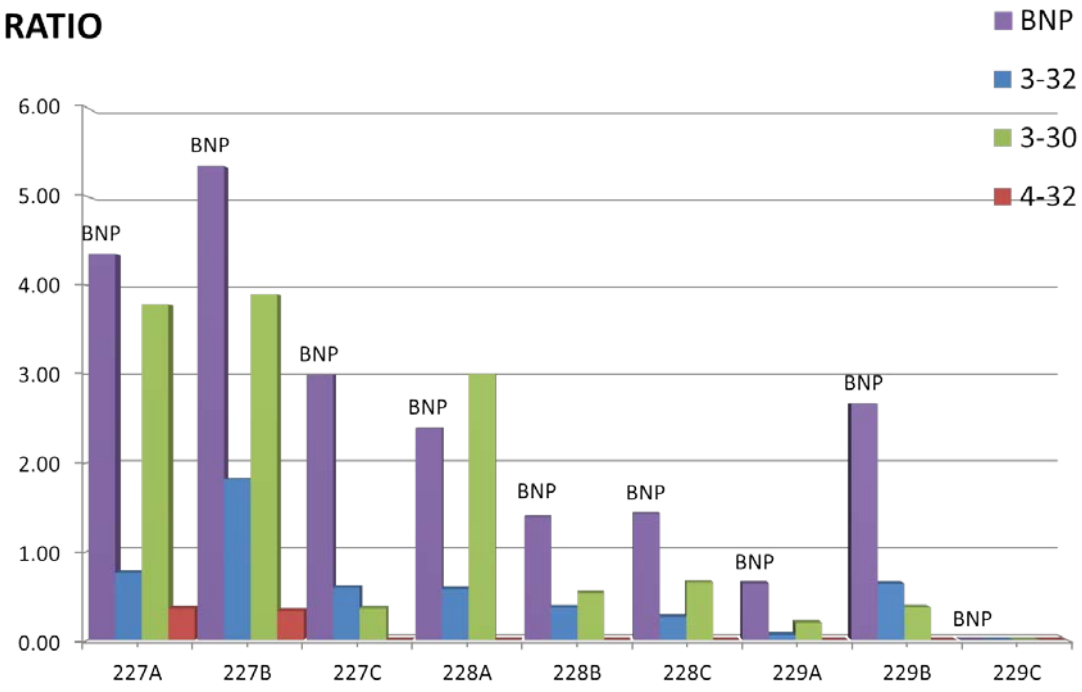

Appendix B 8 BNP quantitation results and degradation profiles of NEQAS samples. Dashed lines: range of the reference method (52-520 pg/g). Dotted lines: lower and higher decision limits (100/500 pg/g). RATIO: BNP, 3-32, 3-30 and 4-32 area over the labelled BNP* area. Results 227-229.

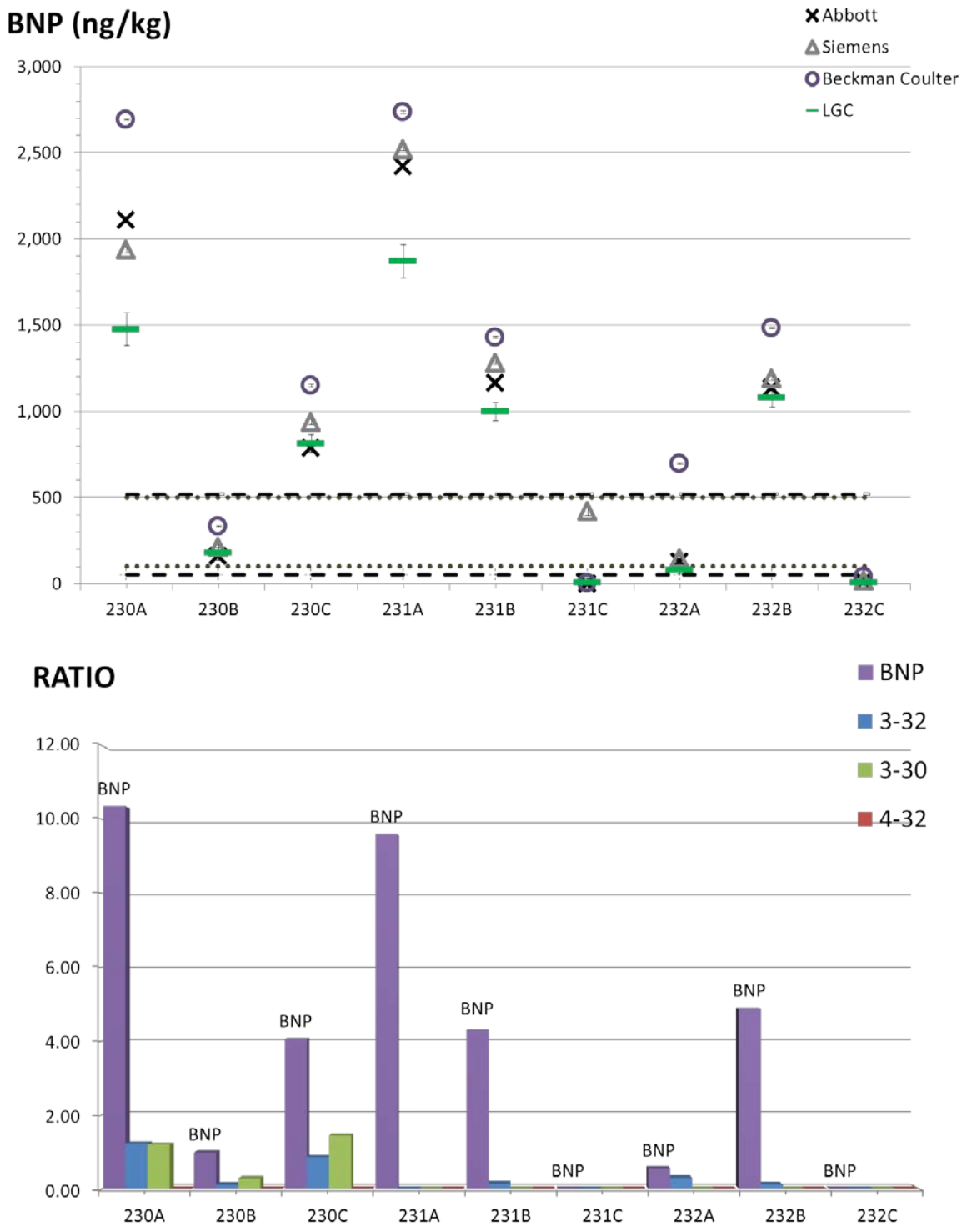

Appendix B 9 BNP quantitation results and degradation profiles of NEQAS samples. Dashed lines: range of the reference method (52-520 pg/g). Dotted lines: lower and higher decision limits (100/500 pg/g). RATIO: BNP, 3-32, 3-30 and 4-32 area over the labelled BNP* area. Results 230-232.

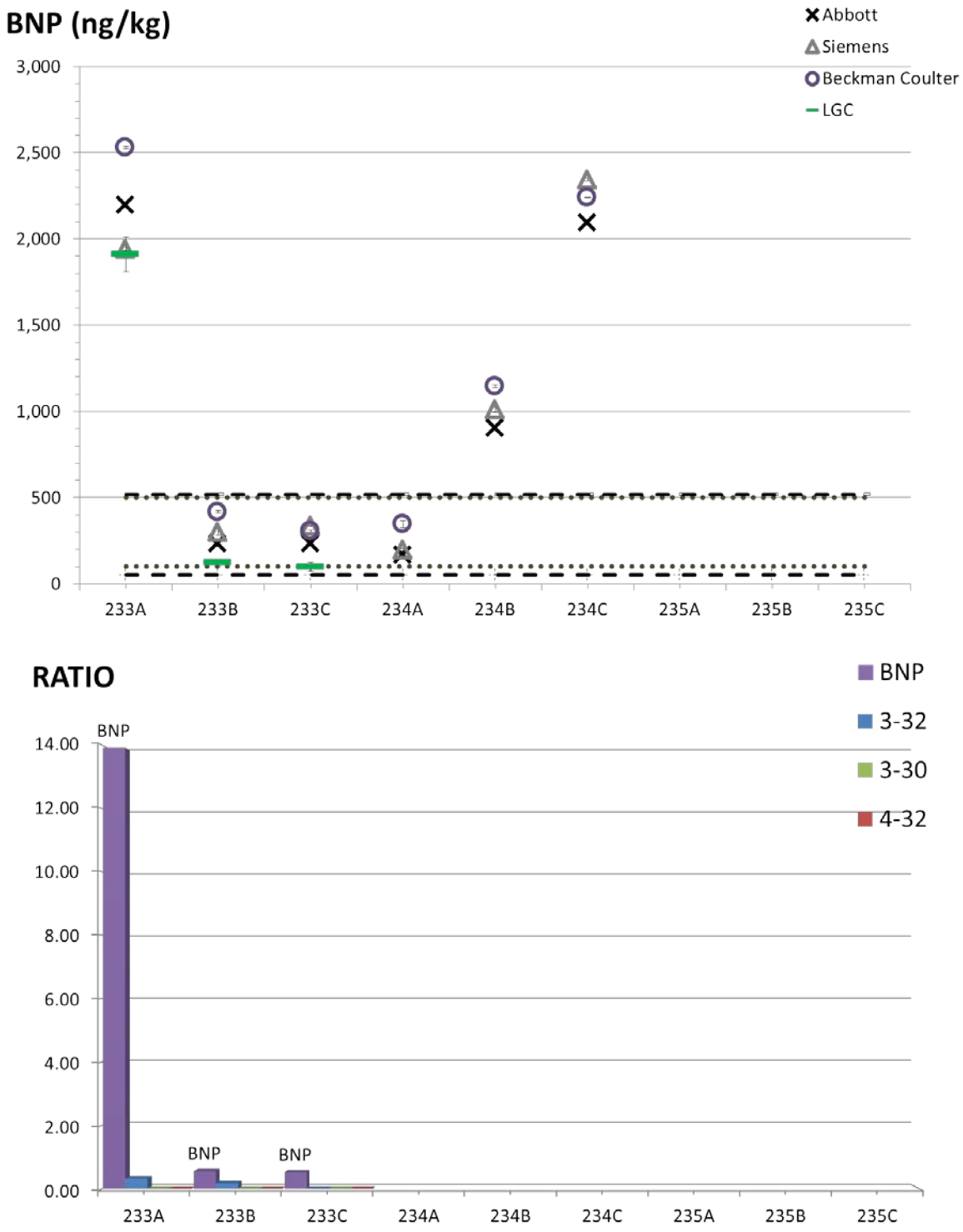

Appendix B 10BNP quantitation results and degradation profiles of NEQAS samples.Dashed lines: range of the reference method (52-520 pg/g). Dotted lines: lower and higher decision limits (100/500 pg/g). RATIO: BNP, 3-32, 3-30 and 4-32 area over the labelled BNP* area. Results 233-235.

Appendix C Related publications

DE GRUYTER Clin Chem Lab Med 2017; 55(9): 1397–1406

Open Access

Attila F. Torma, Kate Groves, Sabine Blesenbruch, Chris Mussell, Alan Reid, Steve Ellison, Rainer Cramer and Milena Quaglia*

A candidate liquid chromatography mass spectrometry reference method for the quantification of the cardiac marker 1-32 B-type natriuretic peptide

DOI 10.1515/cclm-2016-1054
Received November 18, 2016; accepted March 9, 2017; previously published online April 20, 2017

Abstract

Background: B-type natriuretic peptide (BNP) is a 32 amino acid cardiac hormone routinely measured by immunoassays to diagnose heart failure. While it is reported that immunoassay results can vary up to 45%, no attempt of standardization and/or harmonization through the development of certified reference materials (CRMs) or reference measurement procedures (RMPs) has yet been carried out.

Methods: B-type natriuretic peptide primary calibrator was quantified traceably to the International System of Units (SI) by both amino acid analysis and tryptic digestion. A method for the stabilization of BNP in plasma followed by protein precipitation, solid phase extraction (SPE) and liquid chromatography (LC) mass spectrometry (MS) was then developed and validated for the quantification of BNP at clinically relevant concentrations (15–150 fmol/g).

Results: The candidate reference method was applied to the quantification of BNP in a number of samples from the UK NEQAS Cardiac Markers Scheme to demonstrate its applicability to generate reference values and to preliminary evaluate the commutability of a potential CRM. The results from the reference method were consistently lower than the immunoassay results and discrepancy between the immunoassays was observed confirming previous data.

Conclusions: The application of the liquid chromatography-mass spectrometry (LC-MS) method to the UK NEQAS samples and the correlation of the results with the immunoassay results shows the potential of the method to support external quality assessment schemes, to improve understanding of the bias of the assays and to establish RMPs for BNP measurements. Furthermore, the method has the potential to be multiplexed for monitoring circulating truncated forms of BNP.

Keywords: 1-32 B-type natriuretic peptide (BNP) reference method; brain natriuretic peptides; isotope dilution mass spectrometry; standardization.

Introduction

B-type natriuretic peptide (BNP) and N-terminal proBNP (NT-proBNP) are cardiac biomarkers secreted as proBNP, the prohormone of BNP, by the myocytes of the left ventricle in response to volume overload in an event of congestive heart failure [1]. In 2012, specific age-independent decision cut-offs for both BNP (≤100 ng/L) and NT-proBNP (≤300 ng/L) were endorsed [2] and measurements of circulating BNP are currently used in clinical practice for the diagnosis of acute and chronic heart failure, risk stratification and monitoring response to therapy [3].

A number of immunoassays specific for BNP and NT-proBNP analysis are commercially available and studies have been performed to assess their performance [4, 5]. The results of the CardioOrmoCheck study, for example, highlighted discrepancy between immunoassays specific for BNP and discussed the requirement for measurement standardization [6].

*Corresponding author: Dr. Milena Quaglia, LGC Ltd., Science and Innovation, Queens Road, TW11 0LY Teddington, UK, E-mail: Milena.Quaglia@lgcgroup.com
Attila F. Torma, Kate Groves, Sabine Blesenbruch and Steve Ellison: LGC Ltd., Teddington, UK
Chris Mussell: LGC Ltd., Teddington, UK
Alan Reid: UK NEQAS Cardiac Markers – Laboratory Medicine and FM Building, Queen Elizabeth University Hospital, Glasgow, UK
Rainer Cramer: University of Reading – Department of Chemistry, Reading, Berkshire, UK